

Université de Montréal

**Molecular characterization of the contribution of autophagy to  
antigen presentation using quantitative proteomics**

par

Christina Bell

Département de Chimie

Faculté des Arts et des Sciences

Thèse présentée à la Faculté des études supérieures et postdoctorales

en vue de l'obtention du grade de

Philosophiæ Doctor (Ph.D.)

en chimie

July 2014

© Christina Bell, 2014



## Résumé

L'autophagie est une voie hautement conservée de dégradation lysosomale des constituants cellulaires qui est essentiel à l'homéostasie cellulaire et contribue à l'apprêtement et à la présentation des antigènes. Les rôles relativement récents de l'autophagie dans l'immunité innée et acquise sous-tendent de nouveaux paradigmes immunologiques pouvant faciliter le développement de nouvelles thérapies où la dérégulation de l'autophagie est associée à des maladies auto-immunes. Cependant, l'étude *in vivo* de la réponse autophagique est difficile en raison du nombre limité de méthodes d'analyse pouvant fournir une définition dynamique des protéines clés impliquées dans cette voie. En conséquence, nous avons développé un programme de recherche en protéomique intégrée afin d'identifier et de quantifier les protéines associées à l'autophagie et de déterminer les mécanismes moléculaires régissant les fonctions de l'autophagosome dans la présentation antigénique en utilisant une approche de biologie des systèmes. Pour étudier comment l'autophagie et la présentation antigénique sont activement régulés dans les macrophages, nous avons d'abord procédé à une étude protéomique à grande échelle sous différentes conditions connues pour stimuler l'autophagie, tels l'activation par les cytokines et l'infection virale.

La cytokine tumor necrosis factor-alpha (TNF- $\alpha$ ) est l'une des principales cytokines pro-inflammatoires qui intervient dans les réactions locales et systémiques afin de développer une réponse immune adaptative. La protéomique quantitative d'extraits membranaires de macrophages contrôlés et stimulés avec le TNF- $\alpha$  a révélé que l'activation des macrophages a entraîné la dégradation de protéines mitochondriales et des changements d'abondance de plusieurs protéines impliquées dans le trafic vésiculaire et la réponse immunitaire. Nous avons constaté que la dégradation des protéines mitochondriales était sous le contrôle de la voie ATG5, et était spécifique au TNF- $\alpha$ . En outre, l'utilisation d'un nouveau système de présentation antigénique, nous a permis de constater que l'induction de la mitophagie par le TNF- $\alpha$ , a entraînée l'apprêtement et la présentation d'antigènes mitochondriaux par des molécules du CMH de classe I, contribuant ainsi la variation du répertoire immunopeptidomique à la surface cellulaire. Ces résultats mettent en évidence un rôle insoupçonné du TNF- $\alpha$  dans la mitophagie et permet une meilleure compréhension des mécanismes responsables de la présentation d'auto-antigènes par les molécules du CMH de classe I.

Une interaction complexe existe également entre infection virale et l'autophagie. Récemment, notre laboratoire a fourni une première preuve suggérant que la macroautophagie peut contribuer à la présentation de protéines virales par les molécules du CMH de classe I lors de l'infection virale par l'herpès simplex virus de type 1 (HSV-1). Le virus HSV1 fait parti des virus humains les plus complexes et les plus répandues. Bien que la composition des particules virales a été étudiée précédemment, on connaît moins bien l'expression de l'ensemble du protéome viral lors de l'infection des cellules hôtes. Afin de caractériser les changements dynamiques de l'expression des protéines virales lors de l'infection, nous avons analysé par LC-MS/MS le protéome du HSV1 dans les macrophages infectés. Ces analyses nous ont permis d'identifier un total de 67 protéines virales structurales et non structurales (82% du protéome HSV1) en utilisant le spectromètre de masse LTQ-Orbitrap. Nous avons également identifié 90 nouveaux sites de phosphorylation et de dix nouveaux sites d'ubiquitylation sur différentes protéines virales. Suite à l'ubiquitylation, les protéines virales peuvent se localiser au noyau ou participer à des événements de fusion avec la membrane nucléaire, suggérant ainsi que cette modification pourrait influencer le trafic vésiculaire des protéines virales. Le traitement avec des inhibiteurs de la réplication de l'ADN induit des changements sur l'abondance et la modification des protéines virales, mettant en évidence l'interdépendance des protéines virales au cours du cycle de vie du virus. Compte tenu de l'importance de la dynamique d'expression, de l'ubiquitylation et la phosphorylation sur la fonction des protéines virales, ces résultats ouvriront la voie vers de nouvelles études sur la biologie des virus de l'herpès.

Fait intéressant, l'infection HSV1 dans les macrophages déclenche une nouvelle forme d'autophagie qui diffère remarquablement de la macroautophagie. Ce processus, appelé autophagie associée à l'enveloppe nucléaire (nuclear envelope derived autophagy, NEDA), conduit à la formation de vésicules membranaires contenant 4 couches lipidiques provenant de l'enveloppe nucléaire où on retrouve une grande proportion de certaines protéines virales, telle la glycoprotéine B. Les mécanismes régissant NEDA et leur importance lors de l'infection virale sont encore méconnus. En utilisant un essai de présentation antigénique, nous avons pu montrer que la voie NEDA est indépendante d'ATG5 et participe à l'apprêtement et la présentation d'antigènes viraux par le CMH de classe I. Pour comprendre l'implication de NEDA dans la présentation des antigènes, il est essentiel de caractériser le protéome des autophagosomes isolés à partir de macrophages infectés par HSV1. Aussi, nous avons développé une nouvelle approche



de fractionnement basé sur l'isolation de lysosomes chargés de billes de latex, nous permettant ainsi d'obtenir des extraits cellulaires enrichis en autophagosomes. Le transfert des antigènes HSV1 dans les autophagosomes a été déterminé par protéomique quantitative. Les protéines provenant de l'enveloppe nucléaire ont été préférentiellement transférées dans les autophagosome lors de l'infection des macrophages par le HSV1. Les analyses protéomiques d'autophagosomes impliquant NEDA ou la macroautophagie ont permis de découvrir des mécanismes jouant un rôle clé dans l'immunodominance de la glycoprotéine B lors de l'infection HSV1. Ces analyses ont également révélées que diverses voies autophagiques peuvent être induites pour favoriser la capture sélective de protéines virales, façonnant de façon dynamique la nature de la réponse immunitaire lors d'une infection.

En conclusion, l'application des méthodes de protéomique quantitative a joué un rôle clé dans l'identification et la quantification des protéines ayant des rôles importants dans la régulation de l'autophagie chez les macrophages, et nous a permis d'identifier les changements qui se produisent lors de la formation des autophagosomes lors de maladies inflammatoires ou d'infection virale. En outre, notre approche de biologie des systèmes, qui combine la protéomique quantitative basée sur la spectrométrie de masse avec des essais fonctionnels tels la présentation antigénique, nous a permis d'acquérir de nouvelles connaissances sur les mécanismes moléculaires régissant les fonctions de l'autophagie lors de la présentation antigénique. Une meilleure compréhension de ces mécanismes permettra de réduire les effets nuisibles de l'immunodominance suite à l'infection virale ou lors du développement du cancer en mettant en place une réponse immunitaire appropriée.

**Mots-clés:** Autophagie, présentation antigénique, protéomique quantitative, spectrométrie de masse, TNF- $\alpha$ , macrophages, Herpès Simplex Virus



## Abstract

Autophagy is a highly conserved lysosomal-mediated protein degradation pathway that plays a crucial role in maintaining cellular homeostasis and contributes to antigen processing and presentation. The emerging roles of autophagy in both innate and adaptive immunity underpin novel immunological paradigms that may provide opportunities for the development of new therapies where impaired autophagy is associated with autoimmune diseases. However, the *in vivo* study of autophagic response is challenging in view of the limited number of analytical approaches that can provide a dynamic definition of the key proteins involved in this pathway. Accordingly, we developed an integrated proteomics research program to unravel the molecular machines associated with autophagy and to decipher the fine details of the molecular mechanisms governing the functions of the autophagosome in antigen presentation using a systems biology approach. To study how autophagy and antigen presentation are actively modulated in macrophages, we first conducted comprehensive, global proteomics studies under different conditions known to stimulate autophagy. Autophagy is modulated by cytokines as well as by viral infection in various ways.

TNF- $\alpha$  is one of the major proinflammatory cytokines that mediate local and systemic responses and direct the development of adaptive immunity. Label-free quantitative proteomics analysis of membrane extracts from TNF- $\alpha$  activated and resting macrophages revealed that TNF- $\alpha$  activation led to the downregulation of mitochondrial proteins and the differential regulation of several proteins involved in vesicle trafficking and immune response. Importantly, we found that the downregulation of mitochondria proteins occurred through Atg5-dependent mitophagy, and was specific to TNF- $\alpha$ . Furthermore, using a novel antigen presentation system, we observed that the induction of mitophagy by TNF- $\alpha$  enabled the processing and presentation of mitochondrial antigens at the cell surface by MHC class I molecules, suggesting that TNF- $\alpha$  induced mitophagy contributes to the modification of the MHC class I peptide repertoire. These findings highlight an unsuspected role of TNF- $\alpha$  in mitophagy and expanded our understanding of the mechanisms responsible for MHC class I presentation of self-antigens.

A complex interplay also exists between viral infection and autophagy. Recently, our lab provided the first evidence that macroautophagy can contribute to the presentation of viral proteins on MHC class I molecules during Herpes Simplex Virus type 1 (HSV1) infection. HSV1 are among the most complex and widespread human viruses. While the composition of viral particles has been studied, less is known about the expression of the whole viral proteome in infected cells. To comprehensively characterize the system, we analyzed the proteome of the prototypical HSV1 in infected macrophages by LC-MS/MS. We achieved a very high level of protein coverage and identified a total of 67 structural and non-structural viral proteins (82% of the HSV1 proteome) using LC-MS/MS on a LTQ-Orbitrap instrument. We also obtained a comprehensive map of 90 novel phosphorylation sites and ten novel ubiquitylation sites on different viral proteins. Interestingly all ubiquitylated proteins could either localize to the nucleus or participate in membrane fusion events, suggesting that ubiquitylation of viral proteins might affect their trafficking. Treatment with inhibitors of DNA replication induced changes of both viral protein abundance and modifications, highlighting the interdependence of viral proteins during the life cycle of the virus. Given the importance of expression dynamics, ubiquitylation and phosphorylation for protein function, these findings will serve as important tools for future studies on herpes virus biology.

Interestingly, HSV1 infection in macrophages triggers a novel form of autophagy which remarkably differs in many ways from macroautophagy. This process, referred to as nuclear envelope-derived autophagy (NEDA), leads to the formation of 4-membrane layered vesicles originating from the nuclear envelope where some viral protein such as glycoprotein B are highly enriched. To which extent this process differs from macroautophagy and participates in the pathogenesis of HSV infection is still largely unknown. Using a novel antigen presentation assay we could show that NEDA is an Atg5-independent pathway that participates in the capture of viral proteins, and their processing and presentation on MHC class I molecules. To understand the involvement of NEDA in antigen presentation it is crucial to characterize the autophagosomal proteome in HSV1 infected macrophages. We developed a novel isolation method based on the loading of the lysosomal compartment with latex beads, a unique tool to obtain very pure cell extracts, upon autophagy induction. The transfer of HSV1 antigens into autophagosomes was monitored using quantitative proteomics. Nuclear enveloped-derived proteins were preferentially transferred to the autophagosome during HSV1 infection. Detailed proteomics characterization of autophagosomes formed during NEDA

and macroautophagy led to the discovery of mechanisms that play a key role in glycoprotein B immunodominance during HSV1 infection. These analyses also revealed that various autophagic pathways can be induced to promote the capture of selective sets of viral proteins, thus actively shaping the nature of the immune response during infection.

In conclusion, the application of quantitative proteomics methods played a key role in identifying and quantifying important regulators of autophagy in macrophages and allowed us to identify changes occurring during the remodeling of autophagosomes in response to disease and inflammatory conditions such as viral infections. Furthermore, our systems biology approach that combined mass spectrometry-based quantitative proteomics with functional screens such as antigen presentation assays revealed novel biological insights on the molecular mechanisms governing the functions of autophagy in antigen presentation. Harnessing the contribution of autophagy in antigen presentation has the potential to minimize the deleterious effects of immunodominance in viral infection and cancer by shaping an appropriate immune response.

**Keywords:** Autophagy, antigen presentation, quantitative proteomics, mass spectrometry, TNF- $\alpha$ , macrophages, Herpes Simplex Virus



# Table of contents

<b>Résumé .....</b>	<b>i</b>
<b>Abstract .....</b>	<b>v</b>
<b>Table of contents .....</b>	<b>ix</b>
<b>List of tables.....</b>	<b>xvii</b>
<b>List of figures .....</b>	<b>xix</b>
<b>List of abbreviations.....</b>	<b>xxi</b>
<b>Acknowledgements .....</b>	<b>xxv</b>
<b>Chapter 1 : Introduction .....</b>	<b>1</b>
<b>1.1. The immune system.....</b>	<b>2</b>
1.1.1 Innate immunity.....	2
1.1.2. Adaptive immunity.....	3
1.1.2.1. T cells – important effector cells of adaptive immunity .....	3
<b>1.2. Macrophages – key players in innate and adaptive immunity.....</b>	<b>4</b>
1.2.1. Macrophage activation.....	6
<b>1.3. Antigen processing and presentation.....</b>	<b>9</b>
<b>1.4. Autophagy .....</b>	<b>12</b>
1.4.1. Molecular regulation of autophagy and the autophagy pathway.....	14
1.4.2. Signaling pathways regulating autophagy .....	15
1.4.3. Origin of the autophagosomal membrane.....	17
1.4.4. Selective autophagy.....	18

1.4.5.	Mitophagy .....	20
1.4.6.	Autophagy in infection and immunity .....	22
1.4.6.1.	Xenophagy .....	22
1.4.6.2.	Autophagy and antigen presentation .....	23
1.4.6.3.	Cross-talk between autophagy and cytokines .....	25
1.4.6.4.	Autophagy and viral infection .....	26
<b>1.5.</b>	<b>Characteristics of Herpes simplex virus type 1 .....</b>	<b>28</b>
1.5.1.	Virion structure .....	29
1.5.2.	Genome organization .....	30
1.5.3.	Viral life cycle .....	30
1.5.4.	Viral gene expression .....	31
1.5.5.	Latent infection .....	32
1.5.6.	Treatment of HSV infections .....	32
1.5.7.	Viral infection control- Viral evasion .....	33
1.5.8.	HSV-1 and autophagy: a complex interplay .....	34
1.5.8.1.	Nuclear envelope derived autophagy (NEDA) .....	34
<b>1.6.</b>	<b>Mass spectrometry-based proteomics .....</b>	<b>35</b>
1.6.1.	Sample preparation .....	37
1.6.2.	Separation of proteins and peptides .....	37
1.6.3.	Mass spectrometry .....	40
1.6.3.1.	Ionization techniques – Electrospray Ionization .....	40
1.6.3.2.	Tandem mass spectrometry (MS/MS) .....	42
1.6.3.2.1.	<i>Dissociation methods for MS/MS</i> .....	43
1.6.3.2.2.	<i>Nomenclature of fragment ions</i> .....	44
1.6.3.3.	Mass analyzers .....	45
1.6.3.3.1.	<i>Linear quadrupole ion traps (LIT)</i> .....	46
1.6.3.3.2.	<i>Orbitrap Mass Analyzer</i> .....	47
1.6.3.3.3.	<i>LTQ Orbitrap</i> .....	48
1.6.3.3.4.	<i>Orbitrap Elite</i> .....	49
1.6.4.	Quantification in mass spectrometry-based proteomics .....	50
1.6.4.1.	Stable-isotope based methods .....	52
1.6.4.1.1.	<i>Metabolic labeling</i> .....	52
1.6.4.1.2.	<i>Chemical protein and peptide labeling</i> .....	52



1.6.4.2.	Label-free quantitation .....	53
1.6.4.2.1.	<i>Spectral count based approaches</i> .....	53
1.6.4.2.2.	<i>MS<sup>1</sup> intensity based approaches</i> .....	54
1.6.5.	Bioinformatics and data analysis .....	54
1.6.6.	Proteomics of post-translational modifications.....	57
1.6.7.	Contribution of proteomics to the understanding of HSV-1 infection .....	58
1.6.8.	Characterization of autophagy by quantitative proteomics .....	59
<b>1.7.</b>	<b>Research objectives .....</b>	<b>61</b>
<b>1.8.</b>	<b>Thesis overview .....</b>	<b>63</b>
<b>1.9.</b>	<b>References .....</b>	<b>65</b>
 <b>Chapter 2 : Quantitative proteomics reveals the induction of mitophagy in TNF-<math>\alpha</math> activated macrophages.....</b>		<b>93</b>
<b>2.1.</b>	<b>Author contributions .....</b>	<b>96</b>
<b>2.2.</b>	<b>Summary.....</b>	<b>97</b>
<b>2.3.</b>	<b>Introduction .....</b>	<b>98</b>
<b>2.4.</b>	<b>Experimental Procedures.....</b>	<b>101</b>
2.4.1.	Cell lines .....	101
2.4.2.	Raw-Kb construction.....	101
2.4.3.	pIRES-gB <sub>30-694</sub> -Mito vector .....	101
2.4.4.	RAW-Kb-Mito gB <sub>30-694</sub> cell line .....	102
2.4.5.	Crude membrane preparation.....	102
2.4.6.	Protein and peptide fractionation .....	102
2.4.7.	Proteolytic digestion.....	103
2.4.8.	Mass spectrometry.....	104
2.4.9.	Protein identification and quantitative analysis .....	104
2.4.10.	Bioinformatics analysis .....	105
2.4.11.	Western Blot .....	105

2.4.12.	Flow Cytometry Analysis .....	106
2.4.13.	Immunofluorescence .....	106
2.4.14.	Electron microscopy .....	107
2.4.15.	Antigen presentation Assay.....	107
<b>2.5.</b>	<b>Results.....</b>	<b>108</b>
2.5.1.	Quantitative proteomics of TNF- $\alpha$ activated macrophages .....	109
2.5.2.	Protein interaction network analysis of TNF- $\alpha$ activated macrophages uncovers the regulation of mitochondrial proteins.....	113
2.5.3.	TNF- $\alpha$ induces specific autophagic elimination of mitochondria in macrophages.....	116
2.5.4.	Macrophage activation by TNF- $\alpha$ increases MHC Class I presentation of mitochondrial antigens .....	121
<b>2.6.</b>	<b>Discussion .....</b>	<b>124</b>
<b>2.7.</b>	<b>Acknowledgements.....</b>	<b>127</b>
<b>2.8.</b>	<b>Supplemental data.....</b>	<b>128</b>
2.8.1.	Supplementary figures .....	128
2.8.2.	Supplemental tables.....	137
<b>2.9.</b>	<b>References .....</b>	<b>138</b>
 <b>Chapter 3 : Proteomics analysis of Herpes Simplex Virus type 1-infected cells reveals dynamic changes of viral protein expression, ubiquitylation and phosphorylation.....</b>		
<b>3.1.</b>	<b>Author contributions.....</b>	<b>146</b>
<b>3.2.</b>	<b>Abstract.....</b>	<b>147</b>
<b>3.3.</b>	<b>Introduction.....</b>	<b>148</b>
<b>3.4.</b>	<b>Experimental Procedures .....</b>	<b>150</b>

3.4.1.	Cells & viruses .....	150
3.4.2.	Infection & drug treatment.....	150
3.4.3.	SDS-PAGE and Mass Spectrometry .....	150
3.4.4.	Protein identification and data analysis.....	151
3.4.5.	Identification of ubiquitylated and phosphorylated residues .....	151
3.4.6.	Immunoblot .....	152
<b>3.5.</b>	<b>Results &amp; Discussion .....</b>	<b>153</b>
3.5.1.	Coverage of HSV1 proteins .....	153
3.5.2.	Dynamic changes in the HSV1 proteome after inhibition of DNA replication.....	154
3.5.3.	Ubiquitylation might regulate protein trafficking during the viral life cycle....	157
3.5.4.	Phosphorylation of HSV1 regulatory proteins .....	160
3.5.5.	Phosphorylated protein motifs display great variability .....	163
<b>3.6.</b>	<b>Conclusions.....</b>	<b>165</b>
<b>3.7.</b>	<b>Acknowledgement .....</b>	<b>166</b>
<b>3.8.</b>	<b>Abstract figure.....</b>	<b>167</b>
<b>3.9.</b>	<b>Supporting Information .....</b>	<b>168</b>
3.9.1.	Supporting figures.....	168
3.9.2.	Supporting tables .....	169
<b>3.10.</b>	<b>References .....</b>	<b>170</b>
<b>Chapter 4 : Nuclear envelope-derived autophagy contributes to MHC I antigen presentation of a viral protein that resides in the nuclear envelope .....</b>		<b>175</b>
<b>4.1.</b>	<b>Author contributions .....</b>	<b>176</b>
<b>4.2.</b>	<b>Summary.....</b>	<b>177</b>

<b>4.3. Introduction.....</b>	<b>178</b>
<b>4.4. Results.....</b>	<b>180</b>
4.4.1. Contribution of NEDA to viral antigen presentation .....	180
4.4.2. Quantitative proteomics analyses of viral proteins in autophagolysosomes .....	186
<b>4.5. Discussion .....</b>	<b>196</b>
<b>4.6. Experimental Procedures .....</b>	<b>200</b>
4.6.1. Cells, viruses, and antibodies.....	200
4.6.2. Generation of pIRES-gB1-2715 Nuclear Envelope and pIRES-gB1-2094 ER lumen vectors .....	201
4.6.3. Generation of stable RAW gB-nuclear envelope & RAW gB-ER lumen cell lines .....	201
4.6.4. Infection and drug treatment .....	201
4.6.5. Antigen presentation assays .....	202
4.6.6. Autophagolysosome isolation.....	202
4.6.7. Mass spectrometry analysis of APL .....	202
4.6.8. Immunofluorescence .....	203
4.6.9. SDS-PAGE & immunoblots .....	204
4.6.10. Electron microscopy .....	204
<b>4.7. Acknowledgements.....</b>	<b>205</b>
<b>4.8. Supplemental data.....</b>	<b>206</b>
4.8.1. Supplementary figures .....	206
4.8.2. Supplemental tables.....	207
<b>4.9. References .....</b>	<b>208</b>
<b>Chapter 5 : Conclusion .....</b>	<b>213</b>
<b>5.1. Conclusion and Discussion .....</b>	<b>214</b>
5.1.1. An unexpected role for TNF- $\alpha$ in the induction of mitophagy .....	215

5.1.2.	Potential roles of TNF- $\alpha$ induced mitophagy.....	216
5.1.3.	TNF- $\alpha$ induced mitophagy contributes to antigen presentation: 'Shaping an efficient immune response' .....	218
5.1.4.	HSV1 infection and autophagy .....	219
5.1.5.	A comprehensive characterization of viral protein expression in macrophages .....	220
5.1.6.	NEDA is Atg5-independent and contributes to MHC class I antigen presentation .....	221
5.1.7.	A novel autophagosome isolation method .....	221
5.1.8.	Selectivity of NEDA: beneficial for host or virus? .....	222
5.1.9.	Autophagy can shape the immune response by selectively targeting different protein subsets: a novel concept .....	223
<b>5.2.</b>	<b>Future perspectives .....</b>	<b>225</b>
5.2.1.	Iterative proteomics: Autophagy and antigen presentation - 'network of influence' .....	225
5.2.2.	Quantitative proteomics approaches to investigate selectivity in autophagy pathways.....	226
5.2.3.	Modulation of the Immunopeptidome by selective autophagy .....	227
<b>5.3.</b>	<b>References.....</b>	<b>229</b>
<b>Appendix : Scientific Contributions .....</b>		<b>xxix</b>



## List of tables

<b>Table II-1.</b> Changes in abundance of selected macrophage membrane proteins upon TNF- $\alpha$ stimulation.....	111
<b>Table II-S1.</b> Protein identification for different separation platforms: mRP-C18, GELFREE and SCX (CD-ROM). .....	137
<b>Table II-S2.</b> List of peptides identified in each separation platforms (mRP-C18, GELFREE and SCX) (CD-ROM). .....	137
<b>Table II-S3.</b> Quantification of protein abundance changes upon TNF-alpha stimulation (CD-ROM). .....	137
<b>Table II-S4.</b> Ubiquitinated peptides upon TNF-alpha stimulation (CD-ROM).....	137
<b>Table III-1.</b> Ubiquitylation sites in HSV1 proteins. ....	158
<b>Table III-2.</b> Phosphorylation sites identified in HSV1 proteins. ....	161
<b>Table III-S1.</b> Summary of all HSV1 proteins that were identified in this study (under all experimental conditions) (CD-ROM). ....	169
<b>Table III-S2.</b> Summary of detailed peptide identifications in HSV1 infected cells treated with DMSO, acyclovir or PAA (CD-ROM).....	169
<b>Table III-S3.</b> Statistics on peptides identified after DMSO, acyclovir and PAA treatment in replicate experiments (CD-ROM). ....	169
<b>Table III-S4.</b> Organisation of HSV1 proteins in clusters according to sensitivity to acyclovir and PAA (CD-ROM).....	169
<b>Table III-S5.</b> Description of ubiquitylated peptides including links to spectra (CD-ROM). ....	169
<b>Table III-S6.</b> Statistics on ubiquitylated residues detected in replicate experiments (CD-ROM).....	169
<b>Table III-S7.</b> Description of phosphorylated peptides including links to spectra (CD-ROM).....	169
<b>Table III-S8.</b> Statistics on phosphorylated residues detected in replicate experiments (CD-ROM).. .....	169
<b>Table IV-1.</b> Statistics of quantitative proteomics analysis of APL and TCL from HSV1 WT and HSV1 $\Delta$ PP1 $\alpha$ infected macrophages. ....	189
<b>Table IV-S1.</b> HSV1 protein identifications (under all experimental conditions) (CD-ROM).....	207
<b>Table IV-S2.</b> List of ubiquitylated peptides including links to spectra (CD-ROM).....	207





## List of figures

<b>Figure 1.1.</b> Cytokine mediated macrophage activation. ....	8
<b>Figure 1.2.</b> MHC class I and MHC class II antigen processing and presentation pathways. ....	10
<b>Figure 1.3.</b> Autophagy pathway. ....	13
<b>Figure 1.4.</b> Signaling pathways regulating autophagy.....	16
<b>Figure 1.5.</b> Autophagy mechanisms and potential sources of membrane. ....	18
<b>Figure 1.6.</b> Cross-talk between autophagy and cytokines. ....	25
<b>Figure 1.7.</b> HSV virion structure. ....	29
<b>Figure 1.8.</b> General shotgun proteomics workflow.....	36
<b>Figure 1.9.</b> Nomenclature for fragment ions. ....	44
<b>Figure 1.10.</b> Schematics of the LTQ Orbitrap XL and Orbitrap Elite hybrid mass spectrometers. ....	49
<b>Figure 1.11.</b> Overview of quantitative proteomics workflows. ....	51
<b>Figure 1.12.</b> Analytical outcome of a proteomics experiment. ....	56
<b>Figure 2.1.</b> Workflow for large-scale quantitative proteomics analyses of RAW264.7 macrophages. ....	109
<b>Figure 2.2.</b> Large Scale membrane proteome analysis of resting and TNF- $\alpha$ activated macrophages. ....	110
<b>Figure 2.3.</b> Quantitative proteomics analysis of membrane proteins in TNF- $\alpha$ stimulated macrophages identified the overexpression of cPLA <sub>2</sub> . ....	112
<b>Figure 2.4.</b> Bioinformatics analyses of the membrane proteome from TNF- $\alpha$ activated macrophages reveals the downregulation of mitochondria proteins. ....	115
<b>Figure 2.5.</b> Changes in mitochondrial functions associated with TNF- $\alpha$ activated macrophages. ....	118
<b>Figure 2.6.</b> TNF- $\alpha$ induces mitophagy.....	120
<b>Figure 2.7.</b> Influence of TNF- $\alpha$ on antigen presentation. ....	123
<b>Figure 2.S1.</b> Flow cytometry analysis and clone showing the highest fluorescence levels selected, amplified and used.....	128
<b>Figure 2.S2.</b> Fractionation efficiency using immunoblots for several cellular markers. ....	129
<b>Figure 2.S3.</b> Reproducibility of peptide intensities across replicates. ....	130
<b>Figure 2.S4.</b> Comparison of three different fractionation techniques for quantitative membrane proteomics of RAW264.7 macrophages. ....	131
<b>Figure 2.S5.</b> MS/MS spectra of phosphopeptides. (CD-ROM). ....	131
<b>Figure 2.S6.</b> Scatter plots of abundance measurements for peptide ions identified in control and TNF- $\alpha$ stimulated extracts. ....	132
<b>Figure 2.S7.</b> Fold change measurements for citrate synthase and ATP synthase subunit b. ....	133
<b>Figure 2.S8.</b> MS/MS spectra of ubiquitinated peptides. (CD-ROM). ....	134

<b>Figure 2.S9.</b> Abundance of fluorescently-labeled Annexin A5 at the plasma membrane and 7-amino actinomycin D using flow cytometry. ....	134
<b>Figure 2.S10.</b> Lysosomal degradation activities when stained with Lysosensor. ....	135
<b>Figure 2.S11.</b> Integrated model of the TNF- $\alpha$ modulated functions favoring antigen MHC class I presentation. ....	136
<b>Figure 3.1</b> Effect of DNA replication inhibitors on HSV1 protein expression. ....	156
<b>Figure 3.2.</b> Ubiquitylation of HSV1 proteins. ....	159
<b>Figure 3.3.</b> Phosphorylation of HSV1 proteins. ....	162
<b>Figure 3.4.</b> Phosphorylation motifs. ....	164
<b>Figure 3.5.</b> Abstract figure.....	167
<b>Figure 3.S1.</b> Coverage of HSV1 structural proteins and proteins of different kinetic classes. ....	168
<b>Figure 4.1.</b> NEDA is regulated differently than macroautophagy and is Atg5-independent. ....	181
<b>Figure 4.2.</b> NEDA contributes to the presentation of gB to MHC class I molecules...	183
<b>Figure 4.3.</b> NEDA contributes to MHC class I antigen presentation of a nuclear envelope-resident viral antigen. ....	185
<b>Figure 4.4.</b> A novel autophagolysosome isolation method. ....	188
<b>Figure 4.5.</b> Quantitative proteomics analysis of APL extracts.....	191
<b>Figure 4.6.</b> NEDA leads to the enrichment of gB on the APL. ....	193
<b>Figure 4.7.</b> Atg5-dependent transfer of a specific subset of proteins to the APL during $\Delta$ PP1 $\alpha$ infection. ....	195
<b>Figure 4.S1.</b> Atg5 knockdown efficiency. ....	206

## List of abbreviations

1D	One dimensional
2D	Two dimensional
3-MA	3-methyladenine
APC	Antigen presenting cell
APL	Autophagolysosome
ATG	Autophagy related genes
AtgX	Autophagy-related protein X
Baf	Bafilomycin A1
Bcl	B-cell lymphoma
CCCP	Carbonyl cyanide m-chlorophenylhydrazone
CD	Cluster of differentiation
CH	Cycloheximide
CID	Collision-induced dissociation
cPLA <sub>2</sub>	Cytosolic phospholipase A2
DDA	Data-dependent acquisition
DMSO	Dimethylsulfoxide
DNA	Deoxyribonucleic acid
ER	Endoplasmic reticulum
ERK	Extracellular signal-regulated kinase
ESI	Electrospray ionization
ETD	Electron transfer dissociation
FDR	False Discovery Rate
FP	False positive
FPR	False positive rate
FT-ICR	Fourier transform ion cyclotron resonance
GABARAP	$\gamma$ -amino butyric acid receptor-associated protein
GELFREE	Gel-eluted liquid fraction entrapment electrophoresis
GO	Gene Ontology

gX	Glycoprotein X
HBV	Hepatitis B virus
HCD	Higher energy collisional induced dissociation
HSV1	Herpes Simplex Virus type 1
ICP	Infected cell protein
IFN- $\gamma$	Interferon- $\gamma$
IL	Interleukin
IRGM	Human immunity-related GTPase
JC-1	5,5',6,6'-tetrachloro 1,1',3,3'-teramethyl benzimidazol carbo cyanine iodide
LB-C	Latexbead-compartment
LC	Liquid chromatography
LC3	Microtubule-associated protein 1A/1B-light chain 3
LIR	LC3-interacting motif
LIT	Linear ion trap
LTQ	Linear trap quadrupole
$m/z$	Mass-to-charge ratio
MALDI	Matrix-assisted laser desorption/ionization
MAMP	Microbial-associated pattern
MEF	Mouse embryonic fibroblasts
MHC	Major histocompatibility complex
MIIC	MHC class II compartment
MOI	Multiplicity of infection
mRP-C18	Macroporous reversed phase-C18
MS	Mass Spectrometry
MS/MS	Tandem mass spectrometry
mTORC1	Mammalian TOR complex 1
MudPIT	Multidimensional protein identification technology
NEDA	Nuclear envelope derived autophagy
OVA	Ovalbumin

PAA	Phosphonoacetic acid
PAGE	Polyacrylamide gel electrophoresis
PAS	Phagophore assembly site
pi	Post infection
PINK1	PTEN (phosphatase and tensin homolog)-induced putative protein kinase 1
PP1 $\alpha$	Protein Phosphatase $\alpha$
ppm	Parts per million
PSM	Peptide-to-spectrum match
PtdIns3K	Phosphatidylinositol 3-kinase
PTM	Posttranslational modification
pXY	Protein encoded by HSV1 gene XY
rf	Radio frequency
ROS	Reactive oxygen species
RP	Reversed phase
RSD	Relative standard deviation
SCX	Strong cation exchange
SD	Standard deviation
SILAC	Stable isotope labeling with amino acids in cell culture
SQSTM1	Sequestosome
TAP	Transporter associated with antigen processing
TCL	Total cell lysate
T <sub>H</sub> X	T helper type X
TLR	Toll-like receptor
TM	Total membrane
TMD	Transmembrane domain
TNF- $\alpha$	Tumor necrosis factor- $\alpha$
ToF	Time-of-flight
TOR	Target of rapamycin
TP	True positive

TRAP1	TNF receptor-associated protein 1
TSC	Tuberous sclerosis complex
UBL	Ubiquitin like
U <sub>L</sub>	Unique region long
ULK	Unc-51-like kinase
UPS	Ubiquitin dependent proteasome system
U <sub>s</sub>	Unique region short
Vps	Vacuolar protein sorting
WT	Wild Type
XIC	Extracted ion chromatogram

## Acknowledgements

This thesis would never have been possible without the generous advice and support of many people.

I would like to express my deepest gratitude to Prof. Pierre Thibault, my PhD research director at the Institute for Research in Immunology and Cancer at Université de Montréal, who believed in my abilities and offered me this research position in his lab. I am very grateful for the challenge he presented to me in the shape of this project and for the opportunity to perform graduate studies in mass spectrometry-based proteomics. Pierre was always ready and patient to answer my questions concerning my work and listen to my problems. I thankfully acknowledge all his scientific support and advice on science and academic life in general. Thank you for being a great mentor and for making my stay at the IRIC very pleasant. I am very glad that I could be a member of your group.

I would like also like to express my sincere gratitude to Prof. Michel Desjardins, my PhD research co-director, from the Department of Pathology and Cell Biology at Université de Montréal for the opportunity to be a part of his lab and to learn from his expertise. I am thankful for not only his willingness to share his knowledge, but also for always motivating me to explore and develop my research further and thus get better.

Thank you to both of you for encouraging my research and for allowing me to grow as a scientist, while working on a very exciting, interdisciplinary project. Your advice on both research as well as on my career have been precious. I also really appreciate that you made it possible for me to realize a research stay during my PhD in the group of Prof. Markus Wenk at the National University of Singapore, to whom I would also like to express my gratitude. This research stay was a great experience, which not only taught me a lot about lipidomics, but it also significantly expanded my horizons.

I am very much obliged to the past and present lab members of the Thibault and Desjardins labs for sharing their expertise, for their support and for a very friendly atmosphere throughout my thesis work. The privilege to work closely with them, was of great importance to my work. I want to thank Dr. Kerstin Radtke for all her expertise with the viral infection system and for all her advice and help in general. I would also like to thank Dr. Luc English for introducing me to all the concepts of autophagy and antigen presentation and for teaching me several techniques crucial for my PhD project. Also, I

am very grateful to Dr. Jonathan Boulais for sharing his knowledge and teaching me useful bioinformatics tools. He was always ready to answer all my questions, help me with the data analysis and discuss about science. Thank you very much also to Dr. Matthias Trost for sharing his knowledge and experimental skills and for introducing me to my PhD project at first. Thank you to Dr. Diana Matheoud, Angélique Bellemare-Pelletier, Christiane Rondeau, Dr. Francis McManus and Prof. Étienne Gagnon for help and support. I am also very grateful to Dr. Mathieu Courcelles as well as to Olivier Caron-Lizotte for all their help and patience with the analysis of my large proteomics datasets. I would like to especially thank Dr. Eric Bonneil for all his help and expertise with the mass spectrometry equipment as well as all his scientific advice and guidance, and particularly for making every day in the lab much more fun. I really enjoyed working with you.

I would also like to thank Prof. Roger Lippé and his team, especially Johanne Duron, for all their expertise with the viral infection system and for making their equipment available to us.

I would like to express my special appreciation and thanks to Dr. Sonja Hess from California Institute of Technology, who always supported me and gave me valuable advice and who first introduced me to the field of proteomics during my diploma thesis research, which continued to fascinate me ever since.

Finally, I would like to thank the Chemistry department as well the FESP for supporting my application to the Vanier Canada Graduate Scholarship and of course the Natural Sciences and Engineering Research Council (NSERC) for selecting me as a Vanier scholar. It was an honor and a privilege to benefit society through my research as a Vanier scholar. This award not only opened up opportunities for my research, but it also was a constant motivation to fulfill my goals.

Above all, I'm very grateful to my parents Werner and Brunhilde, and my loving family for always being there for me and for accompanying me during this journey from afar. Thank you for always supporting my academic endeavors and for always encouraging me to strive towards my goals and make my dreams come true.

Most of all, I would like to thank Vincent for his relentless support, love, encouragement and understanding. Words cannot express how grateful I am. Thank you for always being there for me and for always staying on my side, especially in hard times.

**Danke! Thank you! Merci!**



You miss 100% of the shots you don't take.

**Wayne Gretzky**



## **Chapter 1 : Introduction**

## **1.1. The immune system**

The immune system is composed of structures and mechanisms that allow an organism to discriminate between "self" and "non-self" <sup>1</sup>. These defense mechanisms provide the body with protection against foreign pathogens such as bacteria, viruses, parasites or fungi and it also prevents autoreactive damage causing autoimmune disease, an immunosurveillance mechanisms referred to as self tolerance<sup>2</sup>. Furthermore, the immune system is also able to recognize an "altered- self" as in the case of cancer cells. The immune system is broadly divided into two main systems composed of innate immunity (or nonspecific immunity) and acquired/adaptive immunity (or specific immunity). Although these two subsystems were often seen as completely separate, the current opinion is that innate immunity and adaptive immunity systems are functionally interconnected and complement each other to contain infectious diseases<sup>3</sup>.

### **1.1.1 Innate immunity**

The innate immune system represents an excellent and rapid first line of defense against microbes. It is composed of physical barriers, antimicrobial substances, inflammatory mechanisms, complement system, leukocytes and fever, which are very effective against a variety of pathogens. The innate immune system recognizes molecular patterns common to various pathogens via a restricted number of receptors on phagocytic cells such as Toll-like receptors and is hence not specific<sup>2</sup>. This initial response is very rapid (in a time frame of hours) as these pathogen receptors are widely expressed on many cells. However, due to the lack of specificity the system rapidly fails when attacked by a pathogen that has evolved to evade the defense mechanisms. The presence of a constant synergizing interaction between innate and adaptive immunity allows the rapid establishment of specific defense mechanisms targeted at the pathogen. For example, phagocytosis and autophagy, two non-specific defense mechanisms for degradation of pathogens that are intra-or extracellular, are now recognized as part of the specific immune response<sup>1, 4</sup>.

### **1.1.2. Adaptive immunity**

Adaptive immunity, which has been acquired later in evolution, comprises a limited number of cells with very specific recognition capabilities for any pathogen. The adaptive immune system uses two types of responses, the cell-mediated response and the humoral response. For each of these responses, specialized cells have evolved that express antigen-specific receptors on their surface to exclusively recognize antigens associated with different pathogens<sup>2</sup>. The antigen receptor, if linked with a specific antigen, generates a clonal expansion of the latter, necessary to obtain enough immune cells to elucidate an efficient immune response. The adaptive immune response is hence slower (in a timeframe of days). In the case of cell-mediated immunity, the main actors are T lymphocytes, previously activated by professional antigen-presenting cells (APCs). To provide humoral immunity and perform the role of APCs, B cells actively produce antibodies after activation by antigen interaction. In addition to the development of effector cells, the adaptive response also enables the development of memory cells, thus providing a more rapid immune response if re-infected with the same pathogen<sup>4</sup>, a mechanism used in vaccination strategies<sup>3</sup>.

#### **1.1.2.1. T cells – important effector cells of adaptive immunity**

Adaptive immune cells that cause cell-mediated immunity originate from pluripotent hematopoietic stem cells in the bone marrow. These pluripotent cells generate multipotent stem cells that give rise to lymphoid and myeloid precursors. These precursors generate all cells comprising the immune system; T cells (derived from lymphoid precursors) and monocytes/macrophages and dendritic cells (formed from myeloid precursors)<sup>5</sup>.

Bone marrow derived T cells undergo a "selection" in the thymus. Thymic selection comprises positive and negative selection<sup>4</sup>. During positive selection only T cells able to bind major histocompatibility (MHC) molecules expressed by the epithelial cells of the thymus cortex with sufficient affinity survive, while others are eliminated by apoptosis<sup>6</sup>. Thereafter, the cells having passed the positive selection, migrate to the thymus to undergo negative selection (or clonal deletion). Here the lack of affinity with peptide-MHC complexes ensures the survival of lymphocytes, since T cells that interact too strongly with "self"-peptide-MHC complexes are eliminated<sup>7</sup>. This last step is crucial to avoid auto-reactive lymphocytes causing autoimmune diseases and plays an important role in

central tolerance<sup>8</sup>. After the thymic selection, “naïve” T cells enter the blood and lymphatic circulation, where they can get activated as “effector” T lymphocytes and / or “memory” T lymphocytes following recognition of specific antigens. The differentiation of naïve T cells into effector T lymphocytes is executed by professional antigen presenting cells, including dendritic cells and macrophages, regulated by co-stimulatory molecules and cytokines, and allows T effector cells to eliminate infected cells<sup>4</sup>.

There are different subgroups of effector T cells. Cluster of differentiation (CD) 4+ T lymphocytes play a central role in the development of the humoral response and cell mediated immune response. CD4+ T cells can differentiate into type I T helper (T<sub>H</sub>1) cells or type II T helper (T<sub>H</sub>2) cells, following binding of a peptide antigen on MHC class II complex from macrophages or dendritic cells and T cell receptor (TCR). T<sub>H</sub>1 and T<sub>H</sub>2 cells differ based on their subsequent production of cytokines. T<sub>H</sub>1 cells modulate cell-mediated immunity by secreting cytokines such as interferon and interleukin-2 (IL-2), whereas T<sub>H</sub>2 cells modulate humoral immunity by secreting IL-4, IL-10 and IL-13<sup>9</sup>.

Naïve CD8 + T cells differentiate into cytotoxic T lymphocytes (CTL) following activation through the interaction of their TCR with peptide-MHC class I and strong co-stimulatory activity on the surface of an APC. The co-stimulatory activity is promoted by the cytokine production of CD4+ T cells, resulting in the increased expression of co-stimulatory molecules. CD8+ T lymphocytes are particularly effective in eliminating virus-infected cells<sup>10</sup>. CD8+ T cells can destroy infected cells directly via the release of serine proteases called granzymes and the protein perforin<sup>11</sup>, which allows granzymes to enter into infected cells.

## **1.2. Macrophages – key players in innate and adaptive immunity**

Macrophages are innate immune cells with well-established roles in the primary response to pathogens, but also in the coordination of the adaptive immune response, inflammation, tissue homeostasis, and repair. Macrophages were initially recognized by Elli Metchnikoff as phagocytic cells responsible for pathogen elimination and housekeeping functions in a wide range of organisms, from invertebrates to vertebrates.

Ellie Metchnikoff, who won the Nobel Prize in Physiology or Medicine in 1908 for his description of phagocytosis, proposed that the key to immunity was to “stimulate the phagocytes”<sup>12</sup>.

Macrophages evolved in simple multicellular organisms to phagocyte and clear dying cells during development, and to protect the host through innate immunity, both as resident tissue macrophages and monocyte-derived cells mobilized during inflammation. Macrophages are very plastic and can change their functional phenotype depending on the environmental stimuli they receive. These cells have a vital role in protecting the host through their ability to kill pathogens and instruct other immune cells, but also contribute to the pathogenesis of inflammatory and degenerative diseases.

Macrophages are present in essentially all tissues. They differentiate from circulating peripheral-blood mononuclear cells (PBMCs), which migrate into tissue in the steady state or in response to inflammation<sup>13</sup>. PBMCs develop from a common myeloid progenitor cell in the bone marrow. This myeloid progenitor cell is the precursor of many different cell types, including, eosinophils, basophils, neutrophils, macrophages, dendritic cells and mast cells. During monocyte development, myeloid progenitor cells (termed granulocyte/macrophage colony-forming units) successively generate monoblasts, pro-monocytes and finally monocytes, which are sent from the bone marrow into the bloodstream<sup>13</sup>. Monocytes travel from the blood into tissue to form long-lived tissue-specific macrophages of the bone (osteoclasts), alveoli, central nervous system (microglial cells), gastrointestinal tract, liver (Kupffer cells), connective tissue (histiocytes), skin (Langerhans cells), peritoneum and spleen. Resident macrophage populations in different organs adjust to their local microenvironment. The stimuli that regulate tissue-specific phenotypes of macrophages include surface and secretory products of neighboring cells and extracellular matrix. Macrophages can respond to endogenous cues that are quickly generated following infection or injury. These early stimuli are typically produced by innate immune cells and can result in a distinct, though usually transient, effect on the physiology of macrophages<sup>14</sup>. Macrophages can also respond to stimuli produced by antigen-specific immune cells. These signals are more specific and prolonged than innate immune stimuli and generally exert longer term alterations in macrophages<sup>15</sup>.

Macrophages are professional phagocytes that internalize large particles like dead cells or pathogens, and play crucial roles in immunity by the initiation of microbicidal

mechanisms as a part of innate immunity<sup>14</sup>. In mammals, the internalization of microorganisms at sites of infection by macrophages proceeds via the internalization of pathogens in phagosomes, where they are killed and degraded by hydrolytic enzymes. Phagosomes obtained these functional properties relatively recently during the evolution of multicellular organisms through the acquisition of molecular machineries that transformed phagosomes from a lytic vacuole into an organelle fully competent for antigen presentation<sup>16</sup>. Indeed, the processing of proteins from internalized pathogens to derive antigens for presentation at the cell surface on major histocompatibility complex (MHC) class I and class II molecules is a key mechanism of adaptive immunity to initiate specific defense mechanisms<sup>17</sup>. Importantly, the initiation of an efficient immune response depends on the capability of APCs such as macrophages to display peptide MHC complexes on their cell surface.

### **1.2.1. Macrophage activation**

Cytokines produced by immune cells can activate macrophages to convey different responses. Classically macrophages are activated in response to interferon- $\gamma$  (IFN- $\gamma$ ), which can be produced during an adaptive immune response by T helper 1 (T<sub>H</sub>1) cells or CD8+ T cells or during an innate immune response by natural killer cells, and tumor necrosis factor (TNF), which is produced by antigen presenting cells (Figure 1.1). The term classically activated has been used to refer to the effector macrophages that are produced during cell-mediated immune responses<sup>14, 15, 18</sup>.

IFN- $\gamma$  activation results in the transcriptional regulation of several genes including nitric oxide synthase-2 and phagocyte oxidase that are associated with reactive oxygen species (ROS) production. ROS are an established feature of the macrophage's microbicidal activity and improve the killing abilities of macrophages<sup>19</sup>. IFN- $\gamma$  transforms resting macrophages into potent cells with increased antigen presenting capacity, increased synthesis of proinflammatory cytokines and toxic mediators, and enhanced complement mediated phagocytosis. Thus, macrophages obtain the capacity to kill bacteria, especially intracellular pathogens. IFN- $\gamma$  also mediates phagosome maturation and antigen loading on MHC class I and class II molecules<sup>20-22</sup> and regulates the upregulation of MHC class I as well as co-stimulatory molecules on macrophages<sup>14</sup>.



Classically activated macrophages secrete pro-inflammatory cytokines such as IL-1, IL-6 and IL-23, a hallmark of the macrophage's microbicidal activity<sup>14</sup>. Proinflammatory cytokines produced by classically activated macrophages are an important feature of the host defense, but they can also cause extensive damage to the host. The expansion of T<sub>H</sub>17 cells has been linked to IL-1, IL-6 and IL-23<sup>23, 24</sup>. These cells produce IL-17, a cytokine that can contribute to inflammatory autoimmune diseases<sup>14</sup>. Interestingly, macrophages activated through Toll-like receptor (TLR) ligand stimulation produce tumor necrosis factor  $\alpha$  (TNF- $\alpha$ ), another important cytokine that synergizes with INF- $\gamma$  to enhance macrophage activation. Macrophages can also be stimulated exogenously from the secretion of this cytokine by antigen presenting cells. TNF- $\alpha$  stimulation is particularly important in *Leishmania* infections as macrophages stimulated with IFN- $\gamma$  alone are less efficient at killing this parasite due to lack of TLR ligands expression. TNF- $\alpha$  also has a central role in inflammatory cell activation and recruitment, and is associated with the development of various chronic inflammatory diseases such as Crohn's disease<sup>25</sup>.

Taken together, classically activated macrophages are products of a cell-mediated immune response. They can also be transiently generated in response to innate stimuli following viral infections or stress. Some pathogens have acquired the ability to interfere with IFN- $\gamma$  signaling and inhibit efficient macrophage activation. Classically activated macrophages are vital components of the host defense, but their activation must be tightly controlled, because the cytokines and mediators they produce can lead to host tissue damage. Indeed classically activated macrophages are key mediators of the immunopathology that occurs during several autoimmune diseases, including rheumatoid arthritis<sup>26</sup> and inflammatory bowel disease<sup>27</sup>.

Similarly to classically activated macrophages, wound healing or alternatively activated macrophages can arise in response to innate or adaptive signals (Figure 1.1). Macrophages are alternatively activated by IL-4 and IL-13<sup>28</sup>, which trigger a distinct phenotype that accounts for allergic, cellular and humoral responses to parasitic and extracellular pathogens<sup>28</sup>. Basophils and mast cells are important early sources of innate IL-4 production, while other granulocytes might also contribute. It is well established that IL-4 and IL-13 are associated with T<sub>H</sub>2 type responses. IL-4- and IL-13 can promote the development of wound-healing macrophages, though this activation yields poor antigen-presenting cells that are less efficient at producing ROS or at clearing intra cellular pathogens than classically activated macrophages<sup>29</sup>.

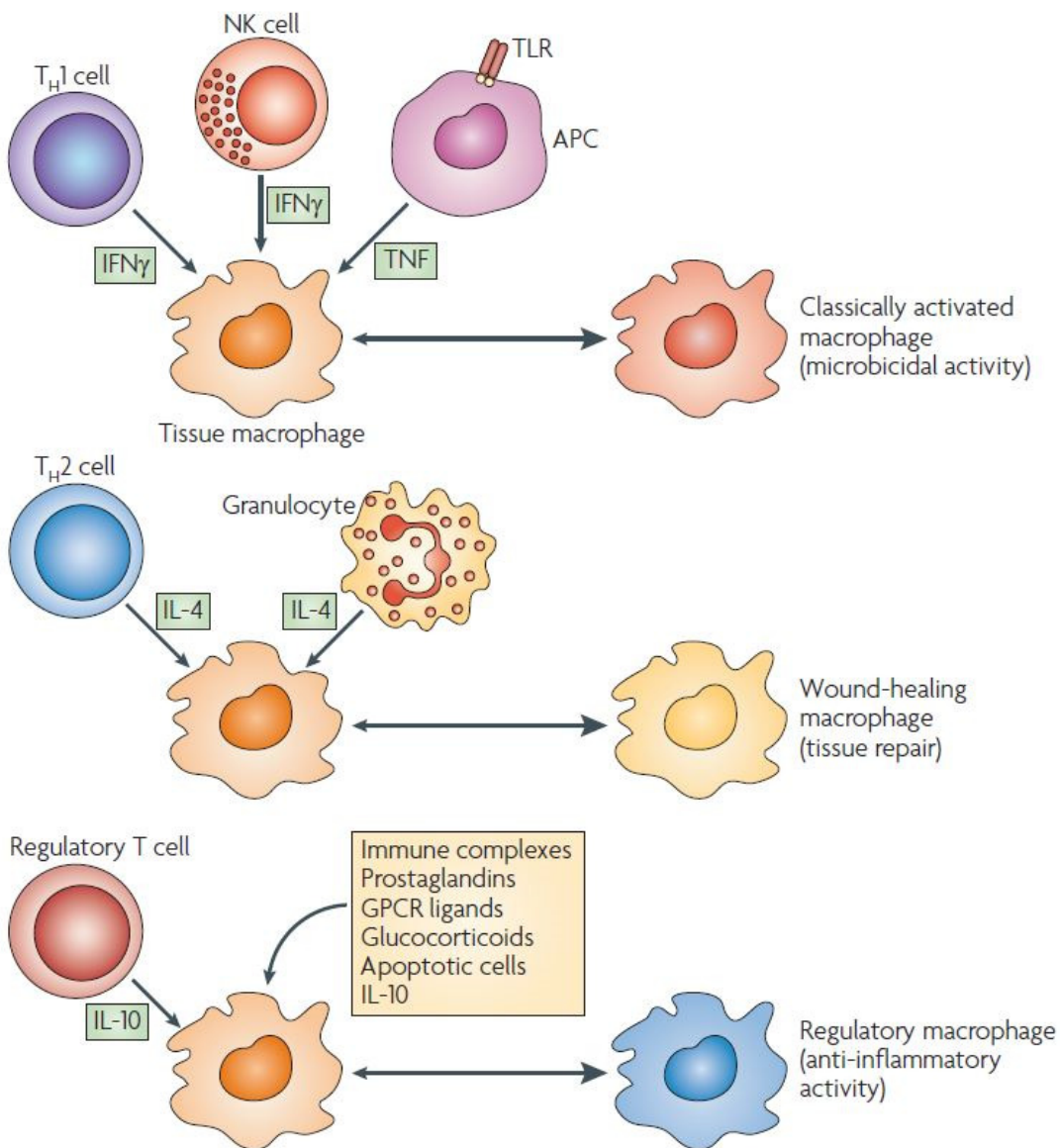


**Figure 1.1. Cytokine mediated macrophage activation.**

Classically activated macrophages are generated from  $\text{IFN-}\gamma$  and  $\text{TNF-}\alpha$  stimulation.  $\text{IL-4}$  stimulation results in wound-healing (alternatively) activated macrophages. Regulatory macrophages are formed in response to various stimuli including glucocorticoids and  $\text{IL-10}$ . From reference<sup>14</sup>.

Due to the role of  $\text{T}_\text{H}1$ -derived interferon- $\gamma$  in cell-mediated immunity to intracellular infection and of  $\text{IL-4}$  ( $\text{T}_\text{H}2$ ) in extracellular parasitic infection, macrophages were designated analogously as M1 (classic) and M2 (alternative) macrophages. This concept was recently extended to a wider range of immune modulatory mediators and functions<sup>30</sup>.

In addition to classically and alternatively activated macrophages, regulatory macrophages develop in response to various stimuli, including immune complexes, glucocorticoids, apoptotic cells, prostaglandins, G-protein coupled receptor ligands or IL-10 (Figure 1.1). This innate or acquired deactivation of macrophages causes the production of IL-10, which suppresses immune responses and is the most important and reliable characteristic of regulatory macrophages<sup>14</sup>.

Taken together, both innate and adaptive signals can influence macrophage physiology and these alteration allow macrophages to participate in homeostatic processes such as tissue remodeling and wound healing as well as in host defense. However, each of these alterations can have potentially dangerous consequences and must be appropriately regulated.

### **1.3. Antigen processing and presentation**

The efficiency of T cell-mediated adaptive immune responses depends on the ability of antigen presenting cells, such as macrophages, to display peptide and MHC complexes on their surface<sup>31</sup>. MHC molecules are divided into MHC class I and MHC class II, where the former presents peptides at the cell surface to CD8+ and the latter to CD4+ T cells. MHC class I and II also differ by the structure of the groove where antigenic peptides are bound. The antigen-binding groove of MHC class I molecules is closed at each end, resulting in the binding of peptides with a defined length (8-10 amino acids)<sup>32</sup>. In contrast, the antigen binding groove of MHC class II molecules has open ends, permitting the loading of peptides of a more variable length (13-25 amino acids).<sup>33</sup>.

While MHC I complexes are expressed ubiquitously by all nucleated cells and recognized by CD8+ T cells, MHC II molecules are limited to professional APCs such as B cells, macrophages and dendritic cells, and are then recognized by CD4+ T cells.<sup>34</sup> However, MHC class II expression can be induced by IFN- $\gamma$  and other stimuli in non-APCs. Non-APCs can express MHC class II molecules in the absence of co-stimulatory molecules to maintain peripheral tolerance<sup>34</sup>.

Membrane trafficking plays a key role in both endogenous and exogenous antigen processing and presentation (see Figure 1.2). Initially, two segregated pathways of antigen presentation were proposed. Endogenous antigens, including viral proteins

synthesized by infected cells, are degraded in the cytoplasm by the proteasome. The resulting peptides are translocated into the endoplasmic reticulum (ER) lumen by the MHC locus-encoded peptide transporter associated with antigen processing (TAP), where they can be further trimmed and are loaded onto nascent MHC class I molecules<sup>35</sup>. The constitutive 26S proteasome is composed of a 20S core barrel that has protease activity<sup>36</sup> and two 19S caps. It generates the bulk peptides for MHC class I molecules. Two alternative proteasomes exist: the immunoproteasome, which is expressed by many immune cells and the thymus specific proteasome, which is expressed in thymic epithelial cells<sup>37</sup>. Immune cell-specific variants of the proteolytic core are incorporated into the 20S barrel altering the degradation pattern of the proteasome<sup>38</sup>.

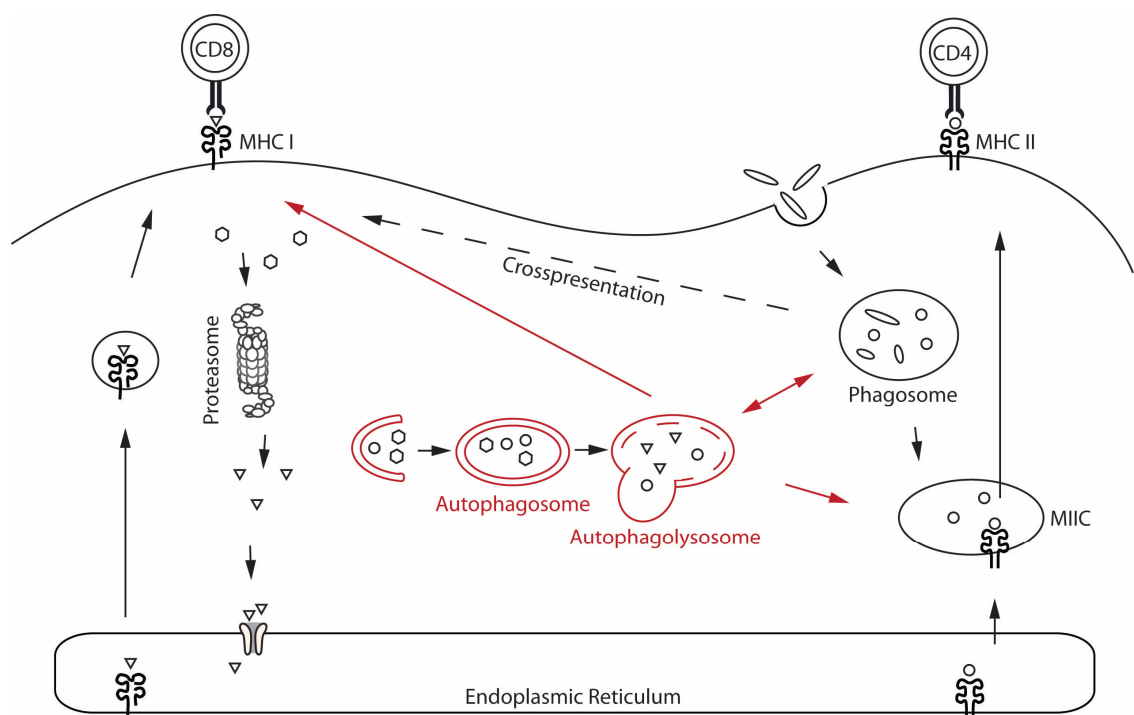


**Figure 1.2. MHC class I and MHC class II antigen processing and presentation pathways.**

Endogenous antigens are degraded in the cytoplasm by the proteasome. The resulting peptides are translocated into the endoplasmic reticulum (ER), where they are loaded on MHC class I molecules and transported to the cell surface to be presented to CD8+ T cells. Exogenous antigens are internalized by endocytosis or phagocytosis, processed by hydrolases, and then loaded onto MHC class II molecules before translocation to the cell surface and presentation to CD4+ T cells. Exogenous antigens can also be presented on MHC class I molecules, a process referred to as cross-presentation. Autophagy contributes to endogenous and exogenous MHC class II antigen processing and presentation by delivering endogenous antigens to MHC class II-containing compartments (MIICs) for lysosomal antigen processing and MHC class II loading of antigens. Autophagy can also contribute to the presentation of endogenous antigens by MHC class I molecules. Endogenous antigens may be transported from the autophagosome to the cytosol to enter the classical pathway, or peptides may be loaded onto MHC class I molecules in the autophagolysosome compartment. Adapted from reference<sup>39</sup>.

In the ER, the MHC class I heterodimer is assembled from a polymorphic heavy chain and a light chain called  $\beta$ 2-microglobulin ( $\beta$ 2m). In order to be stable a peptide in the MHC I binding groove is required. Without peptides, MHC class I molecules are stabilized by ER chaperone proteins such as calreticulin, ERp57, protein disulfide isomerase and the chaperone tapasin. Tapasin interacts with TAP, thus coupling peptide translocation into the ER with peptide delivery to MHC class I molecules. The complex of TAP, tapasin, MHC class I, ERp57 and calreticulin is known as the peptide loading complex (PLC)<sup>34</sup>. Peptides may bind to MHC class I molecules directly or may need further trimming by ER aminopeptidase associated with antigen processing (ERAAP). When peptides bind to MHC class I molecules, the chaperones are released and fully assembled peptide-MHC class I complexes leave the ER and are transported to the cell surface through the secretory pathway (Figure 1.2) for presentation to CD8+ T cells<sup>35, 40</sup>. Peptides and MHC class I molecules that fail to bind are transported back into the cytosol and degraded by the ER-associated protein degradation system (ERAD)<sup>41</sup>.

In contrast, exogenous antigens are internalized by endocytosis or phagocytosis, processed by hydrolases in lytic endovacuolar compartments and the resulting peptides loaded onto MHC class II molecules. The transmembrane  $\alpha$  – and  $\beta$  chains of MHC class II are assembled in the ER and associate with the invariant chain (Ii). The resulting Ii-MHC class II complex is transported to a late endosomal compartment termed the MHC class II compartment (MIIC). Here Ii is cleaved, leaving a residual class II associated Ii peptide (CLIP) in the peptide binding groove of the MHC class II heterodimer. In the MIIC, MHC class II molecules require HLA DM (H2-M in mice) to enable the exchange of the CLIP fragment for a specific peptide derived from the degradation of exogenous proteins in the endosomal pathway. MHC class II molecules are then translocated to the cell surface for presentation of their cargo to CD4+ T cells (Figure 1.2).<sup>34</sup>

Although initially thought to be strictly segregated, these two pathways were revisited to account for the cells' ability to present exogenous antigens on MHC class I molecules, a process referred to as cross-presentation (Figure 1.2)<sup>42</sup>. Different models have been proposed for the cross-presentation pathway. In the phagosome to cytosol model, antigens internalized by phagocytosis are transported across the phagosome membrane into the cytosol, where they can be further processed by the proteasome and enter the classical processing pathway for MHC class I presentation<sup>43</sup>. In the phagosome to cytosol to phagosome model, peptides are loaded on MHC class I molecules in the phagosome

itself. This model involves two transmembrane transport steps of the phagocytosed antigens<sup>44, 45</sup>. The first step transports peptides into the cytoplasm where antigens are further trimmed by the proteasome. The second step enables the re-entry of the processed antigens in the phagosome lumen through TAP<sup>44-46</sup>. It was recently shown that antigenic peptides that bind to MHC class I molecules can also be generated by proteases in the lumen of vacuolar organelles hence avoiding the detour to the proteasome in the cytosol. These peptides are directly loaded on the MHC class I complexes in the "vacuolar pathway"<sup>47</sup>. While the contribution of the endo-phagocytic pathway to the processing of exogenous antigen for MHC class I and II antigen presentation has been recognized for several years, it has been shown only very recently that endogenous and exogenous antigens can also be taken up by autophagosomes and presented on both MHC class I and MHC class II molecules, thus making autophagy an emerging immunological paradigm (see chapter 1.4.6.2 for more details)<sup>48</sup>.

## 1.4. Autophagy

A constant balance between biosynthetic and catabolic processes is crucial for cellular homeostasis. Eukaryotic cells primarily use two distinct mechanisms for large-scale degradation, the ubiquitin dependent proteasome system (UPS) and autophagy. Proteasome-mediated degradation requires previous ubiquitylation of the cargo, which is then recognized by ubiquitin receptors directing it to the 26S proteasome. The UPS rapidly eliminates proteins to regulate many cellular processes, including signal transduction, cell division and gene expression and is considered to be highly selective. Conversely, autophagy, a highly conserved lysosomal degradation pathway, can degrade almost any cargo including whole organelles. Half a century ago, Christian de Duve coined the term "autophagy" (literally, "self-eating") to describe a process whereby cells digest their cytoplasmic materials within lysosomes<sup>49, 50</sup>. This was based on his discovery of lysosomes in 1955<sup>51</sup>, for which he won the Nobel Prize in Physiology or Medicine in 1974<sup>52</sup>.

Half a decade of research has helped to understand that there is not one autophagic pathway, but at least three primary types of autophagy: macroautophagy, microautophagy and chaperone-mediated autophagy (CMA), which share a common

destiny of lysosomal degradation, but are mechanistically different from one another<sup>53, 54</sup>. Both micro and macroautophagy can be selective or non-selective. During microautophagy, lysosomes engulf cytoplasmic materials by inward invagination of the lysosomal membrane. Chaperone-mediated autophagy, mediated by the chaperone hsc70, co-chaperones, and the lysosomal-associated membrane protein type 2A (LAMP2A), transports proteins across the lysosomal membrane without membrane rearrangements<sup>55, 56</sup>. During classical macroautophagy a phagophore is formed at the phagophore assembly site (PAS). The phagophore subsequently engulfs cytosolic components such as organelles and packages them in a two-membrane-bound compartment called the autophagosome. The autophagosome subsequently fuses with the lysosome to form the autophagolysosome in which the content is completely degraded and the resulting macromolecules are released back into the cytosol for reuse (Figure 1.3)<sup>56</sup>.

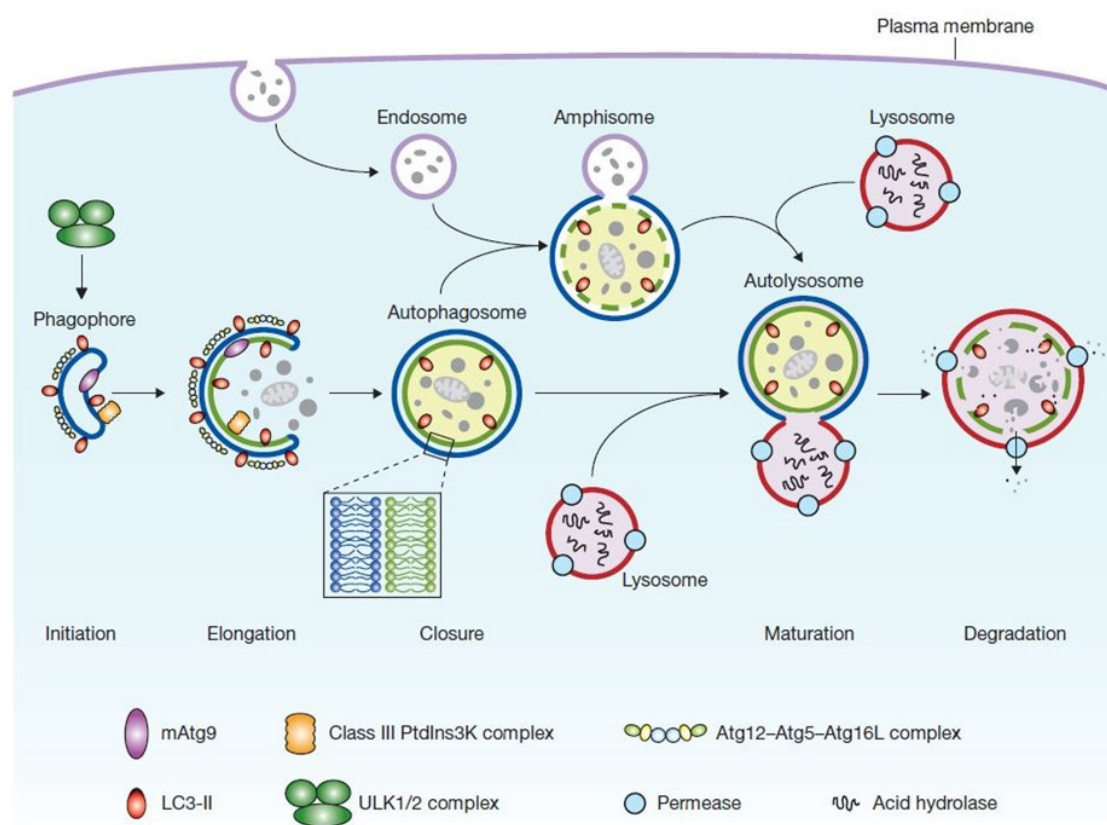


**Figure 1.3. Autophagy pathway.**

Mammalian autophagy proceeds through a series of steps. Upon several, yet unknown signals the phagophore is formed. The phagophore subsequently engulfs cytosolic components such as organelles and packages them in a double-membrane autophagosome. Autophagosome maturation proceeds via fusion with an endosome and/or lysosome, followed by breakdown and degradation of the autophagosome inner membrane and cargo, and recycling of the resulting macromolecules. The core molecular machinery is also shown. Adapted from reference<sup>56</sup>.

### 1.4.1. Molecular regulation of autophagy and the autophagy pathway

Although autophagy was first identified in mammalian cells approximately half a century ago, the transition from morphology to molecular mechanisms only started in the last decade mainly based on the discovery of autophagy related (ATG) genes initially identified in yeast<sup>57</sup>. Mammalian homologs were found soon after<sup>58</sup>. Among these ATG genes, one subgroup comprised of approximately 18 genes is common to the various types of autophagy including non-selective macroautophagy and mitophagy. The corresponding gene products of this subgroup are crucial for autophagosome formation and are thus referred to as the core autophagy machinery<sup>59, 60</sup>. There are four different functional subgroups: (1) the Atg1/unc-51-like kinase (ULK) complex (Atg1, Atg11, Atg13, Atg13, Atg17, Atg29 and Atg31), which plays a role in the initial induction of autophagosome formation; (2) the transmembrane protein Atg9 and associated proteins (Atg2, Atg9 and Atg18), which regulates membrane recruitment to the elongating phagophore after the association of the Atg1 complex at the PAS; (3) the class II phosphatidylinositol 3-kinase (PtdIns3K) complex (Vps (vacuolar protein sorting) 34, Vps15, Vps30/Atg6, and Atg14), which plays a role during vesicle nucleation and is implicated in the targeting of phosphatidylinositol-3-phosphate (PtdIns3P)-binding proteins to the PAS; and (4) two ubiquitin like (UBL) conjugation systems: the Atg12 (Atg5, Atg7, Atg10, Atg12 and Atg16) and Atg8/LC3 (Atg3, Atg4, Atg7 and Atg8) conjugation system, which function in vesicle expansion<sup>61, 62</sup>.

Mammalian autophagy is regulated by the serine/threonine protein kinases ULK1 and ULK2 (mammalian homologues of the yeast autophagy-related protein (Atg1)) and the lipid kinase activity of PtdIns3K Vps34 (Vps-34 in yeast) associated to Beclin 1 (mammalian orthologue of yeast Atg6) and Atg14-like protein (Atg14L). ULK1, ULK2 and the Vps34-Beclin 1-ATG14L complex integrate upstream signaling pathways (see chapter 1.4.4.) and activate the downstream Atg conjugation cascade<sup>62, 63</sup>. Two ubiquitin-like systems regulate autophagosome formation and closure, conjugating three UBL proteins (Atg12, Atg5 and Atg8) to target proteins or membranes<sup>64</sup>. Atg7 and Atg10 exert the conjugation of Atg12 to Atg5 respectively, which forms a complex with Atg16. A complex of Atg12-Atg5-Atg16 together with Atg3 controls conjugation of Atg8 (processed by Atg4) to phosphatidylethanolamine (PE) on the isolation membrane<sup>64</sup>. Although these two UBL systems are dependent on each other, they have distinct functions. The Atg12-Atg5-Atg16 complex localizes transiently to the outer membrane of the PAS. However,



Atg8-PE (also called microtubule-associated protein 1A/1B-light chain 3 (LC3)-II) persists throughout the early phase of formation, cargo sequestration and fusion to the lysosome and is thus often used as marker of autophagic flux<sup>65</sup>.

Together with other components lipidated mammalian homologs of Atg8 serve to assemble, elongate and close the autophagosome. The UBL protein conjugation systems are highly conserved from yeast to mammals. One of the main differences is the existence of multiple homologs of yeast Atg8 in mammals. Two subfamilies of at least seven Atg8 proteins exist: the LC3 proteins LC3a, LC3b, and LC3c, and GABARAP ( $\gamma$ -amino butyric acid receptor-associated protein), GABARAPL1 and GABARAPL2. LC3 plays an important role during phagophore elongation, while GABARAP proteins act at a later stage of maturation. In mammals LC3b is the most prevalent and well-established autophagosome marker<sup>66</sup>.

#### **1.4.2. Signaling pathways regulating autophagy**

Autophagy is regulated by a complex signaling network of diverse stimulatory and inhibitory signals (Figure 1.4). The target of rapamycin (TOR), a highly conserved serine/threonine protein kinase that senses growth factors, nutrients and energy levels, acts as a 'master regulator' of autophagy<sup>67</sup>. TOR occurs in two distinct complexes, TORC1 (target of rapamycin complex 1) and TORC2 that are conserved from yeast to mammals. TORC1 is mainly implicated in autophagy regulation. mTORC1 (mammalian TORC1) is sensitive to rapamycin, which in many conditions induces autophagy. mTORC1/TOR plays a central role in autophagy by integrating the class I PtdIns3K signaling and amino acid-dependent signaling pathways. Activation of growth factor receptors activates the class I PtdIns3K complex and small GTPase Ras, leading to activation of the PtdIns3K-PKB (PtdIns3K-protein kinase B)-TOR pathway and the Raf-1-MEK (Dual specificity mitogen activated protein kinase kinase) 1/2-ERK (extracellular signal-regulated kinase) 1/2 pathway, respectively. PKB and ERK1/2 cause the phosphorylation and inhibition of the tuberous sclerosis complex 1/2 (TSC1-TSC2), resulting in the stabilization of Rheb GTPase, which subsequently activates mTORC1, hence inhibiting autophagy. Activated ERK1/2 also induces autophagy. Amino acids inhibit the Raf-1-MEK1/2-ERK1/2 signaling cascade, hence antagonizing autophagy. High adenosine monophosphate (AMP):adenosine triphosphate (ATP) ratios caused by

metabolic stress and low energy levels, cytokines or increased cytosolic  $\text{Ca}^{2+}$  concentrations, lead to the phosphorylation of the AMP-activated protein kinase (AMPK) and activation by LKB1 (Liver kinase B1). AMPK phosphorylates and activates TSC1/TSC2, causing inactivation of mTORC1/TOR and autophagy induction<sup>56, 60</sup>.

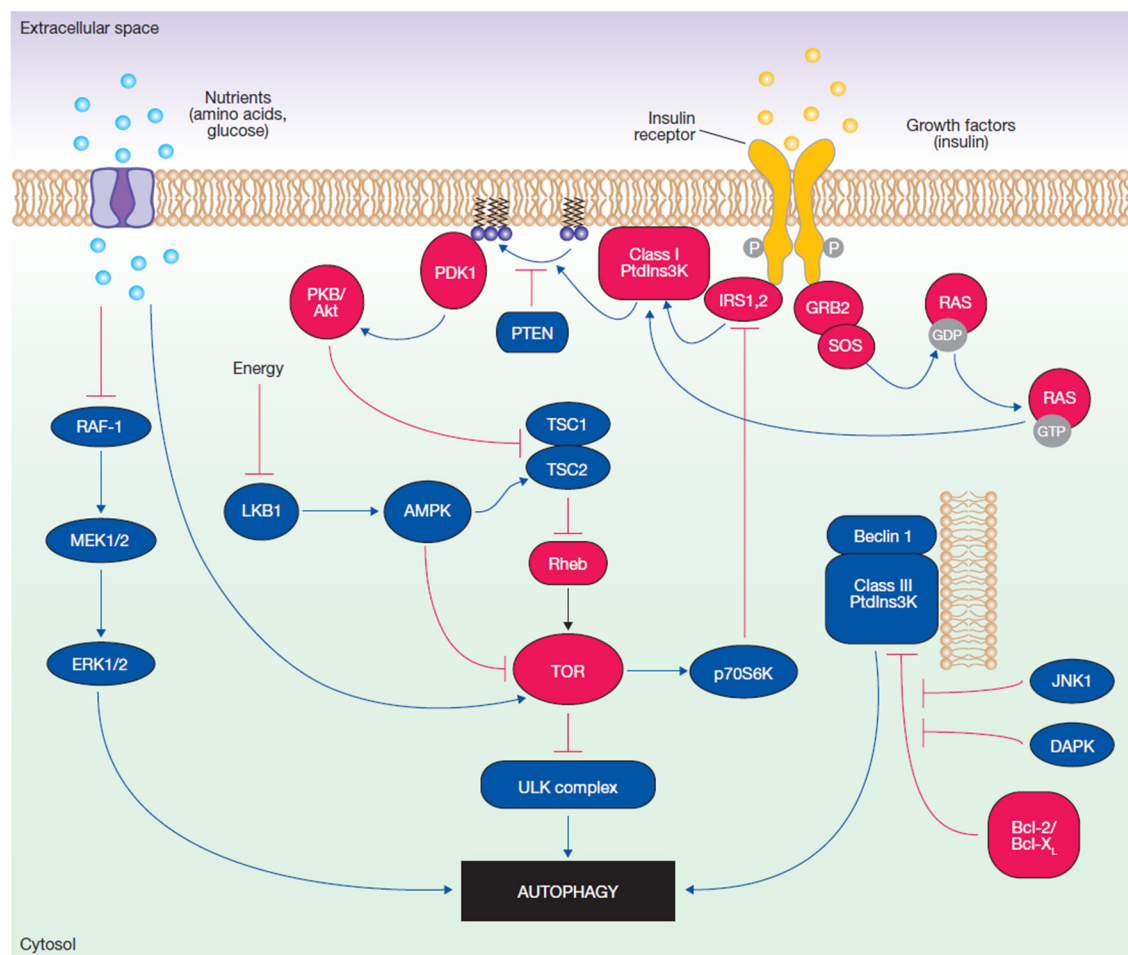


**Figure 1.4. Signaling pathways regulating autophagy.**

Complex signaling events are involved in autophagy regulation including stimulatory (blue arrows) and inhibitory signals (red bars). Blue elements in the figure stimulate autophagy, whereas red elements inhibit autophagy. TOR is a key regulator of autophagy induction. From reference<sup>68</sup>.

TOR-independent autophagy pathways do also exist. Phosphorylation and interruption of the interaction of anti-apoptotic proteins, Bcl-2 (B-cell lymphoma-2) and Bcl-XL with Beclin 1 by the stress-responsive c-Jun amino terminal kinase (JNK1) and death-associated protein kinase (DAPK) stimulates the phagophore-bound Beclin 1-associated class III PtdIns3K complex and induces autophagy<sup>69, 70</sup>. Pharmacological stimulation of autophagy can be achieved by inhibiting negative regulators such as TOR with rapamycin<sup>71</sup>. Targeting the class III PI3K implicated in autophagosome formation with 3-

methylenadenine (3-MA) or Wortmannin inhibits autophagy. Inhibition can also be executed by targeting autophagosome maturation, using inhibitors of the lysosomal proton pump inhibitors such as bafilomycin A1 or lysosomal alkalines such as chloroquine and 3-hydroxychloroquine<sup>71</sup>. It is noteworthy that all these pharmacological treatments are not specific for the autophagy pathway. Consequently, genetic inhibition of autophagy via knockout of ATG genes or knockdown by shRNA (short hairpin ribonucleic acid) resulted in more conclusive information about the biological functions of autophagy in health and disease<sup>72</sup>.

#### **1.4.3. Origin of the autophagosomal membrane**

The source of the isolation membrane that forms the autophagosome has been eagerly debated<sup>39</sup>. The endoplasmic reticulum (ER), mitochondria, the Golgi apparatus, and the plasma membrane represent potential candidates (Figure 1.5)<sup>73-78</sup>. Recent research indicates that several more or less different autophagy pathways exist, using a different source of membrane. While Atg5-dependent macroautophagy might recruit its membrane from the ER<sup>75</sup>, a novel pathway that employs Rab9 but not Atg5, Atg7 or LC3 might originate from the trans-Golgi network<sup>79</sup>. Another LC3b- and LC3a-positive autophagic pathway that is induced in Herpes Simplex Virus type-1 infected cells even uses the nuclear envelope<sup>80, 81</sup>. Taken together, these data indicate that autophagosomes can be formed by very different molecular pathways. However, regardless of their origin, these vesicles ultimately have to reach a lytic vacuole such as a late endosome or a lysosome in order to degrade their cargo. The different ways autophagosomes can form might reflect a finely tuned and differentially controlled machinery that can react to distinct stimuli and fulfill multiple functions.

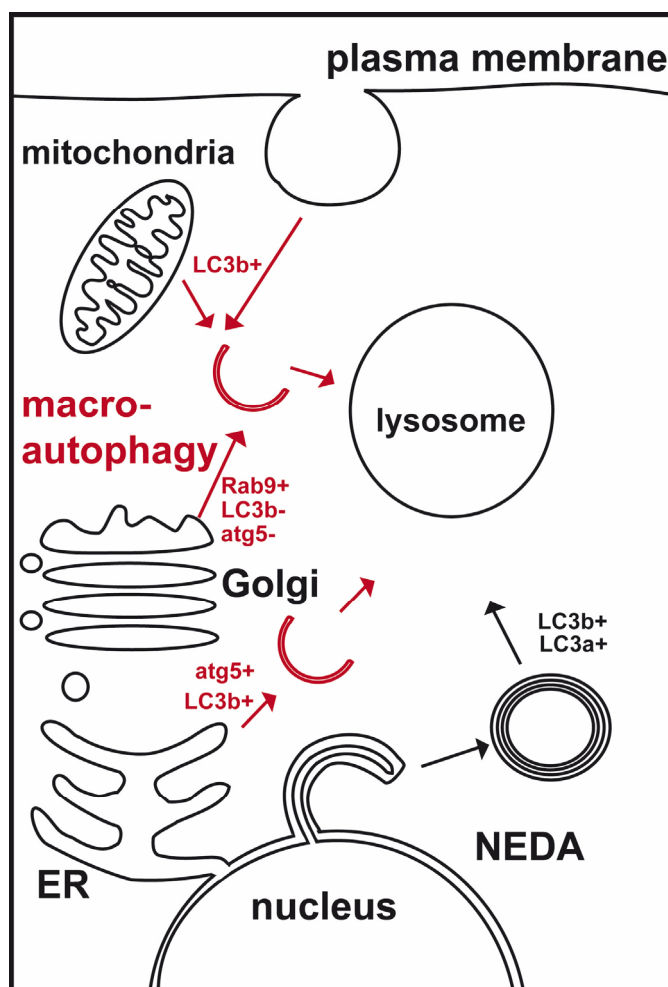


**Figure 1.5. Autophagy mechanisms and potential sources of membrane.**

Distinct mechanisms of autophagy are known. Atg5-dependent macroautophagy might receive its membrane from the ER, while a novel Rab9-dependent pathway might originate from the trans-Golgi network. Another LC3b- and LC3a-positive autophagic pathway that occurs in cells infected with Herpes Simplex Virus type 1 uses the nuclear envelope. Several different cellular compartments contribute to the isolation membrane formed during macroautophagy (red) under different conditions, hence macroautophagy is likely not one uniform pathway. This diversity is further highlighted by differences in the contributing cellular machinery. Adapted from reference<sup>39</sup>.

#### 1.4.4. Selective autophagy

Autophagy was traditionally regarded as a non-selective, bulk degradation process acting as a supplier of energy during starvation. This view has changed strongly during the last decade as several studies suggested that autophagy can be highly selective. The key element of this selectivity is the LC3-interacting motif (LIR), which targets autophagy receptors to LC3 (or other Atg8 family proteins) anchored in the phagophore

membrane<sup>66</sup>. In addition, it emerged that ubiquitin as well as ubiquitin binding proteins (UBPs) play a role in the regulation of selective autophagy<sup>82</sup>. This process refers to the selective degradation of, for example, bacteria (xenophagy), organelles (mitophagy and pexophagy), ribosomes, macromolecular structures, specific proteins and protein aggregates (aggrephagy) by autophagy. During selective autophagy the cargo is recruited to the membrane of the growing phagophore by autophagy receptors that associate with the cargo and with lipidated Atg8/LC3-II via the LIR motif. The phagophore elongates and sequesters the selective cargo to form the double-membrane autophagosome. Fusion of the autophagosome with lysosomes (maturation) forms autolysosomes where the cargo is degraded<sup>66</sup>.

Atg8 family proteins are the only UBL proteins that have been found to be conjugated to lipids. All Atg8 homologues impact autophagosome formation and fusion; however their individual role as cargo receptors is still not clear. Similarly to the UPS, ubiquitylation also plays a crucial role in selective autophagy. Ubiquitin can form multiple ubiquitin chain types that can be recognized by ubiquitin-binding domains (UBDs). p62 or sequestosome (SQSTM1) was identified as the first selective autophagy receptor<sup>83-85</sup>. It was shown that p62 acts as both a selective autophagy substrate and a cargoreceptor for autophagic degradation of ubiquitylated proteins. Subsequently, the related neighbor of BRCA1 gene 1 (NBR1) was discovered as an aggrephagy receptor<sup>86</sup> and nuclear dot protein 52kDa (NDP52) was found to be a xenophagy receptor<sup>87</sup> together with optineurin<sup>88</sup>. These autophagy receptors target their cargo for autophagic degradation using LIR-motif dependent interactions. The LIR motif has also been called Atg8-family interacting motif (AIM)<sup>89</sup>.

The LIR motif of p62 was revealed by detailed deletion mapping and point mutation analysis together with X-ray crystallography and nuclear magnetic resonance (NMR). All LIR motifs contain a core consensus sequence [W/F/Y]xx[L/I/V]<sup>66</sup>. Acidic or hydroxylated residues (E, D, S or T), either N- or C-terminal to the conserved aromatic residue are also important. Interestingly, LIR-independent interaction involving Atg8 proteins also exist. Behrends et al. identified several LIR-independent Atg8-interacting proteins.<sup>90</sup> Importantly, most identified cargo receptors also contain UBDs such as p62, which contains a carboxy-terminal ubiquitin associated (UBA) domain. This suggests that cargo receptors function as adaptors between ubiquitylated proteins and the autophagic

machinery. Taken together, there are basically three types of selective autophagy those dependent on ubiquitin, the LIR motif or both.

#### **1.4.5. Mitophagy**

Selective autophagy of mitochondria, known as mitophagy, is an important mitochondrial quality control mechanism that eliminates damaged or superfluous mitochondria<sup>91</sup>. The mitochondrion plays an important role in eukaryotic cells. While this organelle provides critical metabolic functions in fatty acid oxidation, the citric acid cycle, and oxidative phosphorylation, it can also cause cell damage<sup>92</sup>. Reactive oxygen species (ROS) are formed as a toxic byproduct of oxidative phosphorylation<sup>93</sup>. ROS result in oxidative damage to mitochondrial lipids, DNA (deoxyribonucleic acid), and proteins, which makes mitochondria even more susceptible to ROS production. Damaged mitochondria hence release high levels of  $\text{Ca}^{2+}$  and cytochrome c to the cytosol inducing apoptosis<sup>94</sup>. Consequently, ensuring proper mitochondrial quality control is critical to cellular survival, and mitochondrial damage has been associated to diabetes, aging<sup>95</sup>, and neurodegenerative diseases<sup>93</sup>. Several mechanisms to eliminate dysfunctional mitochondria and prevent cellular damage have evolved in order to preserve a population of healthy mitochondria. The mitochondria's own proteolytic system can degrade misfolded mitochondrial membrane proteins<sup>96</sup>. In addition to proteolytic and proteasomal degradation, a recent study suggests that a lysosomal pathway exists in which vesicles bud from mitochondria, sequester selected mitochondrial cargo and target those mitochondrial components for lysosomal degradation<sup>97</sup>. These mentioned pathways degrade only a subset of mitochondrial proteins, while during mitophagy an entire mitochondrion is sequestered within a double membrane vesicle, the autophagosome, followed by fusion with the lysosome<sup>91</sup>.

Although mitochondrial turnover and clearance of damaged mitochondria may be the primary function of mitophagy, specialized forms of mitophagy exist. During erythrocyte maturation<sup>98</sup> mitophagy completely degrades mitochondria and mitophagy also selectively removes sperm-derived mitochondria after oocyte fertilization<sup>99, 100</sup>. Although mitochondria can be engulfed non-selectively along with other cytosolic components during bulk autophagy<sup>101</sup>, mitophagy represents a selective autophagy pathways selectively degrading damaged or superfluous mitochondria. Depolarization of

mitochondria with the uncoupler carbonyl cyanide m-chlorophenylhydrazone (CCCP)<sup>102</sup> or photoirradiation<sup>103</sup> causes autophagic clearance of mammalian mitochondria, while other organelles are unaffected.

The selectivity of mitophagy is brought about by several factors. In yeast, the mitochondrial outer membrane protein Atg32<sup>104</sup> targets the core autophagic machinery to mitochondria for their selective removal via binding to Atg8 through the adapter protein Atg11<sup>91</sup>. Atg11 and Atg32 do not have homologs in higher eukaryotes<sup>105</sup>, however functional homologues might exist in mammals. The ubiquitin-binding adapter p62(SQSTM1) for example, is enriched on damaged mitochondria and has been reported to target mitochondria to the autophagosome by binding to Atg8/LC3<sup>106</sup>. Nix (BNIP3L; BCL2/adenovirus E1B 19 kDa protein-interacting protein 3-like), a Bcl-2 related mitochondria outer membrane protein enables the elimination of mitochondria in reticulocytes by mitophagy. Nix is necessary for the sequestration of mitochondria into autophagosomes<sup>98, 107</sup>. Nix contains a LIR motif and might thus function as a receptor to recruit mitochondria to autophagosome<sup>108</sup>. Nix and another BH3-only protein BNIP3 (BCL2/adenovirus E1B 19 kDa protein-interacting protein 3), also play a role in hypoxia induced mitophagy in mammalian fibroblasts<sup>108</sup>.

Recently a pathway mediated by PTEN (phosphatase and tensin homolog)-induced putative protein kinase 1 (PINK1) and the E3 ubiquitin ligase Parkin has emerged as a paradigm for mammalian mitophagy.<sup>91</sup> PINK1 is a serine/threonine kinase that localizes to mitochondria due to its mitochondrial targeting sequence<sup>109</sup>. In healthy mitochondria, PINK1 is imported to the inner mitochondrial membrane, cleaved by several proteases including the mitochondrial processing protease, the TIM (transporter inner membrane) complex-associated protease and the inner membrane presenilin-associated rhomboid-like protease PARL, and finally proteolytically degraded<sup>110-112</sup>. In damaged mitochondria the loss of membrane potential inhibits the import of PINK1 causing the accumulation of intact PINK1 on the mitochondrial outer membrane, where it interacts with the TOM (transporter outer membrane) complex<sup>113</sup>. This functions as a sensor for mitochondrial damage and recruits Parkin from the cytosol to damaged mitochondria<sup>114</sup>. Parkin stimulates mitophagy of damaged mitochondria in several ways. Parkin, causes the degradation of its substrates such as Miro and Mitofusins<sup>115, 116</sup>, which results in mitochondrial fragmentation and arrest of motility promoting the autophagosomal sequestration of mitochondria. Parkin also mediates hyper-ubiquitylation of the

mitochondrial outer membrane, which is recognized by ubiquitin binding adapters such as p62, HDAC6 (Histone deacetylase 6) and unknown others. Their interaction with the autophagosomal protein LC3 might target damaged mitochondria to the isolation membrane<sup>91</sup>. Importantly, parkin-mediated mitophagy is dependent on core components of the autophagic machinery. Inhibiting Atg3, Atg5, Atg7 and class III PI3K prevents degradation of CCCP treated mitochondria<sup>102</sup>.

There are still several open questions with regard to the initiation of mitophagy and autophagosome formation. It also still needs to be elucidated how different stimuli initiate the mitophagy cascade and how distinct the mitophagy pathways induced by different stimuli or conditions are. The existence of multiple mitophagy pathways likely represents distinct control mechanisms for the regulation of fast responses to damaged mitochondria, constitutive turnover of mitochondria, changes to mitochondrial status with nutrient accessibility, and highly specialized developmental requirements<sup>91</sup>.

#### **1.4.6. Autophagy in infection and immunity**

Autophagy contributes to both innate and adaptive immunity against many pathogens. Different bacteria and viruses interact in various ways with the autophagic machinery, both to elicit an immune response as well as to evade it. Autophagy contributes to antimicrobial immunity in direct ways by the xenophagic degradation of intracellular pathogens as well as in indirect ways by the modulation of effector cell activation in adaptive immunity<sup>39</sup>.

##### **1.4.6.1. Xenophagy**

Probably the most direct way to fight microbial infection is by degradation of the invading pathogen itself. Xenophagy, an autophagic pathway that specifically targets invading microorganisms and facilitates their lysosomal degradation can exert this defensive strategy. There are various mechanisms of xenophagy and they depend mostly on the subcellular localization of the pathogen<sup>117</sup>. Cytosolic pathogens can be taken up by a phagophore similar to macroautophagy. Pathogens that are internalized via phagocytosis and remain inside the phagosome can be degraded once autophagic proteins (e.g. LC3 or Atg5) are targeted to their phagosomal membrane. These



components then facilitate fusion of the phagosome with lysosomes, without the formation of a new vesicle.<sup>118</sup> However, the life cycle of many pathogens includes both vacuolar and cytosolic stages, hence these autophagic processes are not mutually exclusive.<sup>119</sup> In addition to eliminating invading pathogens, xenophagy might contribute to the adaptive immune response by generating peptides for antigen presentation, and perhaps also by limiting tissue damage caused by a strong pro-inflammatory response<sup>117, 119-121</sup>.

In contrast to some other forms of autophagy, xenophagy is highly selective. The substrate specificity is achieved by at least three different mechanisms: (A) selective ubiquitylation of pathogens is followed by binding to an adaptor protein like p62/sequestosome, NDP52 or optineurin that in turn links the ubiquitylated pathogens to LC3 and thus the nascent xenophagic vesicle; (B) a direct interaction between pathogenic proteins and the autophagic machinery, as is the case for *Shigella* IcsA binding to Atg5; and (C) an interaction between the autophagic machinery and pathogens is mediated by pattern recognition receptor signaling, such as TLR or cytosolic pattern recognition receptor signalling<sup>39, 119, 120</sup>.

#### **1.4.6.2. Autophagy and antigen presentation**

The first indication that autophagy contributes to antigen presentation was derived from studies of endogenous MHC II antigen presentation (Figure 1.2)<sup>122-124</sup>. MHC II presentation of cytosolic neomycin phosphotransferase antigen in Epstein Barr virus transformed cell lines was found to be greatly reduced when autophagy was inhibited.<sup>122</sup> The nuclear antigen 1 of Epstein Barr virus was also degraded in the lysosome, and inhibition of autophagy decreased the presentation of this antigen on MHC II complexes<sup>123</sup>. An analysis of the MHC class II immunopeptidome in different culture conditions revealed that starvation-induced autophagy shifts the pool of MHC II ligands towards a more frequent display of intracellular peptides, including the autophagy protein LC3<sup>125</sup>. This enrichment for cytosolic epitopes suggests that enhancing autophagy or targeting of antigens to autophagosomes by LC3 could increase MHC II antigen presentation. In addition to macroautophagy, a recent study has shown that chaperone-mediated autophagy can also lead to MHC class II presentation of cytosolic self antigens<sup>126</sup>.

In addition to contributing to endogenous MHC II antigen presentation, autophagy is also implicated in MHC II presentation of exogenous antigens (Figure 1.2). Several studies showed that macroautophagy or particular components of its molecular machinery contribute to efficient delivery of extracellular viral or bacterial antigens to lysosomes for their processing. Cells may capture exogenous antigens either by forming autophagosomes *de novo* or by recruiting components of the macroautophagy machinery directly to the phagosomal membrane<sup>127-129</sup>. TLR signaling also links the autophagy pathway to phagocytosis via LC3-associated phagocytosis (LAP)<sup>130</sup>. While the link between autophagy and antigen presentation on MHC II is well established, the contribution of autophagy to MHC I presentation is much less understood. Autophagy does contribute to MHC class I presentation of endogenous viral peptides in infected macrophages (Figure 1.2)<sup>80</sup>. Macroautophagy is also required for the TAP -independent antigen processing of another endogenous viral protein that is presented on MHC class I molecules<sup>131</sup>.

The contribution of autophagy to MHC class I cross presentation is complex. One report showed that autophagy does not affect MHC I cross-presentation in dendritic cells<sup>129</sup>, whereas two other studies show enhanced cross presentation of viral and tumor antigens upon macroautophagy induction in antigen donor cells<sup>132, 133</sup>. The latter observations suggest that autophagosomes serve as effective vehicles for the delivery of exogenous antigens to the cross-presentation pathway in antigen donor cells. In addition, a recent study suggests that autophagy participates in the cross presentation of nanoparticle-associated OVA antigen and proposed that cross presentation occurs in the autophagosome itself<sup>134</sup>. In addition to antigen delivery and processing, autophagy may also traffic MHC I complexes between the plasma membrane and intracellular compartments. In particular, inhibition of autophagy enhances the surface expression of MHC I molecules<sup>135</sup>.

In conclusion, autophagy modulates both MHC class I and class II antigen processing and presentation (Figure 1.2) as well as MHC I shuttling. Furthermore, macroautophagy can promote antigen processing not only by directly enhancing phagosome maturation, but also by delivering hydrolases to the lysosome<sup>136</sup>. Thus, autophagy plays a key role for the regulation of a dynamic adaptive immune response against both intracellular and extracellular pathogens<sup>39</sup>.

#### 1.4.6.3. Cross-talk between autophagy and cytokines

Most of our current knowledge of the impact of cytokines on autophagy / xenophagy comes from studies of the macrophage response to *Mycobacterium tuberculosis*. Xenophagy aids macrophages to overcome the phagosome maturation block induced by mycobacteria and to clear the vacuolar pathogen<sup>137, 138</sup>. Macrophage activation with IFN- $\gamma$  promotes maturation of mycobacteria-containing phagosomes, and the IFN- $\gamma$  inducible GTPase Irgm1 is essential for this protective response<sup>139, 140</sup>. Moreover, IFN- $\gamma$  induces autophagy in macrophages in an Irgm1-dependent manner (Figure 1.6)<sup>137, 138</sup>. The mechanism by which autophagy contributes to IFN- $\gamma$ -induced phagosome maturation in macrophages infected with *M. tuberculosis* is not yet fully understood and needs further research.

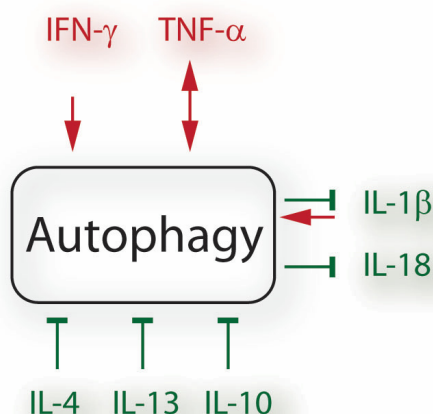


**Figure 1.6. Cross-talk between autophagy and cytokines.**

While cytokines such as IFN- $\gamma$ , TNF- $\alpha$  and IL-1 $\beta$  promote autophagy, IL-4, IL-13 and IL-10 inhibit it. In turn, autophagy also antagonizes the secretion of IL-1 $\beta$  and IL-18 and positively regulates the secretion of TNF- $\alpha$ . From reference<sup>39</sup>.

Remarkably, IFN- $\gamma$  does not stimulate autophagy in all conditions. For example, IL-1 $\beta$  treatment of macrophages infected with Herpes Simplex Virus type 1 increases autophagy and enhances the CD8<sup>+</sup> T cell response to a viral antigen, but IFN- $\gamma$  treatment does not<sup>80</sup>.

TNF- $\alpha$ , another major pro-inflammatory cytokine, plays an important role in the protective immune response to *M. tuberculosis*. In particular, TNF- $\alpha$  is central for the formation and maintenance of granulomas, organized structures of macrophages and highly differentiated cells comprised of foamy cells surrounded by a rim of lymphocytes that are

a hallmark of tuberculosis infection<sup>141</sup>. TNF- $\alpha$  stimulates autophagy in several cell types (Figure 1.6)<sup>142-147</sup>. In turn, autophagy arms these host cells to clear *Toxoplasma gondii*<sup>142, 144</sup>.

While pro-inflammatory cytokines such as IFN- $\gamma$  and TNF- $\alpha$  induce autophagy, IL-4 and IL-13 antagonize it (Figure 1.6)<sup>148</sup>. For example, IL-13 is a potent inhibitor of starvation-induced autophagy in HT-29 epithelial cells<sup>149, 150</sup>. In the context of infection by *M. tuberculosis*, both IL-4 and IL-13 inhibit starvation- or IFN- $\gamma$ -induced autophagy, hence decreasing phagosome maturation and enhancing intracellular survival of the bacteria<sup>151</sup>. Accordingly, modulation of autophagy by cytokines and by pathogens may represent an important battleground in the evolutionary arms race between the host and mycobacteria<sup>152</sup>.

IL-10 also inhibits rapamycin or starvation induced autophagy in murine macrophages (Figure 1.6)<sup>153, 154</sup>. Consequently, since IL-10, IL-4 and IL-13 are mostly secreted by macrophages and lymphocyte subsets, cytokine-mediated regulation of autophagy by leukocytes might influence the specific immune responses to infectious pathogens.

Interestingly, autophagy can also directly control the transcription, processing and secretion of a number of cytokines<sup>148</sup>. IL-1 $\beta$  and IL-18 release is increased when autophagy is inhibited. It was also shown that autophagy is implicated in the regulation of TNF- $\alpha$  secretion by macrophages and dendritic cells (Figure 1.6). In particular, inhibition of autophagy with 3-methyl adenine causes a marked decrease of TLR-dependent secretion of TNF- $\alpha$ <sup>155</sup>.

These results illustrate an extensive crosstalk between autophagy and cytokines. A variety of mechanisms contribute and the degree of integration between these defense pathways depends on multiple factors, including specific receptors and cell types. Autophagy hence potentially represents a key therapeutic target for the regulation of immune responses and inflammation<sup>39</sup>.

#### **1.4.6.4. Autophagy and viral infection**

Autophagy plays a crucial role in the host defense against viral infection, coordinating pathogen degradation (xenophagy), innate immune signaling and aspects of adaptive immunity<sup>156</sup>. To survive and spread within the host, viruses have developed a variety of

strategies to evade autophagy and to exploit the autophagy machinery for their own benefit<sup>156</sup>. During coevolution of viruses and eukaryotes, long-term mutual adaptations resulted in a very complex interplay between autophagy and viruses<sup>55, 157</sup>.

Herpes simplex virus 1 (HSV1) interacts with autophagy in a complex manner and the interactions are discussed in more detail in chapter 1.5.8. Viral infection stimulates autophagy<sup>158</sup>, however the signals that induce autophagy during viral infection are still largely unknown. During viral infection autophagy could be induced by viral entry or replication, viral components, increased energy requirements, unfolded protein responses, and plasma membrane disturbance<sup>156</sup>. Autophagy can have several antiviral effects<sup>156</sup>. Virophagy can degrade cytoplasmic viral components. Virophagy is a form of selective autophagy believed to involve the ubiquitylation of cargo and binding of an adaptor protein to both ubiquitin and LC3. However, it is not clear whether virions can be selectively targeted for autophagy and if so, is virophagy also ubiquitin dependent<sup>156</sup>. Recent studies have established that Sindbis virus nucleocapsids are selectively recruited for autophagic degradation by mechanisms that involve interactions of the nucleocapsids with the well-known adaptor protein p62/SQSTM1, as well as a newly identified adapter protein SMAD ubiquitination regulatory factor 1 (SMURF), an E3 ligase, in an ubiquitin-independent way<sup>159</sup>. Autophagy may also have an antiviral effect by the delivery of viral nucleic acids to endosomal TLRs and hence activate innate immune signaling. TLRs that both recognize viral microbial-associated molecular patterns (MAMPs) and induce autophagy include TLR3 (polyIC/dsRNA) and TLR7 (ssRNA)<sup>160, 161</sup>. The delivery of cytosolic ligands to TLR-containing vesicles may also play a key role for innate recognition of viral pathogens as has been demonstrated for vesicular stomatitis virus and TLR7<sup>162</sup>. Another antiviral function of autophagy is the activation of adaptive immunity by presentation of endogenous viral antigens to MHC class I and MHC class II molecules (as outlined in more detail in section 1.4.6.2.). Finally, autophagy might be antiviral through the regulation of mitochondrial quality control, ROS production and the promotion of cell survival<sup>156, 163</sup>, hence regulating the immune response.

Autophagy can also exert proviral roles<sup>156</sup>. Different viruses have developed various strategies to evade or suppress autophagy degradation and autophagy-mediated immune activation. These viral evasion strategies include the suppression of autophagy initiation, the avoidance of autophagic capture, and the inhibition of autophagosomal maturation<sup>163</sup>. The successful evasion of the antiviral effects of autophagy allows viruses

to manipulate the autophagy pathway and components of the autophagy machinery to facilitate their infection. Dengue virus manipulate lipid metabolism for viral replication via lipophagy<sup>164</sup>. Poliovirus utilize autophagy to promote non-lytic release of virions<sup>165</sup>. Hepatitis C virus (HCV) employ the autophagy machinery to initiate early viral genome replication and also to conceal viral RNA in autophagosome-like double membrane vesicles<sup>166, 167</sup>. Moreover, viruses can exploit autophagy related proteins. Two recent studies on Coxsackievirus B3<sup>168</sup> and Hepatitis B virus (HBV)<sup>169</sup> provide *in vivo* evidence that the Atg5 protein can have proviral functions. Disruption of Atg5 decreases Coxsackievirus B3 replication in the pancreas<sup>168</sup> and liver specific knockout of Atg5 reduces circulating HBV DNA.<sup>169</sup> These *in vivo* studies indicate that for certain viruses inhibition of autophagy might have antiviral effects. However it is not clear whether the *in vivo* phenotypes of Atg5 deficiency on Coxsackievirus B and HBV infection are due to the inhibition of autophagy or the absence of other Atg5-dependent functions. A recent study also proposed that human immunity-related GTPase M (IRGM) and the mouse ortholog Irgm1 may be a common target of RNA viruses that evade autophagy<sup>170</sup>. In this study human IRGM was shown to interact with several core autophagy proteins including Atg5, Atg10 and LC3b as well as with several viral proteins. The precise mechanisms by which viral targeting of IRGM stimulates viral replication remain to be elucidated.

In conclusion, during co-evolution with their hosts, many viruses have developed diverse strategies to evade and manipulate autophagy. Interestingly, even for the same virus, the complex interaction with autophagy can varies depending on the specific cellular target<sup>156</sup>.

## 1.5. Characteristics of Herpes simplex virus type 1

Herpes simplex virus (HSV) or Human herpes virus (HHV) is a human pathogen that infects orofacial mucosal surfaces (HSV1) and genital mucosal surfaces (HSV2). During productive infection, vesicular lesions in the mucosal epithelia are developed, followed by the propagation of the virus to sensory neurons and establishment of a latent infection persisting for the life of the host. Repeated disease at or next to the site of primary infection results from reactivation of dormant virus. Although the common cold sores

caused by HSV1 and the genital herpes lesions caused by HSV2 are not fatal conditions, infections of the cornea (keratitis) or central nervous system (encephalitis) can cause serious pathology, and infection of newborns or immunocompromised individuals can result in severe spread disease<sup>171, 172</sup>.

### 1.5.1. Virion structure

The International Committee on the Taxonomy of Viruses (ICTV) classified HSV1 and HSV2 in the genus *Simplexvirus* in the subfamily *Alphaherpesvirinae* of the family Herpesviridae<sup>171</sup>. HSV is a large (150-200nm diameter) enveloped virus<sup>173</sup> with a virion structure typical for herpes viruses. A mature HSV particle is characterized by four structural elements (Figure 1.7)<sup>174</sup>: 1) a core comprising viral linear dsDNA<sup>175-177</sup> compactly packaged as a torus<sup>178</sup>, 2) an icosahedral capsid, 3) an intermediate phase or 'tegument' and 4) an outer lipid membrane envelope decorated with viral glycoproteins enclosing the structure<sup>179</sup>.

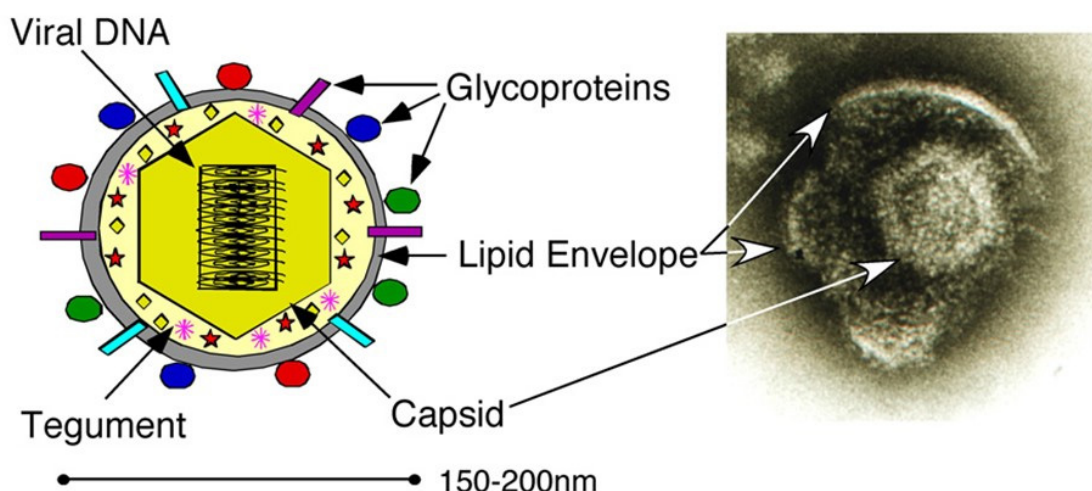


**Figure 1.7. HSV virion structure.**

The HSV1 virion is composed of a tightly packaged viral dsDNA; an icosahedral capsid; a tegument layer comprising various viral proteins; and a glycoprotein-studded lipid membrane envelope. Adapted from reference<sup>171</sup>.

### 1.5.2. Genome organization

The HSV-1 genome, sequenced in 1988, comprises a linear, double stranded DNA of approximately 150,000 base pairs<sup>180, 181</sup>. From this large genome the virus encodes at least 80 gene products<sup>171</sup>. The complex genome contains two covalently linked segments, called Long (L) or Short (S), according to their relative length. Each segment holds unique regions ( $U_L$  or  $U_S$ ) flanked by inverted repeat sequences<sup>182</sup>. There are only single copies of genes present in the unique regions, while genes that are encoded in the repeat regions, such as ICP0 or ICP4, exist in the genome in two copies. Viral genes (and their protein products) are generally named by their relative position from left to right in the  $U_L$  or  $U_S$  region. From the long segments  $U_L$ , 65 viral proteins are expressed, whereas 14 viral proteins are expressed from the short segments  $U_S$ <sup>183</sup>. Many viral proteins are also referred to by alternative names according to their function or properties, for example gB for glycoprotein B, Infected cell protein (ICP) number or Virion Protein (VP) number<sup>171</sup>.

### 1.5.3. Viral life cycle

Productive infection of a cell by HSV follows several key stages including entry, viral gene expression, viral DNA synthesis and assembly and egress of progeny virions<sup>171, 173</sup>. To initiate infection, HSV attaches to at least three different classes of cell-surface receptors and fuses its envelope with the plasma membrane. This process involves the function of several viral envelope proteins, including at least gB, gC, gD and the gH/gL heterodimer<sup>171</sup>. Following fusion, the viral nucleocapsid and tegument proteins are released into the cytoplasm of the host cell. The nucleocapsid and some teguments proteins are then transported to the nuclear pore, through which viral DNA is released into the nucleus. As soon as the viral DNA is in the nucleus, transcription and translation of the viral immediate early (IE) and early (E) genes from the viral DNA begins. In turn, viral DNA is synthesized, viral late (L) genes are transcribed and translated, the capsid is assembled within the nucleus, DNA packaged and finally progeny virions are released.<sup>171</sup>

The pathway of virion egress from an infected cell is still debated. Two pathways have been suggested. In the re-envelopment model<sup>184, 185</sup>, enveloped virions fuse with the



outer nuclear membrane to release free nucleocapsids into the cytoplasm that re-envelope by budding into the Golgi compartment and are subsequently secreted from the cell by vesicles. In the luminal pathway model<sup>186</sup>, enveloped virions migrate in vesicles from the innernuclear space to the Golgi or within the lumen of the endoplasmic reticulum (ER) and are released from the cell via the secretory pathway.

#### **1.5.4. Viral gene expression**

DNA viruses exploit the host cell in many ways to express viral proteins necessary to replicate and propagate. The virus requires the expression of two types of proteins, non-structural proteins essential for viral DNA replication and structural proteins that form the virion and envelope for viral DNA packaging. All viral mRNAs are synthesized by host RNA polymerase II. Herpes viruses are characterized by a temporally regulated gene expression cascade<sup>187</sup>. There are 3 temporal classes of HSV gene expression: immediate early ( $\alpha$ ), early ( $\beta$ ) and late ( $\gamma$ ) genes. Nevertheless, viral gene expression does not take place in distinct stages, but progresses rather gradually. The first genes transcribed during viral infection are the immediate early (IE) genes. IE genes initiate transcription of early (E) genes, whose gene products perform the replication of the viral DNA. Viral DNA replication promotes the expression of the late genes, which encode the structural proteins<sup>171</sup>. IE proteins also promote the transcription of a subset of the late genes prior to DNA replication, called early/late, leaky late or  $\gamma_1$  genes. After the initiation of viral DNA replication<sup>171</sup> a second subgroup of late genes, the true late or  $\gamma_2$  genes, is also transcribed.

During the regulation of gene expression the shutdown of immediate early and early gene expression, which is regulated by ICP4<sup>188-191</sup> and ICP8<sup>192-194</sup> is a key regulatory mechanism. HSV also shuts down host cell RNA, DNA and protein synthesis<sup>195</sup>. HSV seizes these cellular components for its own protein synthesis. HSV achieves this using several mechanisms including the degradation of existing mRNAs<sup>196-198</sup>, by inhibiting RNA maturation<sup>199, 200</sup> or by destabilizing several cellular proteins, especially those involved in the regulation of the host cell cycle<sup>201, 202</sup>.

### 1.5.5. Latent infection

All herpes virus infections are characterized by the development of a latent infection that can last the lifetime of the host. In contrast to a persistent infection, where the virus constantly replicates, during HSV latency, viral progeny are not produced and gene transcription is limited. HSV latent infection is mostly localized in sensory neurons in ganglion tissue, either trigeminal ganglia for HSV1 or sacral ganglia for HSV2. Following the primary infection at an oral or genital mucosal surface, the virus migrates along the innervating neuronal axon to the neuronal cell body<sup>171</sup>. The virus stays in a quiescent state in the neuron and there is no production of lytic gene products. In the latent state, the HSV genome exists in the nucleus of the neuron as circular, extra-chromosomal DNA<sup>203, 204</sup> and only a family of viral RNA transcripts referred to as latency-associated transcripts (LATs) is produced. The virus stays in latency for the life of the host, or until the virus is resuscitated, through specific physical stresses or exposure to ultraviolet radiation<sup>171</sup>, and new progeny are generated, which migrate along the neuron axis to the initial infection site to re-induce a lytic replication cycle<sup>205</sup>.

### 1.5.6. Treatment of HSV infections

The standard therapy for HSV infections constitutes drug treatment with acyclovir, a synthetic acyclic purine-nucleoside analogue<sup>172</sup>. Acyclovir is a prodrug that is processed only in infected cells by the viral thymidine kinase, which phosphorylates, and hence activates the nucleoside analogue drug, which is then incorporated into nascent DNA, where it causes DNA strand termination. There are also precursor drugs currently in use, valaciclovir (converted to acyclovir) and famciclovir (converted to penciclovir), which have better oral bioavailability than acyclovir and penciclovir respectively<sup>206</sup>.

Although, prophylactic vaccination might be difficult to establish as HSV recurs in individuals with humoral and cell mediated immunity<sup>207</sup>, two subunit vaccines have been investigated for therapy and prevention. gB and gD vaccine subunits did not show any prophylactic or therapeutic effect<sup>208</sup>. Potential vaccines include attenuated HSV constructs ( $\gamma$ 34.5 deletion) or disabled infectious single-cycle vaccines, however these constructs require the ability to attenuate a virus that can cause severe mortality if the brain is infected<sup>172</sup>.

### 1.5.7. Viral infection control- Viral evasion

Although the mechanisms leading to the transition from the latency phase to viral reactivation are poorly understood, CD8<sup>+</sup> T cells play a key role in maintaining viral latency<sup>209-212</sup>. CD4<sup>+</sup> T cells also control the infection by promoting the development of cell-mediated immune response carried out by CD8<sup>+</sup> T cells<sup>213</sup>.

During HSV1 infection, viral proteins are degraded by the proteasome to generate peptides that are loaded on MHC class I molecules and presented at the cell surface to stimulate a CD8<sup>+</sup> T cell response. It has been shown that the cytotoxic T cell response to HSV-1 infection in mice is almost entirely directed against a single gB immunodominant epitope corresponding to the peptide SSIEFARL<sup>214</sup>. In fact, more than 50% of the CD8<sup>+</sup> T cells present in infected mice are directed against this single epitope. The other reactive viral epitopes in mice are unknown<sup>215</sup>. A study examining the CD4<sup>+</sup> T cell repertoire in HSV1 infected human patients also detected gB as the most abundantly presented protein, followed by gD, and ICP4<sup>216</sup>. The cellular processes responsible for gB immunodominance are poorly understood, however could represent an immune evasive strategy of the virus. Directing the immune response against a single epitope might result in a limited, inefficient immune response.

The HSV1 virus has developed multiple immune evasion mechanisms. The inhibition of the peptide transporting molecule TAP by the viral protein ICP47 is one of the most well established mechanisms resulting in a strong MHC class I down regulation on the surface of infected cells<sup>217, 218</sup>. HSV1 can also counteract natural killer T (NKT) cell functions by suppression of CD1d recycling<sup>219</sup>. MHC class II presentation can also be blocked by gB, which replaces the invariant chain, thereby preventing binding of antigenic peptides<sup>220, 221</sup>. In addition to inhibiting the adaptive immune response, HSV1 has developed mechanisms to protect itself against the humoral response by bridging the Fc part of antibodies, thereby blocking the antibody's action<sup>222</sup>. HSV1 also established several mechanisms to counteract innate immunity such as the inhibition of the autophagic response to avoid degradation of virions<sup>223</sup>. HSV1 interacts in several additional ways with the autophagy pathway (see section 1.5.8. for more details) and it impedes the interferon-mediated antiviral response<sup>224-226</sup>. Improving our knowledge about these viral immune evasion mechanisms will help us to understand how HSV1 can persist in the body of the host.

### 1.5.8. HSV-1 and autophagy: a complex interplay

The infected cell protein 34.5(ICP34.5), also called  $\gamma$ 34.5<sup>227</sup> is a neurovirulence factor and a potent viral autophagy evasion protein<sup>158</sup>. ICP34.5 contains a GADD homology domain<sup>228, 229</sup> that binds protein phosphatase-1 $\alpha$  (PP1 $\alpha$ ) required for eIF2 $\alpha$  dephosphorylation to reverse host translational shutoff<sup>230</sup>. In addition ICP34.5 contains a Beclin 1 binding domain required for the inhibition of autophagy<sup>223</sup>. ICP34.5 counteracts autophagy by directly targeting Beclin 1 through binding to different regions of Beclin 1<sup>223</sup>. Additionally, ICP34.5 inhibits upstream signals that promote autophagy by reversing protein kinase R (PKR)-mediated eIF2 $\alpha$  phosphorylation<sup>231</sup>. Hence, it seems that ICP34.5 evolved as a multifunctional virulence factor in HSV1 infection. It reverses host cell shutoff through its PP1 $\alpha$  binding domain to ensure viral protein synthesis, and it mediates autophagy evasion through inhibition of PKR signaling and directly antagonizes Beclin 1, which may prevent xenophagic degradation of virions or viral proteins<sup>158</sup>.

#### 1.5.8.1. Nuclear envelope derived autophagy (NEDA)

It was recently described that macroautophagy can contribute to efficient processing and presentation of a viral antigen in murine macrophages during late, but not early stages of HSV-1 infection.<sup>80</sup> Ultrastructural analyses of HSV1 infected macrophages did not only show macroautophagosomes, but also a novel type of autophagosomes that formed at the nuclear envelope and fused with lysosomes.<sup>80</sup>

This novel form of autophagy induced during HSV-1 infection is referred to as nuclear envelope-derived autophagy (NEDA). Remarkably, this autophagic response triggered during HSV1 infection differs in many ways from macroautophagy. This process occurs around 6 hours after infection and leads to the formation of 4-membrane layered structures through coiling from the nuclear envelope where some of the viral proteins, such as gB, are highly abundant.<sup>80</sup> NEDA is characterized by the accumulation of LC3a and LC3b around the nuclear rim. LC3a is a marker for the occurrence of NEDA as it is only detected during NEDA and not during macroautophagy.

NEDA is known to depend on the viral protein ICP34.5. Using mutant viruses, it was shown that NEDA is regulated differently than macroautophagy as binding of Beclin 1 by ICP34.5 had no effect on NEDA. Instead, NEDA is stimulated in response to ICP34.5

binding to protein phosphatase 1 $\alpha$  (PP1 $\alpha$ ). NEDA depends on the expression of late viral proteins and can be inhibited by acyclovir treatment. This suggests that NEDA might be a cellular stress response induced late during HSV-1 infection that compensates for the modulation of the macroautophagy by the virus.<sup>232</sup>

The role of NEDA in the pathogenesis of viral infection, whether it benefits the host or the virus, and how this autophagic process differs from classical macroautophagy is poorly understood. Furthermore, the extent to which this autophagic process is involved in the processing and presentation of viral proteins and peptides remains to be established.

## **1.6. Mass spectrometry-based proteomics**

The field of proteomics, or the study of the full array of proteins expressed by an organism, has become a fundamental tool for molecular and cellular biology. The proteome, in analogy to the genome, is used to describe the entire collection of proteins produced by an organism under a defined set of conditions. In comparison to the genome, the proteome is much more dynamic and complex, constantly changing in response to environmental alterations. A further level of complexity is introduced by the addition of protein post-translational modifications, e.g. phosphorylation or ubiquitylation, an important strategy to influence and modulate protein structure and function. Proteomic profiles of a particular organism, tissue or cell are affected by various environmental stimuli, including those provoked by infectious disease. After the discovery of protein ionization techniques, mass spectrometry has become an indispensable tool in protein analysis and a key technology for proteomics. The ability of mass spectrometry (MS) to identify and quantify thousands of proteins from complex samples impacts broadly on biology and medicine. Mass spectrometry-based proteomics has revolutionized system biology because of its ability to map thousands of proteins and posttranslational modifications (PTMs) in parallel. Systems biology is based on comprehensive data at all molecular levels and mass spectrometry-based proteomics has emerged as a powerful tool, which changed the way in which biological systems are probed.

Numerous experimental strategies and schemes have been devised. A generic shotgun proteomic workflow shown in Figure 1.8 can be divided into (1) sample preparation, (2)

protein and peptide separation, (3) mass spectrometry, and (4) data analysis and allows scientists to put together modular workflows incorporating elements that fit best for a particular biological question<sup>233</sup>.

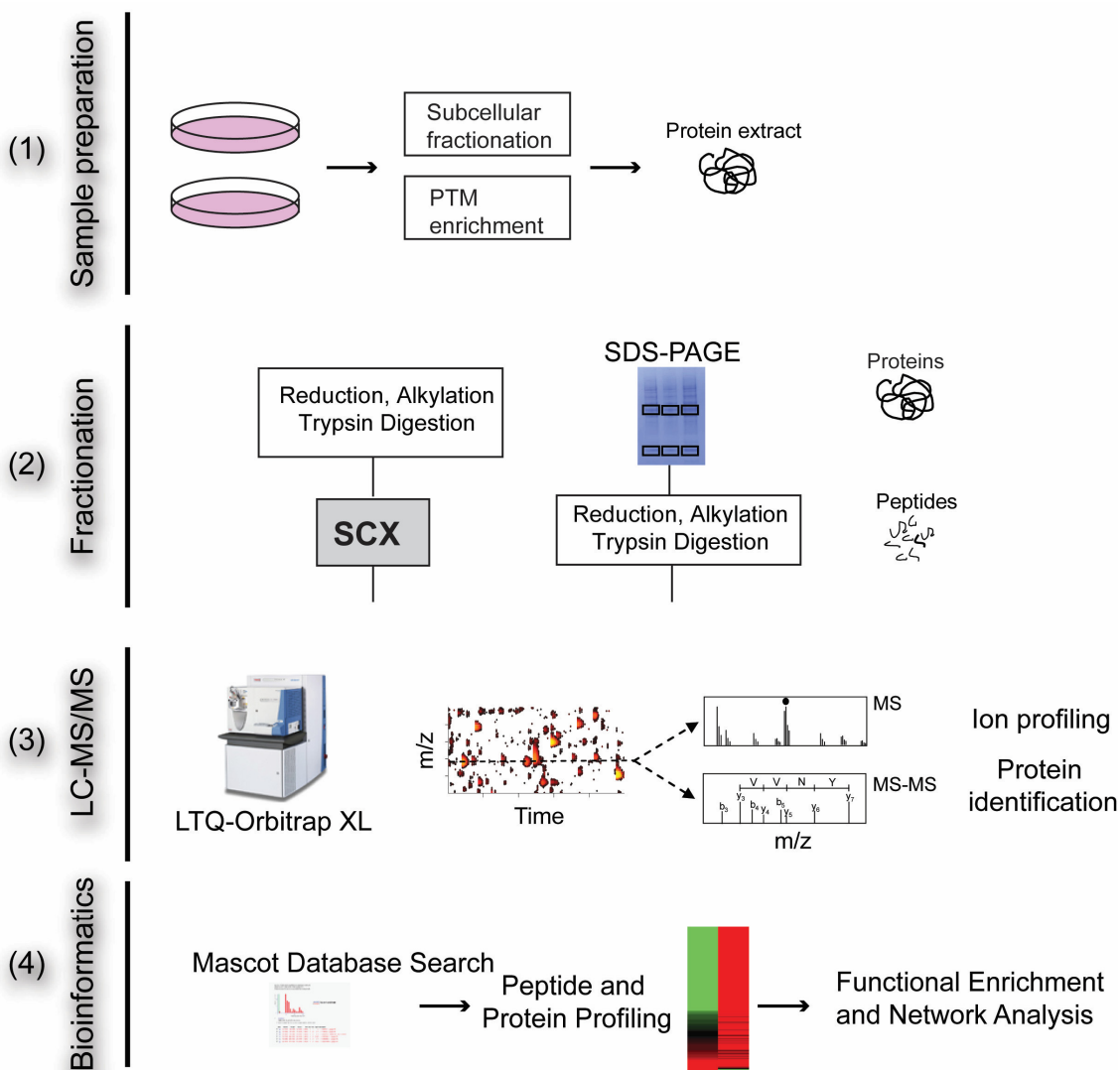


**Figure 1.8. General shotgun proteomics workflow.**

During sample preparation (1), which might include subcellular fractionations or enrichment for post-translational modifications, protein extracts are obtained and subsequently digested with trypsin to obtain peptides. Pre-fractionation at the protein or peptide level (2) such as SDS-PAGE (sodium dodecyl sulfate-polyacrylamide gel electrophoresis) or SCX (strong cation-exchange) fractionation can be introduced. Analysis with liquid chromatography (LC)-mass spectrometry (MS) (3) then results in large datasets of MS and tandem mass spectrometry (MS/MS) data containing quantitative peptide information. Bioinformatics tools (4) such as Mascot are used for peptide and protein identification in combination with quantitative analysis softwares to obtain peptide and protein profiles.

### 1.6.1. Sample preparation

Proteomics can be used to examine various types of input material from prokaryote or eukaryote cells through entire tissues and body fluids. The first step of most sample preparation protocols usually comprises protein extraction from cells or tissues, which can be performed by cell lysis and biochemical fractionation, such as autophagosome isolation, or by affinity selection<sup>234</sup>. The protein content of these samples can be analyzed directly, or depending on the study optional subcellular enrichment, enrichment of PTMs, protein fractionation or affinity purification can be performed. In each condition, in shotgun bottom-up proteomics proteins are digested into peptides (in top down proteomics entire proteins are analyzed)<sup>233</sup>.

In mass spectrometry-based proteomics trypsin is the most popular enzyme used for digestion of proteins into peptides<sup>234</sup>. Trypsin has several advantages for MS-based proteomics. Trypsin has a high cleavage specificity and cleaves peptides C-terminal to arginine or lysine residues. This results in the generation of peptides with a strong-terminal charge in a mass range suitable for effective fragmentation by tandem mass spectrometry (MS/MS). Obtained peptides can be subsequently fractionated to increase the coverage of protein identifications as well as the dynamic range as outlined in more detail below.

### 1.6.2. Separation of proteins and peptides

The analysis of a complex protein samples involves the separation of the proteins or peptides in a sample followed by the identification of the resolved proteins or peptides. There are two main approaches, the gel-based and the gel-free approaches, each involving either single- or multi-dimensional separation of protein extracts. In the gel-based approach one-dimensional sodium dodecyl sulfate-polyacrylamide gel electrophoresis (1D-(SDS)-PAGE) or two-dimensional polyacrylamide gel electrophoresis (2D-PAGE) followed by mass spectrometry are the most widely used methods for protein separation and identification<sup>235, 236</sup>. Proteins can be separated by 1D-PAGE according to their molecular weight (MW), while in 2D-PAGE proteins are first separated by their isoelectric point (pI) and by their molecular weight in a second dimension. Although the resolving power of 2D-PAGE is excellent, the analysis remains

tedious in view of the time requirement for all necessary steps including spot excision, protein digestion and analysis of the corresponding peptides by mass spectrometry. Also, dynamic range and protein solubility issues make the detection and separation of low-abundance and hydrophobic proteins by 2D-PAGE difficult<sup>237-239</sup>. Especially, the analysis of integral membrane proteins remains challenging. In this context, GeLC-MS is more frequently used for the analysis of complex mixtures<sup>234</sup>. This technique is two-dimensional based on a combination of 1D-PAGE, where proteins are digested in gel, peptides are then extracted and separated in the second dimension by Reversed Phase Liquid Chromatography (RPLC). This method is well established and works well with many samples. The relatively large amounts of starting material are sometimes considered a major disadvantage of this approach. The biggest advantage of the approach is the relative ease of use and reduction of the dynamic range of a sample since the proteins are concentrated in one lane and not distributed over multiple fractions as for shotgun approaches discussed below.

The techniques employed for gel-free approaches are shotgun proteomics using 1D-, 2D- or 3D-chromatography coupled online to the MS instrument. The most frequently used chromatographic method for protein and peptide separations is RPLC (Reversed Phase Liquid Chromatography). Here, the analytes are partitioned between a non-polar solid phase, typically made of long alkyl chains chemically bound to silica or polymeric particles packed into a column, and a mobile phase typically water, acid, e.g. acetic acid or formic acid, and a varying portion of organic solvents, such as acetonitrile or methanol. Using C<sub>18</sub> bound columns for peptide separations and C<sub>3</sub>, C<sub>4</sub> or C<sub>8</sub> for proteins, the analytes are separated based on their hydrophobicity. Proteins or peptides are eluted by gradually increasing the amount of the organic solvent, which disrupts hydrophobic interactions and favors the elution of analytes based on their hydrophobicity.

As far as LC separations are concerned there are two major tendencies. The first major tendency in LC separations concerns the RP chromatography system that is directly connected to the mass spectrometer. Long columns (more than 20cm) packed with small particles (3µm or less) and long gradient times (2h or more) are becoming more and more widespread in order to increase peak capacity<sup>240, 241</sup>. The peak capacity is a theoretical measure of the performance of multidimensional separations. The higher the peak capacity, the more peaks can be separated. The second major tendency is the increasing popularity of two-dimensional LC separations. One-dimensional separations



may lack sufficient resolving power to separate all proteins present in complex biological samples or cell preparations. Hence, 2D-chromatography coupled online to MS is often used to achieve better separation and thus improve quantitation accuracy. In this method two independent chromatography and orthogonal phases are commonly used in succession. In addition to a reversed-phase (RP) resin a strong cation-exchange (SCX) resin is typically used. The SCX resin typically consists of negatively charged carboxyl- or sulfate-groups bound to polymeric particles. Peptides are separated based on their charge and fractions are eluted using increasing salt concentrations. Techniques such as strong anion exchange chromatography (SAX)<sup>242</sup> are also gaining popularity to boost the number of identified and quantified proteins in a proteome.

A very useful technique for proteome analysis that may be specifically applied to membrane or organelle proteomics, is the multidimensional protein identification technology (MudPIT) developed by Yates and coworkers in 2001<sup>243, 244</sup>. MudPIT combines multidimensional liquid chromatography with electrospray ionization tandem mass spectrometry. The multidimensional liquid chromatography method integrates a reversed-phase resin, a strong cation-exchange resin and another reversed-phase resin in a triphasic column. The complex peptide mixture is loaded onto the system and the separated peptides are eluted directly off the column and into the mass spectrometer. In the MudPIT approach, the first RP phase guarantees the even application of the sample. Then peptides are systematically separated, depending on the charge in the second dimension (SCX) and hydrophobicity in the third (RP). MudPIT increases peptide separation for mass spectrometry analysis when compared to other techniques. MudPIT has a dynamic range of 10000 to 1 between the most abundant and least abundant proteins/peptides in a complex mixture and has a peak capacity of 23 000<sup>243</sup>. MudPIT is also well established. The increased sample complexity together with reported and experienced reproducibility problems can be considered major disadvantages of the technique. In comparison to GeLC-MS, sample consumption is reduced, which must also be considered advantageous. Two-dimensional LC separations are currently also often used 'off-line' rather than online. The physical separation of the two chromatographic steps allows more flexibility in terms of matching sample quantities and solvents systems between the separation dimensions<sup>245</sup>.

One can summarize that all sample preparation techniques come with advantages and disadvantages and must be considered carefully. For this PhD project, gel-based as well as gel-free approaches were used.

### **1.6.3. Mass spectrometry**

Mass spectrometric measurements are based on the determination of the mass-to-charge ( $m/z$ ) ratio of gas phase ions. All mass spectrometers comprise three main components: an ionization source to create the gas-phase ions, mass analyzer(s) that measures the mass-to-charge ratio ( $m/z$ ) of the ionized analytes, and an ion detector that records the impact of the individual ions.

#### **1.6.3.1. Ionization techniques – Electrospray Ionization**

Electrospray ionization (ESI) and matrix-assisted laser desorption/ionization (MALDI), so called ‘soft ionization’ methods causing the vaporization and ionization of a sample whilst minimizing fragmentation, are the two techniques most frequently used for mass spectrometry analysis<sup>234</sup>. The minimization of fragmentation is especially important for labile, biological molecules, and for the study of complex mixtures, where fragments must not interfere with the mass spectrum when trying to define the original constituents. ESI enables the formation of liquid to gas phase ions and is therefore readily coupled to liquid-chromatography-based separation tools. MALDI sublimates and ionizes the samples out of a dry, crystalline matrix via laser pulses. For the analysis of complex samples integrated liquid-chromatography ESI-MS systems (LC-MS) have emerged as the principal methods of choice today. Since in the current work ESI was exclusively used, this technique will be described in more detail below.

Electrospray involves the dispersion of a solution into electrically charged droplets with subsequent gaseous ion formation. The possibility to create gas phase ions of macromolecules by spraying a solution from the tip of an electrically charged capillary was first recognized by Dole in the 1960s<sup>246</sup>. Yet, the first successful experiments using ESI as a true interface for mass spectrometry of large biomolecules were described by Fenn and co-workers only in 1986<sup>247</sup>. The efforts that lead to the development of electrospray ionization for the analysis of biological macromolecules were awarded with

the attribution of the Nobel Prize in Chemistry to John Bennett Fenn in 2002<sup>248</sup> (shared with Tanaka for his discovery of MALDI<sup>249</sup>, and Wüthrich, who pioneered NMR techniques for biomolecules<sup>250</sup>). In ESI ions are generated at atmospheric pressure by passing a solution-based sample through a small, charged capillary (internal diameter < 250  $\mu\text{m}$ )<sup>251</sup>. The small capillary is at a potential difference to a counter electrode at voltages between +500 and 4,500 V, which depends on both the inner diameter of the needle and the solvents that make up the solution. Generally, higher voltages are necessary for capillaries with larger inner diameters and solvents with higher boiling points.

Electrostatic spraying of a sample solution initially creates an aerosol of charged droplets. Occasionally, mainly at higher flow rates (>5  $\mu\text{L}/\text{min}$ ) a concentric flow of gas, such as  $\text{N}_2$  is employed to facilitate this nebulization process. The resulting field at the capillary tip results in the accumulation of either positive or negative ions on the surface of the emerging liquid. Accordingly, the charged droplets comprising both solvent and analyte molecules have a net positive or negative charge depending on the polarity of the applied voltage. The aerosol is at least partially generated by a process involving the formation of a conical meniscus by the emerging liquid at the tube exit known as a “Taylor Cone”<sup>252</sup>. The “Taylor Cone” is caused by the competition between the surface tension of the liquid and forces owing to the interaction of dipoles in the liquid with the applied field. When the liquid is electrically conducting, a thin jet merges from the tip of the cone. This fine jet breaks up into small, charged droplets, whose diameters are affected by various parameters such as the applied potential, the solution flow rate and the solvent properties. Solvent evaporation shrinks the droplet thereby bringing the surface charges closer together and enhancing the density of charges on the droplet surface to a critical value, the so-called “Rayleigh Limit”, at which the Coulombic repulsion of the surface charges would overcome the surface tension. As predicted theoretically already by Lord Rayleigh in 1882 the resulting instability leads to the disintegration of the droplets into a plurality of offspring droplets.

There are two major competing theories explaining the gas phase ion formation from charged droplets: the charged residue model (CRM) and the ion evaporation model (IEM). Both models assume that sequential evaporation steps followed by droplet fission result in smaller and smaller droplets. In the CRM, which was originally proposed by Dole<sup>246</sup>, this sequence continues until the droplets become so small that each one

contains a single solute molecule. The naked molecule would retain some of its droplets charge to become a free gas ion upon solvent evaporation. The IEM, developed by Iribarne and Thomson<sup>253, 254</sup>, presumes that before ultimate droplets containing only one solute molecule are formed, the field at a droplet's surface intensifies sufficiently to lift a solute ion from the droplet surface into the ambient gas. This means the surface field can release ions from the droplet surface. Irrespective of how the ions are formed, once desolvated, they make their way - directed by the electric field - in to the mass analyzer, where they are separated based on their mass-to-charge-ratio.

Protonation/deprotonation is the main source of charging for biologically relevant ions in ESI. In the positive ion mode (application of a positive capillary potential) the produced protein or peptide ions are protonated on the basic sites within the molecule and ions with the general formula  $[M+nH]^{n+}$  are formed. The multiplicity of protonation is hence correlated to the number of basic amino acid residues in the protein or peptide structure resulted from charge accumulation in the droplets. The generation of multiply charged ions is a hallmark of ESI enabling the use of mass spectrometers with limited  $m/z$  ranges to analyze higher-molecular weight molecules. However, with the increase of charge state, the  $m/z$  becomes lower and the spacing between the isotopomers (peaks due to the presence of other isotopes) is reduced, thereby placing higher requirements on mass spectrometer resolution for proper peak separation.

#### **1.6.3.2. Tandem mass spectrometry (MS/MS)**

The technique of tandem mass spectrometry (MS/MS) is essential for the structural analysis of peptides and proteins. As the name implies MS/MS comprises two stages of MS. In the first stage ions of a selected  $m/z$  are isolated from the rest of the ions originating from the ion source. These ions, termed precursor ions are then activated, leading to the formation of product ions that are subsequently analyzed by the second MS analyzer for sequencing of the peptide. With trap instruments  $MS^n$  experiments are possible, where  $n$  is equal to the number of stages of MS performed.

In discovery proteomics experiments, tandem mass spectrometry (MS/MS) data are usually collected on peptides through automated data-dependent acquisition (DDA). With DDA, mass information on intact peptides in a full-scan mass spectrum ( $MS^1$ ) is used to decide which subset of peptides will be targeted for acquisition of fragmentation (MS/MS)

spectra necessary for sequence identification<sup>255</sup>. Usually “top ten” or “top15” methods are employed, where only the 10 or 15 most intense parent ions in the full scan are selected for fragmentation. An alternative to DDA is data independent acquisition (DIA)<sup>256</sup>. In DIA, MS/MS scans are collected systematically and independently of precursor information.

#### **1.6.3.2.1.      *Dissociation methods for MS/MS***

Ion activation is required to increase the internal energy of the precursor ion and favor its fragmentation. In practice, ion activation and dissociation cannot be separated, consequently ion activation methods are typically referred to as dissociation methods. The internal energy of ions can be enhanced in different ways. The dissociation method almost universally used across all types of mass spectrometers is collision-induced dissociation (CID)<sup>257, 258</sup> also referred to as collisionally activated dissociation (CAD). Recently, also higher energy collisional induced dissociation (HCD)<sup>259, 260</sup> has emerged. HCD provides beam type CID MS/MS with detection of fragment ions at high resolution in the Orbitrap mass analyzer<sup>261</sup>. In addition, there are a few other techniques that can be used. Electron capture dissociation (ECD)<sup>262</sup> and Electron Transfer Dissociation (ETD)<sup>263</sup> are becoming increasingly more widely available.

In linear ion trap based CID the precursor ion collides with a neutral target gas, the so-called collision gas, and a fraction of the kinetic energy of the precursor ion is converted into internal energy. The dissociation is an ergodic process, where the weakest bonds such as backbone amide bonds and post-translational modifications tend to be cleaved off. Low-energy CID (in the range of 1-100 eV) is mostly used in Q-ToF (quadrupole-time-of-flight), LIT (linear ion trap), FT-ICR (Fourier transform ion cyclotron resonance) and Orbitrap instruments<sup>264</sup>. To enhance the efficiency of low-energy CID, ion activation is attained by multiple collisions using heavier gases (N<sub>2</sub>, Ar) and extended collision cells.

HCD employs higher energy dissociations than in ion trap CID, enabling a wider range of fragmentation pathways. HCD fragmentation is available for the LTQ (linear trap quadrupole) Orbitrap, where ions are fragmented in a collision cell rather than an ion trap and then transferred back through the C-trap for analysis at high resolution in the Orbitrap. Compared with traditional ion trap-based CID, HCD fragmentation with Orbitrap detection has several advantages such as no low-mass cutoff, high resolution ion detection, and increased ion fragments resulting in higher quality MS/MS spectra.

However longer spectral acquisition times, as more ions are required for Fourier transform detection in the Orbitrap compared to detection of CID spectra in the ion trap via electron multipliers, are a downside. The use of more efficient HCD collision cells as in the LTQ Orbitrap Velos and Elite instruments has greatly improved the performance of HCD fragmentation, making rapid and routine analysis possible<sup>265</sup>.

#### 1.6.3.2.2. Nomenclature of fragment ions

The nomenclature for fragment ions of peptides is illustrated in Figure 1.9. The classification of the various peptide fragments was initially proposed by Roepstorff and Fohlmann<sup>266</sup> and was later modified by Biemann<sup>267</sup>. The identification of the breakage point of the peptide backbone and the determination of the retained charge on the N- or C-terminus fragment of the peptide is central to this nomenclature.

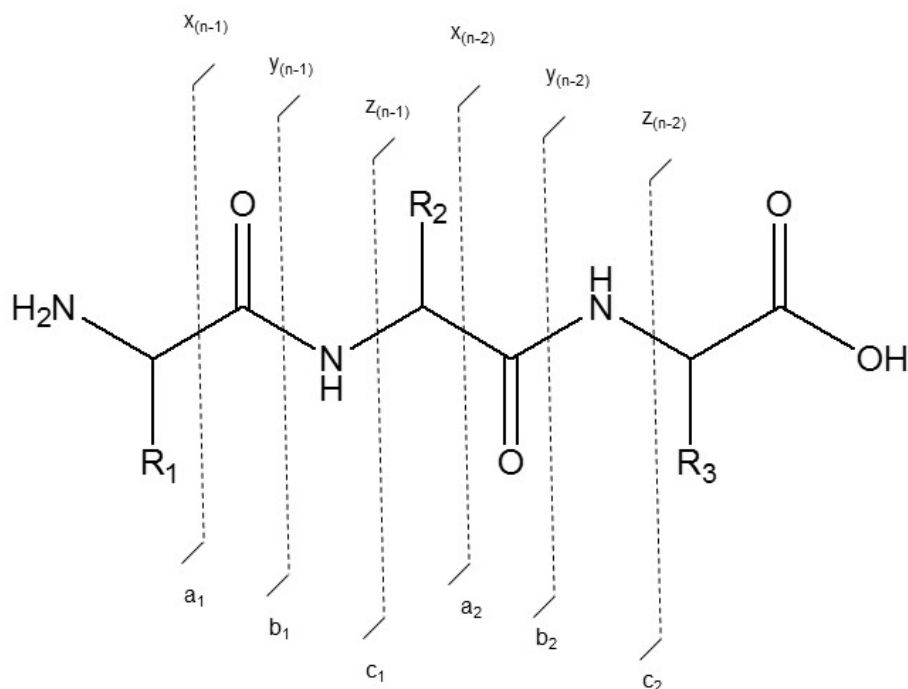


**Figure 1.9. Nomenclature for fragment ions.**

The type of ions produced depends on the cleavage site. Adapted from reference<sup>268</sup>.

The ions are referred to as *a*-, *b*-, or *c*-series if the charge is retained on the N-terminus of the fragment ion. If the C-terminus of the fragment ion is charged, the ions are called *x*-, *y*- and *z*-ion series. The position of the amino acid where fragmentation has occurred is designated by a subscript number, which is counted sequentially from the N- or C-terminus, respectively<sup>269</sup>. Different activation methods result in the formation of different ion series. *b*-ions (acylium-ions) and *y*-ions (ammonium ions), which are shown in Figure 1.9 are formed by low energy collision-induced dissociation typically performed in quadrupole ion traps, quadrupole time-of-flight, Fourier transform ion cyclotron resonance and Orbitrap instruments. The *b*-ions can dissociate into *a*-ions with the concomitant loss of CO. Electron Capture dissociation generates *c*- and *z*-ions.

### 1.6.3.3. Mass analyzers

The different types of mass analyzer measure the mass-to-charge ratio ( $m/z$ ) of the ionized analytes in different ways. Five basic types of mass analyzers are currently employed in proteomics that use three different principles: separation on the basis of time-of-flight (ToF MS), separation by quadrupole electric fields (quadrupole MS) or separation by selective ejection of ions from a three-dimensional trapping field (ion trap, FT-ICR, Orbitrap MS)<sup>234</sup>. For proteomics applications the most important parameters of mass analyzers are the  $m/z$  limit, sensitivity, resolution, mass accuracy and the ability to perform tandem mass spectrometry.

Resolution (R), which is the ability to resolve two adjacent peaks, refers to the precision of the measurement. Resolution is defined by the following equation:

$$\text{Resolution} = \frac{m}{\Delta m} \quad \text{Equation 1.1}$$

$m$  is the  $m/z$  of the peak of interest and  $\Delta m$  is the peak width at a specified height (typically 50%). Hence, the higher the value of R, the better the ability of the mass analyzer to separate two closely spaced  $m/z$  values.

Mass accuracy, generally reported as parts per million (ppm), is the most important parameter in establishing compound identity. Mass accuracy is a measurement of the correlation between the observed  $m/z$  and the “true value”. It can be determined from the following equation:

$$\text{Mass accuracy (ppm)} = \frac{m_{\text{observed}} - m_{\text{theory}}}{m_{\text{theory}}} \times 1000000 \quad \text{Equation 1.2}$$

$m_{\text{observed}}$  is the  $m/z$  of the peak of interest obtained in the mass spectrum and  $m_{\text{theory}}$  is a calculated  $m/z$  expected for the species.

The above mentioned analyzers can be stand-alone or combined in a “hybrid” mass spectrometer to take advantage of the strength of each. In this thesis, we have used two hybrid mass spectrometry instruments, the LTQ-OrbitrapXL (Thermo Scientific) and the more recent generation LTQ Orbitrap Elite. These instruments comprise a linear ion trap (LIT) and a high field Orbitrap for high resolution separation of gas phase ions. The LIT, the Orbitrap and the respective hybrid instruments will be described in more detail below.

#### **1.6.3.3.1. Linear quadrupole ion traps (LIT)**

The LIT is a close relative of the quadrupole mass analyzer. While a quadrupole has electric fields in two dimensions (x and y) and the ions move perpendicular to the field, the LIT has the electric field in all three dimensions. It is a quadrupole with an applied high potential to the front and the back sections. This generates a trapping potential with the ions being trapped in the center section. Ions in a quadrupole field experience restoring forces that drive them back toward the center of the trap. The motion of the ions in the field is defined by solutions to the Mathieu equation<sup>270</sup> and a Mathieu stability diagram applies to the ion trap. Ions are confined radially in the center section by radio frequency (rf) potentials and axially by DC potentials. Ions are extracted through the ion exit slots in the x-rods of the quadrupole. The extraction of ions is important on the one hand in order to avoid space charge effects caused by too many ions in the analyzer cell that interact through Coulombic repulsion, and on the other hand for the isolation of precursor ions in tandem mass spectrometry instruments. To acquire a mass spectrum with an ion trap the ion trajectories must be made unstable. Mass analysis is attained by making ion trajectories unstable in a mass-selective manner. Different techniques for the extraction of ions trapped in a quadrupole field exist. The main principle is to enhance the oscillation amplitude of the selected ions by applying a supplemental resonance voltage to the trap that causes excitation of the ion with corresponding ion resonance. To eject an ion of selected  $m/z$  ratio from a quadrupole trap either dipole or quadrupole excitation can be performed. Ions of a range of  $m/z$  ratios can be ejected in different



ways, for example, by applying a fixed trapping rf voltage with a scanning excitation frequency or by applying a fixed supplemental excitation voltage and a simultaneous change in the main trapping rf voltage. Both options bring ions of a range of  $m/z$  into resonance for a successive ejection. Another way to eject ions of a range of  $m/z$  from a quadrupole trap is a frequency scan, using multiple frequencies or a broadband waveform. In the case of a broadband waveform all frequencies except for the resonant frequency of the ion to be isolated are present and thus all other ions are ejected from the trap. This ejection method needs less time and hence increases the duty cycle of the instrument. The duty cycle refers to the time the detector in fact is measuring ions. It can be determined in this way: (ion detection time/total scan time)  $\times$  100%.<sup>271</sup> The mass accuracy of ion traps is hundreds of ppm. The sensitivity, throughput and ease of use of the LIT, combined with its relatively low cost has led to the widespread use of the LIT in mass spectrometry labs.

#### **1.6.3.3.2. Orbitrap Mass Analyzer**

An Orbitrap mass analyzer is the most recent addition to the set of tools that can be used for the identification, characterization and quantitation of components in biological systems. The proof of principle of the Orbitrap was first described by Makarov<sup>272</sup> and Hardman and Makarov first described the injection of electrosprayed ions into the Orbitrap<sup>273</sup>. With its capacity to deliver low-ppm mass accuracy and extremely high resolving power similar to those achievable with FT-ICR instrumentation, all within a time scale compatible with nano-LC separations, the Orbitrap has become an instrument of choice for many proteomics applications since its commercial introduction in 2005.

The Orbitrap consists of an inner (central) and an outer electrode that are used to trap ions in a quadrolongarithmic electrostatic potential<sup>272, 273</sup>. The electrostatic attraction towards the central electrode is compensated by a centrifugal force arising from the initial tangential velocity of the ions. Ions revolve about the central electrode and oscillate harmonically along its axis (the z-direction) with a frequency characteristic of their  $m/z$  values. The axial component of these oscillations is independent of initial energy, angles and positions. The oscillations of the moving ions induce an image current that is detected via a differential amplifier between the two halves of an electrode encapsulating

the Orbitrap. The  $m/z$  of different ions in the Orbitrap can be determined from respective frequencies of oscillation after a Fourier transformation.

The Orbitrap operates very efficiently as a high resolving accurate mass detector. The literature supports claims of routine mass measurements of less than 2 pm for the analysis of complex peptide mixtures<sup>274</sup> and even intact proteins<sup>275</sup>. The maximum resolving power of the classical Orbitrap is just over 100,000 (referenced to  $m/z$  400)<sup>276</sup>.

#### **1.6.3.3.3. LTQ Orbitrap**

Fig. 1.10 shows a hybrid LTQ Orbitrap. It comprises three main parts: an LTQ linear ion trap mass spectrometer, a C-trap and an Orbitrap mass analyzer. The ions from the electrospray ion source are first transmitted via rf-only multipoles into the first section after the source in a LTQ Orbitrap, the linear ion trap, which is very fast and capable of multiple levels of fragmentation usually referred to as MS<sup>n</sup>. MS and MS<sup>n</sup> spectra are detected at very high sensitivity but relatively low resolution and mass accuracy. Ions stored in the linear ion trap can be released via an rf-only octapole into a C-shaped RF-only quadrupole, the so-called C-trap. In the C-trap, ions are accumulated and their energy is reduced by residual nitrogen gas. Controlling the number of ions transmitted to the C-trap, and then injected into the Orbitrap helps to reduce space charge effects, which can decrease mass resolution and accuracy through non-ideal behavior of the ions in the Orbitrap electrostatic fields. From the C-trap the accumulated ions are filled into the Orbitrap by a pulse and their signal is detected in the Orbitrap. On their way from C-trap, ions pass through three stages of differential pumping until they reach the ultrahigh vacuum compartment of the Orbitrap maintained at  $\approx 2 \times 10^{-10}$  mbar<sup>274</sup>.

The acquisition of MS/MS spectra in the linear ion trap and a high resolution/mass accuracy spectrum of the precursor in the Orbitrap can be done in parallel or series.

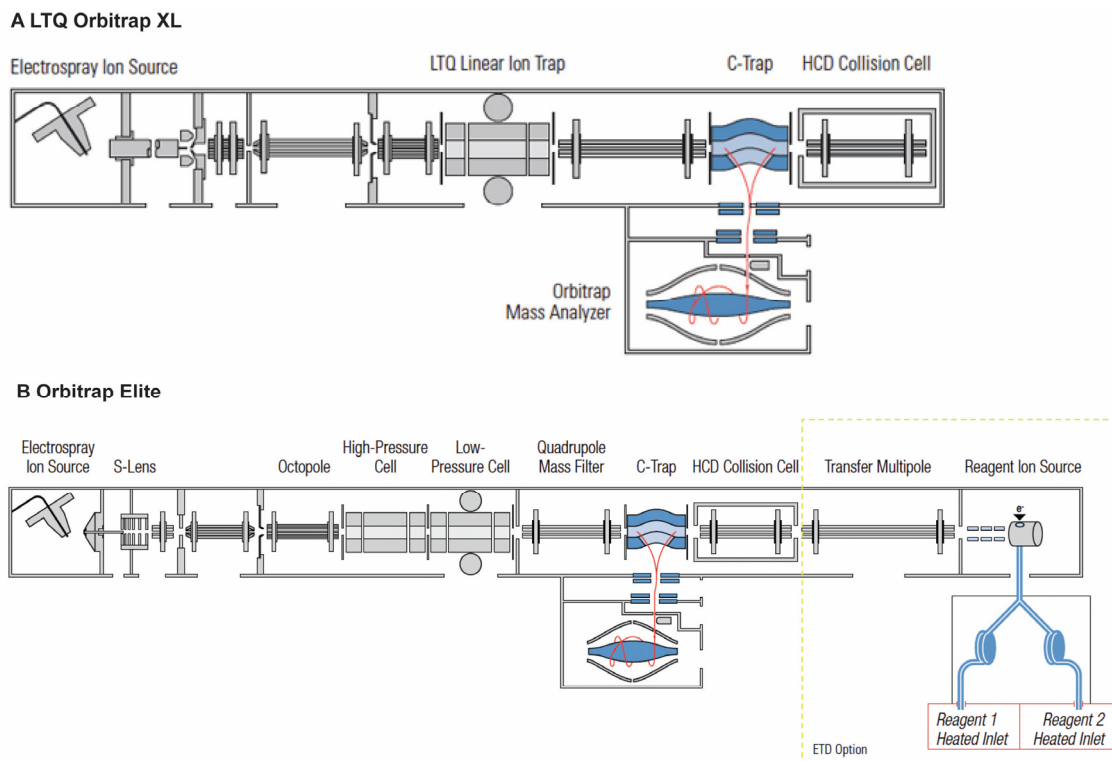


**Figure 1.10. Schematics of the LTQ Orbitrap XL and Orbitrap Elite hybrid mass spectrometers.**

(A) The LTQ Orbitrap XL consists of a LTQ linear ion trap mass spectrometer, a C-trap and an Orbitrap mass analyzer. (B) The Orbitrap Elite contains novel elements such as a dual pressure LIT and a compact high-field Orbitrap analyzer. ETD fragmentation is optional. Adapted from Thermo Scientific (<http://planetorbitrap.com>).

#### 1.6.3.3.4. Orbitrap Elite

The Thermo Scientific Orbitrap Elite mass spectrometer, introduced in 2011 and depicted in Figure 1.10, combines a dual-pressure linear ion trap (Velos Pro) with a novel high-field Orbitrap mass analyzer<sup>277</sup>. The Orbitrap Elite is characterized with enhanced sensitivity and faster scan speed. This was achieved by improvements in several areas. A novel dual-pressure linear ion trap<sup>278</sup> makes it possible to separate capture and fragmentation processes from the mass scanning and detection process with an MS acquisition speed to >12 scan/s. A combination of C-trap and HCD collision cell with an applied axial field enhances extraction of fragment ions and trapping capacities leading to faster MS/MS scans. The injection times required to acquire high resolution, high mass accuracy MS/MS spectra are similar to those previously needed for ion trap fragmentation (“high-low” mode), making routine proteomics analysis in a “high-high”

mode, where not only MS spectra, but also fragmentation spectra have high mass accuracy<sup>278</sup> possible. Additionally, a more robust ion transfer interface was introduced. Most importantly, by employing a compact, high-field Orbitrap analyzer with reduced trap dimensions, the resolving power of the Orbitrap analyzer has been increased two fold for the same transient length. In addition, enhanced Fourier Transform algorithm, which incorporates phase information, increases the resolving power to 240,000 at  $m/z$  400<sup>277</sup>. Enhanced proteome coverage of complex samples can be achieved due to the higher resolution and quality of spectra, as well as the faster scan speed. The availability of multiple fragmentation techniques (CID, HCD and optional ETD) offers new opportunities to approach demanding research objectives<sup>277</sup>.

Recently, there have been more additions to the Orbitrap family of hybrid/tribrid instruments. The Thermo Scientific Q Exactive hybrid quadrupole-Orbitrap mass spectrometer, introduced in 2011 combines quadrupole precursor selection with high-resolution, accurate-mass Orbitrap detection<sup>279</sup>. The Thermo Scientific Orbitrap Fusion Tribid mass spectrometer, the newest addition, introduced in 2013, is a combination of quadrupole, Orbitrap, and ion trap mass analysis in a Tribid architecture that delivers unparalleled analysis capabilities<sup>280</sup>.

In the setup used in this thesis, a precursor scan was performed with the Orbitrap followed by the recording of MS/MS spectra in the linear ion trap on LTQ Orbitrap XL or Orbitrap Elite instruments respectively. The instruments were operated in data dependent acquisition mode using CID as fragmentation.

#### **1.6.4. Quantification in mass spectrometry-based proteomics**

Quantification plays a key role in MS-based proteomics. Proteomics can define the absolute amount of each protein in a mixture or their relative abundance between conditions. Absolute quantification can provide the copy number of proteins in a cell using the AQUA (absolute quantification) method, where an isotopically labeled peptide is synthesized and spiked in known amounts to the sample to absolutely quantify its endogenous counterpart<sup>281</sup>.

There are two main approaches used for relative quantitation in proteomics –label-free or stable-isotope based methods (Figure 1.11).

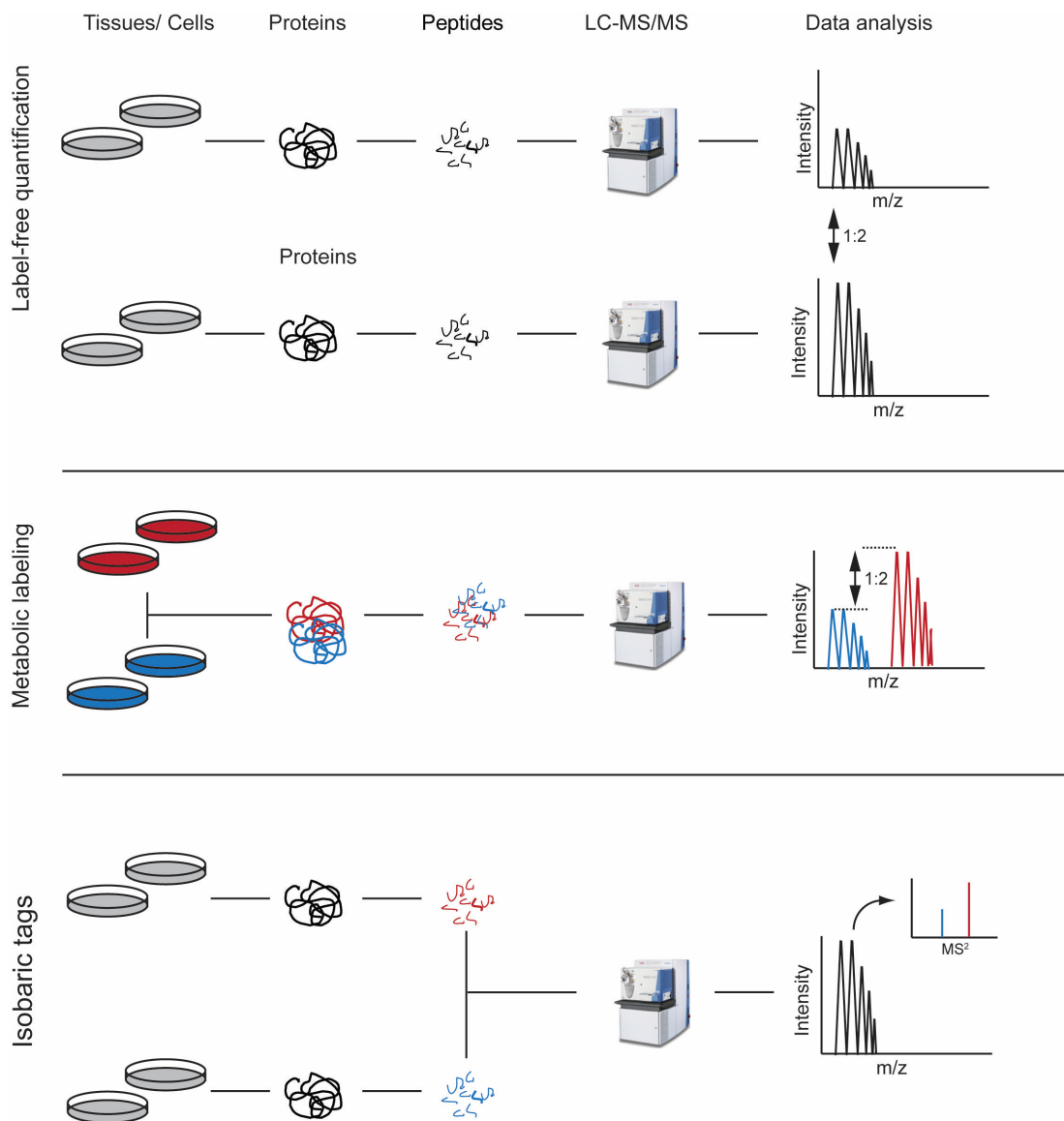


**Figure 1.11. Overview of quantitative proteomics workflows.**

In label-free quantification workflows unlabeled samples are individually analyzed and quantitation is performed based on spectral counting or MS<sup>1</sup> based approaches (depicted). Metabolic labeling is characterized by the isotopic labeling of proteins in vivo (indicated by blue - light and red - heavy), after which the samples are combined and processed for quantitative analysis. With isobaric tags, protein extraction is performed prior to labeling. Isobaric tags yield peptide fragment ion spectra through LC-MS/MS analysis generated in MS<sup>1</sup> and the cleaved tag spectra generated in MS<sup>2</sup>, which are used for peptide identification and relative quantitation. Adapted from Thermo Scientific (<http://www.piercenet.com/method/quantitative-proteomics>).

#### **1.6.4.1. Stable-isotope based methods**

Stable-isotope labeling for peptide and protein quantification is based on the principally identical physicochemical properties of labeled and natural peptides. Hence, relative and absolute quantification of a sample of interest can be performed by comparing its MS intensity with that of a labeled peptide standard present in the same sample<sup>245</sup>. Stable-isotope labeling can be performed based on metabolic or chemical labeling.

##### **1.6.4.1.1. Metabolic labeling**

In metabolic labeling strategies, cells are cultured in defined isotope media (Figure 1.11). The isotope label is introduced into every protein during cell growth and division, which creates labeled standards for every protein in a sample of interest. The introduction of the isotope label at the earliest possible step in a proteomic workflow, results in both high quantification accuracy and high precision as systematic errors arising from sample handling can be eliminated. Stable isotope labeling with amino acids in cell culture (SILAC), introduced more than a decade ago, is the method of choice in mammalian systems<sup>282</sup>. In the classical SILAC experiment, arginine and lysine are provided in light and heavy forms (isotopically labelled with  $^{13}\text{C}$  and  $^{15}\text{N}$ ) to two cell populations and are incorporated into each protein after several cell doublings. The MS intensities of the isotope clusters of the labeled and unlabeled peptides are compared for relative quantification. The combination of several conditions is possible, however a maximum of three samples is typically compared. A drawback of multiplexing SILAC-labeled samples is the likelihood of overlapping isotope clusters, complicating proper quantification<sup>245</sup>. The use of SILAC has recently been extended to entire organisms and even to human tissue. In the super SILAC approach, unlabeled tissues from patients or an animal model system are compared to a representative mix of different heavy-labeled SILAC cell lines used as a common internal standard<sup>283</sup>.

##### **1.6.4.1.2. Chemical protein and peptide labeling**

Popular implementations of chemical derivatization for quantification are tandem mass tags (TMT-tags)<sup>284</sup> and iTRAQ (isobaric tags for absolute and relative quantification)<sup>285, 286</sup>, both of which chemically derivatize primary amines of the peptides. Differential labelling with these reagents generates peptides with identical mass (isobaric), which

can be distinguished following fragmentation by the isotope encoded reporter ions in the lower mass range region of MS/MS spectra. The intensities of the reporter ions are used for the quantification (Figure 1.11). Isobaric labeling has several advantages for the multiplexed analysis of different biological samples. TMT reagents, for example, are now available in up to 10 different versions, allowing for the comparison of 10 conditions in a single experiment. Furthermore, the peptides labeled with isobaric tags co-elute during LC separations resulting in no increase of the complexity. Even more the complexity of peptide mass spectra is not increased because differentially labelled peptides are isobaric<sup>245</sup>.

An alternative for the chemical labeling of protein digests is stable-isotope dimethyl labeling<sup>287, 288</sup>. Here, primary amines of peptides are labeled by formaldehyde through reductive amination using cyanoborohydride. Different combinations of reagent isotopomers result in many possible label combinations with distinct mass shifts. Generally, duplex and triplex reactions, which introduce mass differences of a minimum of 4 Da are used to avoid overlapping isotope envelopes. Dimethyl labeling has several advantages. It is inexpensive and it can be performed in solution or directly in reversed phase chromatography columns which avoids sample loss. One limitation is the use of deuterium as part of the labels which can lead to small retention time shifts of labeled peptides during LC-MS/MS analysis.

#### **1.6.4.2. Label-free quantitation**

Label-free quantitative proteomics aims at the quantification of peptides and proteins without the use of stable-isotope labels. Label-free quantitation is a rapidly growing area in proteomics and it can be roughly divided into spectrum count approaches or MS<sup>1</sup>-intensity-based approaches.

##### **1.6.4.2.1. Spectral count based approaches**

Spectral counting is a simple quantification method in which the number of peptide fragmentation events is used as a proxy for the protein amount. Spectrum count approaches are based on the observation that the number of peptide-to-spectrum matches (PSMs; spectrum count), the number of identified distinct peptides, and the

protein sequence coverage in an LC-MS/MS experiment correlate with protein abundance<sup>245</sup>. Filtering of PSMs for protein quantification is important as it has been demonstrated that considering only high-confidence PSMs allows for the detection of smaller abundance changes with statistical significance compared to the application of less stringent criteria<sup>289</sup>. However, including low-scoring PSMs results in a higher dynamic range and more accurate quantification of low-abundance proteins<sup>289, 290</sup>. In label free studies samples are analyzed separately by LC-MS/MS. Consequently stable and reproducible mass spectrometry analysis has to be guaranteed and is generally best achieved by the analysis of all samples in a single sequence in the same instrument<sup>245</sup>.

#### **1.6.4.2.2. *MS<sup>1</sup> intensity based approaches***

Intensity-based label-free quantification uses the MS signal response of peptides for quantification (Figure 1.11). In bottom-up proteomics this can either be achieved using the peak height intensity values or by integrating the area under the curve (AUC) of the peptide peak<sup>245</sup>. Classically, full scan survey spectra are used to obtain extracted ion chromatograms (XICs). A robust LC-MS/MS setup is required for accurate quantification. Narrow LC peak widths yield better signal-to-noise ratios, hence extending the dynamic range of quantification<sup>245</sup>. In cases where peptides were not identified in all conditions, XICs are mapped by the alignment of accurate mass and retention time. Retention time stability and reproducibility are thus key in label-free quantitative proteomics.

When large datasets need to be compared the number of conditions that can be compared using label-free approaches is not predefined and intensity-based or spectral count based relative quantification is hence particularly attractive.

#### **1.6.5. Bioinformatics and data analysis**

Proteomic studies generate a lot of data. The analysis and interpretation of the vast volumes of proteomics data still remains demanding. Hence, the development of transparent tools for proteomic data analysis using statistical principles is a fundamental challenge<sup>291</sup>. A key breakthrough was the development of algorithms for protein identification from mass spectrometric data. Peptides matching to the spectra are identified. Proteins are inferred from the identified peptides. Nowadays MS/MS data of



individual peptides are commonly used. MS/MS data provides information about the peptide sequence and important additional structural information in addition to the peptide mass. Thus, database searching with tandem mass spectrometry data is more specific and discriminating.

For protein identifications, spectra acquired by MS/MS are scanned against comprehensive protein sequence databases e.g. NCBI<sup>292</sup> or Uniprot<sup>293</sup> using one of various algorithms. There are three main approaches<sup>234</sup>. In the “peptide sequence tag” approach a short, unambiguous amino acid sequence from the peak pattern is extracted and combined with the mass information. Together, this represents a specific probe to define the origin of the peptide<sup>294</sup>. The cross-correlation method utilizes theoretical constructed mass spectra corresponding to peptide sequences from the database under certain fragmentation conditions. The best match is established by the overlap or “cross-correlation” of these predicted spectra with the measured mass spectra<sup>295</sup>. In the third approach, “probability based matching”, which is implemented in the Mascot search engine<sup>296, 297</sup>, calculated fragments from peptide sequences in the database are compared to observed experimental peaks starting with the most intense ions in the spectra in order to find the best matching peptide. From this comparison an identification score is calculated:

$$\text{Identification Score} = -10\log(P) \quad \text{Equation 1.3}$$

$P$  represents the probability that the number of fragment matches is a random event. The identification score reveals the statistical significance of the match between the experimental spectrum and the sequences in a database. All these approaches produce a compilation of the identified peptides into a protein “hit list”.

Database search engines like Mascot<sup>297</sup> or SEQUEST<sup>295</sup> are known to generate a significant number of incorrect peptide assignments<sup>298</sup>, because protein hits might just be randomly assigned hits. These data analyses limitations can be significantly decreased by adopting statistical models for validation of peptide assignments<sup>291</sup>. Usually target decoy database search strategies are used to discriminate correct from incorrect peptide assignments<sup>299</sup> as implemented in the proteoconnections software<sup>300</sup> used in this study. This allows filtering of large-scale proteomics data sets with predictable sensitivity and False Discovery Rates (FDR). Determining the False Discovery Rate (FDR) is an important statistical parameter employed in proteomics analysis to estimate error rates

of protein or peptide identifications. In addition, a false-positive rate (FPR) exists, which is widely used (and sometimes confused with FDR) in the proteomics community as well and it is important to note the difference between the FPR and the FDR as it applies to protein identifications. Figure 1.12 shows the analytical outcome of a proteomics experiment. The search engine, for example Mascot, returns protein hits, which can be true protein identifications present in the analyzed sample, so-called True Positives (TP) or they can be just random hits, which are not true protein identifications, namely False Positives (FP). Besides this, there are protein identifications, which are true proteins in the analyzed sample, but which are not returned as a protein hit in the output of the search engine, so-called False Negatives (FN). Those proteins that are not returned by the search engine and also are not present, are called True Negatives (TN). Ideally, a proteomics experiment should only result in TP. In reality, FP are regularly detected and cannot necessarily be discriminated from TP based on their scores alone.

		Search Engine	
		Returned	Not Returned
Truth "Goldstandard"	Yes	TP	FN
	No	FP	TN

**Figure 1.12. Analytical outcome of a proteomics experiment.**

TP – True Positives, FP – False Positives, FN – False Negatives, TN – True Negatives. From reference<sup>268</sup>.

False Discovery Rate and False Positive Rate are defined in Equations 1.4 and 1.5.

$$FDR = \frac{FP}{FP + TP} \quad \text{Equation 1.4}$$

$$FPR = \frac{FP}{FP + TN} \quad \text{Equation 1.5}$$

The FDR is the rate of random protein assignments to true protein assignments, whereas the FPR is the fraction of proteins not present in the analyzed sample that appear in the final protein list. In a proteomics experiment the FDR is required to be around 1-2% percent.

Quantitative proteomics involves additional data extraction and processing. Intensity-based label-free quantification procedures typically require mass calibration, noise and data reduction steps, followed by feature detection and generation of peptide elution profiles or peptide maps. In turn, peptide features from different LC-MS/MS experiments are aligned in the time and mass dimensions, and intensities are normalized. Finally, relative quantification is achieved by clustering the intensities of the individual peptide features across all experiments in the dataset<sup>245</sup>. For this purpose in this study our in house developed label-free quantitation software 'Proteoprofile', which quantified peptides and proteins based on the peptide ion peak heights was used. There are also public, free tools available including OpenMS<sup>301</sup>, Census<sup>302</sup>, and Superhirn<sup>303</sup>. For stable isotope based labelling MaxQuant<sup>304</sup> is the most established software and it is especially optimized for SILAC-based quantitation.

Finally, it is important to integrate the proteomics dataset with several bioinformatics tools such as Gene ontology<sup>305</sup> term enrichment analysis, pathway analysis<sup>306</sup> or protein interaction<sup>307</sup> network analysis data in a biologically meaningful way, so that hypotheses about specific biological phenomenon can be generated and ultimately tested.

#### **1.6.6. Proteomics of post-translational modifications**

Mass spectrometry is the tool of choice for the analysis of posttranslational modifications (PTMs) such as phosphorylation or ubiquitylation, because it can discover them, it can locate the PTM with single amino acid resolution and it can be much more specific and quantitative than antibody based methods. The main challenge in PTM analysis is the low abundance of modified peptides.

Phosphopeptides, for example, are very low abundant in protein digests and can display a wide dynamic range of site occupancy on proteins. Consequently, enrichment techniques to increase the relative proportion of phosphopeptides from protein digests are necessary to perform large-scale phosphoproteomics experiments by MS.<sup>308</sup>. Several approaches have been developed to increase selectivity including LC fractionation, such as hydrophilic interaction or ion exchange chromatography<sup>309-311</sup>. The most popular enrichment methodologies for phosphopeptide enrichment are immobilized metal affinity chromatography (IMAC) with Fe3+<sup>312, 313</sup> and metal oxide affinity

chromatography with TiO<sub>2</sub> beads<sup>314</sup>. Nevertheless, various complementary approaches have also been established, including phosphotyrosine immunoaffinity purification<sup>315</sup>.

Several biological pathways are known to be regulated by ubiquitylation, however the large-scale identification of ubiquitylated proteins is still challenging. Similarly to phosphoproteomics experiments, the low occupancy of ubiquitylation makes the detection of endogenously modified proteins by MS very difficult. However, the chemical properties of the isopeptide bond, formed between the C-terminal glycine in ubiquitin and the  $\epsilon$ -amino group of lysine residues in substrates, provide a possibility for the specific detection of ubiquitylated targets by MS. Tryptic digestion of ubiquitin conjugates yields characteristic “diGly remnants” due to cleavage of the C-terminal Arg-Gly-Gly sequence of ubiquitin. To globally characterize the ubiquitinome, enrichment strategies have been developed based on affinity capture of the diGly remnant by diGly specific antibodies<sup>316</sup>. The inhibition of the proteasome is also commonly used to increase the number of ubiquitylated substrates in the cell and thus increase the chance of their detection by MS.

#### **1.6.7. Contribution of proteomics to the understanding of HSV-1 infection**

MS-based proteomics has contributed to the understanding of HSV1-host interactions. Previous proteomics analysis focused mostly on the analysis of the HSV1 protein interactome or on differential quantitative proteomics to analyze virally induced changes in the host cellular proteome<sup>317</sup>. Several immediate early viral-protein interactomes have been characterized. Interaction partner and host-viral complexes have been characterized using immunoaffinity purification procedures for viral proteins ICP27<sup>318</sup>, ICP8<sup>319</sup>, ICP4<sup>320</sup>, UL46<sup>321</sup>. A few studies also characterized the composition of purified mature and immature extracellular and perinuclear virions by proteomics<sup>322-324</sup>.

Proteomics studies focused on the elucidation of host proteome modifications during early stages of HSV-1 infection. Using subcellular proteomics important insights on the mechanisms altered in the host during HSV1 infection were obtained. Ribosomes extracted from mock or HSV1 infected HeLa cells were compared<sup>325</sup>, cytosolic and microsomal proteomes at different early time points during infection in HuH7 cells were compared<sup>326</sup> as well as the host cells nuclear proteome alterations were investigated in HSV1 infected HuH7 cells<sup>327</sup>. Recently, a global secretome characterization of HSV-

infected human primary macrophages by proteomics was described<sup>328</sup>. In addition to subcellular studies, Antrobus et al. recently analyzed whole cell extracts from mock- and HSV-1-infected HEp-2 cells in the first global comparative analysis of HSV-1 infected cells and provided an important insight into host cell proteome changes during the early stages of HSV-1 infection<sup>329</sup>.

However, until now all proteomics studies investigated early, but not late time points of HSV1 infection. In addition, the intracellular HSV1 proteome has not yet been characterized, and it would be crucial to investigate the temporal expression profiles of HSV1 proteins in the host cell. Furthermore, no large scale study was yet performed to investigate PTMs on HSV1 proteins. Obtaining a distribution of HSV1 phosphorylation, ubiquitylation or glycosylation sites would provide an important resource for HSV1 biology.

#### **1.6.8. Characterization of autophagy by quantitative proteomics**

A few recent studies used MS-based proteomics to investigate global proteome changes during autophagy<sup>330</sup>. SILAC-based quantification was used to determine the relative abundance of proteins in mammalian cells during amino acid starvation, and their kinetic profiles suggested an ordered degradation of cellular components during starvation-induced autophagy<sup>331</sup>. A few protein-protein interaction studies using proteomics in context of autophagy were also described. In a recent landmark study, Behrends et al. used affinity purification MS to obtain a human autophagy protein interaction network of 409 proteins and 751 interactions<sup>90</sup>. Quantitative proteomics was also applied to elucidate the regulation of early signaling events upon autophagy and to characterize the temporal phosphorylation dynamics after starvation and rapamycin treatment. A comprehensive distribution of phosphorylation kinetics within the first 30 min upon induction of autophagy was obtained with both treatments affecting widely different cellular processes<sup>332</sup>.

However, proteomics analyses of the autophagosome proteome composition are scarce. Only four previous studies described the use of MS to identify autophagosomal proteins<sup>333-336</sup>. In a first report, autophagosomes were analyzed using a 2-D gel approach and MALDI-TOF-MS, and identified relatively few proteins (39 enriched proteins), most

of which were associated to metabolic processing<sup>336</sup>. The conclusions from this study were limited by the fact that autophagosomes were isolated by density gradient centrifugation<sup>337</sup>, an approach where organelles are only partially separated from each other based on their intrinsic density. In a second report, autophagosomes were purified using antibodies against GFP (green fluorescence protein)-tagged LC3 in combination with magnetic beads<sup>333</sup> and 101 proteins were identified, most of which have unknown functions in autophagy. Similar approaches based on density gradient centrifugation were used in 2 more recent large-scale mass spectrometry studies<sup>334, 335</sup>. Dengjel *et al.* used density gradient centrifugation relying on protein correlation profiling in combination with LC3-GFP pulldown assays to identify more than 700 putative autophagosome associated proteins from human breast cancer cells<sup>334</sup>. The most recent study from Mancias *et al.* identified a cohort of novel and known autophagosome enriched proteins in human cells, including cargo receptors<sup>335</sup>. They used a density gradient centrifugation based approach combined to high stringency filtering for abundance in the total proteome to remove proteins that were unspecifically captured during bulk autophagy. The overlap between all four autophagosomal proteomes is alarmingly low<sup>335</sup>, raising questions about the co-purification of contaminants or unselective capture during cytosolic bulk degradation.

Accordingly, thorough characterization of the autophagosome proteome and how it is modulated under different conditions is still awaiting the development of efficient protocols for the isolation of these organelles.

## 1.7. Research objectives

My research project focuses on the definition of the molecular mechanisms governing the involvement of autophagy in innate and adaptive immunity using novel quantitative proteomics methods together with functional assays as part of an integrated research program. Accordingly, this thesis was centered on the following objectives:

- 1) Determine the role and specificity of cytokines such as TNF- $\alpha$  in the activation of macrophages using quantitative proteomics
- 2) Identify the distribution of HSV1 proteins and their post-translational modifications following macrophage infection.
- 3) Develop an efficient cell fractionation method to characterize the composition of autophagic vesicles such as autophagolysosomes.
- 4) Determine the global changes in the viral proteome during host infection by HSV1 to identify proteins that are differentially abundant in total cell lysate and autophagolysosome extracts.

TNF- $\alpha$  is one of the major proinflammatory cytokines that mediate local and systemic responses and direct the development of adaptive immunity. Based on these considerations, the first study of my PhD project was motivated by the objectives to perform the first comprehensive characterization of pathways and molecular mechanisms involved in the activation of macrophages by TNF- $\alpha$  in order to identify novel and alternative pathways induced by TNF- $\alpha$  stimulation as well as their functional role. To investigate the molecular mechanisms of TNF- $\alpha$  we profiled the changes in abundance in resting and activated RAW264.7 mouse macrophages using label-free quantitative proteomics. Importantly, we also integrated our proteomics dataset with several functional validation steps including flow cytometry, immunofluorescence microscopy as well as novel antigen presentation assays to perform a comprehensive characterization of TNF- $\alpha$  activated macrophages.

Viral infection also regulates autophagy. Recently, our lab provided the first evidence that autophagy can contribute to the presentation of viral proteins on MHC class I molecules during Herpes Simplex Virus type 1 (HSV1) infection<sup>80</sup>. HSV1 are among the most complex and prevalent human viruses. While the composition of viral particles has been

investigated, less is known about the expression of the whole viral proteome in infected cells and no comprehensive analysis of viral protein expression kinetics in an infected cells have been performed to date. In order to obtain meaningful insights on how viral infection modulates autophagy, we first needed to comprehensively characterize the system. Using our well established high sensitivity mass spectrometry workflow, we analyzed the proteome of the prototypical HSV1 in infected macrophages by LC-MS/MS. In addition to protein expression levels, post translational modifications such ubiquitylation and phosphorylation modulate HSV1 protein function, subcellular localization or stability. Consequently, this study also aimed to obtain ubiquitylation and phosphorylation patterns for HSV1 proteins during infection of macrophages with the overall goal to generate a map of protein expression profiles as well as phosphorylation and ubiquitylation sites as an important resources for HSV1 biology.

Remarkably, the autophagic response triggered during HSV1 infection differs in many ways from macroautophagy. This process, referred to as nuclear envelope-derived autophagy (NEDA), leads to the formation of 4-membrane layered structures originating from the nuclear envelope<sup>80</sup>. The discovery of this novel autophagy pathway was very exciting, but it also opened up several questions that we needed to address with regard to the protein content of NEDA-autophagosomes as well as their implication for antigen presentation. The characterization of the autophagosomal proteome in HSV1 infected cells is crucial to our understanding of the involvement of autophagy in antigen presentation. However, to date no efficient autophagosome isolation method that can be interfaced to MS-based proteomics has been established. My PhD project was thus motivated by the development of a new isolation method to obtain enriched autophagosome extracts during HSV1 infection of macrophages that could subsequently be analyzed by quantitative proteomics. The developed method allowed us to monitor the transfer of HSV1 antigens into autophagosomes using our well-established quantitative proteomics workflow. Furthermore, in-house developed novel antigen presentation assays allowed us to shed some light on the functional consequences of antigen relocation on antigen presentation.

In conclusion, the application of quantitative proteomics methods in a systems biology approach allowed us to identify changes occurring during the remodeling of autophagosomes in response to disease and inflammatory conditions such as viral infections.



## 1.8. Thesis overview

The first chapter presents a literature review of the current knowledge on macrophage biology, autophagy and its role in innate and adaptive immunity as well as HSV1 infection. An overview of state-of-the-art techniques used in mass spectrometry-based proteomics is also given. Furthermore, the current knowledge was put into perspective with regard to the research project investigated in this thesis.

The second chapter presents my first article describing the use of label-free quantitative proteomics to profile the dynamic changes of proteins from resting and TNF- $\alpha$  activated mouse macrophages published in ***Molecular and Cellular Proteomics***<sup>338</sup>. These analyses revealed that TNF- $\alpha$  activation of macrophages led to the downregulation of mitochondrial proteins and the differential regulation of several proteins involved in vesicle trafficking and immune response. Importantly, we found that the downregulation of mitochondria proteins occurred through mitophagy and was specific to TNF- $\alpha$ . Furthermore, using a novel antigen presentation system, we observed that the induction of mitophagy by TNF- $\alpha$  enabled the processing and presentation of mitochondrial antigens at the cell surface by MHC class I molecules.

The third chapter presents the analysis of the proteome of the prototypical HSV1 in infected macrophages by mass spectrometry published as my second article in ***Journal of Proteome Research***<sup>339</sup>. Using a high sensitivity LTQ-Orbitrap, we achieved a very high level of protein coverage and identified a total of 67 structural and non-structural viral proteins. We also identified 90 novel phosphorylation sites and ten novel ubiquitylation sites on different viral proteins. Treatment with inhibitors of DNA replication induced changes of both viral protein abundance and modifications, highlighting the interdependence of viral proteins during the life cycle. Given the importance of expression dynamics, ubiquitylation and phosphorylation for protein function, these findings will serve as important tools for future studies on herpes virus biology.

The fourth chapter presents the investigation of the contribution of NEDA to antigen presentation. Our results indicate that NEDA is an Atg5-independent autophagic process distinct from macroautophagy. Using a novel antigen presentation assay, we could show that NEDA improves presentation of viral antigens to CD8+ T cells. Detailed proteomics characterization of autophagosomes formed during NEDA and macroautophagy

revealed the interesting finding that various autophagic pathways can be induced to promote the capture of selective sets of viral proteins, thus actively shaping the nature of the immune response during infection. This work is currently in preparation for submission to *Immunity*.

Finally, the fifth chapter presents a discussion of the results obtained in this study as well as a conclusion that links all the work and findings of this thesis. Potential future perspectives and implications of the findings of this thesis are also discussed.

## 1.9. References

1. Delves, P. J., Martin, S. J., Burton, D. R., and Roitt, I. M. (2011) *Roitt's essential immunology*, John Wiley & Sons
2. Chaplin, D. D. (2010) Overview of the immune response. *Journal of Allergy and Clinical Immunology* 125, S3-S23
3. Blackwell, J. M., Jamieson, S. E., and Burgner, D. (2009) HLA and infectious diseases. *Clinical microbiology reviews* 22, 370-385
4. William, E. P. (2013) *Fundamental Immunology*, Philadelphia : Wolters Kluwer Health/Lippincott Williams & Wilkins, c2013, United States
5. Laiosa, C. V., Stadtfeld, M., and Graf, T. (2006) DETERMINANTS OF LYMPHOID-MYELOID LINEAGE DIVERSIFICATION. *Annual Review of Immunology* 24, 705-738
6. Klein, L., Hinterberger, M., Wirnsberger, G., and Kyewski, B. (2009) Antigen presentation in the thymus for positive selection and central tolerance induction. *Nature Reviews Immunology* 9, 833-844
7. Starr, T. K., Jameson, S. C., and Hogquist, K. A. (2003) POSITIVE AND NEGATIVE SELECTION OF T CELLS. *Annual Review of Immunology* 21, 139-176
8. Carpenter, A. C., and Bosselut, R. (2010) Decision checkpoints in the thymus. *Nature immunology* 11, 666-673
9. Jenkins, M. K., Khoruts, A., Ingulli, E., Mueller, D. L., McSorley, S. J., Reinhardt, R. L., Itano, A., and Pape, K. A. (2001) IN VIVO ACTIVATION OF ANTIGEN-SPECIFIC CD4 T CELLS. *Annual Review of Immunology* 19, 23-45
10. Wong, P., and Pamer, E. G. (2003) CD8 T CELL RESPONSES TO INFECTIOUS PATHOGENS. *Annual Review of Immunology* 21, 29-70
11. Bonilla, F. A., and Oettgen, H. C. (2010) Adaptive immunity. *Journal of Allergy and Clinical Immunology* 125, S33-S40
12. Nathan, C. (2008) Metchnikoff's Legacy in 2008. *Nature immunology* 9, 695-698
13. Gordon, S., and Taylor, P. R. (2005) Monocyte and macrophage heterogeneity. *Nature Reviews Immunology* 5, 953-964
14. Mosser, D. M., and Edwards, J. P. (2008) Exploring the full spectrum of macrophage activation. *Nature Reviews Immunology* 8, 958-969
15. Gordon, S. (2007) The macrophage: past, present and future. *European journal of immunology* 37, S9-S17

16. Boulais, J., Trost, M., Landry, C. R., Dieckmann, R., Levy, E. D., Soldati, T., Michnick, S. W., Thibault, P., and Desjardins, M. (2010) Molecular characterization of the evolution of phagosomes. *Molecular systems biology* 6
17. Jutras, I., and Desjardins, M. (2005) Phagocytosis: at the crossroads of innate and adaptive immunity. *Annu. Rev. Cell Dev. Biol.* 21, 511-527
18. O'Shea, J. J., and Murray, P. J. (2008) Cytokine signaling modules in inflammatory responses. *Immunity* 28, 477-487
19. Ehrt, S., Schnappinger, D., Bekiranov, S., Drenkow, J., Shi, S., Gingeras, T. R., Gaasterland, T., Schoolnik, G., and Nathan, C. (2001) Reprogramming of the Macrophage Transcriptome in Response to Interferon- $\gamma$  and Mycobacterium tuberculosis: Signaling Roles of Nitric Oxide Synthase-2 and Phagocyte Oxidase. *The Journal of Experimental Medicine* 194, 1123-1140
20. Watts, C., and Amigorena, S. (2001) Phagocytosis and antigen presentation. *Seminars in immunology*, pp. 373-379, Elsevier
21. Trost, M., English, L., Lemieux, S., Courcelles, M., Desjardins, M., and Thibault, P. (2009) The phagosomal proteome in interferon- $\gamma$ -activated macrophages. *Immunity* 30, 143-154
22. Jutras, I., Houde, M., Currier, N., Boulais, J., Duclos, S., LaBoissière, S., Bonneil, E., Kearney, P., Thibault, P., and Paramithiotis, E. (2008) Modulation of the phagosome proteome by interferon- $\gamma$ . *Molecular & Cellular Proteomics* 7, 697-715
23. Langrish, C. L., Chen, Y., Blumenschein, W. M., Mattson, J., Basham, B., Sedgwick, J. D., McClanahan, T., Kastelein, R. A., and Cua, D. J. (2005) IL-23 drives a pathogenic T cell population that induces autoimmune inflammation. *The Journal of experimental medicine* 201, 233-240
24. Bettelli, E., Carrier, Y., Gao, W., Korn, T., Strom, T. B., Oukka, M., Weiner, H. L., and Kuchroo, V. K. (2006) Reciprocal developmental pathways for the generation of pathogenic effector TH17 and regulatory T cells. *Nature* 441, 235-238
25. Van Dullemen, H. M., van Deventer, S. J., Hommes, D. W., Bijl, H. A., Jansen, J., Tytgat, G. N., and Woody, J. (1995) Treatment of Crohn's disease with anti-tumor necrosis factor chimeric monoclonal antibody (cA2). *Gastroenterology* 109, 129-135
26. Szekanecz, Z., and Koch, A. E. (2007) Macrophages and their products in rheumatoid arthritis. *Current opinion in rheumatology* 19, 289-295
27. Zhang, X., and Mosser, D. (2008) Macrophage activation by endogenous danger signals. *The Journal of pathology* 214, 161-178
28. Gordon, S. (2003) Alternative activation of macrophages. *Nature reviews immunology* 3, 23-35

29. Edwards, J. P., Zhang, X., Frauwirth, K. A., and Mosser, D. M. (2006) Biochemical and functional characterization of three activated macrophage populations. *Journal of leukocyte biology* 80, 1298-1307
30. Martinez, F. O., and Gordon, S. (2014) The M1 and M2 paradigm of macrophage activation: time for reassessment. *F1000prime reports* 6
31. Chemali, M., Radtke, K., Desjardins, M., and English, L. (2011) Alternative pathways for MHC class I presentation: a new function for autophagy. *Cellular and Molecular Life Sciences* 68, 1533-1541
32. Falk, K., Rötzschke, O., Stevanović, S., Jung, G., and Rammensee, H.-G. (1991) Allele-specific motifs revealed by sequencing of self-peptides eluted from MHC molecules. *Nature* 351, 290-296
33. Brown, J. H., Jardetzky, T. S., Gorga, J. C., Stern, L. J., Urban, R. G., Strominger, J. L., and Wiley, D. C. (1993) Three-dimensional structure of the human class II histocompatibility antigen HLA-DR1. *NATURE-LONDON* 364, 33-33
34. Neefjes, J., Jongsma, M. L. M., Paul, P., and Bakke, O. (2011) Towards a systems understanding of MHC class I and MHC class II antigen presentation. *Nat Rev Immunol* 11, 823-836
35. York, I. A., and Rock, K. L. (1996) Antigen processing and presentation by the class I major histocompatibility complex 1. *Annual review of immunology* 14, 369-396
36. Sauer, R. T., and Baker, T. A. (2011) AAA+ proteases: ATP-fueled machines of protein destruction. *Annual review of biochemistry* 80, 587-612
37. Sijs, E., and Kloetzel, P.-M. (2011) The role of the proteasome in the generation of MHC class I ligands and immune responses. *Cellular and Molecular Life Sciences* 68, 1491-1502
38. Toes, R., Nussbaum, A., Degermann, S., Schirle, M., Emmerich, N., Kraft, M., Laplace, C., Zwiderman, A., Dick, T., and Müller, J. (2001) Discrete cleavage motifs of constitutive and immunoproteasomes revealed by quantitative analysis of cleavage products. *The Journal of experimental medicine* 194, 1-12
39. Bell, C., Desjardins, M., Thibault, P., and Radtke, K. (2014 expected) Autophagy's contribution to innate and adaptive immunity: an overview. In: Jackson, W., ed. *Autophagy, Infection and the Immune Response*, John Wiley & Sons Inc.
40. Vyas, J. M., Van der Veen, A. G., and Ploegh, H. L. (2008) The known unknowns of antigen processing and presentation. *Nature Reviews Immunology* 8, 607-618
41. Hughes, E. A., Hammond, C., and Cresswell, P. (1997) Misfolded major histocompatibility complex class I heavy chains are translocated into the cytoplasm and degraded by the proteasome. *Proceedings of the National Academy of Sciences* 94, 1896-1901

42. Ackerman, A. L., and Cresswell, P. (2004) Cellular mechanisms governing cross-presentation of exogenous antigens. *Nature immunology* 5, 678-684
43. Kovacsics-Bankowski, M., and Rock, K. (1995) A phagosome-to-cytosol pathway for exogenous antigens presented on MHC class I molecules. *Science* 267, 243-246
44. Houde, M., Bertholet, S., Gagnon, E., Brunet, S., Goyette, G., Laplante, A., Princiotta, M. F., Thibault, P., Sacks, D., and Desjardins, M. (2003) Phagosomes are competent organelles for antigen cross-presentation. *Nature* 425, 402-406
45. Ackerman, A. L., Kyritsis, C., Tampé, R., and Cresswell, P. (2003) Early phagosomes in dendritic cells form a cellular compartment sufficient for cross presentation of exogenous antigens. *Proceedings of the National Academy of Sciences* 100, 12889-12894
46. Guermonprez, P., Saveanu, L., Kleijmeer, M., Davoust, J., van Endert, P., and Amigorena, S. (2003) ER-phagosome fusion defines an MHC class I cross-presentation compartment in dendritic cells. *Nature* 425, 397-402
47. Shen, L., Sigal, L. J., Boes, M., and Rock, K. L. (2004) Important role of cathepsin S in generating peptides for TAP-independent MHC class I crosspresentation in vivo. *Immunity* 21, 155-165
48. Deretic, V. (2012) Autophagy: an emerging immunological paradigm. *The Journal of Immunology* 189, 15-20
49. de Duve, C., and Wattiaux, R. (1966) Functions of lysosomes. *Annual review of physiology* 28, 435-492
50. De Duve, C., De Reuck, A. V., and Cameron, M. P. (1963) *Ciba Foundation Symposium: Lysosomes: Proceedings*, Churchill
51. De Duve, C., Pressman, B., Gianetto, R., Wattiaux, R., and Appelmans, F. (1955) Tissue fractionation studies. 6. Intracellular distribution patterns of enzymes in rat-liver tissue. *Biochemical Journal* 60, 604
52. Duve, C. (1975) Exploring cells with a centrifuge. *Science* 189, 186-194
53. Klionsky, D. J. (2005) The molecular machinery of autophagy: unanswered questions. *Journal of cell science* 118, 7-18
54. Massey, A. C., Zhang, C., and Cuervo, A. M. (2006) Chaperone-mediated autophagy in aging and disease. *Current topics in developmental biology* 73, 205-235
55. Deretic, V., and Levine, B. (2009) Autophagy, immunity, and microbial adaptations. *Cell Host Microbe* 5, 527-549
56. Yang, Z., and Klionsky, D. J. (2010) Eaten alive: a history of macroautophagy. *Nat Cell Biol* 12, 814-822

57. Klionsky, D. J., Cregg, J. M., Dunn, W. A., Emr, S. D., Sakai, Y., Sandoval, I. V., Sibirny, A., Subramani, S., Thumm, M., and Veenhuis, M. (2003) A unified nomenclature for yeast autophagy-related genes. *Developmental cell* 5, 539-545
58. Yang, Z., and Klionsky, D. J. (2009) An overview of the molecular mechanism of autophagy. *Curr Top Microbiol Immunol* 335, 1-32
59. Feng, Y., He, D., Yao, Z., and Klionsky, D. J. (2013) The machinery of macroautophagy. *Cell research*
60. Yang, Z., and Klionsky, D. J. Mammalian autophagy: core molecular machinery and signaling regulation. *Curr Opin Cell Biol* 22, 124-131
61. Suzuki, K., Kubota, Y., Sekito, T., and Ohsumi, Y. (2007) Hierarchy of Atg proteins in pre-autophagosomal structure organization. *Genes to Cells* 12, 209-218
62. Mizushima, N., Yoshimori, T., and Ohsumi, Y. (2011) The role of Atg proteins in autophagosome formation. *Annual review of cell and developmental biology* 27, 107-132
63. Deretic, V., Saitoh, T., and Akira, S. (2013) Autophagy in infection, inflammation and immunity. *Nature Reviews Immunology* 13, 722-737
64. Popovic, D., and Dikic, I. (2012) The molecular basis of selective autophagy. *Biochemist* 34, 24-30
65. Ohsumi, Y., and Mizushima, N. (2004) Two ubiquitin-like conjugation systems essential for autophagy. *Seminars in cell & developmental biology*, pp. 231-236, Academic Press
66. Birgisdottir, Å. B., Lamark, T., and Johansen, T. (2013) The LIR motif—crucial for selective autophagy. *Journal of cell science* 126, 3237-3247
67. Yang, Z., and Klionsky, D. J. (2010) Mammalian autophagy: core molecular machinery and signaling regulation. *Current Opinion in Cell Biology* 22, 124-131
68. Cao, Y., Nair, U., Yasumura-Yorimitsu, K., and Klionsky, D. J. (2009) A multiple ATG gene knockout strain for yeast two-hybrid analysis. *Autophagy* 5, 699-705
69. Wei, Y., Pattingre, S., Sinha, S., Bassik, M., and Levine, B. (2008) JNK1-mediated phosphorylation of Bcl-2 regulates starvation-induced autophagy. *Molecular cell* 30, 678-688
70. Zalckvar, E., Berissi, H., Mizrachy, L., Idelchuk, Y., Koren, I., Eisenstein, M., Sabanay, H., Pinkas-Kramarski, R., and Kimchi, A. (2009) DAP-kinase-mediated phosphorylation on the BH3 domain of beclin 1 promotes dissociation of beclin 1 from Bcl-XL and induction of autophagy. *EMBO reports* 10, 285-292
71. Rubinsztein, D. C., Gestwicki, J. E., Murphy, L. O., and Klionsky, D. J. (2007) Potential therapeutic applications of autophagy. *Nature reviews Drug discovery* 6, 304-312

72. Levine, B., and Kroemer, G. (2008) Autophagy in the Pathogenesis of Disease. *Cell* 132, 27-42
73. Yla-Anttila, P., Vihinen, H., Jokitalo, E., and Eskelinen, E. L. (2009) Monitoring autophagy by electron microscopy in Mammalian cells. *Methods Enzymol* 452, 143-164
74. Hailey, D. W., Rambold, A. S., Satpute-Krishnan, P., Mitra, K., Sougrat, R., Kim, P. K., and Lippincott-Schwartz, J. (2010) Mitochondria supply membranes for autophagosome biogenesis during starvation. *Cell* 141, 656-667
75. Hayashi-Nishino, M., Fujita, N., Noda, T., Yamaguchi, A., Yoshimori, T., and Yamamoto, A. (2010) Electron tomography reveals the endoplasmic reticulum as a membrane source for autophagosome formation. *Autophagy* 6, 301-303
76. Ravikumar, B., Moreau, K., Jahreiss, L., Puri, C., and Rubinsztein, D. C. (2010) Plasma membrane contributes to the formation of pre-autophagosomal structures. *Nat Cell Biol* 12, 747-757
77. van der Vaart, A., and Reggiori, F. (2010) The Golgi complex as a source for yeast autophagosomal membranes. *Autophagy* 6, 800-801
78. Yen, W. L., Shintani, T., Nair, U., Cao, Y., Richardson, B. C., Li, Z., Hughson, F. M., Baba, M., and Klionsky, D. J. (2010) The conserved oligomeric Golgi complex is involved in double-membrane vesicle formation during autophagy. *J Cell Biol* 188, 101-114
79. Nishida, Y., Arakawa, S., Fujitani, K., Yamaguchi, H., Mizuta, T., Kanaseki, T., Komatsu, M., Otsu, K., Tsujimoto, Y., and Shimizu, S. (2009) Discovery of Atg5/Atg7-independent alternative macroautophagy. *Nature* 461, 654-658
80. English, L., Chemali, M., Duron, J., Rondeau, C., Laplante, A., Gingras, D., Alexander, D., Leib, D., Norbury, C., Lippe, R., and Desjardins, M. (2009) Autophagy enhances the presentation of endogenous viral antigens on MHC class I molecules during HSV-1 infection. *Nat Immunol* 10, 480-487
81. Radtke, K., English, L., Rondeau, C., Leib, D., Lippé, R., and Desjardins, M. (2013) Inhibition of the Host Translation Shutoff Response by Herpes Simplex Virus 1 Triggers Nuclear Envelope-Derived Autophagy. *Journal of Virology* 87, 3990-3997
82. Kraft, C., Peter, M., and Hofmann, K. (2010) Selective autophagy: ubiquitin-mediated recognition and beyond. *Nature cell biology* 12, 836-841
83. Bjørkøy, G., Lamark, T., Brech, A., Outzen, H., Perander, M., Øvervatn, A., Stenmark, H., and Johansen, T. (2005) p62/SQSTM1 forms protein aggregates degraded by autophagy and has a protective effect on huntingtin-induced cell death. *The Journal of Cell Biology* 171, 603-614
84. Komatsu, M., Waguri, S., Koike, M., Sou, Y.-s., Ueno, T., Hara, T., Mizushima, N., Iwata, J.-i., Ezaki, J., and Murata, S. (2007) Homeostatic levels of p62 control cytoplasmic inclusion body formation in autophagy-deficient mice. *Cell* 131, 1149-1163



85. Pankiv, S., Clausen, T. H., Lamark, T., Brech, A., Bruun, J.-A., Outzen, H., Øvervatn, A., Bjørkøy, G., and Johansen, T. (2007) p62/SQSTM1 Binds Directly to Atg8/LC3 to Facilitate Degradation of Ubiquitinated Protein Aggregates by Autophagy. *Journal of Biological Chemistry* 282, 24131-24145
86. Kirkin, V., Lamark, T., Sou, Y.-S., Bjørkøy, G., Nunn, J. L., Bruun, J.-A., Shvets, E., McEwan, D. G., Clausen, T. H., and Wild, P. (2009) A role for NBR1 in autophagosomal degradation of ubiquitinated substrates. *Molecular cell* 33, 505-516
87. Thurston, T. L., Ryzhakov, G., Bloor, S., von Muhlinen, N., and Randow, F. (2009) The TBK1 adaptor and autophagy receptor NDP52 restricts the proliferation of ubiquitin-coated bacteria. *Nature immunology* 10, 1215-1221
88. Wild, P., Farhan, H., McEwan, D. G., Wagner, S., Rogov, V. V., Brady, N. R., Richter, B., Korac, J., Waidmann, O., Choudhary, C., Dötsch, V., Bumann, D., and Dikic, I. (2011) Phosphorylation of the Autophagy Receptor Optineurin Restricts Salmonella Growth. *Science* 333, 228-233
89. Noda, N. N., Ohsumi, Y., and Inagaki, F. (2010) Atg8-family interacting motif crucial for selective autophagy. *FEBS letters* 584, 1379-1385
90. Behrends, C., Sowa, M. E., Gygi, S. P., and Harper, J. W. (2010) Network organization of the human autophagy system. *Nature* 466, 68-76
91. Ashrafi, G., and Schwarz, T. (2012) The pathways of mitophagy for quality control and clearance of mitochondria. *Cell Death & Differentiation* 20, 31-42
92. Saraste, M. (1999) Oxidative Phosphorylation at the fin de siècle. *Science* 283, 1488-1493
93. Wallace, D. C. (2005) A MITOCHONDRIAL PARADIGM OF METABOLIC AND DEGENERATIVE DISEASES, AGING, AND CANCER: A Dawn for Evolutionary Medicine. *Annual Review of Genetics* 39, 359-407
94. Parsons, M. J., and Green, D. R. (2010) Mitochondria in cell death. *Essays Biochem* 47, 99-114
95. Hagen, T. M., Yowe, D. L., Bartholomew, J. C., Wehr, C. M., Do, K. L., Park, J.-Y., and Ames, B. N. (1997) Mitochondrial decay in hepatocytes from old rats: Membrane potential declines, heterogeneity and oxidants increase. *Proceedings of the National Academy of Sciences* 94, 3064-3069
96. Langer, T., Kaser, M., Klanner, C., and Leonhard, K. (2001) AAA proteases of mitochondria: quality control of membrane proteins and regulatory functions during mitochondrial biogenesis. *Biochemical Society Transactions* 29, 431-435
97. Soubannier, V., McLelland, G.-L., Zunino, R., Braschi, E., Rippstein, P., Fon, Edward A., and McBride, Heidi M. (2012) A Vesicular Transport Pathway Shuttles Cargo from Mitochondria to Lysosomes. *Current Biology* 22, 135-141

98. Sandoval, H., Thiagarajan, P., Dasgupta, S. K., Schumacher, A., Prchal, J. T., Chen, M., and Wang, J. (2008) Essential role for Nix in autophagic maturation of erythroid cells. *Nature* 454, 232-235
99. Sato, M., and Sato, K. (2011) Degradation of Paternal Mitochondria by Fertilization-Triggered Autophagy in *C. elegans* Embryos. *Science* 334, 1141-1144
100. Al Rawi, S., Louvet-Vallée, S., Djeddi, A., Sachse, M., Culetto, E., Hajjar, C., Boyd, L., Legouis, R., and Galy, V. (2011) Postfertilization Autophagy of Sperm Organelles Prevents Paternal Mitochondrial DNA Transmission. *Science* 334, 1144-1147
101. Kiššová, I. B., Salin, B., Schaeffer, J., Bhatia, S., Manon, S., and Camougrand, N. (2007) Selective and Non-Selective Autophagic Degradation of Mitochondria in Yeast. *Autophagy* 3, 329-336
102. Narendra, D., Tanaka, A., Suen, D.-F., and Youle, R. J. (2008) Parkin is recruited selectively to impaired mitochondria and promotes their autophagy. *The Journal of Cell Biology* 183, 795-803
103. Kim, I., and Lemasters, J. J. (2011) Mitophagy selectively degrades individual damaged mitochondria after photoirradiation. *Antioxidants & redox signaling* 14, 1919-1928
104. Kanki, T., Wang, K., Cao, Y., Baba, M., and Klionsky, D. J. (2009) Atg32 is a mitochondrial protein that confers selectivity during mitophagy. *Dev Cell* 17, 98-109
105. Kanki, T., Wang, K., Baba, M., Bartholomew, C. R., Lynch-Day, M. A., Du, Z., Geng, J., Mao, K., Yang, Z., and Yen, W.-L. (2009) A genomic screen for yeast mutants defective in selective mitochondria autophagy. *Molecular biology of the cell* 20, 4730-4738
106. Narendra, D., Kane, L. A., Hauser, D. N., Fearnley, I. M., and Youle, R. J. (2010) p62/SQSTM1 is required for Parkin-induced mitochondrial clustering but not mitophagy; VDAC1 is dispensable for both. *Autophagy* 6, 1090-1106
107. Schweers, R. L., Zhang, J., Randall, M. S., Loyd, M. R., Li, W., Dorsey, F. C., Kundu, M., Opferman, J. T., Cleveland, J. L., Miller, J. L., and Ney, P. A. (2007) NIX is required for programmed mitochondrial clearance during reticulocyte maturation. *Proceedings of the National Academy of Sciences* 104, 19500-19505
108. Novak, I., and Dikic, I. (2011) Autophagy receptors in developmental clearance of mitochondria. *Autophagy* 7, 301-303
109. Youle, R. J., and Narendra, D. P. (2011) Mechanisms of mitophagy. *Nat Rev Mol Cell Biol* 12, 9-14
110. Meissner, C., Lorenz, H., Weihofen, A., Selkoe, D. J., and Lemberg, M. K. (2011) The mitochondrial intramembrane protease PARL cleaves human Pink1 to regulate Pink1 trafficking. *Journal of Neurochemistry* 117, 856-867

111. Deas, E., Plun-Favreau, H., Gandhi, S., Desmond, H., Kjaer, S., Loh, S. H. Y., Renton, A. E. M., Harvey, R. J., Whitworth, A. J., Martins, L. M., Abramov, A. Y., and Wood, N. W. (2011) PINK1 cleavage at position A103 by the mitochondrial protease PARL. *Human Molecular Genetics* 20, 867-879
112. Greene, A. W., Grenier, K., Aguilera, M. A., Muise, S., Farazifard, R., Haque, M. E., McBride, H. M., Park, D. S., and Fon, E. A. (2012) Mitochondrial processing peptidase regulates PINK1 processing, import and Parkin recruitment. *EMBO reports* 13, 378-385
113. Lazarou, M., Jin, Seok M., Kane, Lesley A., and Youle, Richard J. (2012) Role of PINK1 Binding to the TOM Complex and Alternate Intracellular Membranes in Recruitment and Activation of the E3 Ligase Parkin. *Developmental Cell* 22, 320-333
114. Narendra, D. P., Jin, S. M., Tanaka, A., Suen, D.-F., Gautier, C. A., Shen, J., Cookson, M. R., and Youle, R. J. (2010) PINK1 is selectively stabilized on impaired mitochondria to activate Parkin. *PLoS biology* 8, e1000298
115. Chan, N. C., Salazar, A. M., Pham, A. H., Sweredoski, M. J., Kolawa, N. J., Graham, R. L. J., Hess, S., and Chan, D. C. (2011) Broad activation of the ubiquitin–proteasome system by Parkin is critical for mitophagy. *Human Molecular Genetics* 20, 1726-1737
116. Tanaka, A., Cleland, M. M., Xu, S., Narendra, D. P., Suen, D.-F., Karbowski, M., and Youle, R. J. (2010) Proteasome and p97 mediate mitophagy and degradation of mitofusins induced by Parkin. *The Journal of Cell Biology* 191, 1367-1380
117. Levine, B. (2005) Eating oneself and uninvited guests: autophagy-related pathways in cellular defense. *Cell* 120, 159-162
118. Sanjuan, M. A., Dillon, C. P., Tait, S. W., Moshiah, S., Dorsey, F., Connell, S., Komatsu, M., Tanaka, K., Cleveland, J. L., Withoff, S., and Green, D. R. (2007) Toll-like receptor signalling in macrophages links the autophagy pathway to phagocytosis. *Nature* 450, 1253-1257
119. Knodler, L. A., and Celli, J. (2011) Eating the strangers within: host control of intracellular bacteria via xenophagy. *Cell Microbiol* 13, 1319-1327
120. Choy, A., and Roy, C. R. (2013) Autophagy and bacterial infection: an evolving arms race. *Trends Microbiol* 21, 451-456
121. Jo, E. K., Yuk, J. M., Shin, D. M., and Sasakawa, C. (2013) Roles of autophagy in elimination of intracellular bacterial pathogens. *Front Immunol* 4, 97
122. Nimmerjahn, F., Milosevic, S., Behrends, U., Jaffee, E. M., Pardoll, D. M., Bornkamm, G. W., and Mautner, J. (2003) Major histocompatibility complex class II-restricted presentation of a cytosolic antigen by autophagy. *European Journal of Immunology* 33, 1250-1259
123. Paludan, C., Schmid, D., Landthaler, M., Vockerodt, M., Kube, D., Tuschl, T., and Münz, C. (2005) Endogenous MHC Class II Processing of a Viral Nuclear Antigen After Autophagy. *Science* 307, 593-596

124. Schmid, D., Pypaert, M., and Münz, C. (2007) Antigen-Loading Compartments for Major Histocompatibility Complex Class II Molecules Continuously Receive Input from Autophagosomes. *Immunity* 26, 79-92
125. Dengjel, J., Schoor, O., Fischer, R., Reich, M., Kraus, M., Müller, M., Kreymborg, K., Altenberend, F., Brandenburg, J., Kalbacher, H., Brock, R., Driessen, C., Rammensee, H.-G., and Stevanovic, S. (2005) Autophagy promotes MHC class II presentation of peptides from intracellular source proteins. *Proceedings of the National Academy of Sciences* 102, 7922-7927
126. Zhou, D., Li, P., Lin, Y., Lott, J. M., Hislop, A. D., Canaday, D. H., Bratkiewicz, R. R., and Blum, J. S. (2005) Lamp-2a Facilitates MHC Class II Presentation of Cytoplasmic Antigens. *Immunity* 22, 571-581
127. Blanchet, F. P., Moris, A., Nikolic, D. S., Lehmann, M., Cardinaud, S., Stalder, R., Garcia, E., Dinkins, C., Leuba, F., Wu, L., Schwartz, O., Deretic, V., and Piguet, V. (2010) Human Immunodeficiency Virus-1 Inhibition of Immunoamphisomes in Dendritic Cells Impairs Early Innate and Adaptive Immune Responses. *Immunity* 32, 654-669
128. Cooney, R., Baker, J., Brain, O., Danis, B., Pichulik, T., Allan, P., Ferguson, D. J. P., Campbell, B. J., Jewell, D., and Simmons, A. (2010) NOD2 stimulation induces autophagy in dendritic cells influencing bacterial handling and antigen presentation. *Nat Med* 16, 90-97
129. Lee, H. K., Mattei, L. M., Steinberg, B. E., Alberts, P., Lee, Y. H., Chervonsky, A., Mizushima, N., Grinstein, S., and Iwasaki, A. (2010) In Vivo Requirement for Atg5 in Antigen Presentation by Dendritic Cells. *Immunity* 32, 227-239
130. Sumpter Jr, R., and Levine, B. (2010) Autophagy and innate immunity: triggering, targeting and tuning. *Seminars in cell & developmental biology*, pp. 699-711, Elsevier
131. Tey, S.-K., and Khanna, R. (2012) Autophagy mediates transporter associated with antigen processing-independent presentation of viral epitopes through MHC class I pathway. *Blood* 120, 994-1004
132. Li, Y., Wang, L.-X., Yang, G., Hao, F., Urba, W. J., and Hu, H.-M. (2008) Efficient Cross-presentation Depends on Autophagy in Tumor Cells. *Cancer Research* 68, 6889-6895
133. Uhl, M., Kepp, O., Jusforgues-Saklani, H., Vicencio, J. M., Kroemer, G., and Albert, M. L. (2009) Autophagy within the antigen donor cell facilitates efficient antigen cross-priming of virus-specific CD8+ T cells. *Cell Death Differ* 16, 991-1005
134. Li, H., Li, Y., Jiao, J., and Hu, H.-M. (2011) Alpha-alumina nanoparticles induce efficient autophagy-dependent cross-presentation and potent antitumour response. *Nat Nano* 6, 645-650
135. Li, B., Lei, Z., Lichty, B., Li, D., Zhang, G.-M., Feng, Z.-H., Wan, Y., and Huang, B. (2010) Autophagy facilitates major histocompatibility complex class I expression induced by IFN- $\gamma$  in B16 melanoma cells. *Cancer Immunol Immunother* 59, 313-321

136. Ireland, J. M., and Unanue, E. R. (2011) Autophagy in antigen-presenting cells results in presentation of citrullinated peptides to CD4 T cells. *The Journal of Experimental Medicine* 208, 2625-2632
137. Gutierrez, M. G., Master, S. S., Singh, S. B., Taylor, G. A., Colombo, M. I., and Deretic, V. (2004) Autophagy Is a Defense Mechanism Inhibiting BCG and Mycobacterium tuberculosis Survival in Infected Macrophages. *Cell* 119, 753-766
138. Singh, S. B., Davis, A. S., Taylor, G. A., and Deretic, V. (2006) Human IRGM Induces Autophagy to Eliminate Intracellular Mycobacteria. *Science* 313, 1438-1441
139. Schaible, U. E., Sturgill-Koszycki, S., Schlesinger, P. H., and Russell, D. G. (1998) Cytokine Activation Leads to Acidification and Increases Maturation of Mycobacterium avium-Containing Phagosomes in Murine Macrophages. *The Journal of Immunology* 160, 1290-1296
140. MacMicking, J. D., Taylor, G. A., and McKinney, J. D. (2003) Immune Control of Tuberculosis by IFN- $\gamma$ -Inducible LRG-47. *Science* 302, 654-659
141. Flynn, J. L., and Chan, J. (2001) IMMUNOLOGY OF TUBERCULOSIS. *Annual Review of Immunology* 19, 93-129
142. Andrade, R. M., Wessendarp, M., Gubbels, M.-J., Striepen, B., and Subauste, C. S. (2006) CD40 induces macrophage anti-Toxoplasma gondii activity by triggering autophagy-dependent fusion of pathogen-containing vacuoles and lysosomes. *The Journal of Clinical Investigation* 116, 2366-2377
143. Jia, G., Cheng, G., Gangahar, D. M., and Agrawal, D. K. (2006) Insulin-like growth factor-1 and TNF-[alpha] regulate autophagy through c-jun N-terminal kinase and Akt pathways in human atherosclerotic vascular smooth cells. *Immunol Cell Biol* 84, 448-454
144. Ling, Y. M., Shaw, M. H., Ayala, C., Coppens, I., Taylor, G. A., Ferguson, D. J. P., and Yap, G. S. (2006) Vacuolar and plasma membrane stripping and autophagic elimination of Toxoplasma gondii in primed effector macrophages. *The Journal of Experimental Medicine* 203, 2063-2071
145. Baregamian, N., Song, J., Bailey, C. E., Papaconstantinou, J., Evers, B. M., and Chung, D. H. (2009) Tumor Necrosis Factor- $\alpha$ ; and Apoptosis Signal-Regulating Kinase 1 Control Reactive Oxygen Species Release, Mitochondrial Autophagy and C-Jun N-Terminal Kinase/P38 Phosphorylation During Necrotizing Enterocolitis. *Oxidative Medicine and Cellular Longevity* 2, 297-306
146. Harris, J., and Keane, J. (2010) How tumour necrosis factor blockers interfere with tuberculosis immunity. *Clinical & Experimental Immunology* 161, 1-9
147. Keller, C. W., Fokken, C., Turville, S. G., Lünemann, A., Schmidt, J., Münz, C., and Lünemann, J. D. (2011) TNF- $\alpha$  Induces Macroautophagy and Regulates MHC Class II Expression in Human Skeletal Muscle Cells. *Journal of Biological Chemistry* 286, 3970-3980
148. Harris, J. (2011) Autophagy and cytokines. *Cytokine* 56, 140-144

149. Petiot, A., Ogier-Denis, E., Blommaert, E. F. C., Meijer, A. J., and Codogno, P. (2000) Distinct Classes of Phosphatidylinositol 3'-Kinases Are Involved in Signaling Pathways That Control Macroautophagy in HT-29 Cells. *Journal of Biological Chemistry* 275, 992-998
150. Arico, S., Petiot, A., Bauvy, C., Dubbelhuis, P. F., Meijer, A. J., Codogno, P., and Ogier-Denis, E. (2001) The Tumor Suppressor PTEN Positively Regulates Macroautophagy by Inhibiting the Phosphatidylinositol 3-Kinase/Protein Kinase B Pathway. *Journal of Biological Chemistry* 276, 35243-35246
151. Harris, J., De Haro, S. A., Master, S. S., Keane, J., Roberts, E. A., Delgado, M., and Deretic, V. (2007) T Helper 2 Cytokines Inhibit Autophagic Control of Intracellular Mycobacterium tuberculosis. *Immunity* 27, 505-517
152. Harris, J., Master, S. S., De Haro, S. A., Delgado, M., Roberts, E. A., Hope, J. C., Keane, J., and Deretic, V. (2009) Th1–Th2 polarisation and autophagy in the control of intracellular mycobacteria by macrophages. *Veterinary Immunology and Immunopathology* 128, 37-43
153. Van Grol, J., Subauste, C., Andrade, R. M., Fujinaga, K., Nelson, J., and Subauste, C. S. (2010) HIV-1 Inhibits Autophagy in Bystander Macrophage/Monocytic Cells through Src-Akt and STAT3. *PLoS ONE* 5, e11733
154. Park, H.-J., Lee, S. J., Kim, S.-H., Han, J., Bae, J., Kim, S. J., Park, C.-G., and Chun, T. (2011) IL-10 inhibits the starvation induced autophagy in macrophages via class I phosphatidylinositol 3-kinase (PI3K) pathway. *Molecular Immunology* 48, 720-727
155. Crişan, T. O., Plantinga, T. S., van de Veerdonk, F. L., Farcaş, M. F., Stoffels, M., Kullberg, B.-J., van der Meer, J. W. M., Joosten, L. A. B., and Netea, M. G. (2011) Inflammasome-Independent Modulation of Cytokine Response by Autophagy in Human Cells. *PLoS ONE* 6, e18666
156. Dong, X., and Levine, B. (2013) Autophagy and viruses: adversaries or allies? *Journal of innate immunity* 5, 480-493
157. Levine, B., Mizushima, N., and Virgin, H. W. (2011) Autophagy in immunity and inflammation. *Nature* 469, 323-335
158. Orvedahl, A., and Levine, B. (2009) Autophagy in mammalian antiviral immunity. *Autophagy in Infection and Immunity*, pp. 267-285, Springer
159. Orvedahl, A., Sumpter Jr, R., Xiao, G., Ng, A., Zou, Z., Tang, Y., Narimatsu, M., Gilpin, C., Sun, Q., and Roth, M. (2011) Image-based genome-wide siRNA screen identifies selective autophagy factors. *Nature* 480, 113-117
160. Delgado, M. A., Elmaoued, R. A., Davis, A. S., Kyei, G., and Deretic, V. (2008) Toll-like receptors control autophagy. *EMBO J* 27, 1110-1121
161. Shi, C.-S., and Kehrl, J. H. (2008) MyD88 and Trif Target Beclin 1 to Trigger Autophagy in Macrophages. *Journal of Biological Chemistry* 283, 33175-33182

162. Lee, H. K., Lund, J. M., Ramanathan, B., Mizushima, N., and Iwasaki, A. (2007) Autophagy-Dependent Viral Recognition by Plasmacytoid Dendritic Cells. *Science* 315, 1398-1401
163. Deretic, V., and Levine, B. (2009) Autophagy, immunity, and microbial adaptations. *Cell host & microbe* 5, 527-549
164. Singh, R., Kaushik, S., Wang, Y., Xiang, Y., Novak, I., Komatsu, M., Tanaka, K., Cuervo, A. M., and Czaja, M. J. (2009) Autophagy regulates lipid metabolism. *Nature* 458, 1131-1135
165. Jackson, W. T., Giddings Jr, T. H., Taylor, M. P., Mulinyawe, S., Rabinovitch, M., Kopito, R. R., and Kirkegaard, K. (2005) Subversion of cellular autophagosomal machinery by RNA viruses. *PLoS biology* 3, e156
166. Ait-Goughoulte, M., Kanda, T., Meyer, K., Ryerse, J. S., Ray, R. B., and Ray, R. (2008) Hepatitis C virus genotype 1a growth and induction of autophagy. *Journal of virology* 82, 2241-2249
167. Sir, D., Kuo, C.-f., Tian, Y., Liu, H. M., Huang, E. J., Jung, J. U., Machida, K., and Ou, J.-h. J. (2012) Replication of hepatitis C virus RNA on autophagosomal membranes. *Journal of Biological Chemistry* 287, 18036-18043
168. Alirezaei, M., Flynn, C. T., Wood, M. R., and Whitton, J. L. (2012) Pancreatic acinar cell-specific autophagy disruption reduces coxsackievirus replication and pathogenesis in vivo. *Cell host & microbe* 11, 298-305
169. Tian, Y., Sir, D., Kuo, C.-f., Ann, D. K., and Ou, J.-h. J. (2011) Autophagy required for hepatitis B virus replication in transgenic mice. *Journal of virology* 85, 13453-13456
170. Grégoire, I. P., Richetta, C., Meyniel-Schicklin, L., Borel, S., Pradezynski, F., Diaz, O., Deloire, A., Azocar, O., Baguet, J., and Le Breton, M. (2011) IRGM is a common target of RNA viruses that subvert the autophagy network. *PLoS pathogens* 7, e1002422
171. Taylor, T. J., Brockman, M. A., McNamee, E. E., and Knipe, D. M. (2002) Herpes simplex virus. *Frontiers in bioscience: a journal and virtual library* 7, d752-764
172. Whitley, R. J., and Roizman, B. (2001) Herpes simplex virus infections. *The Lancet* 357, 1513-1518
173. Roizman, B. (2001) *Herpes simplex viruses and their replication*, Lippincott, Williams and Wilkins, Philadelphia, PA
174. Wildy, P., Russell, W., and Horne, R. (1960) The morphology of herpes virus. *Virology* 12, 204-222
175. Becker, Y., Dym, H., and Sarov, I. (1968) Herpes simplex virus DNA. *Virology* 36, 184-192

176. Kieff, E. D., Bachenheimer, S. L., and Roizman, B. (1971) Size, composition, and structure of the deoxyribonucleic acid of herpes simplex virus subtypes 1 and 2. *Journal of virology* 8, 125-132
177. Plummer, G., Goodheart, C., Henson, D., and Bowling, C. (1969) A comparative study of the DNA density and behavior in tissue cultures of fourteen different herpesviruses. *Virology* 39, 134-137
178. Furlong, D., Swift, H., and Roizman, B. (1972) Arrangement of herpesvirus deoxyribonucleic acid in the core. *Journal of virology* 10, 1071-1074
179. Zhou, Z. H., Chen, D. H., Jakana, J., Rixon, F. J., and Chiu, W. (1999) Visualization of tegument-capsid interactions and DNA in intact herpes simplex virus type 1 virions. *Journal of virology* 73, 3210-3218
180. McGeoch, D., Dalrymple, M., Davison, A., Dolan, A., Frame, M., McNab, D., Perry, L., Scott, J., and Taylor, P. (1988) The complete DNA sequence of the long unique region in the genome of herpes simplex virus type 1. *J. gen. Virol* 69, 1531-1574
181. McGeoch, D. J., Dolan, A., Donald, S., and Brauer, D. H. (1986) Complete DNA sequence of the short repeat region in the genome of herpes simplex virus type 1. *Nucleic acids research* 14, 1727-1745
182. Wadsworth, S., Jacob, R., and Roizman, B. (1975) Anatomy of herpes simplex virus DNA. II. Size, composition, and arrangement of inverted terminal repetitions. *Journal of virology* 15, 1487-1497
183. Roizman, B., and Campadelli-Fiume, G. (2007) Alphaherpes viral genes and their functions.
184. Siminoff, P., and Menefee, M. (1966) Normal and 5-bromodeoxyuridine-inhibited development of herpes simplex virus: An electron microscope study. *Experimental cell research* 44, 241-255
185. Stackpole, C. W. (1969) Herpes-type virus of the frog renal adenocarcinoma: I. Virus development in tumor transplants maintained at low temperature. *Journal of virology* 4, 75
186. Enquist, L., Husak, P. J., Banfield, B. W., and Smith, G. A. (1998) INFECTION AND SPREAD OF ALPI—IAHERPESVIRUSES IN THE NERVOUS SYSTEM. *Advances in virus research* 51, 237
187. Honess, R. W., and Roizman, B. (1974) Regulation of herpesvirus macromolecular synthesis I. Cascade regulation of the synthesis of three groups of viral proteins. *Journal of virology* 14, 8-19
188. Faber, S. W., and Wilcox, K. W. (1986) Association of the herpes simplex virus regulatory protein ICP4 with specific nucleotide sequences in DNA. *Nucleic acids research* 14, 6067-6083



189. Kristie, T. M., and Roizman, B. (1984) Separation of sequences defining basal expression from those conferring alpha gene recognition within the regulatory domains of herpes simplex virus 1 alpha genes. *Proceedings of the National Academy of Sciences* 81, 4065-4069
190. Muller, M. T. (1987) Binding of the herpes simplex virus immediate-early gene product ICP4 to its own transcription start site. *Journal of virology* 61, 858-865
191. Leopardi, R., Michael, N., and Roizman, B. (1995) Repression of the herpes simplex virus 1 alpha 4 gene by its gene product (ICP4) within the context of the viral genome is conditioned by the distance and stereoaxial alignment of the ICP4 DNA binding site relative to the TATA box. *Journal of virology* 69, 3042-3048
192. Godowski, P. J., and Knipe, D. M. (1983) Mutations in the major DNA-binding protein gene of herpes simplex virus type 1 result in increased levels of viral gene expression. *Journal of virology* 47, 478-486
193. Godowski, P. J., and Knipe, D. M. (1985) Identification of a herpes simplex virus function that represses late gene expression from parental viral genomes. *Journal of virology* 55, 357-365
194. Godowski, P. J., and Knipe, D. M. (1986) Transcriptional control of herpesvirus gene expression: gene functions required for positive and negative regulation. *Proceedings of the National Academy of Sciences* 83, 256-260
195. Roizman, B., and Tognon, M. (1983) Restriction endonuclease patterns of herpes simplex virus DNA: application to diagnosis and molecular epidemiology. *New Developments in Diagnostic Virology*, pp. 273-286, Springer
196. Zelus, B. D., Stewart, R. S., and Ross, J. (1996) The virion host shutoff protein of herpes simplex virus type 1: messenger ribonucleolytic activity in vitro. *Journal of virology* 70, 2411-2419
197. Karr, B. M., and Read, G. S. (1999) The< i> Virion Host Shutoff</i> Function of Herpes Simplex Virus Degrades the 5' End of a Target mRNA before the 3' End. *Virology* 264, 195-204
198. Kwong, A., Kruper, J. A., and Frenkel, N. (1988) Herpes simplex virus virion host shutoff function. *Journal of virology* 62, 912-921
199. Sandri-Goldin, R. M., Hibbard, M. K., and Hardwicke, M. A. (1995) The C-terminal repressor region of herpes simplex virus type 1 ICP27 is required for the redistribution of small nuclear ribonucleoprotein particles and splicing factor SC35; however, these alterations are not sufficient to inhibit host cell splicing. *Journal of virology* 69, 6063-6076
200. Sandri-Goldin, R. M., and Hibbard, M. K. (1996) The herpes simplex virus type 1 regulatory protein ICP27 coimmunoprecipitates with anti-Sm antiserum, and the C terminus appears to be required for this interaction. *Journal of virology* 70, 108-118

201. Advani, S., Brandimarti, R., Weichselbaum, R., and Roizman, B. (2000) The disappearance of cyclins A and B and the increase in activity of the G2/M-phase cellular kinase cdc2 in herpes simplex virus 1-infected cells require expression of the  $\alpha 22$ /US1.5 and UL13 viral genes. *Journal of virology* 74, 8-15
202. Advani, S. J., Weichselbaum, R. R., and Roizman, B. (2000) E2F proteins are posttranslationally modified concomitantly with a reduction in nuclear binding activity in cells infected with herpes simplex virus 1. *Journal of virology* 74, 7842-7850
203. Rock, D., and Fraser, N. (1985) Latent herpes simplex virus type 1 DNA contains two copies of the virion DNA joint region. *Journal of virology* 55, 849-852
204. Mellerick, D., and Fraser, N. (1987) Physical state of the latent herpes simplex virus genome in a mouse model system: evidence suggesting an episomal state. *Virology* 158, 265-275
205. Carton, C. A., and Kilbourne, E. D. (1952) Activation of latent herpes simplex by trigeminal sensory-root section. *New England Journal of Medicine* 246, 172-176
206. Balfour Jr, H. H. (1999) Antiviral drugs. *The New England journal of medicine* 340, 1255-1268
207. Burke, R. (1993) Current status of HSV vaccine development. *The Human Herpesvirus. New York: Raven*, 367-379
208. Corey, L., Langenberg, A. G., Ashley, R., Sekulovich, R. E., Izu, A. E., Douglas Jr, J. M., Handsfield, H. H., Warren, T., Marr, L., and Tyring, S. (1999) Recombinant glycoprotein vaccine for the prevention of genital HSV-2 infection: two randomized controlled trials. *Jama* 282, 331-340
209. Ship, I., Ashe, W., and Scherp, H. (1961) Recurrent "fever blister" and "canker sore" tests for herpes simplex and other viruses with mammalian cell cultures. *Archives of oral biology* 3, 117-1111
210. Knickelbein, J. E., Khanna, K. M., Yee, M. B., Baty, C. J., Kinchington, P. R., and Hendricks, R. L. (2008) Noncytotoxic lytic granule-mediated CD8<sup>+</sup> T cell inhibition of HSV-1 reactivation from neuronal latency. *Science* 322, 268-271
211. Liu, T., Khanna, K. M., Chen, X., Fink, D. J., and Hendricks, R. L. (2000) CD8<sup>+</sup> T cells can block herpes simplex virus type 1 (HSV-1) reactivation from latency in sensory neurons. *The Journal of experimental medicine* 191, 1459-1466
212. Liu, T., Khanna, K. M., Carriere, B. N., and Hendricks, R. L. (2001) Gamma interferon can prevent herpes simplex virus type 1 reactivation from latency in sensory neurons. *Journal of virology* 75, 11178-11184
213. Rajasagi, N. K., Kassim, S. H., Kollias, C. M., Zhao, X., Chervenak, R., and Jennings, S. R. (2009) CD4<sup>+</sup> T cells are required for the priming of CD8<sup>+</sup> T cells following infection with herpes simplex virus type 1. *Journal of virology* 83, 5256-5268

214. Wallace, M. E., Keating, R., Heath, W. R., and Carbone, F. R. (1999) The Cytotoxic T-Cell Response to Herpes Simplex Virus Type 1 Infection of C57BL/6 Mice Is Almost Entirely Directed against a Single Immunodominant Determinant. *Journal of Virology* 73, 7619-7626
215. Sheridan, P. A., and Beck, M. A. (2009) The dendritic and T cell responses to herpes simplex virus-1 are modulated by dietary vitamin E. *Free Radical Biology and Medicine* 46, 1581-1588
216. Jing, L., Schiffer, J. T., Chong, T. M., Bruckner, J. J., Davies, D. H., Felgner, P. L., Haas, J., Wald, A., Verjans, G. M. G. M., and Koelle, D. M. (2013) CD4 T-Cell Memory Responses to Viral Infections of Humans Show Pronounced Immunodominance Independent of Duration or Viral Persistence. *Journal of Virology* 87, 2617-2627
217. Orr, M. T., Edelmann, K. H., Vieira, J., Corey, L., Raulet, D. H., and Wilson, C. B. (2005) Inhibition of MHC class I is a virulence factor in herpes simplex virus infection of mice. *PLoS pathogens* 1, e7
218. Goldsmith, K., Chen, W., Johnson, D. C., and Hendricks, R. L. (1998) Infected cell protein (ICP) 47 enhances herpes simplex virus neurovirulence by blocking the CD8+ T cell response. *The Journal of experimental medicine* 187, 341-348
219. Yuan, W., Dasgupta, A., and Cresswell, P. (2006) Herpes simplex virus evades natural killer T cell recognition by suppressing CD1d recycling. *Nature immunology* 7, 835-842
220. Sievers, E., Neumann, J., Raftery, M., SchÖnrich, G., Eis-Hübinger, A. M., and Koch, N. (2002) Glycoprotein B from strain 17 of herpes simplex virus type I contains an invariant chain homologous sequence that binds to MHC class II molecules. *Immunology* 107, 129-135
221. Neumann, J., Eis-Hübinger, A. M., and Koch, N. (2003) Herpes simplex virus type 1 targets the MHC class II processing pathway for immune evasion. *The Journal of Immunology* 171, 3075-3083
222. Van Vliet, K., De Graaf-Miltenburg, L., Verhoef, J., and Van Strijp, J. (1992) Direct evidence for antibody bipolar bridging on herpes simplex virus-infected cells. *Immunology* 77, 109
223. Orvedahl, A., Alexander, D., Tallóczy, Z., Sun, Q., Wei, Y., Zhang, W., Burns, D., Leib, D. A., and Levine, B. (2007) HSV-1 ICP34.5 Confers Neurovirulence by Targeting the Beclin 1 Autophagy Protein. *Cell Host & Microbe* 1, 23-35
224. Johnson, K. E., Song, B., and Knipe, D. M. (2008) Role for herpes simplex virus 1 ICP27 in the inhibition of type I interferon signaling. *Virology* 374, 487-494
225. Eisemann, J., Mühl-Zürbes, P., Steinkasserer, A., and Kummer, M. (2008) Infection of mature dendritic cells with herpes simplex virus type 1 interferes with the interferon signaling pathway. *Immunobiology* 212, 877-886

226. Melroe, G. T., DeLuca, N. A., and Knipe, D. M. (2004) Herpes simplex virus 1 has multiple mechanisms for blocking virus-induced interferon production. *Journal of virology* 78, 8411-8420
227. Chou, J., Kern, E. R., Whitley, R. J., and Roizman, B. (1990) Mapping of herpes simplex virus-1 neurovirulence to gamma 134.5, a gene nonessential for growth in culture. *Science* 250, 1262-1266
228. Chou, J., and Roizman, B. (1994) Herpes simplex virus 1 gamma(1)34.5 gene function, which blocks the host response to infection, maps in the homologous domain of the genes expressed during growth arrest and DNA damage. *Proceedings of the National Academy of Sciences* 91, 5247-5251
229. He, B., Chou, J., Liebermann, D. A., Hoffman, B., and Roizman, B. (1996) The carboxyl terminus of the murine MyD116 gene substitutes for the corresponding domain of the gamma (1) 34.5 gene of herpes simplex virus to preclude the premature shutoff of total protein synthesis in infected human cells. *Journal of virology* 70, 84-90
230. He, B., Gross, M., and Roizman, B. (1997) The  $\gamma$ 134.5 protein of herpes simplex virus 1 complexes with protein phosphatase 1 $\alpha$  to dephosphorylate the  $\alpha$  subunit of the eukaryotic translation initiation factor 2 and preclude the shutoff of protein synthesis by double-stranded RNA-activated protein kinase. *Proceedings of the National Academy of Sciences* 94, 843-848
231. Tallóczy, Z., Jiang, W., Virgin, H. W., Leib, D. A., Scheuner, D., Kaufman, R. J., Eskelinen, E.-L., and Levine, B. (2002) Regulation of starvation- and virus-induced autophagy by the eIF2 $\alpha$  kinase signaling pathway. *Proceedings of the National Academy of Sciences* 99, 190-195
232. Radtke, K., English, L., Rondeau, C., Leib, D., Lippe, R., and Desjardins, M. (2013) Inhibition of the Host Translation Shut-off Response by Herpes Simplex Virus 1 triggers Nuclear Envelope-derived Autophagy. *J Virol* 87, 3990-3997
233. Cox, J., and Mann, M. (2011) Quantitative, high-resolution proteomics for data-driven systems biology. *Annual review of biochemistry* 80, 273-299
234. Aebersold, R., and Mann, M. (2003) Mass spectrometry-based proteomics. *Nature* 422, 198-207
235. Hanash, S. M. (2000) Biomedical applications of two-dimensional electrophoresis using immobilized pH gradients: Current status. *Electrophoresis* 21, 1202-1209
236. Pandey, A., and Mann, M. (2000) Proteomics to study genes and genomes. *Nature* 405, 837-846
237. Gygi, S. P., Rochon, Y., Franza, B. R., and Aebersold, R. (1999) Correlation between protein and mRNA abundance in yeast. *Molecular and cellular biology* 19, 1720-1730
238. Santoni, V., Molloy, M., and Rabilloud, T. (2000) Membrane proteins and proteomics: un amour impossible? *Electrophoresis* 21, 1054-1070

239. Gygi, S. P., Corthals, G. L., Zhang, Y., Rochon, Y., and Aebersold, R. (2000) Evaluation of two-dimensional gel electrophoresis-based proteome analysis technology. *Proceedings of the National Academy of Sciences* 97, 9390-9395
240. Eeltink, S., Dolman, S., Swart, R., Ursem, M., and Schoenmakers, P. J. (2009) Optimizing the peak capacity per unit time in one-dimensional and off-line two-dimensional liquid chromatography for the separation of complex peptide samples. *Journal of Chromatography A* 1216, 7368-7374
241. Nagaraj, N., Kulak, N. A., Cox, J., Neuhauser, N., Mayr, K., Hoerning, O., Vorm, O., and Mann, M. (2012) System-wide perturbation analysis with nearly complete coverage of the yeast proteome by single-shot ultra HPLC runs on a bench top Orbitrap. *Molecular & Cellular Proteomics* 11, M111. 013722
242. Wisniewski, J. R., Nagaraj, N., Zougman, A., Gnäd, F., and Mann, M. (2010) Brain phosphoproteome obtained by a FASP-based method reveals plasma membrane protein topology. *Journal of proteome research* 9, 3280-3289
243. Wolters, D. A., Washburn, M. P., and Yates, J. R. (2001) An automated multidimensional protein identification technology for shotgun proteomics. *Analytical chemistry* 73, 5683-5690
244. Washburn, M. P., Wolters, D., and Yates, J. R. (2001) Large-scale analysis of the yeast proteome by multidimensional protein identification technology. *Nature biotechnology* 19, 242-247
245. Bantscheff, M., Lemeer, S., Savitski, M. M., and Kuster, B. (2012) Quantitative mass spectrometry in proteomics: critical review update from 2007 to the present. *Analytical and bioanalytical chemistry* 404, 939-965
246. Dole, M., Mack, L., Hines, R., Mobley, R., Ferguson, L., and Alice, M. d. (1968) Molecular beams of macroions. *The Journal of Chemical Physics* 49, 2240-2249
247. Fenn, J. B., Mann, M., Meng, C. K., Wong, S. F., and Whitehouse, C. M. (1989) Electrospray ionization for mass spectrometry of large biomolecules. *Science* 246, 64-71
248. Fenn, J. B. (2003) Electrospray wings for molecular elephants (Nobel lecture). *Angewandte Chemie International Edition* 42, 3871-3894
249. Tanaka, K. (2003) The origin of macromolecule ionization by laser irradiation (Nobel lecture). *Angewandte Chemie International Edition* 42, 3860-3870
250. Wüthrich, K. (2003) NMR studies of structure and function of biological macromolecules (Nobel Lecture). *Angewandte Chemie International Edition* 42, 3340-3363
251. Glish, G. L., and Vachet, R. W. (2003) The basics of mass spectrometry in the twenty-first century. *Nature Reviews Drug Discovery* 2, 140-150

252. Taylor, G. (1964) Disintegration of water drops in an electric field. *Proceedings of the Royal Society of London. Series A. Mathematical and Physical Sciences* 280, 383-397
253. Iribarne, J., and Thomson, B. (1976) On the evaporation of small ions from charged droplets. *The Journal of Chemical Physics* 64, 2287-2294
254. Thomson, B., and Iribarne, J. (1979) Field induced ion evaporation from liquid surfaces at atmospheric pressure. *The Journal of Chemical Physics* 71, 4451-4463
255. Stahl, D., Swiderek, K., Davis, M., and Lee, T. (1996) Data-controlled automation of liquid chromatography/tandem mass spectrometry analysis of peptide mixtures. *J Am Soc Mass Spectrom* 7, 532-540
256. Egertson, J. D., Kuehn, A., Merrihew, G. E., Bateman, N. W., MacLean, B. X., Ting, Y. S., Canterbury, J. D., Marsh, D. M., Kellmann, M., Zabrouskov, V., Wu, C. C., and MacCoss, M. J. (2013) Multiplexed MS/MS for improved data-independent acquisition. *Nat Meth* 10, 744-746
257. McLuckey, S. A. (1992) Principles of collisional activation in analytical mass spectrometry. *J Am Soc Mass Spectrom* 3, 599-614
258. Shukla, A. K., and Futrell, J. H. (2000) Tandem mass spectrometry: dissociation of ions by collisional activation. *Journal of Mass Spectrometry* 35, 1069-1090
259. Olsen, J. V., Macek, B., Lange, O., Makarov, A., Horning, S., and Mann, M. (2007) Higher-energy C-trap dissociation for peptide modification analysis. *Nature methods* 4, 709-712
260. McAlister, G. C., Phanstiel, D. H., Brumbaugh, J., Westphall, M. S., and Coon, J. J. (2011) Higher-energy collision-activated dissociation without a dedicated collision cell. *Molecular & Cellular Proteomics* 10, O111. 009456
261. Jedrychowski, M. P., Huttlin, E. L., Haas, W., Sowa, M. E., Rad, R., and Gygi, S. P. (2011) Evaluation of HCD-and CID-type fragmentation within their respective detection platforms for murine phosphoproteomics. *Molecular & Cellular Proteomics* 10, M111. 009910
262. Zubarev, R. A., Horn, D. M., Fridriksson, E. K., Kelleher, N. L., Kruger, N. A., Lewis, M. A., Carpenter, B. K., and McLafferty, F. W. (2000) Electron capture dissociation for structural characterization of multiply charged protein cations. *Analytical chemistry* 72, 563-573
263. Syka, J. E., Coon, J. J., Schroeder, M. J., Shabanowitz, J., and Hunt, D. F. (2004) Peptide and protein sequence analysis by electron transfer dissociation mass spectrometry. *Proceedings of the National Academy of Sciences of the United States of America* 101, 9528-9533
264. Sleno, L., and Volmer, D. A. (2004) Ion activation methods for tandem mass spectrometry. *Journal of mass spectrometry* 39, 1091-1112

265. Pekar Second, T., Blethrow, J. D., Schwartz, J. C., Merrihew, G. E., MacCoss, M. J., Swaney, D. L., Russell, J. D., Coon, J. J., and Zabrouskov, V. (2009) Dual-pressure linear ion trap mass spectrometer improving the analysis of complex protein mixtures. *Analytical chemistry* 81, 7757-7765
266. Roepstorff, P., Fohlmann, J. (1984) Proposal for a common nomenclature for sequence ions in mass spectra of peptides. *Biomed Mass Spectrom* 11, 601
267. Biemann, K. (1992) Mass spectrometry of peptides and proteins. *Annual review of biochemistry* 61, 977-1010
268. Bell, C. (2009) Characterization of *Mycobacterium tuberculosis* membrane proteins by liquid chromatography mass spectrometry-based proteomics techniques. *Diplomarbeit, Fachbereich Chemie, Pharmazie und Geowissenschaften, Johannes Gutenberg-Universität Mainz*
269. Steen, H., and Mann, M. (2004) The ABC's (and XYZ's) of peptide sequencing. *Nature reviews Molecular cell biology* 5, 699-711
270. March, R. E. (1997) An introduction to quadrupole ion trap mass spectrometry. *Journal of mass spectrometry* 32, 351-369
271. Volmer, D. A., and Sleno, L. (2005) Mass Analyzers: An overview of several designs and their applications, part II. *Spectroscopy* 20, 90-95
272. Makarov, A. (2000) Electrostatic axially harmonic orbital trapping: a high-performance technique of mass analysis. *Analytical chemistry* 72, 1156-1162
273. Hardman, M., and Makarov, A. A. (2003) Interfacing the orbitrap mass analyzer to an electrospray ion source. *Analytical chemistry* 75, 1699-1705
274. Yates, J. R., Cociorva, D., Liao, L., and Zabrouskov, V. (2006) Performance of a linear ion trap-Orbitrap hybrid for peptide analysis. *Analytical chemistry* 78, 493-500
275. Macek, B., Waanders, L. F., Olsen, J. V., and Mann, M. (2006) Top-down protein sequencing and MS3 on a hybrid linear quadrupole ion trap-orbitrap mass spectrometer. *Molecular & Cellular Proteomics* 5, 949-958
276. Scigelova, M., and Makarov, A. (2006) Orbitrap mass analyzer—overview and applications in proteomics. *Proteomics* 6, 16-21
277. Michalski, A., Damoc, E., Lange, O., Denisov, E., Nolting, D., Müller, M., Viner, R., Schwartz, J., Remes, P., and Belford, M. (2012) Ultra high resolution linear ion trap Orbitrap mass spectrometer (Orbitrap Elite) facilitates top down LC MS/MS and versatile peptide fragmentation modes. *Molecular & Cellular Proteomics* 11, O111. 013698
278. Olsen, J. V., Schwartz, J. C., Griep-Raming, J., Nielsen, M. L., Damoc, E., Denisov, E., Lange, O., Remes, P., Taylor, D., and Splendore, M. (2009) A dual pressure linear ion trap Orbitrap instrument with very high sequencing speed. *Molecular & Cellular Proteomics* 8, 2759-2769

279. Michalski, A., Damoc, E., Hauschild, J.-P., Lange, O., Wiegand, A., Makarov, A., Nagaraj, N., Cox, J., Mann, M., and Horning, S. (2011) Mass spectrometry-based proteomics using Q Exactive, a high-performance benchtop quadrupole Orbitrap mass spectrometer. *Molecular & Cellular Proteomics* 10, M111. 011015
280. Senko, M. W., Remes, P. M., Canterbury, J. D., Mathur, R., Song, Q., Eliuk, S. M., Mullen, C., Earley, L., Hardman, M., Blethrow, J. D., Bui, H., Specht, A., Lange, O., Denisov, E., Makarov, A., Horning, S., and Zabrouskov, V. (2013) Novel Parallelized Quadrupole/Linear Ion Trap/Orbitrap Tribrid Mass Spectrometer Improving Proteome Coverage and Peptide Identification Rates. *Analytical Chemistry* 85, 11710-11714
281. Gerber, S. A., Rush, J., Stemman, O., Kirschner, M. W., and Gygi, S. P. (2003) Absolute quantification of proteins and phosphoproteins from cell lysates by tandem MS. *Proceedings of the National Academy of Sciences* 100, 6940-6945
282. Ong, S.-E., Blagoev, B., Kratchmarova, I., Kristensen, D. B., Steen, H., Pandey, A., and Mann, M. (2002) Stable isotope labeling by amino acids in cell culture, SILAC, as a simple and accurate approach to expression proteomics. *Molecular & cellular proteomics* 1, 376-386
283. Geiger, T., Cox, J., Ostasiewicz, P., Wisniewski, J. R., and Mann, M. (2010) Super-SILAC mix for quantitative proteomics of human tumor tissue. *Nature methods* 7, 383-385
284. Thompson, A., Schäfer, J., Kuhn, K., Kienle, S., Schwarz, J., Schmidt, G., Neumann, T., and Hamon, C. (2003) Tandem mass tags: a novel quantification strategy for comparative analysis of complex protein mixtures by MS/MS. *Analytical chemistry* 75, 1895-1904
285. Ross, P. L., Huang, Y. N., Marchese, J. N., Williamson, B., Parker, K., Hattan, S., Khainovski, N., Pillai, S., Dey, S., Daniels, S., Purkayastha, S., Juhasz, P., Martin, S., Bartlett-Jones, M., He, F., Jacobson, A., and Pappin, D. J. (2004) Multiplexed Protein Quantitation in *Saccharomyces cerevisiae* Using Amine-reactive Isobaric Tagging Reagents. *Molecular & Cellular Proteomics* 3, 1154-1169
286. Wiese, S., Reidegeld, K. A., Meyer, H. E., and Warscheid, B. (2007) Protein labeling by iTRAQ: a new tool for quantitative mass spectrometry in proteome research. *Proteomics* 7, 340-350
287. Boersema, P. J., Aye, T. T., van Veen, T. A. B., Heck, A. J. R., and Mohammed, S. (2008) Triplex protein quantification based on stable isotope labeling by peptide dimethylation applied to cell and tissue lysates. *PROTEOMICS* 8, 4624-4632
288. Boersema, P. J., Raijmakers, R., Lemeer, S., Mohammed, S., and Heck, A. J. R. (2009) Multiplex peptide stable isotope dimethyl labeling for quantitative proteomics. *Nat. Protocols* 4, 484-494
289. Cooper, B., Feng, J., and Garrett, W. (2010) Relative, label-free protein quantitation: Spectral counting error statistics from nine replicate MudPIT samples. *J Am Soc Mass Spectrom* 21, 1534-1546



290. Zhou, J.-Y., Schepmoes, A. A., Zhang, X., Moore, R. J., Monroe, M. E., Lee, J. H., Camp, D. G., Smith, R. D., and Qian, W.-J. (2010) Improved LC-MS/MS Spectral Counting Statistics by Recovering Low-Scoring Spectra Matched to Confidently Identified Peptide Sequences. *Journal of Proteome Research* 9, 5698-5704
291. Keller, A., Nesvizhskii, A. I., Kolker, E., and Aebersold, R. (2002) Empirical statistical model to estimate the accuracy of peptide identifications made by MS/MS and database search. *Analytical chemistry* 74, 5383-5392
292. Pruitt, K. D., Tatusova, T., and Maglott, D. R. (2005) NCBI Reference Sequence (RefSeq): a curated non-redundant sequence database of genomes, transcripts and proteins. *Nucleic acids research* 33, D501-D504
293. Consortium, U. (2008) The universal protein resource (UniProt). *Nucleic acids research* 36, D190-D195
294. Mann, M., and Wilm, M. (1994) Error-tolerant identification of peptides in sequence databases by peptide sequence tags. *Analytical chemistry* 66, 4390-4399
295. Eng, J. K., McCormack, A. L., and Yates, J. R. (1994) An approach to correlate tandem mass spectral data of peptides with amino acid sequences in a protein database. *J Am Soc Mass Spectrom* 5, 976-989
296. Mann, M., Hendrickson, R. C., and Pandey, A. (2001) Analysis of proteins and proteomes by mass spectrometry. *Annual review of biochemistry* 70, 437-473
297. Cottrell, J. S., and London, U. (1999) Probability-based protein identification by searching sequence databases using mass spectrometry data. *Electrophoresis* 20, 3551-3567
298. Keller, A., Purvine, S., Nesvizhskii, A. I., Stolyar, S., Goodlett, D. R., and Kolker, E. (2002) Experimental protein mixture for validating tandem mass spectral analysis. *Omics: a journal of integrative biology* 6, 207-212
299. Elias, J., and Gygi, S. (2010) Target-Decoy Search Strategy for Mass Spectrometry-Based Proteomics. In: Hubbard, S. J., and Jones, A. R., eds. *Proteome Bioinformatics*, pp. 55-71, Humana Press
300. Courcelles, M., Lemieux, S., Voisin, L., Meloche, S., and Thibault, P. (2011) ProteoConnections: a bioinformatics platform to facilitate proteome and phosphoproteome analyses. *Proteomics* 11, 2654-2671
301. Sturm, M., Bertsch, A., Gröpl, C., Hildebrandt, A., Hussong, R., Lange, E., Pfeifer, N., Schulz-Trieglaff, O., Zerck, A., and Reinert, K. (2008) OpenMS—an open-source software framework for mass spectrometry. *BMC bioinformatics* 9, 163
302. Park, S. K., Venable, J. D., Xu, T., and Yates, J. R. (2008) A quantitative analysis software tool for mass spectrometry-based proteomics. *Nature methods* 5, 319-322

303. Mueller, L. N., Rinner, O., Schmidt, A., Letarte, S., Bodenmiller, B., Brusniak, M. Y., Vitek, O., Aebersold, R., and Müller, M. (2007) SuperHirn—a novel tool for high resolution LC-MS-based peptide/protein profiling. *Proteomics* 7, 3470-3480
304. Cox, J., and Mann, M. (2008) MaxQuant enables high peptide identification rates, individualized ppb-range mass accuracies and proteome-wide protein quantification. *Nature biotechnology* 26, 1367-1372
305. Ashburner, M., Ball, C. A., Blake, J. A., Botstein, D., Butler, H., Cherry, J. M., Davis, A. P., Dolinski, K., Dwight, S. S., and Eppig, J. T. (2000) Gene Ontology: tool for the unification of biology. *Nature genetics* 25, 25-29
306. Kanehisa, M., and Goto, S. (2000) KEGG: kyoto encyclopedia of genes and genomes. *Nucleic acids research* 28, 27-30
307. Franceschini, A., Szklarczyk, D., Frankild, S., Kuhn, M., Simonovic, M., Roth, A., Lin, J., Minguez, P., Bork, P., von Mering, C., and Jensen, L. J. (2013) STRING v9.1: protein-protein interaction networks, with increased coverage and integration. *Nucleic Acids Research* 41, D808-D815
308. Roux, P. P., and Thibault, P. (2013) The Coming of Age of Phosphoproteomics—from Large Data Sets to Inference of Protein Functions. *Molecular & Cellular Proteomics* 12, 3453-3464
309. Ficarro, S. B., Zhang, Y., Carrasco-Alfonso, M. J., Garg, B., Adelmant, G., Webber, J. T., Luckey, C. J., and Marto, J. A. (2011) Online nanoflow multidimensional fractionation for high efficiency phosphopeptide analysis. *Molecular & Cellular Proteomics* 10, O111. 011064
310. Villén, J., and Gygi, S. P. (2008) The SCX/IMAC enrichment approach for global phosphorylation analysis by mass spectrometry. *Nature protocols* 3, 1630-1638
311. McNulty, D. E., and Annan, R. S. (2008) Hydrophilic interaction chromatography reduces the complexity of the phosphoproteome and improves global phosphopeptide isolation and detection. *Molecular & Cellular Proteomics* 7, 971-980
312. Nühse, T., Yu, K., and Salomon, A. (2007) Isolation of phosphopeptides by immobilized metal ion affinity chromatography. *Current protocols in molecular biology*, 18.13. 11-18.13. 23
313. Thingholm, T. E., and Jensen, O. N. (2009) Enrichment and characterization of phosphopeptides by immobilized metal affinity chromatography (IMAC) and mass spectrometry. *Phospho-Proteomics*, pp. 47-56, Springer
314. Larsen, M. R., Thingholm, T. E., Jensen, O. N., Roepstorff, P., and Jørgensen, T. J. D. (2005) Highly Selective Enrichment of Phosphorylated Peptides from Peptide Mixtures Using Titanium Dioxide Microcolumns. *Molecular & Cellular Proteomics* 4, 873-886

315. Rikova, K., Guo, A., Zeng, Q., Possemato, A., Yu, J., Haack, H., Nardone, J., Lee, K., Reeves, C., and Li, Y. (2007) Global survey of phosphotyrosine signaling identifies oncogenic kinases in lung cancer. *Cell* 131, 1190-1203
316. Kim, W., Bennett, E. J., Huttlin, E. L., Guo, A., Li, J., Possemato, A., Sowa, M. E., Rad, R., Rush, J., and Comb, M. J. (2011) Systematic and quantitative assessment of the ubiquitin-modified proteome. *Molecular cell* 44, 325-340
317. Santamaría, E., Sánchez-Quiles, V., Fernández-Irigoyen, J., and Corrales, F. (2012) Contribution of MS-based proteomics to the understanding of Herpes Simplex virus type 1 interaction with host cells. *Frontiers in microbiology* 3
318. Fontaine-Rodriguez, E. C., Taylor, T. J., Olesky, M., and Knipe, D. M. (2004) Proteomics of herpes simplex virus infected cell protein 27: association with translation initiation factors. *Virology* 330, 487-492
319. Taylor, T. J., and Knipe, D. M. (2004) Proteomics of herpes simplex virus replication compartments: association of cellular DNA replication, repair, recombination, and chromatin remodeling proteins with ICP8. *Journal of virology* 78, 5856-5866
320. Lester, J. T., and DeLuca, N. A. (2011) Herpes simplex virus 1 ICP4 forms complexes with TFIID and mediator in virus-infected cells. *Journal of virology* 85, 5733-5744
321. Lin, A. E., Greco, T. M., Döhner, K., Sodeik, B., and Cristea, I. M. (2013) A Proteomic Perspective of Inbuilt Viral Protein Regulation: pUL46 Tegument Protein is Targeted for Degradation by ICP0 during Herpes Simplex Virus Type 1 Infection. *Molecular & Cellular Proteomics* 12, 3237-3252
322. Loret, S., Guay, G., and Lippé, R. (2008) Comprehensive characterization of extracellular herpes simplex virus type 1 virions. *Journal of virology* 82, 8605-8618
323. Padula, M. E., Sydnor, M. L., and Wilson, D. W. (2009) Isolation and preliminary characterization of herpes simplex virus 1 primary enveloped virions from the perinuclear space. *Journal of virology* 83, 4757-4765
324. Lippé, R. (2012) Deciphering novel host-herpesvirus interactions by virion proteomics. *Frontiers in microbiology* 3
325. Greco, A., Bienvenut, W., Sanchez, J. C., Kindbeiter, K., Hochstrasser, D., Madjar, J. J., and Diaz, J. J. (2001) Identification of ribosome-associated viral and cellular basic proteins during the course of infection with herpes simplex virus type 1. *Proteomics* 1, 545-549
326. Santamaría, E., Mora, M. I., Potel, C., Fernández-Irigoyen, J., Carro-Roldán, E., Hernández-Alcoceba, R., Prieto, J., Epstein, A. L., and Corrales, F. J. (2009) Identification of Replication-competent HSV-1 Cgal+ Strain Signaling Targets in Human Hepatoma Cells by Functional Organelle Proteomics. *Molecular & Cellular Proteomics* 8, 805-815

327. Sánchez-Quiles, V., Mora, M. I., Segura, V., Greco, A., Epstein, A. L., Foschini, M. G., Dayon, L., Sanchez, J.-C., Prieto, J., Corrales, F. J., and Santamaría, E. (2011) HSV-1 Cgal+ Infection Promotes Quaking RNA Binding Protein Production and Induces Nuclear-Cytoplasmic Shuttling of Quaking I-5 Isoform in Human Hepatoma Cells. *Molecular & Cellular Proteomics* 10
328. Miettinen, J. J., Matikainen, S., and Nyman, T. A. (2012) Global secretome characterization of herpes simplex virus 1-infected human primary macrophages. *Journal of virology* 86, 12770-12778
329. Antrobus, R., Grant, K., Gangadharan, B., Chittenden, D., Everett, R. D., Zitzmann, N., and Boutell, C. (2009) Proteomic analysis of cells in the early stages of herpes simplex virus type-1 infection reveals widespread changes in the host cell proteome. *PROTEOMICS* 9, 3913-3927
330. Zimmermann, A. C., Zarei, M., Eiselein, S., and Dengjel, J. (2010) Quantitative proteomics for the analysis of spatio-temporal protein dynamics during autophagy. *Autophagy* 6, 1009-1016
331. Kristensen, A. R., Schandorff, S., Hoyer-Hansen, M., Nielsen, M. O., Jaattela, M., Dengjel, J., and Andersen, J. S. (2008) Ordered organelle degradation during starvation-induced autophagy. *Molecular & Cellular Proteomics*
332. Rigbolt, K. T., Zarei, M., Sprenger, A., Becker, A. C., Diedrich, B., Huang, X., Eiselein, S., Kristensen, A. R., Gretzmeier, C., and Andersen, J. S. (2013) Characterization of early autophagy signaling by quantitative phosphoproteomics. *Autophagy* 10, 17-32
333. Gao, W., Kang, J. H., Liao, Y., Ding, W.-X., Gambotto, A. A., Watkins, S. C., Liu, Y.-J., Stolz, D. B., and Yin, X.-M. (2010) Biochemical Isolation and Characterization of the Tubulovesicular LC3-positive Autophagosomal Compartment. *Journal of Biological Chemistry* 285, 1371-1383
334. Dengjel, J., Høyer-Hansen, M., Nielsen, M. O., Eisenberg, T., Harder, L. M., Schandorff, S., Farkas, T., Kirkegaard, T., Becker, A. C., Schroeder, S., Vanselow, K., Lundberg, E., Nielsen, M. M., Kristensen, A. R., Akimov, V., Bunkenborg, J., Madeo, F., Jäättelä, M., and Andersen, J. S. (2012) Identification of Autophagosome-associated Proteins and Regulators by Quantitative Proteomic Analysis and Genetic Screens. *Molecular & Cellular Proteomics* 11
335. Mancias, J. D., Wang, X., Gygi, S. P., Harper, J. W., and Kimmelman, A. C. (2014) Quantitative proteomics identifies NCOA4 as the cargo receptor mediating ferritinophagy. *Nature* 509, 105-109
336. Øverbye, A., Brinchmann, M. F., and Seglen, P. O. (2007) Proteomic Analysis of Membrane-Associated Proteins from Rat Liver Autophagosomes. *Autophagy* 3, 300-322
337. Strømhaug, P. E., Berg, T. O., Fengsrud, M., and Seglen, P. O. (1998) Purification and characterization of autophagosomes from rat hepatocytes. *Biochem. J.* 335, 217-224

338. Bell, C., English, L., Boulais, J., Chemali, M., Caron-Lizotte, O., Desjardins, M., and Thibault, P. (2013) Quantitative Proteomics Reveals the Induction of Mitophagy in Tumor Necrosis Factor- $\alpha$ -activated (TNF $\alpha$ ) Macrophages. *Molecular & Cellular Proteomics* 12, 2394-2407
339. Bell, C., Desjardins, M., Thibault, P., and Radtke, K. (2013) Proteomics Analysis of Herpes Simplex Virus Type 1-Infected Cells Reveals Dynamic Changes of Viral Protein Expression, Ubiquitylation, and Phosphorylation. *Journal of Proteome Research* 12, 1820-1829

Parts of 'chapter 1.4. Autophagy' (1.4.3.; 1.4.6.) are adapted from the book chapter: 'Bell, C. et al.: Autophagy's contribution to innate and adaptive immunity: an overview'<sup>39</sup> from the book: 'Autophagy, Infection and the Immune Response'. This material is reproduced with permission from John Wiley & Sons Inc..

Parts of 'chapter 1.6. Mass spectrometry-based proteomics' (1.6.2.; 1.6.3.; 1.6.5.) are adapted from: Christina Bell. 'Characterization of *Mycobacterium tuberculosis* membrane proteins by liquid chromatography mass spectrometry-based proteomics techniques'. Diplomarbeit 2009, Fachbereich Chemie, Pharmazie und Geowissenschaften, Johannes Gutenberg-Universität Mainz<sup>268</sup>.



## **Chapter 2 : Quantitative proteomics reveals the induction of mitophagy in TNF- $\alpha$ activated macrophages**

Christina Bell<sup>1,2</sup>, Luc English<sup>3</sup>, Jonathan Boulais<sup>3</sup>, Magali Chemali<sup>3</sup>,  
Olivier Caron-Lizotte<sup>1</sup>, Michel Desjardins<sup>3\*</sup>, Pierre Thibault<sup>1,2\*</sup>

*Mol Cell Proteomics*, 2013 September, 12 (9): 2394-407

Included with permission of

© The American Society for Biochemistry and Molecular Biology

Institute for Research in Immunology and Cancer<sup>1</sup>, Department of Chemistry<sup>2</sup>,  
Department of Pathology and Cell Biology<sup>3</sup>, Université de Montréal, P.O. Box 6128,  
Station. Centre-ville, Montréal, Québec, Canada H3C 3J7

\*Corresponding authors.

**Running Title: TNF- $\alpha$  induces mitophagy in macrophages**

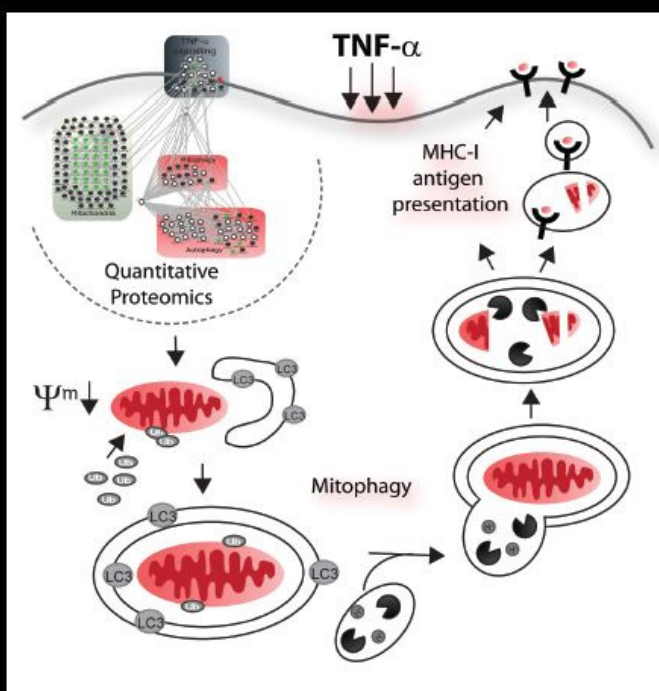




# MOLECULAR & CELLULAR PROTEOMICS

WWW.MCPONLINE.ORG

SEPTEMBER 2013



**ASBMB**  
Published by the  
American Society for Biochemistry  
and Molecular Biology

**On the cover (September 2013):** Quantitative proteomics analyses revealed the specific autophagic degradation of mitochondria in TNF- $\alpha$  activated macrophages. TNF- $\alpha$  induced mitophagy enabled the processing and presentation of mitochondrial antigens at the cell surface by MHC-class-I molecules. These findings highlight an unsuspected role of TNF- $\alpha$  in macrophage activation and expanded our understanding of the mechanisms responsible for the modification of the MHC class I peptide repertoire

## **2.1. Author contributions**

Christina Bell designed, executed and analyzed experiment, wrote the first complete draft and generated the figures. Luc English contributed to project conception and experimental design. Jonathan Boulais and Olivier Caron-Lizotte helped with bioinformatics analyses and Magali Chemali contributed to molecular biology experiments. Pierre Thibault and Michel Desjardins designed the study, analyzed data, discussed results, wrote the manuscript and contributed as senior authors.

## 2.2. Summary

Macrophages play an important role in innate and adaptive immunity as professional phagocytes capable of internalizing and degrading pathogens to derive antigens for presentation to T cells. They also produce pro-inflammatory cytokines such as tumor necrosis factor alpha (TNF- $\alpha$ ) that mediate local and systemic responses and direct the development of adaptive immunity. The present work describes the use of label-free quantitative proteomics to profile the dynamic changes of proteins from resting and TNF- $\alpha$  activated mouse macrophages. These analyses revealed that TNF- $\alpha$  activation of macrophages led to the downregulation of mitochondrial proteins and the differential regulation of several proteins involved in vesicle trafficking and immune response. Importantly, we found that the downregulation of mitochondria proteins occurred through mitophagy and was specific to TNF- $\alpha$ , since other cytokines such as IL-1 $\beta$  and IFN- $\gamma$  had no effect on mitochondria degradation. Furthermore, using a novel antigen presentation system, we observed that the induction of mitophagy by TNF- $\alpha$  enabled the processing and presentation of mitochondrial antigens at the cell surface by MHC class I molecules. These findings highlight an unsuspected role of TNF- $\alpha$  in mitophagy and expanded our understanding of the mechanisms responsible for MHC presentation of self-antigens.

### 2.3. Introduction

Macrophages are professional phagocytes that internalize large particles like dead cells or microorganisms, and play important roles in immunity, inflammation and tissue repair<sup>1</sup>. In mammals, the internalization of microorganisms at sites of infection by macrophages proceeds via a sequential chain of events that leads to sequestration of pathogens in phagosomes where they are killed and degraded by hydrolytic enzymes. The functional properties of phagosomes appeared relatively recently in the evolution of multicellular organisms through the acquisition of molecular machineries that transformed phagosomes from a lytic vacuole into an organelle fully competent for antigen presentation<sup>2</sup>. Indeed, the processing of proteins from internalized microorganisms to derive antigens for presentation at the cell surface on major histocompatibility complex (MHC) class I and class II molecules is a key mechanism of adaptive immunity<sup>3</sup>.

Macrophages are immune effector cells that mediate defence of the host against a variety of bacteria, viruses, and other microorganisms. Classical activation of macrophages involves Toll-like receptor (TLR) ligands (e.g. lipopolysaccharides, LPS) and pro-inflammatory cytokines such as interferon- $\gamma$  (IFN- $\gamma$ ) produced by natural killer (NK) cells or activated T-helper 1 (T<sub>H</sub>1) lymphocytes<sup>4,5</sup>. IFN- $\gamma$  activation results in the transcriptional regulation of hundreds of genes including nitric oxide synthase-2 and phagocyte oxidase that are associated with the production of reactive oxygen species (ROS), and provide enhanced killing abilities to macrophages<sup>6</sup>. This cytokine also mediates phagosome maturation and antigen loading on MHC class I and class II molecules<sup>7-11</sup>. Alternate activation of macrophages by interleukin 4 (IL-4) and IL-13 cytokines produced by T<sub>H</sub>2 cells have also been proposed to account for allergic, cellular and humoral responses to parasitic and extracellular pathogens<sup>12</sup>. These cytokines can promote the development of wound-healing macrophages, though this activation result in poor antigen-presenting cells that are less efficient at producing ROS or at killing intra cellular pathogens than classically activated macrophages<sup>13</sup>.

Classically activated macrophages can also secrete pro-inflammatory cytokines such as IL-1, IL-6 and IL-23 that can lead to the expansion of T<sub>H</sub>17 cells associated with autoimmune responses<sup>14</sup>. Interestingly, macrophages activated in a MyD88-dependent manner through TLR ligand stimulation produce tumor necrosis factor  $\alpha$  (TNF- $\alpha$ ), another

important cytokine that synergizes with INF- $\gamma$  to enhance macrophage activation. Exogenous stimulation of macrophages by TNF- $\alpha$  can also arise from the secretion of this cytokine by antigen presenting cells (APC). The significance of TNF- $\alpha$  in mounting an appropriate immune response is of particular importance in *Leishmania* infections as macrophages stimulated with INF- $\gamma$  alone are less efficient to clear this parasite due to lack of TLR ligands expression. TNF- $\alpha$  is playing an important role in inflammatory cell activation and recruitment, and is associated with the development of many chronic inflammatory diseases such as rheumatoid arthritis <sup>15</sup> and Crohn's disease <sup>16</sup>

Relatively few studies have investigated the molecular mechanisms and signaling associated with the activation of macrophages by TNF- $\alpha$ . Previous reports using TAP purification and mass spectrometry have provided a physical and functional map of the human TNF- $\alpha$  pathway <sup>17</sup>. Stable isotope labeling by amino acids in cell culture (SILAC) was previously used to identify changes in the phosphoproteome of HeLa cells in response to TNF- $\alpha$  <sup>18</sup>, and to determine the dynamic profiles of TNF- $\alpha$ -induced nuclei-associated proteins in HEK293 cells <sup>19</sup>. More recently, label-free quantitative proteomics was used to identify secreted proteins from human adipose tissue-derived mesenchymal stem cells during inflammation <sup>20</sup> and Choi *et al.* utilized a bio-orthogonal non-canonical amino acid tagging (BONCAT) in combination with proteomics and isobaric tags (iTRAQ) to identify newly synthesized proteins induced by TNF- $\alpha$  and IL-1 $\beta$  in human monocytic THP-1 cells <sup>21</sup>.

To investigate the molecular mechanisms of TNF- $\alpha$ , we profiled the changes in protein abundance in resting and activated RAW264.7 mouse macrophages using label-free quantitative proteomics. We evaluated three independent separation protocols enabling the fractionation of intact proteins (GELFREE and macroporous RP) and peptides (SCX) prior to the analysis of the corresponding tryptic digests by LC-MS/MS on a LTQ-Orbitrap mass spectrometer to obtain a comprehensive view of the macrophage proteome. Importantly, quantitative proteomics analyses of TNF- $\alpha$  activated macrophages highlighted the down regulation of several mitochondria proteins. This observation was also correlated by flow cytometry, biochemical assays and immunofluorescence microscopy experiments, and indicated that TNF- $\alpha$  impaired mitochondria functions in activated macrophages. The Atg5 dependent degradation of mitochondria and the

presentation of mitochondrial antigens by MHC class I molecules suggest that TNF- $\alpha$  macrophage stimulation led to mitophagy and contribute to the modification of the MHC class I peptide repertoire.

## 2.4. Experimental Procedures

### 2.4.1. Cell lines

Raw264.7 macrophage cell lines and RAW-Kb-Mito gB<sub>30-694</sub> cell lines were grown in DMEM containing 10% FBS supplemented with glutamine and penicillin/streptomycin. MEF wildtype and Atg5<sup>-/-</sup> cells were grown in DMEM containing 10% FBS supplemented with glutamine and penicillin/streptomycin. The lacZ-inducible gB HSV-specific CD8<sup>+</sup> T cell hybridoma HSV-2.3.2E2 was maintained in RPMI-1640 medium supplemented with 5% fetal bovine serum, 2 mM glutamine, 100 units/ml penicillin, and 100 µg/ml streptomycin.

### 2.4.2. Raw-Kb construction

cDNA was prepared from purified mRNA extracted (Macherey-Nagel, Nucleospin RNA II) from the BMA3.1A7 cell line (haplotype H-2Kb). cDNA of H-2Kb was amplified by PCR using the primers GTGAATTCGCCACCATGGTACCGTG and GATCTCGAGTCACGCTAGAGAATG and the 1125 bp PCR product was cloned into the pUB6/V5-His A vector (Invitrogen) using the EcoRI and XhoI restriction sites. This plasmid was then transfected into RAW264.7 cells and stably transfected cells were selected using Blasticidin 3 µg/ml added 24 h after transfection, for a period of one week. Resistant cells were scraped and surface labelled with anti H-2Kb mouse antibody PE (BD Biosciences) using conditions that preserved cell integrity. Cells exhibiting the highest levels of fluorescence were sorted into 96-well plates (one cell per well) (BD FACS Vantage cell sorter) and amplified in culture for 2 weeks. Cell surface expression levels of H-2Kb in each clone were then tested by surface labelling (see above) followed by flow cytometry analysis and the clone showing the highest fluorescence levels was selected, amplified and used in the subsequent experiments (supplemental Fig. 2.S1).

### 2.4.3. pIRES-gB<sub>30-694</sub>-Mito vector

The sequence coding for amino acids 30 to 694 of HSV-1 gB (gB<sub>30-694</sub>) was cloned from purified HSV-1 DNA (strain F) kindly provided by Johanne Duron (Université de Montréal) using the primers GTAAGTAGTGCTCCGACTTCCCCCG and GTAGATATCCTTGATCTCGTGGCGGGTGTA containing respectively the restriction

sites *SpeI* and *EcoRV*. gB<sub>30-694</sub> lacked both the signal peptide and the transmembrane domain of the viral gB, but included the sequence gB<sub>498-505</sub> coding for the H-2Kb restricted SSIEFARL peptide.

gB<sub>30-694</sub> was cloned in pIRES2-EGFP-Mito kindly provided by Claude Perreault (Université de Montréal). The resulting vector displays the backbone of pIRES2-EGFP including, in the MCS, a cassette containing the mitochondrial matrix-targeting sequence (from human cytochrome c oxidase, MSVLTPLLLRGLTGSARRLPVPRAKIHSL) followed by gB<sub>30-694</sub>.

#### **2.4.4. RAW-Kb-Mito gB<sub>30-694</sub> cell line**

The pIRES-gB<sub>30-694</sub>-Mito vector was transfected in RAW-Kb cells. Stably transfected cells were selected by addition of G418 at 0,5 mg/ml in the culture medium 24 h after transfection. After 8 days, cells displaying high GFP levels were sorted in 96-well plates (one cell per well, BD FACS Vantage cell sorter). After 2 weeks of culture, expression and proper processing of the endogenous fusion protein in the different clones were tested in presentation assays. Each clone was co-cultured with gB HSV-specific CD8<sup>+</sup> T cell hybridoma HSV-2.3.2E2 overnight, and the level of activation of the gB-specific hybridoma was tested as described below. The clone displaying the highest presentation levels of the gB SSIEFARL epitope was amplified and used in subsequent experiments.

#### **2.4.5. Crude membrane preparation**

Control cells or cells stimulated with TNF- $\alpha$  (10 ng/ml) for 24h were lysed in HB buffer (8.5% sucrose, 3 mM imidazole, protease and phosphatase inhibitors, pH 7.4). The cell homogenate was centrifuged at 3000 rpm (4°C) for 5 min to remove the nuclei. The crude membrane extract was isolated by ultracentrifugation at 50000G at 4°C for 30 min and the pellet was resuspended in 8 M urea, 10 mM ammonium bicarbonate, 1mM TCEP.

#### **2.4.6. Protein and peptide fractionation**

Three different methods were used to separate proteins or peptides prior to LC-MS/MS analyses. First, membrane proteins (200  $\mu$ g/replicate; 6 M urea, 1% acetic acid) were separated on Macroporous Reversed-Phase C18-chromatography (mRP-C18) using an



Agilent 1200 LC system (Agilent Technologies). The LC column was maintained at 80 °C and chromatographic separations were achieved using a multi-segment elution gradient, with eluent A (0.1% trifluoroacetic acid, TFA in water, v/v) and eluent B (0.1% TFA in acetonitrile, ACN v/v). The gradient conditions consisted of two steps with increasing concentration of the eluent B (3-80% B 6-49 min; 80-100% B 49-59 min) followed by a re-equilibration at B: 3% for 15.0 min. The flow rate was maintained at 0.75 mL/min, and a total of 12 fractions were collected.

The second method used a gel-eluted liquid fraction entrapment electrophoresis (GELFREE) 8100 system (Protein Discovery) that enabled the separations of membrane proteins (200 µg/replicate in Laemmli buffer) into 12 fractions across the mass range 30-150kDa. SDS was removed from fractions by buffer exchange to 8M urea using Ultracel – 10 Multiscreen filterplates (Millipore) before proteolytic digestion.

Third, membrane protein extracts (200 µg/replicate) were digested with trypsin (sequencing grade, Promega) and the resulting peptides were separated on a strong cation exchange (SCX) column (Polysulfoethyl A, PolyLC Inc.). Chromatographic separations were achieved on an Agilent 1200 LC system using a multi-segment elution gradient with 10 mM Ammonium formate, 25% ACN, pH 3.1 (buffer A) and 500 mM ammonium formate, 25 % ACN, pH 6.7 (buffer B). The gradient conditions consisted of two steps with increasing concentrations of the eluent B (0-65% B 10-65 min; 65-100% B 65-71 min) followed by a re-equilibration at B: 0% for 15.0 min. The flow rate was maintained at 0.3 mL/min, and a total of 12 fractions were collected.

#### **2.4.7. Proteolytic digestion**

Proteins fractionated by mRP or GELFREE were digested by Lys-C and trypsin as follows. Lyophilized protein samples (10-20 µg) were resolubilized in 40 µl of 8 M urea, 50 mM ammonium bicarbonate and reduced by incubation with 3 mM TCEP (Thermo Scientific) for 20 min at room temperature (RT). Reduced cysteines were alkylated with 10 mM chloroacetamide (Sigma) and incubated for 15 min at RT in the dark. Samples were diluted to a final concentration of 2 M urea with 50 mM ammonium bicarbonate, 1 mM CaCl<sub>2</sub> and digested with 0.5 µg of trypsin overnight at 37 °C. The digestion was subsequently quenched by adding formic acid to a final concentration of 5%.

#### 2.4.8. Mass spectrometry

Peptides were separated on a 150  $\mu$ m ID, 10 cm reversed phase nano-LC column (Jupiter C18, 3  $\mu$ m, 300 Å, Phenomenex) with a loading buffer of 0.2% formic acid (FA). Peptide elution was achieved using a linear gradient of 5-40% ACN in 90 min on an Eksigent 2D-nanoLC (Dublin, CA) with a flow-rate of 600 nL/min. The nano-LC was coupled to an LTQ-Orbitrap XL mass spectrometer (Thermo-Electron, Bremen, Germany) and samples were injected in an interleaved manner. The mass spectrometer was operated in a data-dependent acquisition mode with a 1 sec full range mass scan at 60,000 resolution, followed by five product ion scans (MS/MS) of the most abundant precursors above a threshold of 10,000 counts. CID was performed in the LTQ at 35% collision energy and an Activation Q of 0.25.

#### 2.4.9. Protein identification and quantitative analysis

The centroided MS/MS data were merged into single peak-list files for each of the three fractionation platforms used (Distiller, V2.4.2.0) and searched with the Mascot search engine v2.3.01 (Matrix Science) against a concatenated forward and reversed mouse IPI database (IPI mouse rel. 3.54) containing 55 987 forward protein sequences. Mascot was searched with a parent ion tolerance of 10 ppm and a fragment ion mass tolerance of 0.5 Da. Carbamidomethylation of cysteine, oxidation of methionine, deamidation, phosphorylation of serine, threonine and tyrosine residues and ubiquitination of lysine residues (GlyGly) were specified as variable modifications. The confidence in ubiquitination site assignments was determined using a probability score function based on the method of Olsen et al.<sup>22</sup> integrated in the proteoconnections platform.<sup>23</sup> The false discovery rate (FDR), was calculated as the percentage of positive hits in the decoy database *versus* the target database, and a FDR of 2% was considered for both proteins and peptides. Protein identification are reported only for those assigned with a minimum of 2 peptides per protein.

Label-free quantitative proteomics was used to profile protein abundance across sample sets, as reported previously<sup>8, 24</sup>. Briefly, Mascot peptide identifications were matched to ion intensity (MS peak intensity, minimum threshold: 8000 counts) extracted from the aligned MS raw data files (tolerances set to m/z: 15 ppm and RT: 1 minute). For each LC-MS run, we normalized peptide ratios so that the median of their logarithms was zero,

to account for unequal protein amounts across conditions and replicates. Intensities were summed across fractions for peptides of identical sequences, and protein ratios were calculated as the median of all peptide ratios, while minimizing the effect of outliers. Only proteins defined by two or more peptide quantification events were considered. Relative standard deviation was below 58% for 95% of the detected proteins. Proteins with a 2-fold variation and a p-value below 0.1 were considered differentially regulated.

#### **2.4.10. Bioinformatics analysis**

Transmembrane proteins were predicted using TMHMM 2.0.<sup>25</sup> Gene Ontology annotations for cellular component, biological process and molecular function were obtained from the Gene Ontology project using the DAVID Bioinformatics resources (<http://david.abcc.ncifcrf.gov/>)<sup>26, 27</sup>. To identify cellular components or biological processes that were statistically over represented in our protein list, we used the binomial statistics tool to compare classifications of multiple clusters of lists to a reference list (*Mus musculus* total proteome). Only terms that were significantly enriched/depleted with a p-value <0.05 were used for the analysis. A global protein-protein interaction network was generated using Cytoscape Version 2.8.0<sup>28</sup> by submitting all MS-identified proteins to the Cytoscape plugin Bisogenet Version 1.41<sup>29</sup>. By using the gene names of MS-identified proteins, this plugin allowed us to query simultaneously 6 human protein-protein interaction databases: Biogrid, Intact, Mint, Dip, Bind and HPRD, in order to generate a global interactome that contains neighbours of MS-identified proteins up to a distance of 1. Subnetworks were created by manually annotating the MS-identified proteins with the Uniprot database<sup>30</sup> and by functionally clustering the proteins of the global protein-protein interaction network.

#### **2.4.11. Western Blot**

Protein samples were separated by 4-12% SDS-PAGE (Invitrogen) and transferred onto nitrocellulose membrane (Pall Corporation, USA). Proteins of interest were detected using a rabbit polyclonal anti-cPLA<sub>2</sub> (cytosolic phospholipase A2) antibody (Cell Signaling) or a mouse monoclonal anti-GAPDH (Glyceraldehyde 3-phosphate

dehydrogenase) antibody (Millipore), followed by a secondary antibody coupled to horseradish peroxidase (Millipore) for ECL detection (GE Healthcare).

#### **2.4.12. Flow Cytometry Analysis**

JC-1 Mitochondrial Membrane Potential Assay Kit (Cayman Chemical Company, Ann Arbor, MI) was used to quantify the amount of mitochondria in control and TNF- $\alpha$  stimulated cells (24h) by flow cytometry on a FACSCalibur flow cytometer (BD Biosciences). RAW 267.4 macrophages or mouse embryonic fibroblasts (MEF) were incubated with the JC-1 dye for 30 minutes. Cells were harvested and analyzed immediately after. Healthy, functional mitochondria with a high potential contained red JC-1 J-aggregates that were quantified in the FL2 channel (Excitation: 520-570 nm: Emission: 570-610 nm). Apoptotic, unhealthy mitochondria with low potential contained mainly green JC-1 monomers detectable in the FL1 channel (Excitation: 485 nm: Emission: 535 nm). Mitochondria were quantified using relative fluorescence intensities on a gated population of a uniform cell population. Autophagy was blocked using 3-methyl adenine, 3-MA (10 mM, Sigma-Aldrich) for the last 3 h of the TNF- $\alpha$  stimulation. Lysosensor (Invitrogen) was used to quantify the acidity of lysosomes by flow cytometry on a FACSCalibur flow cytometer (BD Biosciences). RAW 267.4 macrophages were incubated with lysosensor. Cells were harvested and analyzed immediately after. The acidification of lysosomes was quantified using relative fluorescence intensities on a gated population of a uniform cell population.

#### **2.4.13. Immunofluorescence**

Cells were fixed and permeabilized according to the manufacturer's indications (Cytofix/Cytoperm Kit, BD). Mitochondria were labelled using a Tim23 or Tom20 antibodies (BD Biosciences), and we used antibodies against LC3 (Abgen) and gB (Santa Cruz) to label autophagosomes or gB glycoprotein, respectively. Antibodies were revealed using IgG Alexa-488- and 568-coupled secondary antibodies (Invitrogen). Samples were analyzed using a confocal laser scanning microscope (Zeiss LSM510) with a 63x objective.

#### 2.4.14. Electron microscopy

For morphological analyses, cells were fixed overnight at 4°C, in 2.5% glutaraldehyde (Canemco) in 0,1M Na Cacodylate (Canemco) buffer, followed by a post-fixation in 1% osmium tetroxide (Canemco) in 0,1M Na Cacodylate buffer for 1 hour at 4°C. Contrast of cell membranes was enhanced by uranyl acetate (Mecalab) treatment. Cells were dehydrated in ethanol, followed by 1:1 mixture of ethanol/Epon, embedded in Epon, and then polymerized at 60°C for 3 days. Sections were examined on a Phillips CM 100 Transmission Electron Microscope.

#### 2.4.15. Antigen presentation Assay

RAW-Kb-Mito gB<sub>30-694</sub> cells (75 x 10<sup>4</sup> cells) treated with TNF- $\alpha$  (10 ng/mL) for 24h and 3-MA (10mM, Sigma Aldrich), Rapamycin (10  $\mu$ g/ml, Calbiochem) or CCCP (carbonyl cyanide *m*-chlorophenyl hydrazone; 20  $\mu$ M; Sigma Aldrich) for 3h were fixed for 10 min at 23 °C with 1% (w/vol) paraformaldehyde, followed by three washes in complete DMEM. Antigen presentation assays were performed as described previously<sup>31</sup>. Briefly, antigen-presenting cells were cultured for 12 h at 37°C together with 4 x 10<sup>5</sup> HSV-2.3.2E2 cells ( $\beta$ -galactosidase-inducible, gB-specific CD8<sup>+</sup> T cell hybridoma) for analysis of the activation of T cells. Cells were then lysed (0.125 M Tris base, 0.01 M cyclohexane diaminotetraacetic acid, 50% glycerol (v:v), 0.025% (v:v) Triton X-100 and 0.003 M dithiothreitol, pH 7.8). A  $\beta$ -galactosidase substrate buffer (0.001 M MgSO<sub>4</sub> x 7 H<sub>2</sub>O, 0.01 M KCl, 0.39 M NaH<sub>2</sub>PO<sub>4</sub> x H<sub>2</sub>O, 0.6 M Na<sub>2</sub>HPO<sub>4</sub> x 7 H<sub>2</sub>O, 100 mM 2-mercaptoethanol and 0.15 mM chlorophenol red  $\beta$ -D-galactopyranoside, pH 7.8) was added for 2–4 h at 37 °C. Cleavage of the chromogenic substrate chlorophenol red-  $\beta$ -D-galactopyranoside was quantified in a Gemini plate reader (Molecular Devices) at 595 nm. The data and error bars are shown as means of three replicate experiments with their respective relative standard deviation.

## 2.5. Results

To obtain a full repertoire of proteins associated with TNF- $\alpha$  activated macrophages we isolated crude membrane extracts from post-nuclear supernatant of mouse macrophage RAW264.7 cells using ultra-centrifugation, and monitored the fractionation efficiency using immunoblots for several cellular markers (supplemental Fig. 2.S2). This cell fractionation afforded protein extracts of reduced sample complexity while simultaneously enriching for potentially interesting organellar and vesicular proteins. Preliminary proteomics analyses of crude membrane extracts (200  $\mu$ g aliquots each) were performed using three independent separation platforms namely mRP-C18, GELFREE, and SCX fractionation to obtain a comprehensive identification of the corresponding samples. While the first two platforms separated intact proteins, SCX enabled efficient separation of peptides following tryptic digestion of the crude membrane extract. In each case, three biological replicates were separated into 12 fractions. Fractionated proteins (mRP-C18, GELFREE) were digested by trypsin, and fractions from all three separation platforms were analyzed on a LTQ-Orbitrap mass spectrometer. We compared the distribution of quantifiable peptides detected in one, two, or three replicates using label-free quantitative proteomics (supplemental Fig 2.S3), and observed that mRP-C18 provided the highest number of reproducibly detected peptides in all replicates (91 %) compared to SCX (88%) and GELFREE (47%). The reproducibility of protein fractionation across biological replicates and the enhanced sequence coverage observed for mRP-C18 compared to the other two platforms provided significant advantages for quantitative proteomics. Supplemental Fig 2.S4 shows the overlap in protein identification and sequence coverage obtained for each platform, and the list of protein and peptide identifications are provided as supplemental Tables II-S1 and II-S2, respectively. Phosphopeptide identifications obtained from these analyses are provided as supplemental Fig. 2.S5. These experiments indicated that mRP-C18 enabled more accurate measurements of peptide abundance compared to the other two platforms examined, and was selected in subsequent quantitative proteomics experiments. The experimental workflow used in the present study is summarized in Figure 2.1.

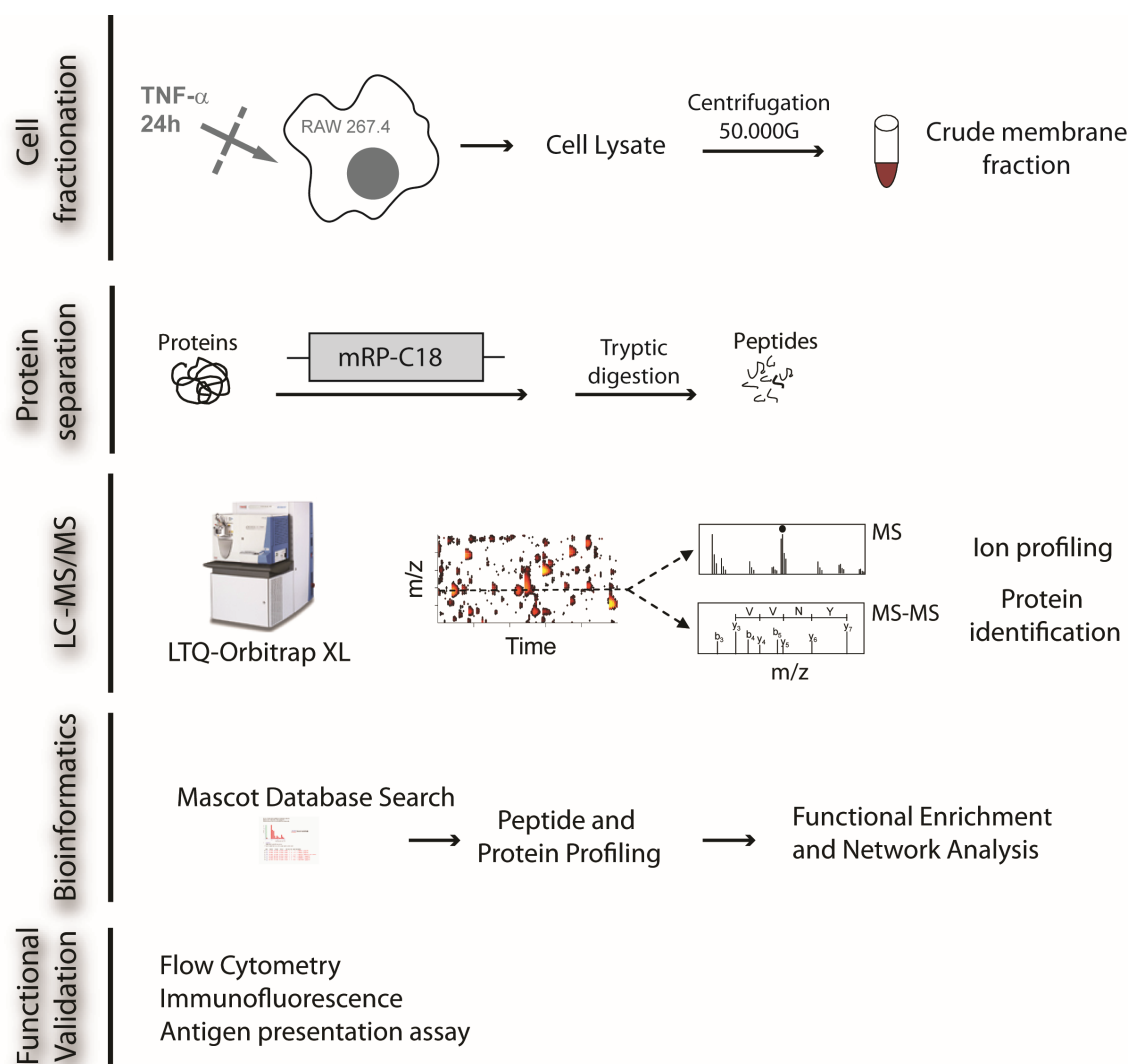


**Figure 2.1. Workflow for large-scale quantitative proteomics analyses of RAW264.7 macrophages.**

Crude membrane extracts were obtained from resting or TNF- $\alpha$  stimulated (24h) macrophages by ultracentrifugation. Protein extracts (n=3) were fractionated by macroporous reversed phase followed by tryptic digestion. Peptides were analysed by LC-MS/MS on a LTQ-Orbitrap XL mass spectrometer. Label-free quantitative proteomics was used to correlate changes in protein abundances across control and TNF- $\alpha$  activated macrophage extracts. GO terms enrichment and protein network were obtained from identified proteins. The proteomics dataset was validated functionally by several biochemical assays.

### 2.5.1. Quantitative proteomics of TNF- $\alpha$ activated macrophages

Label-free quantitative proteomics experiments were performed on mRP-C18 fractions to identify differentially regulated proteins upon TNF- $\alpha$  stimulation of macrophages. The database search enabled the identification of 13808 peptides and 1516 proteins with a 2% FDR (see Experimental Procedures). We identified 1373 proteins with at least two or

more unique peptides with quantifiable abundance measurements (supplemental Table II-S3). Scatter plots of abundance measurements for peptide ions identified in either control or TNF- $\alpha$  stimulated extracts indicated that 95 % of all ions showed RSD values less than 58 % across all three biological replicates, attesting of the reproducibility of the method (supplemental Fig. 2.S6). The consistency of fold change measurements is also shown in supplemental Fig. 2.S7 for citrate synthase and ATP synthase subunit b, each identified with 9 peptides. The distribution of fold-change vs. p-values is represented in the volcano plot of Fig. 2.2.

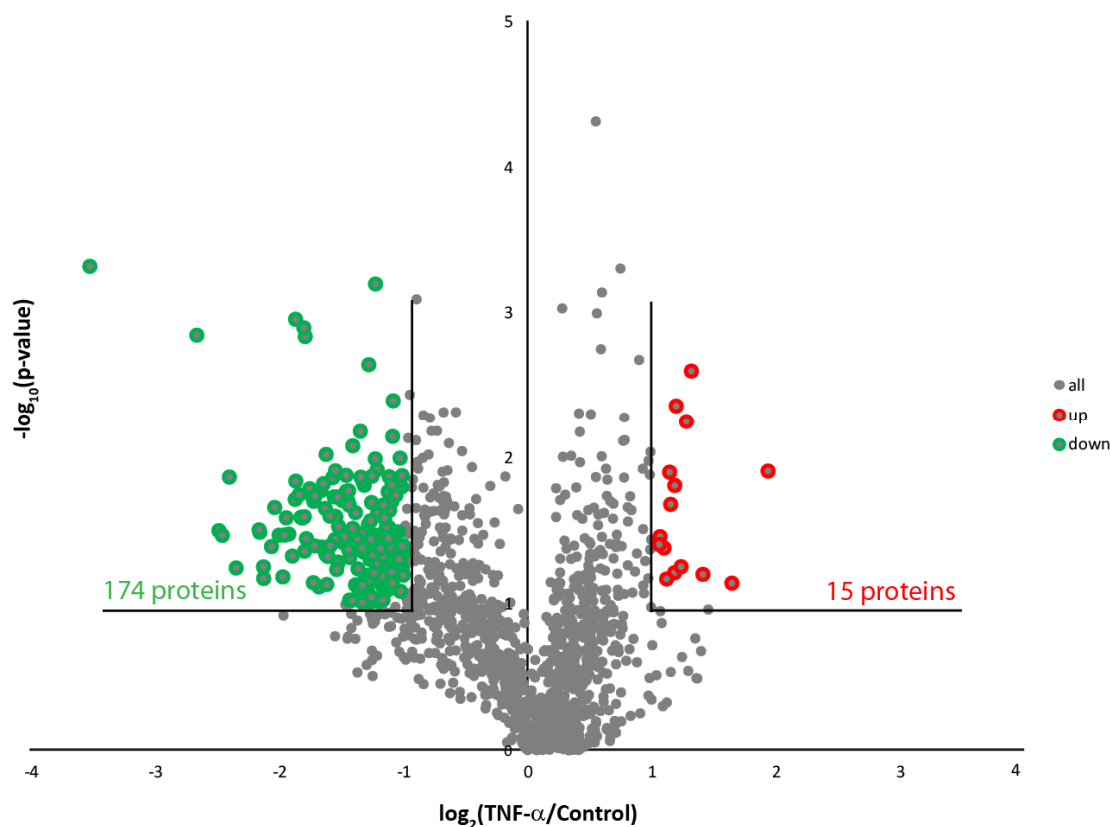


**Figure 2.2. Large Scale membrane proteome analysis of resting and TNF- $\alpha$  activated macrophages.**

Volcano plot representation of protein abundance changes upon TNF- $\alpha$  activation. A total of 189 differentially regulated proteins with fold change  $\geq 2$  and p-values  $< 0.1$  were identified upon TNF- $\alpha$  stimulation.

Based on the reproducibility of abundance measurements, we used a fold change of  $\geq 2$  and p-values  $\leq 0.1$  to define differential regulation across biological replicates. Peptides assigned to the same protein were regrouped together to determine the overall fold-change of abundance upon TNF- $\alpha$  stimulation. Out of 1373 proteins, we identified 174



and 15 proteins that were down- and up-regulated upon TNF- $\alpha$  stimulation, respectively. Several proteins previously reported to be modulated by TNF- $\alpha$  included TNF receptor-associated protein 1 (TRAP1) and cytosolic phospholipase A2 (cPLA<sub>2</sub>) (Table II-1). The overexpression of cPLA<sub>2</sub> upon TNF- $\alpha$  stimulation was validated by immunoblots (Fig. 2.3A) and confirmed the abundance measurement obtained by mass spectrometry (Figs. 2.3B, 2.3C).

**Table II-1.** Changes in abundance of selected macrophage membrane proteins upon TNF- $\alpha$  stimulation.

	Expression $\log_2(\text{TNF-}\alpha/\text{control})$	Sequence Coverage
<b><i>Known TNF-<math>\alpha</math> modulated proteins</i></b>		
Cytosolic phospholipase A2	1.2	9%
Keratin 17	1.4	11%
TNFR-associated protein 1 (HSP75)	-1.3	43%
<b><i>Mitochondrial proteins</i></b>		
Enoyl-CoA hydratase	-1.9	31%
Mitochondrial 2-oxoglutarate/malate carrier	-2.1	40%
Trifunctional enzyme subunit alpha	-1.1	37%
Mitochondrial import receptor subunit TOM22 homolog	-1.3	47%
<b><i>Cytoskeleton proteins</i></b>		
Actin cytoplasmic 1	-1.1	75%
Tubulin alpha-4A chain	-1.3	52%
<b><i>Vesicle trafficking and lysosome</i></b>		
Cathepsin Z	1.2	9%
Vesicle trafficking protein SEC22b	-1.6	32%
Translocon-associated protein subunit beta (Ssr2)	1.1	5%
Sorting nexin-1	-1.1	18%
Lysosome-associated membrane glycoprotein 1 (LAMP1)	-1.3	13%
<b><i>Immune response</i></b>		
Osteopontin	1.1	15%
H-2 class I histocompatibility antigen K-D alpha chain	-1.1	29%
<b><i>Protein degradation</i></b>		
Proteasome activator complex subunit 1	-1.0	26%
Ubiquitin carrier protein	-1.2	26%
<b><i>Autophagy related proteins</i></b>		
HSP90 $\alpha$	-1.4	49%
HSP90 $\beta$	-1.3	53%
14-3-3 protein epsilon	-1.7	60%

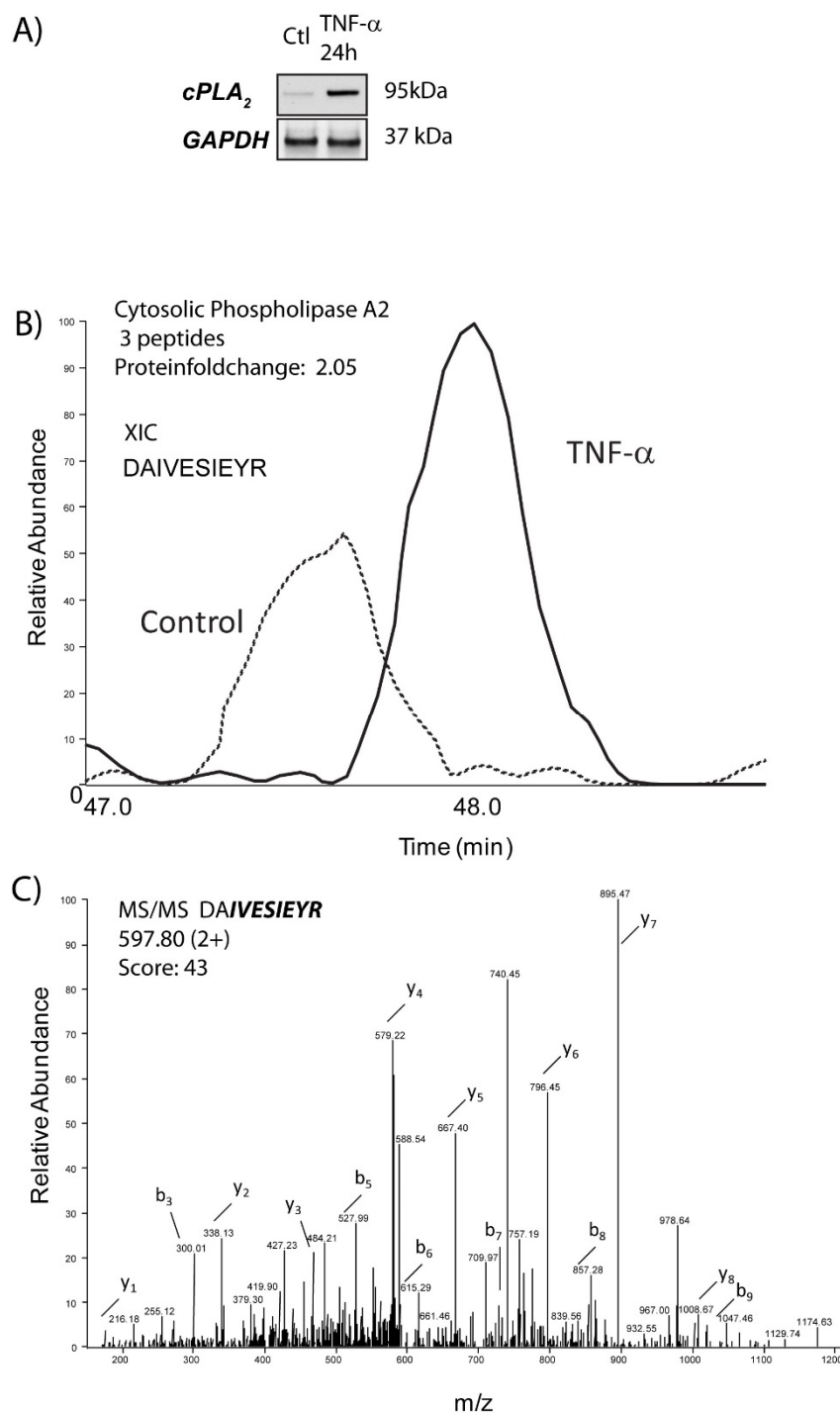


**Figure 2.3. Quantitative proteomics analysis of membrane proteins in TNF- $\alpha$  stimulated macrophages identified the overexpression of cPLA<sub>2</sub>.** (A) Immunoblot showing the increased abundance of cPLA<sub>2</sub> upon TNF- $\alpha$  stimulation. (B) Extracted ion chromatogram of m/z 597.8<sup>2+</sup> corresponding to the peptide DAIVESIEYR from cPLA<sub>2</sub> in control (dashed black) and TNF- $\alpha$  activated macrophage extracts (black). (C) MS/MS spectrum of m/z 597.8<sup>2+</sup> confirming the peptide identification.

Our quantitative proteomics analyses also revealed the differential regulation of several proteins involved in lysosomal degradation (e.g. Cathepsin Z) and vesicle trafficking (e.g. Sec22b, Sorting nexin1). Previous studies have indicated a role for TNF- $\alpha$  in stimulating autophagy in different cell types though the exact mechanism is presently unknown<sup>32-34</sup>. Interestingly, we observed that 37 mitochondrial proteins, accounting for 21 % of all down regulated proteins, were modulated by TNF- $\alpha$ . An example is shown in supplemental Fig. 2.S7 for citrate synthase, an acetyl-CoA dependent mitochondrial enzyme involved in the conversion of oxaloacetate into citrate. We obtained a sequence coverage of 33 % and all corresponding peptides showed a consistent decrease in abundance following activation of macrophages with TNF- $\alpha$ . Interestingly, we also noted that a number of mitochondrial proteins such as DNA topoisomerase 1 mitochondrial and ATP-dependent Clp protease ATP-binding subunit clpX-like mitochondrial were ubiquitinated in response to TNF- $\alpha$  (Supplemental Table II-S4, supplemental Fig. 2.S8). This result is consistent with a recent report indicating the activation of the ubiquitin-proteasome system in mitophagy<sup>35</sup>

### **2.5.2. Protein interaction network analysis of TNF- $\alpha$ activated macrophages uncovers the regulation of mitochondrial proteins**

To obtain additional functional insights into proteins and pathways that are differentially regulated in macrophages, we conducted bioinformatics analyses of our proteomics data sets. First, we grouped differentially abundant proteins according to their GO terms compared to those of the mouse reference proteome. GO-terms were considered significant when they had p-values <0.05 in a Fisher exact test, resulting in 168 significant terms. Protein groups were then sorted according to Cellular Component, Biological Processes and Molecular Function GO categories (Fig. 2.4A).

Upregulated proteins comprised GO terms associated with cytoskeleton and structural molecule activity. Interestingly, we also observed the enrichment for hydrolase activity and cellular nitrogen metabolic processes. Proteins that did not show any significant change in abundance upon TNF- $\alpha$  activation were enriched in mostly basal processes and non redundant pathways (data not shown). Downregulated proteins were mostly associated to vesicles and mitochondrial functions. Interestingly, proteins located at the mitochondrial inner membrane showed a more pronounced enrichment than those

located at the mitochondrial outer membrane, suggesting that specific subsets of proteins are downregulated upon TNF- $\alpha$  stimulation. More specifically, we noted that proteins implicated in energy generation or cellular respiration were represented in the subset of downregulated proteins. Taken together these analyses suggest that TNF- $\alpha$  activation resulted in extensive cytoskeleton remodeling and vesicular trafficking, and contributed to the downregulation of mitochondrial proteins involved in metabolism and in energy generation.

Next, we used the protein expression data to develop a protein interaction network using Cytoscape. The combination of interactions found in mouse and their human orthologs resulted in a network of 7439 proteins (nodes) and 80449 connections (edges). From this complex network we extracted sub-networks using Uniprot annotations. We identified several groups of membrane proteins modulated by TNF- $\alpha$ , including subnetworks comprising proteins involved in TNF- $\alpha$  signalling, vesicular trafficking, immune response, ROS and mitochondria, and mitophagy and autophagy (Fig. 2.4B). This network highlights the perturbation of different mitochondria functions in response to TNF- $\alpha$  activation of macrophages. However, not all mitochondrial proteins were affected equally by TNF- $\alpha$ . Several mitochondrial proteins involved in ROS were downregulated upon TNF- $\alpha$  activation, while mitochondrial ribosomes were unaffected. This interaction network further underscores the modulation of different Rab and effector proteins involved in the control of membrane trafficking such as Rab5, Rab10 and Rab11 together with the downregulation of several proteins participating in SNAREs fusion including AnxA7, Vti1b, Vapb and Vat1. Importantly, we also identified subnetworks related to immune response (e.g. proteasome, antigen processing) and autophagy that were regulated by TNF- $\alpha$ , suggesting a potential association between autophagy and antigen presentation and processing.

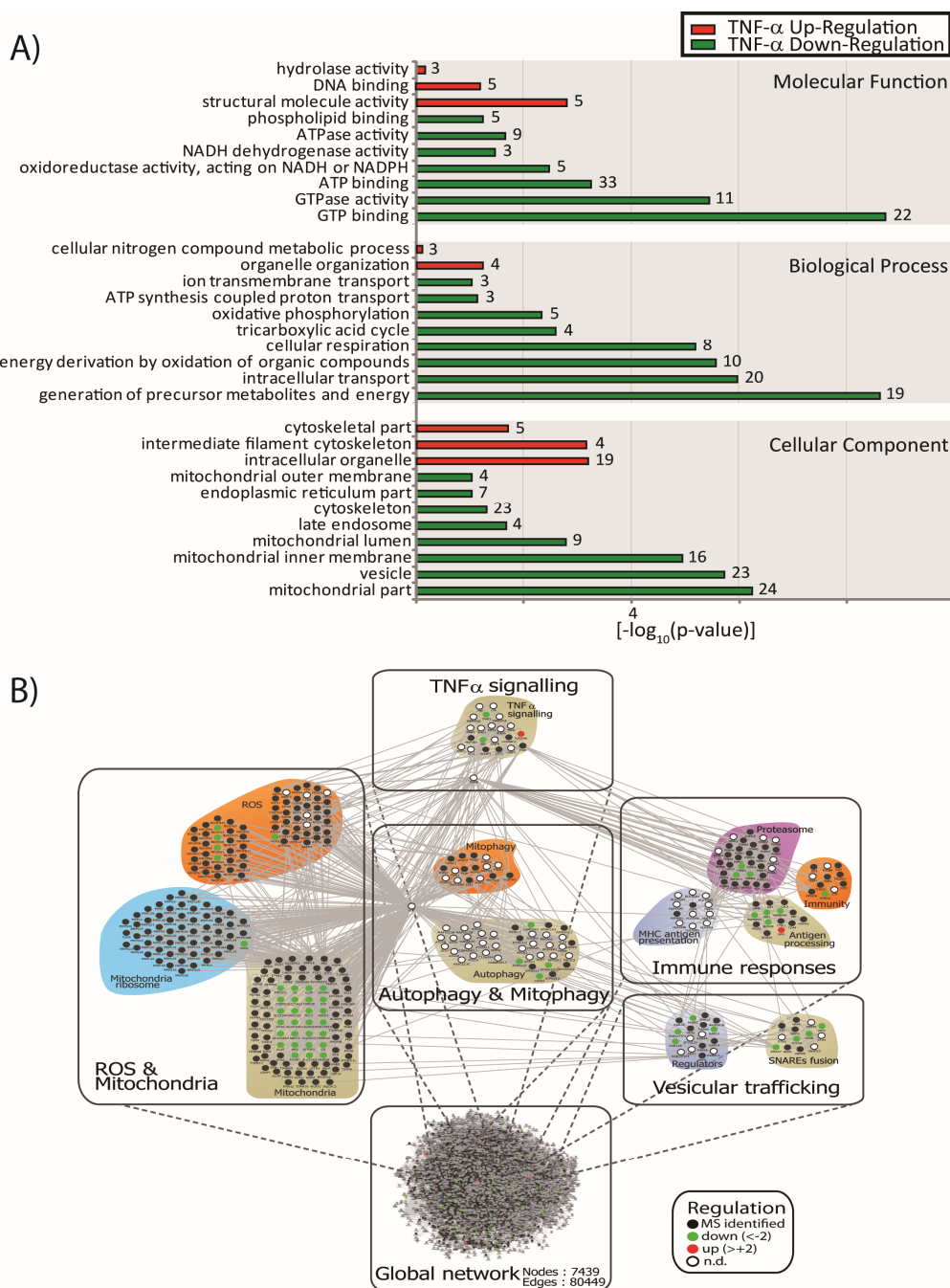


**Figure 2.4. Bioinformatics analyses of the membrane proteome from TNF- $\alpha$  activated macrophages reveals the downregulation of mitochondria proteins.**

(A) Gene Ontology enrichment analysis of upregulated proteins shows a strong enrichment for terms related to mitochondria and energy production while terms associated with vesicle trafficking and mitochondrial functions are downregulated. (Numbers represent distinct proteins)

(B) Global protein-protein interaction network comprising 7439 nodes and 80 449 edges. Subnetworks were created by manually annotating the MS-identified proteins with the Uniprot database and by functionally clustering the proteins from the global protein-protein interaction network. Subnetworks affected by TNF- $\alpha$  activation, such as immune response, ROS & mitochondria and vesicular trafficking are displayed.

### 2.5.3. TNF- $\alpha$ induces specific autophagic elimination of mitochondria in macrophages

Our quantitative proteomics analyses indicated that mitochondria proteins were down-regulated in TNF- $\alpha$  activated macrophages. This cytokine is known to induce several types of cell signaling events including apoptosis, activation of NF- $\kappa$ B and activation of different kinases (e.g. p38, c-Jun, and the extracellular signal regulated kinase, ERK) <sup>36</sup>. Mitochondria are key components in a pathway to programmed cell death, through the release of death-promoting factors (e.g. cytochrome c, Smac, and endonuclease G) from the intermembrane space <sup>37</sup>. To determine if reduced mitochondrial proteins arose from pre-apoptotic signal, we monitored the abundance of fluorescently-labeled Annexin A5 at the plasma membrane using flow cytometry (Supplemental Fig. 2.S9). Annexin A5 is used as a probe to detect cells that express phosphatidylserine on the cell surface, an event associated with apoptosis and other forms of cell death <sup>38</sup>. Flow cytometry analyses revealed that apoptotic and dead cells represented approximately 15 % of the cell population in both control and TNF- $\alpha$  activated macrophages. Similar results were also obtained when cells were stained with 7-amino actinomycin D, a compound that intercalates with double-stranded DNA and penetrates cell membranes of necrotic or dead cells but is excluded from viable cells (Supplemental Fig. 2.S9). Furthermore, no significant change in cell count was observed between control and activated macrophages, confirming that TNF- $\alpha$  does not impair cell viability (data not shown).

To determine the extent of changes in mitochondrial functions associated with TNF- $\alpha$ , we examined the effect of this cytokine on the opening of the mitochondrial permeability transition pore, a property that reflects the integrity of the mitochondrial membrane and its transmembrane potential,  $\Delta\Psi_{mt}$ . We used JC-1 (5,5',6,6'-tetrachloro1,1',3,3'-tetramethyl benzimidazolyl carbocyanine iodide), a fluorescent dye that is taken up by cells and specifically accumulates inside mitochondria. The fluorescence of JC-1 shifts from 527 nm to 590 nm upon aggregation, and the ratio of the green/red fluorescence is used to probe changes in  $\Delta\Psi_{mt}$  and provided a direct measurement of the population of healthy (high potential) versus impaired mitochondria (low potential). We first compared the flow cytometry profile of control macrophages stained with JC-1 to those of cells stimulated for 24 h with different cytokines. We observed that macrophages activated by IL-4, IL-13, IL-10, IL-1 $\beta$  had ratios of healthy to impaired mitochondria comparable to those of control cells (Fig. 2.5A). However, macrophages stimulated with TNF- $\alpha$  and IFN-

$\gamma$  showed a 30 % decrease and 25 % increase in the ratio of healthy to impaired mitochondria, respectively (Fig. 2.5A). The increase in mitochondrial activity upon IFN- $\gamma$  stimulation is consistent with previous reports indicating that activated macrophages utilize significant amounts of glycolytically generated ATP to maintain high  $\Delta\Psi_{mt}$  and prevent apoptosis <sup>39</sup>. In contrast, the decrease in mitochondrial potential in non apoptotic macrophages suggests that TNF- $\alpha$  induced selective degradation of mitochondria, in agreement with our quantitative proteomics experiments. Importantly, these results also indicated that TNF- $\alpha$  is the only major immune response modulating cytokine leading to a decrease in healthy mitochondria in activated macrophages.

The selective degradation of mitochondria proteins upon TNF- $\alpha$  activation prompted us to examine the mechanism by which this could take place and the effect of this cytokine on other cell types. We used mouse embryonic fibroblast (MEF) cells that are morphologically and functionally similar to mouse macrophages. MEF cells stimulated with TNF- $\alpha$  led to a decrease in the ratios of healthy to impaired mitochondria comparable to those observed for RAW 264.7 macrophages (Fig. 2.5B). Also, TNF- $\alpha$  activation of MEF cells did not lead to decreased cell counts or increased apoptosis (data not shown). We surmised that the impaired mitochondrial activities observed in both TNF- $\alpha$  activated macrophages and MEF cells could arise from an autophagy-mediated degradation of mitochondria, or mitophagy <sup>40</sup>. To verify this proposal, we compared the change in mitochondrial potential of TNF- $\alpha$  activated macrophages with and without 3-methyl adenine (3-MA), a compound that prevent autophagy by blocking the formation of autophagosome via the inhibition of phosphatidylinositol 3-kinases (PI-3Ks) <sup>41</sup>. These experiments indicated that 3-MA restored normal mitochondrial activities in TNF- $\alpha$  activated macrophages (Fig. 2.5B). Furthermore, the effects of TNF- $\alpha$  on mitochondrial functions were also abrogated in MEF cells isolated from Atg5 <sup>-/-</sup> mice (Fig. 2.5B). The autophagy-related protein Atg5 is required in the formation of autophagosome, a vacuole in which intracellular components like mitochondria are sequestered before their degradation in the lysosome <sup>42</sup>. Consistent with this observation, we also noted that macrophages stimulated with TNF- $\alpha$  displayed increased lysosomal degradation activities when stained with LysoSensor, a pH-sensitive fluorescent probe that accumulates in acidic organelles (Supplemental Fig. 2.S10).

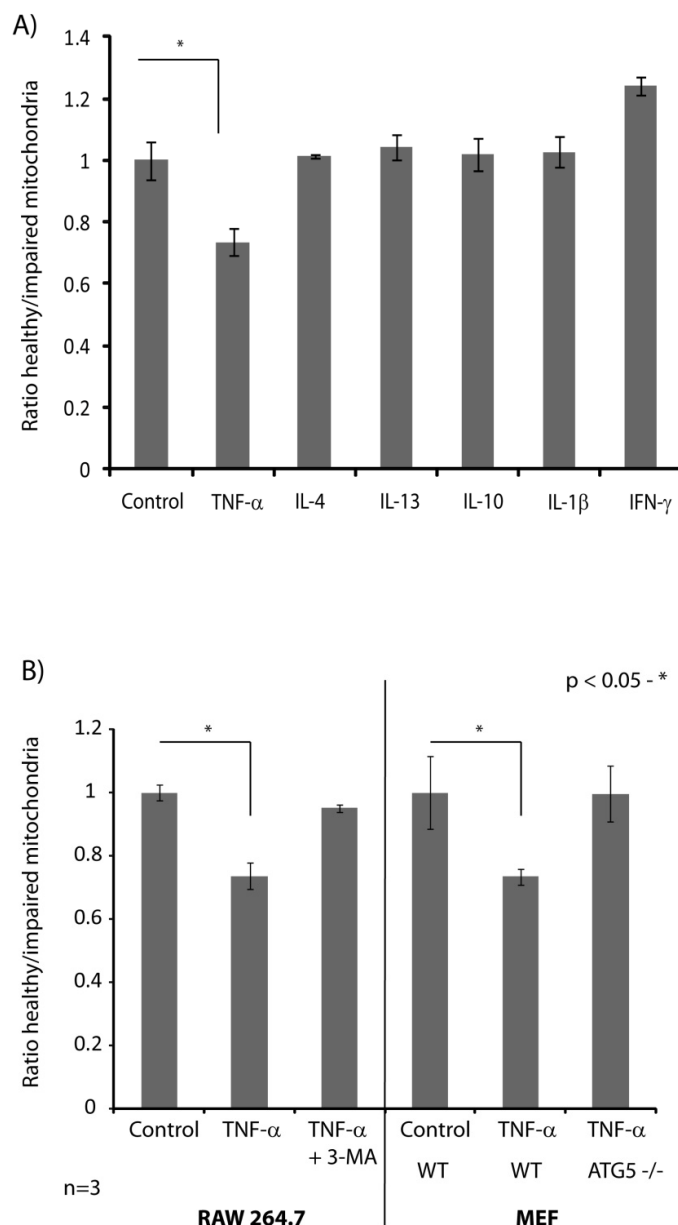


**Figure 2.5. Changes in mitochondrial functions associated with TNF- $\alpha$  activated macrophages.**

(A) Flow Cytometry analysis of changes in mitochondrial membrane potential using JC-1 in RAW264.7 macrophages following stimulation with TNF- $\alpha$ , IL-4, IL-13, IL-10, IL-1 $\beta$  and IFN- $\gamma$ . Macrophages were stimulated with cytokines for 24 hr and the proportion of healthy versus functionally impaired mitochondria in macrophages was determined using mean fluorescence values of monomeric JC-1 or J-aggregates. TNF- $\alpha$  strongly reduces the ratio of healthy to functionally impaired macrophages, while the other cytokines have no significant effect on the mitochondrial membrane potential. (B) Flow Cytometry analysis of changes in mitochondrial membrane potential using JC-1 in RAW264.7 macrophages and MEF stimulated with TNF- $\alpha$  for 24h. The ratio of healthy versus functionally impaired mitochondria in macrophages was determined using mean fluorescence values of monomeric JC-1 or J-aggregates. Treatment with the autophagy inhibitor 3-methyladenine for 3h abolished the effect of TNF- $\alpha$  on mitochondrial potential. Knock-down of Atg5 restored original ratio of healthy mitochondria in TNF- $\alpha$  activated MEF cells.



We used immunofluorescence microscopy to confirm that mitochondria were degraded in autophagosomes upon TNF- $\alpha$  activation. Macrophage cells were stained for the mitochondrion inner membrane protein Tim23 and the autophagic marker LC-3 II to monitor their respective subcellular distribution. In unstimulated cells, Tim23 was evenly distributed across cells while LC3 II was barely detectable (Fig 2.6A). A significant increase in LC3 II abundance was observed following 24 h stimulation with TNF- $\alpha$ , confirming the autophagic activation and the formation of characteristic cellular autophagosome punctae containing LC3 II (Fig. 2.6A). Interestingly, we noted the co-localization of mitochondria and autophagosomes, and the striking disappearance of mitochondria in regions where autophagosomes were more densely distributed, consistent with increased mitophagy activities. A salient feature of autophagy is the sequestration of cytosolic organelles and protein aggregates in double membrane-bound compartments to be transported to and degraded in the lysosomal vacuoles <sup>43</sup>. Morphological analyses performed using electron microscopy revealed the encapsulation of mitochondria by a double-membrane in TNF- $\alpha$  activated macrophages (Fig. 2.6B). Under control conditions mitochondria appeared intact while TNF- $\alpha$  activation of macrophages led to impaired mitochondrial structure. In addition, we observed that mitochondria fused with lysosomes upon TNF- $\alpha$  stimulation. Collectively, these results confirmed that TNF- $\alpha$  selectively led to the degradation of mitochondria via the induction of autophagy.

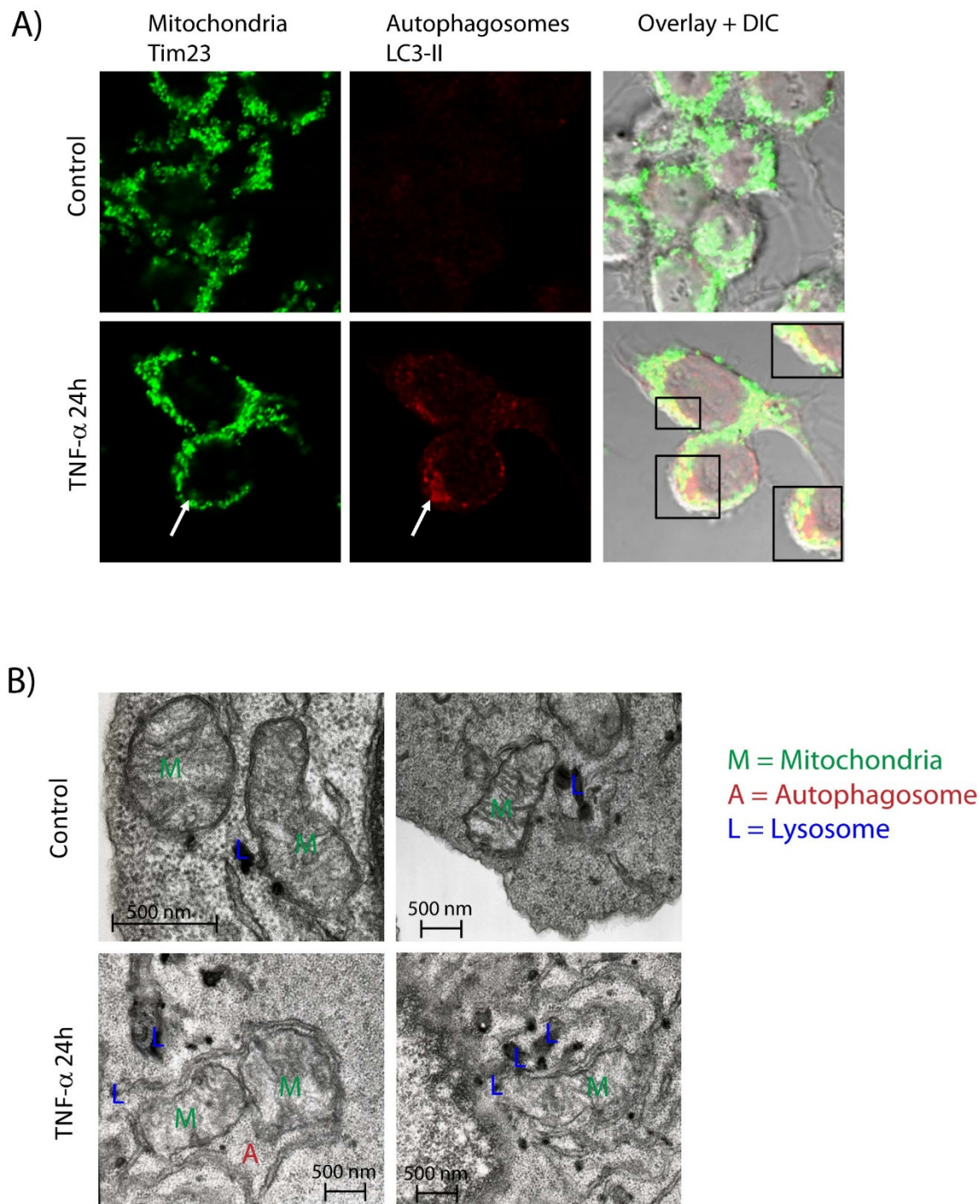


**Figure 2.6. TNF- $\alpha$  induces mitophagy.**

(A) TNF- $\alpha$  stimulation for 24h induces LC3-II punctae (red), and confirmed the colocalization of autophagosomes and mitochondria. In control cells, no LC3-II punctae are detected and mitochondria are distributed throughout the cell. (B) Morphological analyses using electron microscopy (EM) of control and TNF- $\alpha$  stimulated macrophages. Electron micrograph images showed the presence of functionally impaired mitochondria in TNF- $\alpha$  stimulated RAW264.7 macrophages. Mitochondria from TNF- $\alpha$  activated macrophages are enclosed by autophagosomal-like double-membrane vesicles while healthy and functional mitochondria are observed in control cells.

#### **2.5.4. Macrophage activation by TNF- $\alpha$ increases MHC Class I presentation of mitochondrial antigens**

Autophagy is not limited to the clearance of intracellular components, but also plays important roles in both innate and adaptive immunity<sup>44, 45</sup>. Previous reports highlighted the significance of autophagy in promoting the presentation of endogenous antigens on MHC class II molecules, thus leading to the activation of CD4<sup>+</sup> T cells<sup>46, 47</sup>. Interestingly, recent studies also proposed the regulation of macroautophagy and MHC class II expression by TNF- $\alpha$ <sup>34</sup>, and a potential interplay between the vacuolar and MHC class I presentation pathways in IL-1 $\beta$ -activated autophagy<sup>31</sup>. Results from this proteomics study suggest a strong modulation of proteins involved in MHC class I antigen presentation in TNF- $\alpha$ -activated macrophages. In particular, in TNF- $\alpha$  regulated proteins we observed several proteins involved in vesicular trafficking (e.g. sorting nexin-1 and 2, vesicle-trafficking protein SEC22b) and degradation (e.g. LAMP1 and beta-hexosaminidase  $\alpha$  and  $\beta$  subunits) as well as proteins directly implicated in antigen presentation (e.g. H2 class I histocompatibility antigen K-D, D-D and L-D alpha chain, protein transport protein SEC61 $\beta$ ) and proteasomal degradation (e.g. proteasome activator complex subunit I, 26S proteasome non-ATPase regulatory subunit 14, proteasome subunit beta type-3). To our knowledge, the role of the MHC class I presentation machinery in displaying intracellular antigens following the activation of autophagy by TNF- $\alpha$  has not been described thus far. To further investigate the influence of TNF- $\alpha$  on the presentation of mitochondrial antigens via the MHC class I pathway, we developed a system allowing us to study and compare the molecular mechanisms involved in the processing and presentation of endogenous antigens by macrophages. We produced a RAWKb macrophage cell line that stably expressed a truncated form of glycoprotein B (gB) from Herpes Simplex Virus 1 (HSV-1), and targeted its localization to mitochondria using a mitochondrial matrix targeting sequence from cytochrome c oxidase. The vacuolar response initiated by autophagy increases the processing and presentation of gB antigens on MHC class I molecules that can be monitored via the activation of CD8<sup>+</sup> T cells.

The subcellular distribution of HSV-1 gB was determined by immunofluorescence microscopy and confirmed its co-localization with the mitochondrial marker Tom20 (Fig. 2.7A). Next, we cultured these cells for 24 h with TNF- $\alpha$  and/or specific pharmacological inhibitors to evaluate their functional effects on antigen presentation. Following

stimulation, cells were fixed with paraformaldehyde and then co-cultured with lacZ-inducible gB-specific CD8<sup>+</sup> T cell hybridoma to measure T cell activation against the HSV-1 gB antigen 12 h later. We observed a 30% increase in MHC class I presentation of gB antigens for macrophages stimulated by TNF- $\alpha$  (Fig. 2.7B). Stimulation of the CD8<sup>+</sup> T cell hybridoma was decreased after treatment of activated macrophages with PI-3K inhibitor 3-MA, further supporting the proposal that autophagy contributes to the vacuolar processing and presentation of gB antigen on MHC class I molecules. The effect of mitophagy on antigen presentation was confirmed separately using carbonyl cyanide *m*-chlorophenyl hydrazone (CCCP), a protonophore that lead to rapid membrane depolarization and degradation of mitochondria (Fig. 2.7B). Interestingly, macrophages treated with rapamycin, an inhibitor of the kinase mTOR that normally induce autophagy, had no effect on CD8<sup>+</sup> T cell stimulation. Together, these results indicate that TNF- $\alpha$  promoted the selective vacuolar processing of mitochondria proteins and improved the ability of activated macrophages to cross present mitochondrial antigens to CD8<sup>+</sup> T cells.

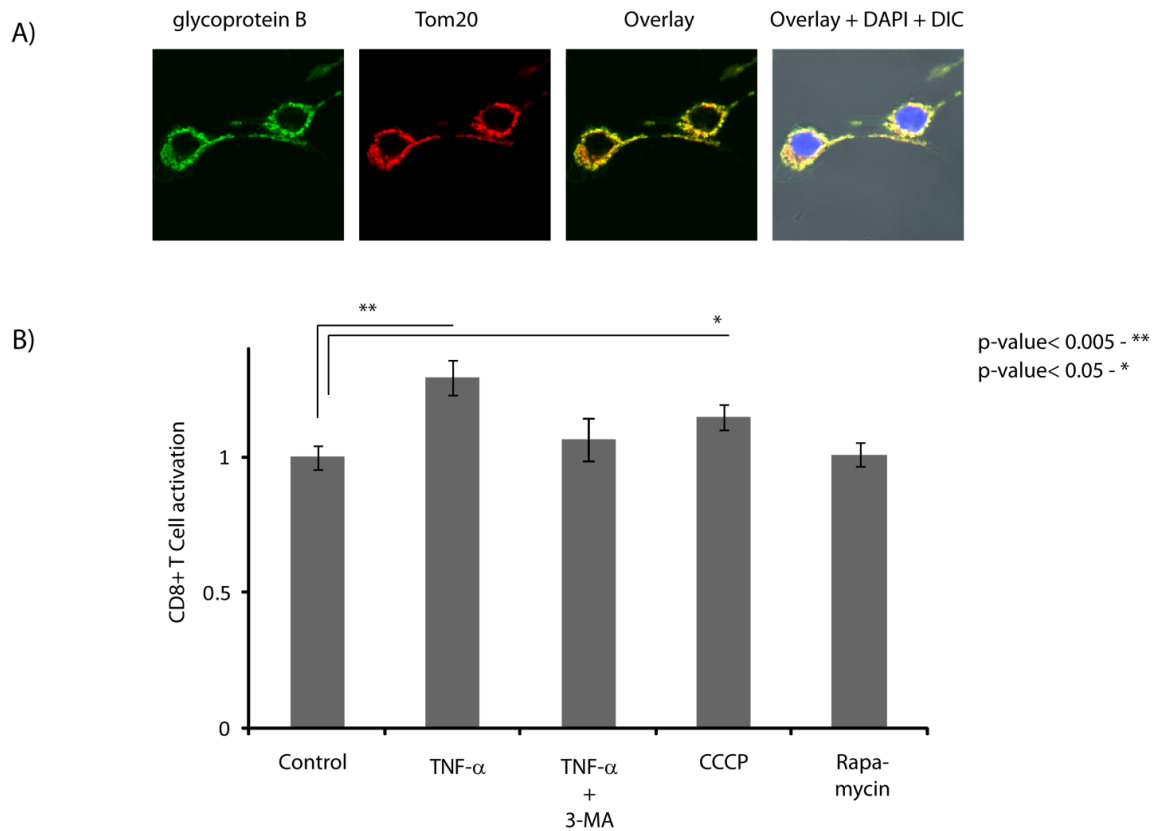


**Figure 2.7. Influence of TNF- $\alpha$  on antigen presentation.**

(A) gB antigen peptide (green) expressed in RAW264.7 cells is targeted to mitochondria and co-localized with Tim23 (red). (B) TNF- $\alpha$  enhanced MHC class I cross presentation of gB antigen. RAW macrophages (control or 24 hr following TNF- $\alpha$  activation) were incubated with different pharmacological inhibitors. Macrophages were fixed and co-cultured with lacZ-inducible gB HSV-specific CD8+ T cell hybridoma for 12 hr, and cell activation was measured using UV-VIS spectrometer following the hydrolysis of  $\beta$ -Gal.

## 2.6. Discussion

In this report, we described a comprehensive proteomics study aimed at characterizing the proteome of resting and TNF- $\alpha$ -activated mouse macrophages. Label-free quantitative proteomics analysis of crude membrane extracts from TNF- $\alpha$  stimulated macrophages revealed the differential regulation of several proteins involved in vesicular trafficking, protein degradation, and immune response (Table II-1). These analyses also confirmed the identification of several proteins known to be modulated by TNF- $\alpha$  such as cPLA<sub>2</sub> and TRAP1. Previous reports have described the activation of cPLA<sub>2</sub> upon TNF- $\alpha$  activation of macrophages<sup>48, 49</sup>. This protein is activated by calcium and comprise both lysophospholipase and transacylase activities. cPLA<sub>2</sub> selectively hydrolyzes arachidonyl phospholipids in the sn-2 position releasing arachidonic acid, and this enzyme plays a major role in the initiation of the inflammatory response. In comparison, TRAP1, also referred to as heat shock protein 75, is a member of the HSP90 family<sup>50</sup> that interacts with the intracellular domain of type I TNF receptor. TRAP1 was found to localize to mitochondria and exhibited ATPase activities, but does not form stable complex with classic HSP90 co-chaperones<sup>51</sup>.

It is noteworthy that the activation of cPLA<sub>2</sub> increases the intracellular levels of arachidonic acid and mediates the production of ROS. While low levels of ROS act as signaling molecules, their prolonged production can impair mitochondrial functions through oxidative damage<sup>52</sup> and depolarization of the transmembrane potential,  $\Delta\Psi_{mt}$  (Fig. 2.5). Interestingly, we observed a consistent downregulation of mitochondrial proteins in response to TNF- $\alpha$  activation (Fig. 2.4 and supplemental Fig. 2.S7). We also noted that mitochondrial proteins were not all affected in a similar manner upon TNF- $\alpha$  activation, and downregulated proteins represented mostly enzymes (65%) and transporters (30%), while proteins associated with mitochondrial ribosomes remained largely unaffected.

Importantly, we observed that TNF- $\alpha$  was the only molecule amongst all cytokines examined that led to the selective degradation of mitochondria in lytic vesicles through autophagy. Several studies have suggested a role for TNF- $\alpha$  in stimulating autophagy in human and murine macrophages<sup>32-34, 53</sup>, but the exact mechanism by which TNF- $\alpha$  stimulates autophagy is not fully understood, and may differ depending on cell types.

This process is initiated by damaged mitochondria which upon loss of  $\Delta\Psi_{mt}$  stabilize the voltage-sensitive kinase Pink1 on the outer mitochondrial membrane leading to the recruitment of the E3 ubiquitin ligase Parkin and the ubiquitination of mitochondrial proteins <sup>54, 55</sup>. It is noteworthy that the regulation of Pink, Parkin, or Nix upon TNF- $\alpha$  stimulation was not determined in the present study, and that macroautophagy could possibly be involved in the elimination of mitochondria. Interestingly, we noted that a number of mitochondrial proteins were ubiquitinated including DNA topoisomerase 1 mitochondrial. The accumulation of ubiquitylated mitochondrial proteins is thought to facilitate the recruitment of the ubiquitin-binding protein p62 (sequestosome-1), an adaptor protein that binds to Lys-63 polyubiquitin chains of ubiquitylated substrates and mediates the interaction with LC3 to facilitate the autophagosomal degradation of the damaged mitochondria <sup>56</sup>. A schematic representation of the autophagic pathways is presented in Supplemental Fig. 2.S11.

Impaired mitochondria are first encapsulated in a characteristic double-membrane structure known as the autophagosome prior to fusing with lysosome where their cargo are degraded (Fig. 2.6B). This double-membrane can arise from an extension of endoplasmic reticulum (ER) known as the omegasome that contributes important components to the formation of autophagosomes <sup>57</sup>. These vesicles are coated with the autophagosome marker microtubule associated protein 1 (MAP1) light chain 3 (LC3), an ubiquitin-like protein that is covalently attached to phosphatidylethanolamine during their biogenesis. Consistent with this notion, immunofluorescence microscopy experiments indicated that LC3-II punctae were present in TNF- $\alpha$  stimulated macrophages but not in resting macrophages (Fig. 2.6A). We also confirmed that the selective degradation of mitochondria was dependent on both PI-3K and Atg5 (Fig. 2.5B). During the induction of autophagy, Atg5 conjugates to the ubiquitin-like protein, Atg12, and interacts with Atg16 to form an oligomeric complex that localizes to nascent autophagosomes <sup>58</sup>. The formation of the Atg12-Atg5-Atg16 complex is a prerequisite to the lipidation of LC3 and its targeting to autophagosomes prior to their fusion with either late endosomes (amphisomes) or lysosomes (autolysosomes) <sup>59, 60</sup>.

In addition to the elimination of dysfunctional mitochondria, autophagy also plays important roles in innate and adaptive immunity via the processing and presentation of endogenously expressed antigens by MHC class I and class II molecules <sup>61-63</sup>. The notion that the degradation of intracellular antigens after autophagy is used by the mammalian

immune system to display intracellular antigens on MHC class II for CD4<sup>+</sup> T cell stimulation was recently expanded to include antigen processing via MHC class I presentation<sup>31</sup>. Indeed, previous results from our group indicated that in addition to the classical MHC class I pathway, viral proteins can be engulfed later during HSV-1 infection by autophagosomes formed from the membrane of the outer nuclear envelope. Inhibition of autophagy was confirmed by siRNA silencing of the Atg5 gene and abrogated HSV-1 specific CD8<sup>+</sup> T cell stimulation<sup>31</sup>. In the present study, we further expanded the role of autophagy in the processing of intracellular antigens and their presentation by MHC class I molecules. Using a RAWKb macrophage cell line that stably expressed a truncated form of gB from HSV-1 targeted to mitochondria, we showed that autophagy increased the processing and presentation of mitochondrial viral antigens on MHC class I molecules following TNF- $\alpha$  activation (Fig. 2.7). CD8<sup>+</sup> T cell activation was modulated by PI-3K inhibition and loss of  $\Delta\Psi_{mt}$  consistent with the notion that autophagy contributes to the processing and presentation of mitochondria-specific gB antigen on MHC class I molecules. This pathway is independent of autophagy induced by mTORC1 inhibition as macrophages treated with rapamycin showed no increase in CD8<sup>+</sup> T cell stimulation. Taken together, these findings highlight a novel role for TNF- $\alpha$  in mitophagy and in the processing and presentation of mitochondrial antigens by MHC class I molecules. It is interesting to note that increased ROS production and oxidative stress induced by the accumulation of damaged mitochondria can lead to a host danger signal initiated by NLRP3 inflammasomes often associated with many chronic inflammatory diseases<sup>64</sup>. NLRP3 inflammasome is negatively regulated by autophagy, and targeted removal of dysfunctional mitochondria following TNF- $\alpha$  prevents progressive cell damage and inflammation.



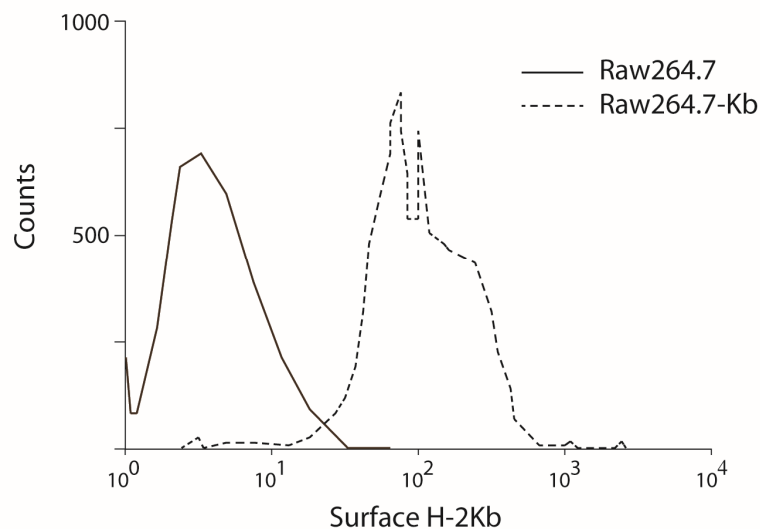
## 2.7. Acknowledgements

We thank Christiane Rondeau and Eric Bonneil for assistance with electron microscopy and mass spectrometry analyses, G. Arthur (University of Manitoba) for the wild-type and *Atg5*<sup>-/-</sup> mouse embryonic fibroblasts produced by N. Mizushima (Medical and Dental University, Tokyo). CB holds a Vanier Canada Graduate Scholarship from the Natural Science and Engineering Research Council (NSERC). This work was supported by a Canadian Institutes of Health Research grant to MD and PT. MD and PT hold Canada Research Chairs in Cellular Microbiology and Proteomics and Bioanalytical Spectrometry, respectively. IRIC is supported in part by the Canadian Center of Excellence in Commercialization and Research, the Canada Foundation for Innovation (CFI) and the Fonds de Recherche du Québec en Santé (FRQS).

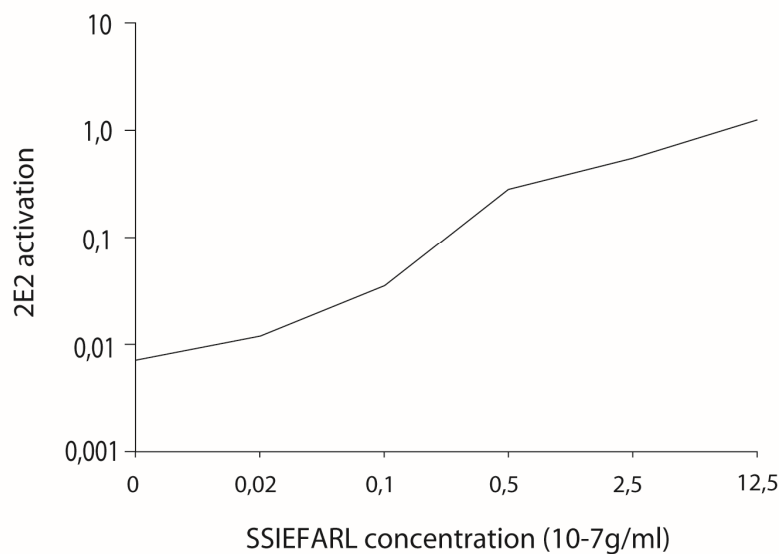
## 2.8. Supplemental data

### 2.8.1. Supplementary figures

A)



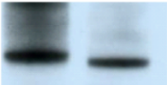


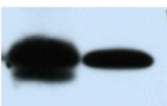


B)



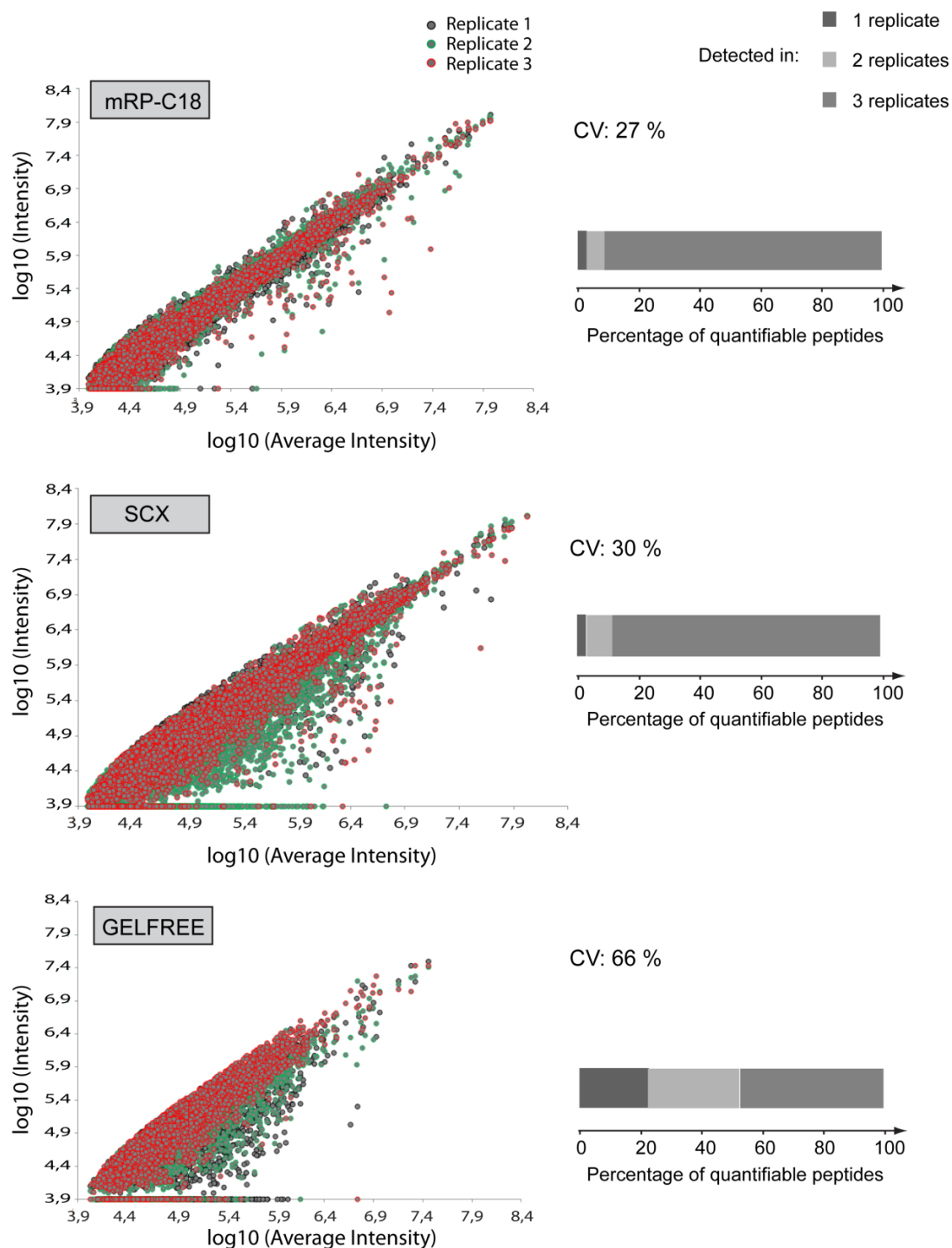
**Supplementary Figure 2.S1. Flow cytometry analysis and clone showing the highest fluorescence levels selected, amplified and used.**

(A) Kb heavy chain of the MHC class I molecule is expressed at the cell surface of Raw-Kb murine macrophages. (B) Kb efficiently binds the Kb-restricted epitope SSIEFARL (derived from gB), as revealed by the strong 2E2 activation when exogenous peptide was added to the culture medium for 30 minutes before fixation and addition of the CD8<sup>+</sup> T cells. 2E2 activation is measured by quantifying beta-galactosidase produced by the hybridoma.

Cellular Compartment	Fraction	
	TM	TCL
Cytoplasm		<b>Actin</b>
Nucleus		<b>Nucleoporin p62</b>
Plasmamembrane		<b>Na<sup>+</sup>/K<sup>+</sup> ATPase</b>
		<b>Annexin II</b>
Lysosomal membrane		<b>LAMP1</b>
Mitochondrial membrane		<b>Tom20</b>

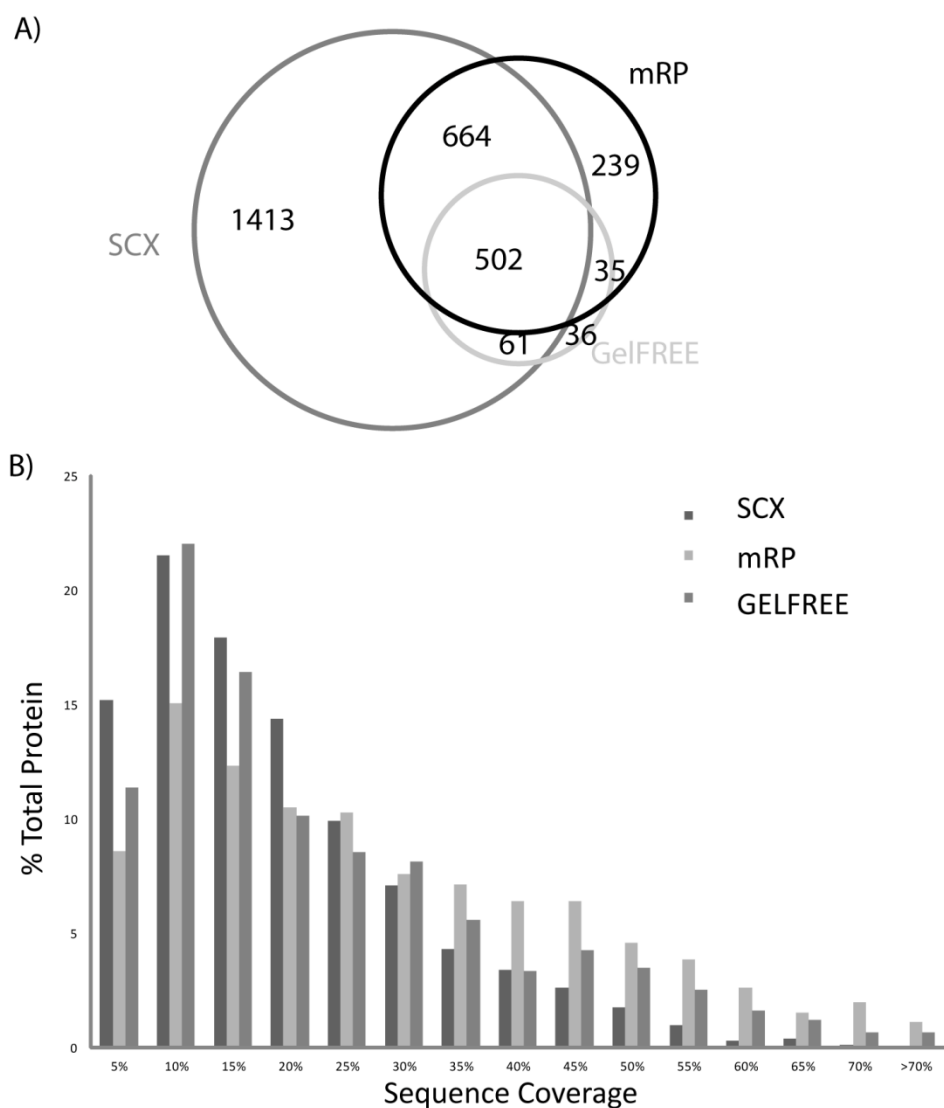
**Supplementary Figure 2.S2. Fractionation efficiency using immunoblots for several cellular markers.**

Western blot analysis of 10 µg of protein of total membrane (TM) and total cell lysate (TCL) preparations of RAW 267.4 mouse macrophages. Western blots confirm the high purity of our TM preparations. The following antibodies were used: gamma-actin (actin, cytoplasm), nucleoporin p62 (nucleus), Na<sup>+</sup>/K<sup>+</sup> ATPase (Plasmamembrane), Annexin II (Plasmamembrane), lysosome-associated membrane glycoprotein 1 (LAMP1, lysosomal membrane), mitochondrial import receptor subunit Tom20 (Tom20, mitochondrial membrane).



**Supplementary Figure 2.S3. Reproducibility of peptide intensities across replicates.**

Scatter plots of abundance measurements for peptide ions identified using mRP-C18, SCX and GELFREE as first dimension of separation. While SCX and GELFREE display quite wide distributions of peptide intensities, mRP-C18 displays a very narrow distribution. mRP-C18 also has the lowest CV of 27% attesting its reproducibility. 91% of quantified peptides using mRP-C18 have been detected in 3 replicates, while in GELFREE only 46% have been detected in 3 replicates respectively.

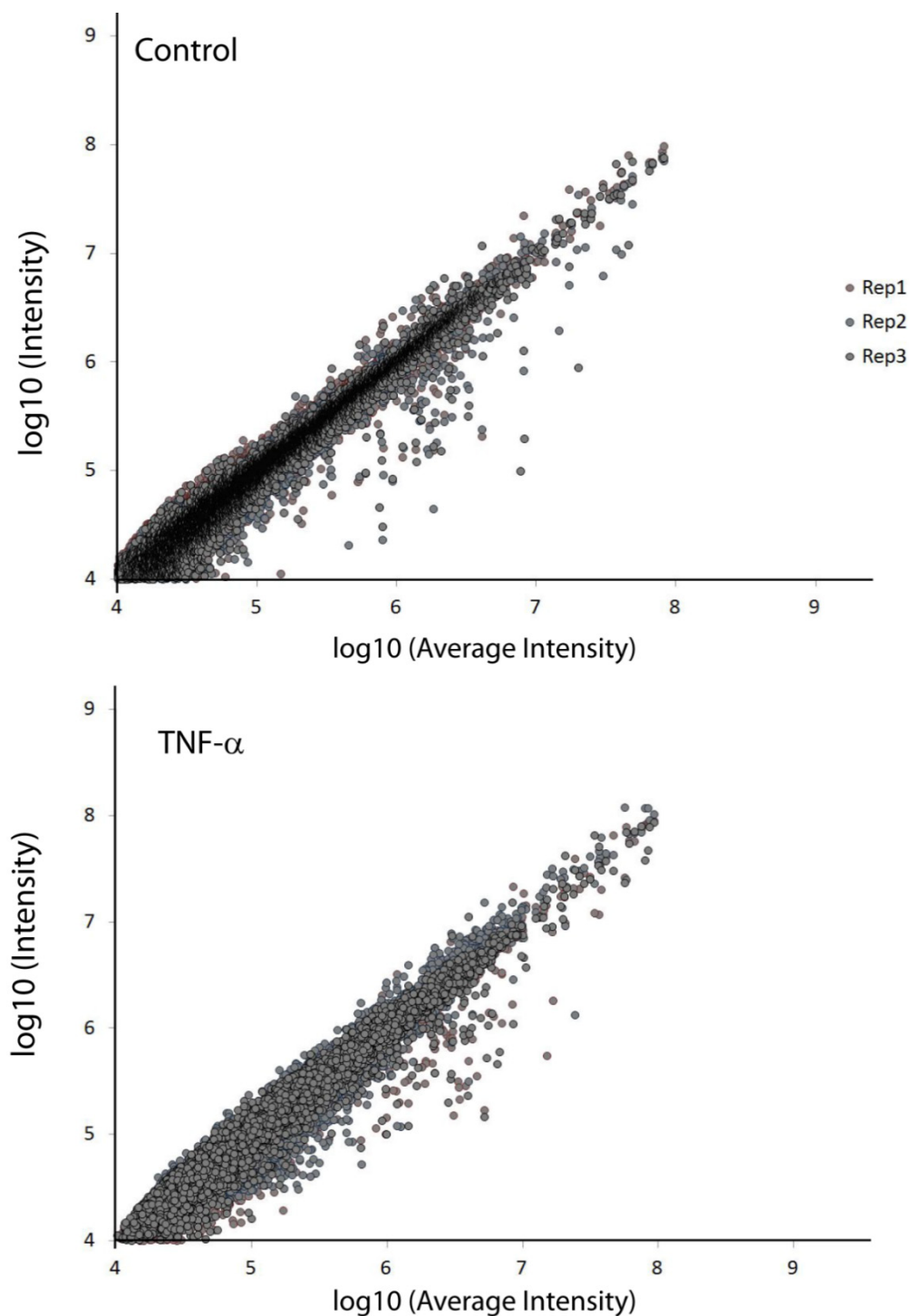


**Supplementary Figure 2.S4. Comparison of three different fractionation techniques for quantitative membrane proteomics of RAW264.7 macrophages.**

(A) Venn diagram representation of protein identification obtained using strong cation exchange (SCX), GelfREE and macroporous reversed phase (mRP) fractionation of macrophage membrane proteins. Different fractionation techniques complement each other for comprehensive large-scale proteomics. (B) Distribution of sequence coverage for separation techniques. A higher sequence coverage of identified proteins is typically obtained using mRP fractionation compared to SCX and GELFREE.

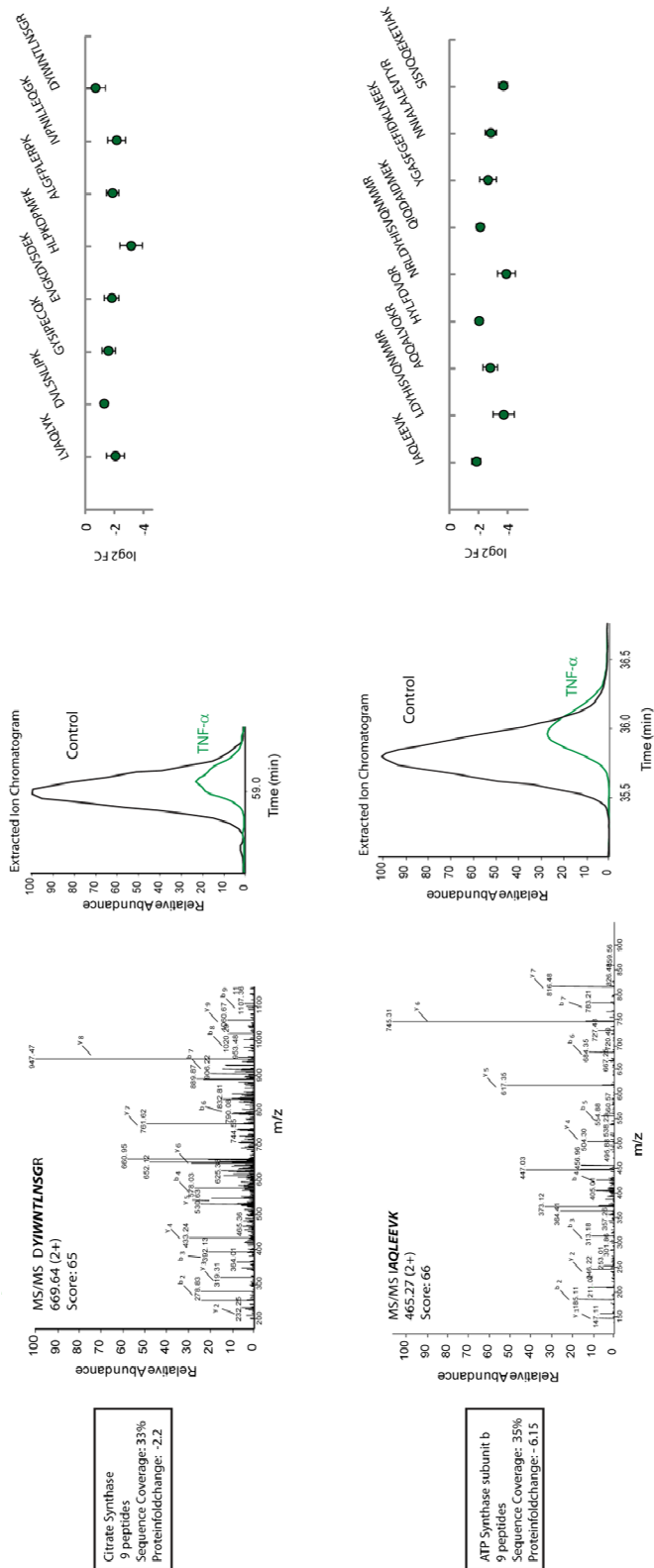
**Supplementary Figure 2.S5. MS/MS spectra of phosphopeptides (CD-ROM).**

Annotated MS/MS spectra of phosphopeptides identified in experiments from fractionation of membrane proteins using SCX, GELFREE and mRP.



**Supplementary Figure 2.S6. Scatter plots of abundance measurements for peptide ions identified in control and TNF- $\alpha$  stimulated extracts.**

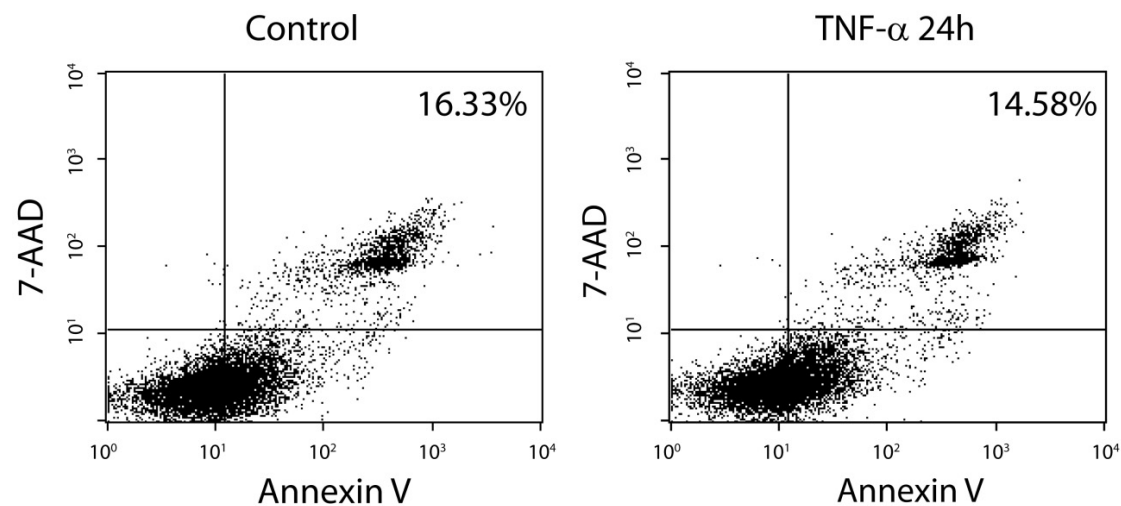
Peptide ion intensity distributions for 3 replicates are very narrow in control and TNF- $\alpha$  stimulated macrophages. 95 % of all ions showed RSD values less than 58 % across all three biological replicates, attesting of the reproducibility of the method.



**Supplementary Figure 2.S7. Fold change measurements for citrate synthase and ATP synthase subunit b.**  
The consistency of fold change measurements is shown for citrate synthase and ATP synthase subunit b, each identified with 9 peptides. The extracted ion chromatogram shows the decrease in peptide ion abundance for a selected peptide. Our workflow enabled accurate detection of protein with high reproducibility as shown by consistent fold changes for all peptides assigned to a specific protein.

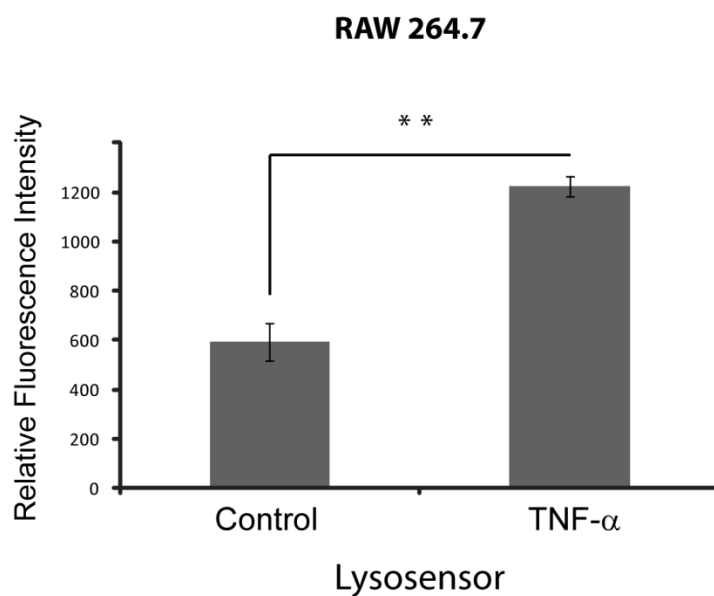
**Supplementary Figure 2.S8: MS/MS spectra of ubiquitinated peptides (CD-ROM).**

Annotated MS/MS spectra of ubiquitinated peptides identified in TNF- $\alpha$  activated macrophages.

**Supplementary Figure 2.S9. Abundance of fluorescently-labeled Annexin A5 at the plasma membrane and 7-amino actinomycin D using flow cytometry.**

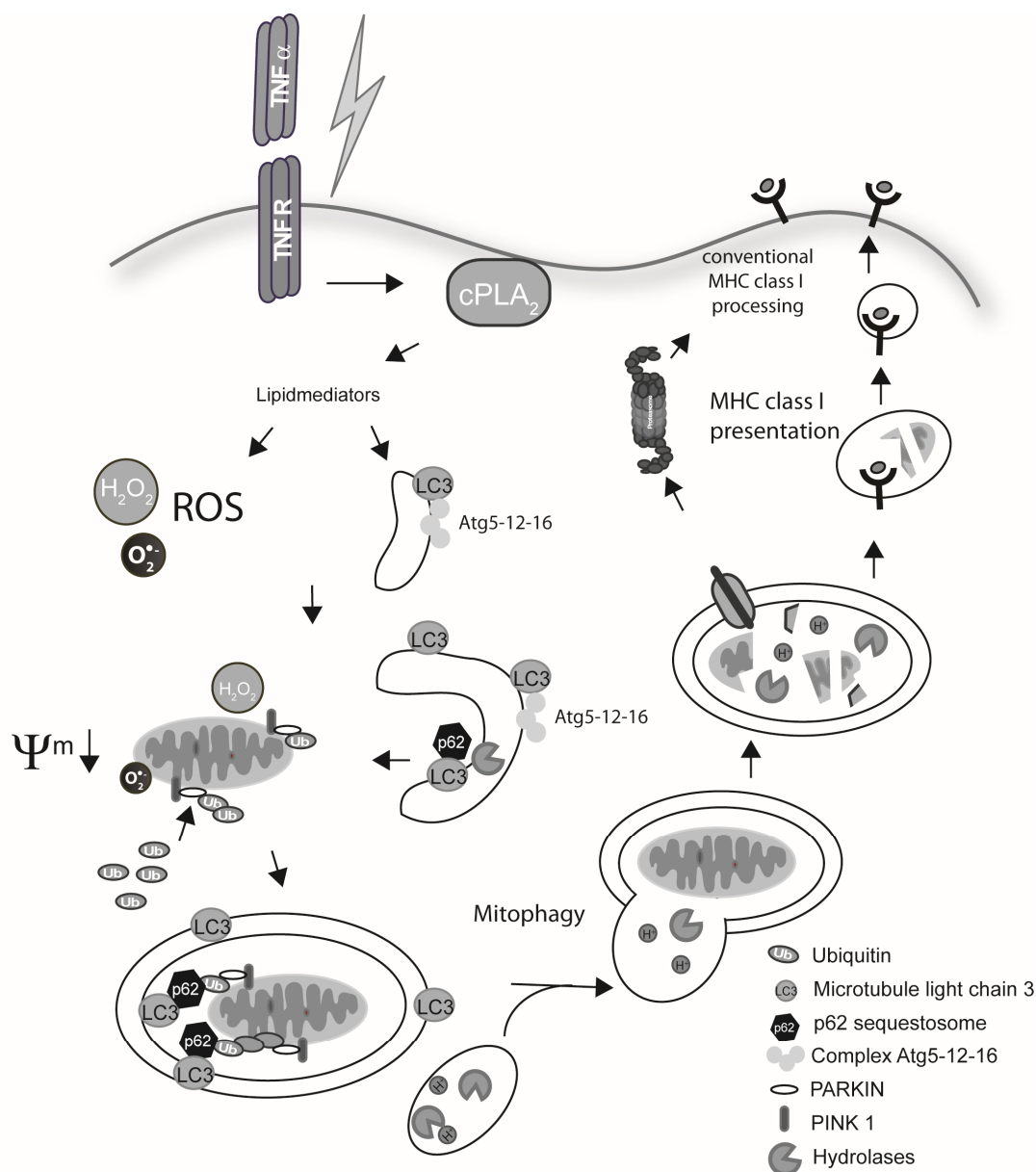
Flow cytometry analyses revealed that apoptotic and dead cells represented approximately 15 % of the cell population in both control and TNF- $\alpha$  activated macrophages. Similar results were also obtained when cells were stained with 7-amino actinomycin D.





**Supplementary Fig. 2.S10. Lysosomal degradation activities when stained with LysoSensor.**

Macrophages stimulated with TNF- $\alpha$  displayed increased lysosomal degradation activities when stained with LysoSensor, a pH-sensitive fluorescent probe that accumulates in acidic organelles.



**Supplementary Figure 2.S11. Integrated model of the TNF- $\alpha$  modulated functions favoring antigen MHC class I presentation.**

TNF- $\alpha$  can mediate the induction of mitophagy in murine macrophages through the activation of cPLA<sub>2</sub>. This activation leads to the induction of lipid mediators such as arachidonic acid, which promotes the formation of reactive oxygen species. Increased ROS levels can impair mitochondrial functions resulting in a decrease in their transmembrane potential,  $\Delta\Psi_{mt}$ . Impaired mitochondrial proteins are engulfed in a double membrane organelle called the autophagosome that later fuses with lysosomes to form autophagolysosomes where they are degraded. Mitochondrial peptides/antigens engulfed in the autophagolysosome can be retrotranslocated into the cytosol where they can be further degraded by the proteasome and processed by the conventional MHC class I machinery. Alternatively, they can remain within the vacuolar compartment where they are degraded by lysosomal proteases, and the resulting peptides are cross-presented to MHC class I molecules.

### 2.8.2. Supplemental tables

**Table II-S1:** Protein identification for different separation platforms: mRP-C18, GELFREE and SCX (CD-ROM).

**Table II-S2:** List of peptides identified in each separation platforms (mRP-C18, GELFREE and SCX) (CD-ROM).

**Table II-S3:** Quantification of protein abundance changes upon TNF-alpha stimulation (CD-ROM).

**Table II-S4:** Ubiquitinated peptides upon TNF-alpha stimulation (CD-ROM).

## 2.9. References

1. Mosser, D. M., and Edwards, J. P. (2008) Exploring the full spectrum of macrophage activation. *Nat Rev Immunol* 8, 958-969
2. Boulais, J., Trost, M., Landry, C. R., Dieckmann, R., Levy, E. D., Soldati, T., Michnick, S. W., Thibault, P., and Desjardins, M. (2010) Molecular characterization of the evolution of phagosomes. *Mol Syst Biol* 6, 423
3. Jutras, I., and Desjardins, M. (2005) Phagocytosis: at the crossroads of innate and adaptive immunity. *Annu Rev Cell Dev Biol* 21, 511-527
4. Plataniias, L. C. (2005) Mechanisms of type-I- and type-II-interferon-mediated signalling. *Nat Rev Immunol* 5, 375-386
5. Murray, P. J., and Wynn, T. A. (2011) Protective and pathogenic functions of macrophage subsets. *Nat Rev Immunol* 11, 723-737
6. Ehrt, S., Schnappinger, D., Bekiranov, S., Drenkow, J., Shi, S., Gingeras, T. R., Gaasterland, T., Schoolnik, G., and Nathan, C. (2001) Reprogramming of the macrophage transcriptome in response to interferon-gamma and Mycobacterium tuberculosis: signaling roles of nitric oxide synthase-2 and phagocyte oxidase. *J Exp Med* 194, 1123-1140
7. Watts, C., and Amigorena, S. (2001) Phagocytosis and antigen presentation. *Semin Immunol* 13, 373-379
8. Trost, M., English, L., Lemieux, S., Courcelles, M., Desjardins, M., and Thibault, P. (2009) The Phagosomal Proteome in Interferon- $\gamma$ -Activated Macrophages. *Immunity* 30, 143-154
9. Jutras, I., Houde, M., Currier, N., Boulais, J., Duclos, S., LaBoissière, S., Bonneil, E., Kearney, P., Thibault, P., Paramithiotis, E., Hugo, P., and Desjardins, M. (2008) Modulation of the Phagosome Proteome by Interferon- $\gamma$ . *Molecular & Cellular Proteomics* 7, 697-715
10. Houde, M., Bertholet, S., Gagnon, E., Brunet, S., Goyette, G., Laplante, A., Princiotta, M. F., Thibault, P., Sacks, D., and Desjardins, M. (2003) Phagosomes are competent organelles for antigen cross-presentation. *Nature* 425, 402-406
11. Guermonprez, P., Saveanu, L., Kleijmeer, M., Davoust, J., Van Endert, P., and Amigorena, S. (2003) ER-phagosome fusion defines an MHC class I cross-presentation compartment in dendritic cells. *Nature* 425, 397-402
12. Gordon, S. (2003) Alternative activation of macrophages. *Nat Rev Immunol* 3, 23-35
13. Edwards, J. P., Zhang, X., Frauwirth, K. A., and Mosser, D. M. (2006) Biochemical and functional characterization of three activated macrophage populations. *J Leukoc Biol* 80, 1298-1307

14. Kolls, J. K., and Linden, A. (2004) Interleukin-17 family members and inflammation. *Immunity* 21, 467-476
15. Maini, R., Elliott, M., Brennan, F., and Feldmann, M. (1995) Beneficial effects of tumour necrosis factor-alpha (TNF-alpha) blockade in rheumatoid arthritis (RA). *Clinical and experimental immunology* 101, 207
16. van Dullemen, H. M., van Deventer, S. J. H., Hommes, D. W., Bijl, H. A., Jansen, J., Tytgat, G. N. J., and Woody, J. (1995) Treatment of Crohn's disease with anti-tumor necrosis factor chimeric monoclonal antibody (cA2). *Gastroenterology* 109, 129-135
17. Bouwmeester, T., Bauch, A., Ruffner, H., Angrand, P.-O., Bergamini, G., Coughton, K., Cruciat, C., Eberhard, D., Gagneur, J., Ghidelli, S., Hopf, C., Huhse, B., Mangano, R., Michon, A.-M., Schirle, M., Schlegl, J., Schwab, M., Stein, M. A., Bauer, A., Casari, G., Drewes, G., Gavin, A.-C., Jackson, D. B., Joberty, G., Neubauer, G., Rick, J., Kuster, B., and Superti-Furga, G. (2004) A physical and functional map of the human TNF-[alpha]/NF-[kappa]B signal transduction pathway. *Nat Cell Biol* 6, 97-105
18. Cantin, G. T., Venable, J. D., Cociorva, D., and Yates, J. R. (2005) Quantitative Phosphoproteomic Analysis of the Tumor Necrosis Factor Pathway. *Journal of Proteome Research* 5, 127-134
19. Ma, D.-j., Li, S.-J., Wang, L.-S., Dai, J., Zhao, S.-l., and Zeng, R. (2009) Temporal and spatial profiling of nuclei-associated proteins upon TNF-[alpha]/NF-[kappa]B signaling. *Cell Res* 19, 651-664
20. Lee, M. J., Kim, J., Kim, M. Y., Bae, Y. S., Ryu, S. H., Lee, T. G., and Kim, J. H. (2010) Proteomic analysis of tumor necrosis factor-alpha-induced secretome of human adipose tissue-derived mesenchymal stem cells. *J Proteome Res* 9, 1754-1762
21. Choi, K. Y., Lippert, D. N., Ezzatti, P., and Mookherjee, N. (2012) Defining TNF-alpha and IL-1beta induced nascent proteins: Combining bio-orthogonal non-canonical amino acid tagging and proteomics. *J Immunol Methods*
22. Olsen, J. V., Blagoev, B., Gnadt, F., Macek, B., Kumar, C., Mortensen, P., and Mann, M. (2006) Global, in vivo, and site-specific phosphorylation dynamics in signaling networks. *Cell* 127, 635-648
23. Courcelles, M., Lemieux, S., Voisin, L., Meloche, S., and Thibault, P. (2011) ProteoConnections: A bioinformatics platform to facilitate proteome and phosphoproteome analyses. *PROTEOMICS* 11, 2654-2671
24. Trost, M., Sauvageau, M., Herault, O., Deleris, P., Pomies, C., Chagraoui, J., Mayotte, N., Meloche, S., Sauvageau, G., and Thibault, P. (2012) Posttranslational regulation of self-renewal capacity: insights from proteome and phosphoproteome analyses of stem cell leukemia. *Blood* 120, e17-27
25. Sonnhammer, E., Von Heijne, G., and Krogh, A. (1998) A hidden Markov model for predicting transmembrane helices in protein sequences. pp. 175-182

26. Sherman, B. T., and Lempicki, R. A. (2009) Bioinformatics enrichment tools: paths toward the comprehensive functional analysis of large gene lists. *Nucleic Acids Research* 37, 1-13
27. Da Wei Huang, B. T. S., and Lempicki, R. A. (2008) Systematic and integrative analysis of large gene lists using DAVID bioinformatics resources. *Nature protocols* 4, 44-57
28. Cline, M. S., Smoot, M., Cerami, E., Kuchinsky, A., Landys, N., Workman, C., Christmas, R., Avila-Campilo, I., Creech, M., and Gross, B. (2007) Integration of biological networks and gene expression data using Cytoscape. *Nature protocols* 2, 2366-2382
29. Martin, A., Ochagavia, M. E., Rabasa, L. C., Miranda, J., Fernandez-de-Cossio, J., and Bringas, R. (2010) BisoGenet: a new tool for gene network building, visualization and analysis. *BMC bioinformatics* 11, 91
30. Consortium, U. (2012) Reorganizing the protein space at the Universal Protein Resource (UniProt). *Nucleic Acids Res* 40, D71-D75
31. English, L., Chemali, M., Duron, J., Rondeau, C., Laplante, A., Gingras, D., Alexander, D., Leib, D., Norbury, C., Lippe, R., and Desjardins, M. (2009) Autophagy enhances the presentation of endogenous viral antigens on MHC class I molecules during HSV-1 infection. *Nat Immunol* 10, 480-487
32. Baregamian, N. (2009) Tumor necrosis factor- $\alpha$  and apoptosis signal-regulating kinase 1 control reactive oxygen species release, mitochondrial autophagy and c-Jun N-terminal kinase/p38 phosphorylation during necrotizing enterocolitis. *Oxidative medicine and cellular longevity* 2, 297
33. Jia, G., Cheng, G., Gangahar, D. M., and Agrawal, D. K. (2006) Insulin-like growth factor-1 and TNF- $\alpha$  regulate autophagy through c-jun N-terminal kinase and Akt pathways in human atherosclerotic vascular smooth cells. *Immunology and cell biology* 84, 448-454
34. Keller, C. W., Fokken, C., Turville, S. G., Lünemann, A., Schmidt, J., Münz, C., and Lünemann, J. D. (2011) TNF- $\alpha$  Induces Macroautophagy and Regulates MHC Class II Expression in Human Skeletal Muscle Cells. *Journal of Biological Chemistry* 286, 3970-3980
35. Chan, N. C., Salazar, A. M., Pham, A. H., Sweredoski, M. J., Kolawa, N. J., Graham, R. L. J., Hess, S., and Chan, D. C. (2011) Broad activation of the ubiquitin-proteasome system by Parkin is critical for mitophagy. *Human molecular genetics* 20, 1726-1737
36. Aggarwal, B. B., Gupta, S. C., and Kim, J. H. (2012) Historical perspectives on tumor necrosis factor and its superfamily: 25 years later, a golden journey. *Blood* 119, 651-665

37. Saelens, X., Festjens, N., Vande Walle, L., van Gorp, M., van Loo, G., and Vandenabeele, P. (2004) Toxic proteins released from mitochondria in cell death. *Oncogene* 23, 2861-2874
38. Vermes, I., Haanen, C., Steffens-Nakken, H., and Reutelingsperger, C. (1995) A novel assay for apoptosis. Flow cytometric detection of phosphatidylserine expression on early apoptotic cells using fluorescein labelled Annexin V. *J Immunol Methods* 184, 39-51
39. Garedew, A., Henderson, S. O., and Moncada, S. (2010) Activated macrophages utilize glycolytic ATP to maintain mitochondrial membrane potential and prevent apoptotic cell death. *Cell Death Differ* 17, 1540-1550
40. Kim, I., Rodriguez-Enriquez, S., and Lemasters, J. J. (2007) Selective degradation of mitochondria by mitophagy. *Archives of Biochemistry and Biophysics* 462, 245-253
41. Petiot, A., Ogier-Denis, E., Blommaert, E. F., Meijer, A. J., and Codogno, P. (2000) Distinct classes of phosphatidylinositol 3'-kinases are involved in signaling pathways that control macroautophagy in HT-29 cells. *J Biol Chem* 275, 992-998
42. Mizushima, N., Sugita, H., Yoshimori, T., and Ohsumi, Y. (1998) A new protein conjugation system in human. The counterpart of the yeast Apg12p conjugation system essential for autophagy. *J Biol Chem* 273, 33889-33892
43. Nakatogawa, H., Suzuki, K., Kamada, Y., and Ohsumi, Y. (2009) Dynamics and diversity in autophagy mechanisms: lessons from yeast. *Nat Rev Mol Cell Biol* 10, 458-467
44. Levine, B., and Deretic, V. (2007) Unveiling the roles of autophagy in innate and adaptive immunity. *Nat Rev Immunol* 7, 767-777
45. Schmid, D., and Munz, C. (2007) Innate and adaptive immunity through autophagy. *Immunity* 27, 11-21
46. Dengjel, J., Schoor, O., Fischer, R., Reich, M., Kraus, M., Muller, M., Kreymborg, K., Altenberend, F., Brandenburg, J., Kalbacher, H., Brock, R., Driessen, C., Rammensee, H. G., and Stevanovic, S. (2005) Autophagy promotes MHC class II presentation of peptides from intracellular source proteins. *Proc Natl Acad Sci U S A* 102, 7922-7927
47. Paludan, C., Schmid, D., Landthaler, M., Vockerodt, M., Kube, D., Tuschl, T., and Munz, C. (2005) Endogenous MHC class II processing of a viral nuclear antigen after autophagy. *Science* 307, 593-596
48. Lee, C.-W., Lin, C.-C., Lee, I. T., Lee, H.-C., and Yang, C.-M. (2011) Activation and induction of cytosolic phospholipase A2 by TNF- $\alpha$  mediated through Nox2, MAPKs, NF- $\kappa$ B, and p300 in human tracheal smooth muscle cells. *Journal of Cellular Physiology* 226, 2103-2114

49. McPhillips, K., Janssen, W. J., Ghosh, M., Byrne, A., Gardai, S., Remigio, L., Bratton, D. L., Kang, J. L., and Henson, P. (2007) TNF- $\alpha$  inhibits macrophage clearance of apoptotic cells via cytosolic phospholipase A2 and oxidant-dependent mechanisms. *J Immunol* 178, 8117-8126
50. Song, H. Y., Dunbar, J. D., Zhang, Y. X., Guo, D., and Donner, D. B. (1995) Identification of a protein with homology to hsp90 that binds the type 1 tumor necrosis factor receptor. *Journal of Biological Chemistry* 270, 3574
51. Felts, S. J., Owen, B. A. L., Nguyen, P. M., Trepel, J., Donner, D. B., and Toft, D. O. (2000) The hsp90-related protein TRAP1 is a mitochondrial protein with distinct functional properties. *Journal of Biological Chemistry* 275, 3305-3312
52. Lee, J., Giordano, S., and Zhang, J. (2012) Autophagy, mitochondria and oxidative stress: cross-talk and redox signalling. *Biochem J* 441, 523-540
53. Ling, Y. M., Shaw, M. H., Ayala, C., Coppens, I., Taylor, G. A., Ferguson, D. J. P., and Yap, G. S. (2006) Vacuolar and plasma membrane stripping and autophagic elimination of *Toxoplasma gondii* in primed effector macrophages. *The Journal of experimental medicine* 203, 2063
54. Chan, N. C., Salazar, A. M., Pham, A. H., Sweredoski, M. J., Kolawa, N. J., Graham, R. L., Hess, S., and Chan, D. C. (2011) Broad activation of the ubiquitin-proteasome system by Parkin is critical for mitophagy. *Hum Mol Genet* 20, 1726-1737
55. Geisler, S., Holmstrom, K. M., Skujat, D., Fiesel, F. C., Rothfuss, O. C., Kahle, P. J., and Springer, W. (2010) PINK1/Parkin-mediated mitophagy is dependent on VDAC1 and p62/SQSTM1. *Nat Cell Biol* 12, 119-131
56. Okatsu, K., Saisho, K., Shimanuki, M., Nakada, K., Shitara, H., Sou, Y., Kimura, M., Sato, S., Hattori, N., Komatsu, M., Tanaka, K., and Matsuda, N. (2010) p62/SQSTM1 cooperates with Parkin for perinuclear clustering of depolarized mitochondria. *Genes to Cells* 15, 887-900
57. Walker, S., Chandra, P., Manifava, M., Axe, E., and Ktistakis, N. T. (2008) Making autophagosomes. *Autophagy* 4, 1093-1096
58. Mizushima, N., Kuma, A., Kobayashi, Y., Yamamoto, A., Matsubae, M., Takao, T., Natsume, T., Ohsumi, Y., and Yoshimori, T. (2003) Mouse Apg16L, a novel WD-repeat protein, targets to the autophagic isolation membrane with the Apg12-Apg5 conjugate. *J Cell Sci* 116, 1679-1688
59. Fujita, N., Itoh, T., Omori, H., Fukuda, M., Noda, T., and Yoshimori, T. (2008) The Atg16L complex specifies the site of LC3 lipidation for membrane biogenesis in autophagy. *Mol Biol Cell* 19, 2092-2100
60. Hanada, T., Noda, N. N., Satomi, Y., Ichimura, Y., Fujioka, Y., Takao, T., Inagaki, F., and Ohsumi, Y. (2007) The Atg12-Atg5 conjugate has a novel E3-like activity for protein lipidation in autophagy. *J Biol Chem* 282, 37298-37302



61. Levine, B., Mizushima, N., and Virgin, H. W. (2011) Autophagy in immunity and inflammation. *Nature* 469, 323-335
62. Deretic, V. (2011) Autophagy in immunity and cell-autonomous defense against intracellular microbes. *Immunological reviews* 240, 92-104
63. Münz, C. (2010) Antigen processing via autophagy--not only for MHC class II presentation anymore? *Current opinion in immunology* 22, 89-93
64. Zhou, R., Yazdi, A. S., Menu, P., and Tschopp, J. (2011) A role for mitochondria in NLRP3 inflammasome activation. *Nature* 469, 221-225



# **Chapter 3 : Proteomics analysis of Herpes Simplex Virus type 1-infected cells reveals dynamic changes of viral protein expression, ubiquitylation and phosphorylation**

Christina Bell<sup>1,2</sup>, Michel Desjardins<sup>3</sup>, Pierre Thibault<sup>1,2</sup>, Kerstin Radtke<sup>3\*</sup>

*J Proteome Res*, 2013 April, 5 12(4): 1820-9

Included with permission of  
© American Chemical Society

Département de Chimie<sup>1</sup>, Proteomics and Mass Spectrometry Research Unit, Institute for Research in Immunology and Cancer<sup>2</sup>, Département de Pathologie et Biologie Cellulaire<sup>3</sup>, Université de Montréal, C.P. 6128 – Succursale Centre-Ville, Montréal (Québec) H3C 3J7, Canada

\*Corresponding author

**Running title: Proteomics analysis of HSV1 infected cells**

**Key words:** Herpes Simplex Virus, phosphorylation, ubiquitylation, gene expression, proteome, DNA replication, late proteins, protein trafficking

### **3.1. Author contributions**

Christina Bell designed, executed and analyzed experiment, wrote the first complete draft and generated the figures. Michel Desjardins and Pierre Thibault contributed to project conception, experimental design and editing of the manuscript. Kerstin Radtke designed the study, analyzed data, discussed results, wrote the manuscript and contributed as senior author.

### **3.2. Abstract**

Herpesviruses are among the most complex and widespread human viruses, and cause a number of diseases ranging from cold sores to genital infections and encephalitis. While the composition of viral particles has been studied, less is known about the expression of the whole viral proteome in infected cells. Here, we analysed the proteome of the prototypical Herpes Simplex Virus type 1 (HSV1) in infected cells by mass spectrometry (MS). Using a high sensitivity LTQ-Orbitrap, we achieved a very high level of protein coverage and identified a total of 67 structural and non-structural viral proteins. We also identified 90 novel phosphorylation sites and ten novel ubiquitylation sites on different viral proteins. Ubiquitylation was observed on nine HSV1 proteins. We identified phosphorylation sites on about half of the detected viral proteins; many of the highly phosphorylated ones are known to regulate gene expression. Treatment with inhibitors of DNA replication induced changes of both viral protein abundance and modifications, highlighting the interdependence of viral proteins during the life cycle. Given the importance of expression dynamics, ubiquitylation and phosphorylation for protein function, these findings will serve as important tools for future studies on herpesvirus biology.

### 3.3. Introduction

Herpes Simplex Virus type 1 (HSV1) is the prototype of a family of viruses that cause numerous diseases ranging in severity from the common cold sore and genital herpes to life threatening encephalitis in humans<sup>1</sup> or Aujeszky's Disease in swine<sup>2</sup>. About 80% of the world's population is infected with HSV1, although many people may never show any sign or symptom of infection<sup>1</sup>. After a primary infection that often occurs in early childhood, the virus establishes a latent infection in the cranial ganglia. Reactivation is triggered by various stimuli including a compromised immune system or UV light.

Mature viral particles consist of three layers: the icosahedral capsid that contains the viral DNA genome, a less structured protein layer that is called tegument, and an envelope consisting of a host-derived membrane studded with viral membrane proteins<sup>3</sup>. The viral genome encodes at least 82 proteins<sup>4</sup>, granting HSV1 a place among the most complex human viruses. In comparison, Hepatitis C Virus consists of only 11 proteins<sup>5</sup>, and the genome of Human Immunodeficiency Virus comprises only nine open reading frames<sup>6</sup>.

During an active lytic infection, HSV1 gene expression is tightly regulated, and proteins are expressed in at least four kinetic classes. The proteins that are expressed first are called immediate early proteins. They prepare the cell for its new role as a virus replication machine, and can also prevent it from alerting immune cells and neighbouring cells e.g. by interfering with antigen presentation<sup>4, 7</sup>. The immediate early proteins also regulate the expression of the next set of viral proteins, the early proteins. This group contains proteins that catalyze viral DNA replication. This process in turn constitutes a check-point that allows the large scale production of structural viral proteins, and thus assembly of new viral particles that can spread the infection within or between hosts<sup>8</sup>. This last kinetic wave of proteins is broadly classified as 'late'. But not all late proteins are expressed simultaneously. Rather, they can be further divided into leaky late proteins that are expressed at low levels prior to the onset of viral DNA replication and at high levels thereafter, while true late proteins are only expressed after the onset of viral DNA replication and are thought to require continuous DNA replication<sup>8</sup>.

In addition to protein expression levels, ubiquitylation and phosphorylation are likely to influence HSV1 protein function, subcellular localisation, or stability. This has been shown previously for some viral proteins<sup>4, 9-11</sup>.

Previous proteomics analyses of herpes viruses have focused on identifying components of mature and immature viral particles<sup>12-16</sup>, and on changes of the host cell proteome or macrophage secretome induced by infection<sup>17-20</sup>. Here, we performed a comprehensive quantitative analysis of the HSV1 proteome of infected cells with and without inhibition of DNA replication. Furthermore, we analysed the HSV1 proteome for the presence of modified residues and identified 90 novel phosphorylation and 10 novel ubiquitylation sites on HSV1 proteins. The inhibitors affected not only the expression of late, but also some early proteins, highlighting a dynamic and probably highly interdependent regulation of protein expression and stability within the HSV1 proteome. In addition to protein expression, phosphorylation and ubiquitylation patterns were also altered by the inhibitors, stressing the highly dynamic nature of these modifications.

### **3.4. Experimental Procedures**

#### **3.4.1. Cells & viruses**

The BMA3.1A7 macrophage cell line was derived from C56/BL6 mice<sup>21</sup> and cultured in DMEM containing 10% (v/v) FCS and 2 mM glutamine. HSV1 17<sup>+</sup> was kindly provided by Roger Lippé (Université de Montréal), and stocks were propagated in BHK-21 (ATCC CCL-10) and titered on Vero cells (ATCC CCL-81) as described previously<sup>22</sup>.

#### **3.4.2. Infection & drug treatment**

Cells were inoculated at a multiplicity of infection (moi) of 5 on a rocking platform at 37°C for 30min. The inoculum was replaced by medium, and infected cells were incubated until 8h post infection (pi). Acyclovir, phosphonoacetic acid (PAA) and cycloheximide (CH) were purchased from Sigma-Aldrich (Oakville, Canada), and added directly after inoculation for 8h at final concentrations of 400 µM, 4 mg/ml or 0.5 mM, respectively. At 8h pi, cells were washed once with PBS, sedimented and taken up in sample buffer (10% β-mercaptoethanol, 5% SDS, 20% glycerol, 200 mM Tris-HCl pH 6.8, 0.05% bromophenol blue).

#### **3.4.3. SDS-PAGE and Mass Spectrometry**

Twenty µg of total cell lysate proteins were separated on a 4-12% pre-cast NuPAGE gel (Invitrogen). The gel was Coomassie stained and the lanes were cut into 12 equal-sized pieces using an in-house cutting device. The gel pieces were reduced with tris(2-carboxyethyl)phosphine (Pierce), alkylated with chloroacetamide (Sigma-Aldrich, Oakville Canada) and digested with trypsin. Peptides were extracted three times with 90% acetonitrile/0.5 M urea. Combined extracts were dried and re-suspended in 5% acetonitrile, 0.1% formic acid for MS analyses. Peptides were separated on a 150 µm ID, 15 cm reversed phase nano-LC column (Jupiter C18, 3 µm, 300 Å, Phenomex) with a loading buffer of 0.2% formic acid. Peptide elution was achieved by a gradient of 5-40% acetonitrile in 70 min on an Eksigent 2D-nanoLC (Dublin, CA) operating at a flow-rate of 600 nL/min. The nano-LC was coupled to an LTQ-Orbitrap XL mass spectrometer



(Thermo-Electron, Bremen, Germany) and samples were injected in an interleaved manner. The mass spectrometer was operated in a data-dependent acquisition mode with a 1s survey scan at 60,000 resolution, followed by six product ion scans (MS/MS) of the most abundant precursors above a threshold of 10,000 counts in the ion trap.

#### **3.4.4. Protein identification and data analysis**

The centroided MS/MS data were merged into single peak-list files (Distiller, v2.4.2.0) and searched with the Mascot search engine v2.3.01 (Matrix Science) against the forward and reversed HSV1 Uniprot release 2011 database. Mascot was searched with a parent ion tolerance of 10 ppm and a fragment ion mass tolerance of 0.5 Da. Carbamidomethylation of cysteine, oxidation of methionine, deamidation, phosphorylation of serine, threonine and tyrosine and ubiquitylation (GlyGly) of lysine, serine, cysteine and threonine residues were specified as variable modifications. Proteins were identified when the combined score of unique peptide identifications exceeded the score of the first reversed-database hit reaching 1%. This resulted in a false-discovery rate of <1 % at the peptide level. Relative protein abundance was determined using a redundant peptide counting approach (spectral counts)<sup>23-25</sup>. The value of redundant peptide counts from 3 identification cycles (on 3 independent biological replicates, %SD 17-24%) was used to generate heatmaps. Unsupervised clustering was performed using the Graphical Proteomics Data Explorer (GProX) software platform in default settings<sup>26</sup>.

#### **3.4.5. Identification of ubiquitylated and phosphorylated residues**

Phosphorylation and ubiquitylation sites were determined and validated using the Proteoconnection bioinformatics platform<sup>27</sup>. Ubiquitylation was detected by the ubiquitylation signature di-glycine remnant of ubiquitin following trypsin cleavage (114.043 Da) on lysine, serine, cysteine and threonine residues. Ubiquitylation site assignments were then evaluated based on a scoring threshold (Mascot Score: 15) followed by manual verification and validation. Peptides that were extensively modified (chemically and posttranslationally) were excluded from our dataset. In addition peptides with a GlyGly residue on the C-terminal lysine were discarded. Phosphorylation on

serine, threonine and tyrosine residues was detected by the neutral loss of H<sub>3</sub>PO<sub>4</sub> (98 Da). The confidence in the location of phosphorylation sites was determined using a probability score function<sup>28</sup> integrated in the proteoconnections platform and only high confidence assignments (>75%) were considered for inclusion in our study. Motif-x (<http://motif-x.med.harvard.edu>) was used to extract overrepresented patterns from our phosphopeptides sequence data set through comparison to the total HSV1 proteome statistical background<sup>29</sup>.

#### **3.4.6. Immunoblot**

Protein samples were separated by linear 4 – 15% SDS-PAGE (BioRad) and transferred onto nitrocellulose membrane (Pall Corporation, USA). Proteins of interest were detected using a rabbit polyclonal anti-HSV1 antibody (RB-1425-A, Neomarkers) or a rabbit polyclonal anti-calnexin antibody (kindly provided by John Bergeron, McGill University, Montreal, Canada), followed by a secondary antibody coupled to horse-radish peroxidase (Jackson ImmunoResearch, West Grove, USA) for ECL detection (PerkinElmer, Waltham, USA).

### 3.5. Results & Discussion

In this study, we performed a comprehensive quantitative analysis of the HSV1 proteome in infected cells to assess expression levels and posttranslational modifications of both structural and non-structural proteins with and without inhibition of DNA replication. Briefly, we obtained lysates of cells that had been infected with HSV1 wt for 8h, a time when immediate early, early and late viral proteins were expected to be present in the cell. Proteins were separated by SDS-PAGE followed by tryptic in-gel digestion. The corresponding peptides were subsequently analyzed by LC-MS/MS on a LTQ-Orbitrap XL mass spectrometer.

#### 3.5.1. Coverage of HSV1 proteins

The HSV1 proteome comprises at least 82 proteins that promote and regulate viral infection and spread<sup>4</sup>. MS/MS analyses of the corresponding protein extracts enabled the identification of 67 out of the 82 predicted HSV1 gene products with two or more unique peptides (see Supplementary Tables III-S1 for proteome coverage & and Supplementary Table III-S2 for details on identified peptides). Of the 15 unidentified gene products, eight do not yield unique peptides since they represent shorter versions of other proteins (pUL8.5, pUL9.5, pUL12.5, pUL20.5, pUL26.5, pUL27.5, pUL43.5 and pUS1.5)<sup>4</sup>. They might have been detected in our samples, but since we could not distinguish them from the larger proteins, we assumed only the presence / detection of the largest form (denoted as pULX and not pULX.5). Taking this into consideration, our analyses covered 90% of all expected HSV1 proteins. The remaining seven proteins (pUL11, pUL20, pUL33, pUL43, pUL49.5, pUS5 and LAT) might not have been detected due to technical limitations like insufficient solubility or masquing by highly abundant host proteins, or they might not have been expressed under our experimental conditions.

Of the 53 predicted structural proteins that form the viral particle, we detected 49 proteins with two or more unique peptides (Supplementary Figure 3.S1 A). For comparison, a previously published analysis of purified extracellular virions reported the identification of 37 of these predicted structural proteins with two or more peptides<sup>12</sup>. We detected 91% of all capsid proteins and 96% of all tegument proteins, but only 79% of envelope proteins. The lower number of identified envelope proteins might be due to the fact that most of these viral components are transmembrane or membrane associated proteins,

which are notoriously difficult to analyze by MS because of their hydrophobicity and limited number of proteolytic peptides. Indeed, four of the seven proteins we did not detect are membrane-associated proteins (pUL20, pUL43, pUL49.5 and pUS5).

We detected more than 80% each of viral proteins expressed with immediate early, early or late expression kinetics, suggesting that all three classes of HSV1 proteins were present after the selected infection period (Supplementary Figure 3.S1 B). Since our analysis covered nearly the whole HSV1 proteome, and proteins of all kinetic classes were detected with similar efficiency, we concluded that our proteomics platform could be used to monitor HSV1 protein expression under experimental conditions known to influence HSV1 protein expression.

### **3.5.2. Dynamic changes in the HSV1 proteome after inhibition of DNA replication**

We analyzed the effects of two different inhibitors of DNA replication, acyclovir and PAA, on HSV1 protein levels to assess the influence of DNA replication on late protein expression. Acyclovir is a prodrug of an acyclic nucleoside analogue that is processed only in infected cells, and incorporated into nascent DNA where it causes DNA strand termination<sup>30</sup>. This compound is the active ingredient of many common anti-cold sore drugs, such as Zovirax. In contrast, PAA binds to and inhibits the DNA polymerase directly<sup>31</sup>. Since one drug acts as a substrate and the other inhibits the enzymatic activity of the DNA polymerase, we assumed that the latter would more efficiently inhibit DNA replication and thus late protein production. We determined the levels of HSV1 proteins expressed in untreated cells or in the presence of acyclovir or PAA using MS/MS analysis on three biological replicates (statistics shown in Supplementary Table III-S3). Redundant peptide count was used to monitor protein expression. Changes in protein abundance were visualized on the heat map shown in Figure 3.1 A. Proteins were grouped into four distinct clusters depending on their sensitivity to both drugs (Supplementary Table III-S4). The first cluster contained proteins whose expression was strongly down regulated by PAA but less so by acyclovir. Proteins in the second cluster were affected equally by both inhibitors. The third cluster contained proteins that were not significantly affected by either drug, and the fourth cluster contained proteins that were affected only by PAA, but not acyclovir. While both acyclovir and PAA reduced protein abundance levels compared to untreated samples, PAA had a more pronounced

effect and affected a broader range of proteins. Western blot analysis with a polyclonal anti-HSV1 antibody confirmed these findings (Figure 3.1 B).

Next, we analyzed how our clusters correlated with previously published kinetics of HSV1 protein expression<sup>4</sup> (Figure 3.1 C). The majority of immediate early and early proteins was not significantly affected by acyclovir or PAA, and grouped into cluster 3. This observation supported the hypothesis that these proteins were expressed independently of DNA replication. Some immediate early and early proteins were grouped into clusters 1 and 4, indicating that they were sensitive to PAA but not or to a lesser extent to acyclovir. Two early proteins, pUL52 and pUL9, were grouped into cluster 2 since their expression was strongly affected by both drugs.

About 40% of the late proteins were grouped into cluster 1, and 8% into cluster 4, indicating that almost half of the late proteins were more sensitive to PAA than to acyclovir. Since these proteins were still produced at high levels in the presence of acyclovir, their expression did not appear to require efficient DNA replication. However, their sensitivity to PAA indicated that their expression was less effective when DNA replication was strongly repressed. Only 23% of late proteins were grouped into cluster 2, since they were strongly affected by both inhibitors, suggesting that their expression strictly depended on continuous DNA replication. Interestingly, 29% of late proteins were not strongly affected by the inhibitors, like the majority of immediate early and early proteins. This insensitivity of some late proteins to DNA replication inhibition, as well as the sensitivity of some early and immediate early proteins, was unexpected. It does not quite fit the current model of HSV1 protein expression regulation. A similar slight deviation from previously published expression kinetics has been observed by Wagner and colleagues, who have studied HSV1 gene expression at the mRNA level<sup>32</sup>. These deviations could be explained by an interdependency of HSV1 proteins for expression as well as for protein or mRNA stability. Variations between different cell lines might be another factor, and have indeed been previously reported<sup>32</sup>. Together, these data suggest that protein expression might be controlled in a more complex manner than previously assumed, and that the classification into immediate early, early and late proteins might not sufficiently describe the more subtle differences between individual proteins. Clearly, kinetic experiments analyzing the expression of the whole HSV1 proteome at various times of infection will be required to understand these differences in more detail, and to determine the changes in abundance of individual proteins in correlation to their putative viral and cellular regulators.

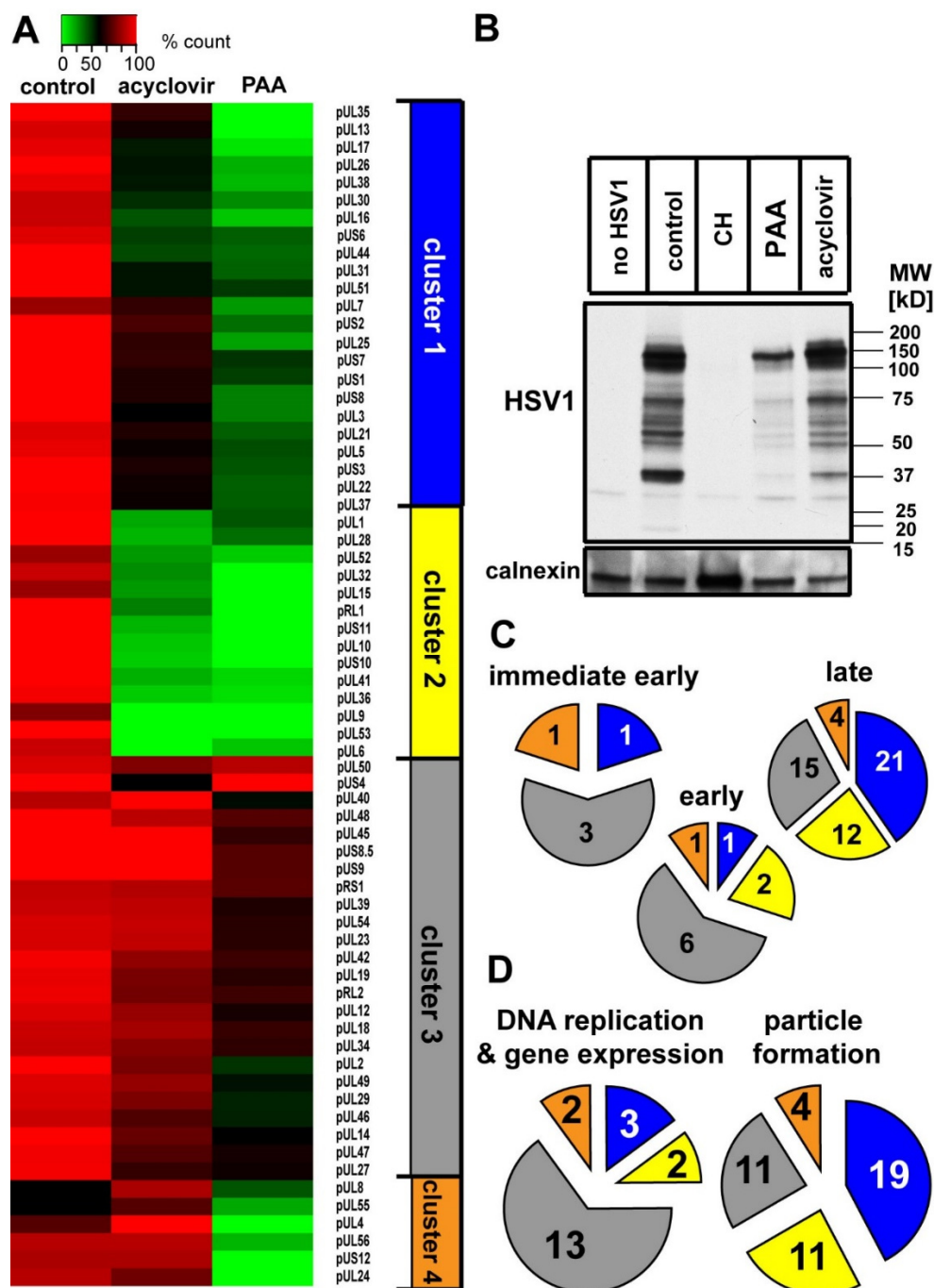


**Figure 3.1. Effect of DNA replication inhibitors on HSV1 protein expression.**

A: Heatmap of relative HSV1 protein abundance in control and treated cells. red: Protein amount equal to 100% redundant peptide count (%count), green: downregulation by 40% or more. HSV1 proteins were sorted according to a hierarchical unsupervised clustering by the effect of acyclovir and PAA. B: Immunoblot of cell lysates treated with acyclovir or PAA. The general translation inhibitor cycloheximide (CH) was used as a control. HSV1 proteins were labelled with a polyclonal antibody, and calnexin was used as a loading control. C: Immediate early, early and late proteins were distributed differently among the clusters specified in A (blue cluster 1, yellow cluster 2, grey cluster 3, orange cluster 4; number of proteins given in pie segments). D: Most proteins involved in DNA replication and gene expression were found in cluster 3, and most proteins involved in virus particle formation in cluster 1.

Next, we wanted to assess whether proteins involved in viral DNA replication and gene expression were down regulated by PAA and acyclovir (Figure 3.1 D). About 65% of these viral proteins were found in cluster three, and thus their expression levels were not significantly affected by either inhibitor. The remaining 35% might be down regulated indirectly, e.g. because a stabilizing interaction partner was missing. For comparison, proteins involved in viral particle formation were found in all four clusters, with a slight preference for cluster one. Thus, these proteins displayed a variable sensitivity to the inhibitors, and were generally more down regulated than proteins involved in DNA replication.

### **3.5.3. Ubiquitylation might regulate protein trafficking during the viral life cycle**

Post-translational modifications such as ubiquitylation play important roles in the regulation of cellular protein stability and localization. Depending on the number and branching of ubiquitin chains, ubiquitylation can control several cellular pathways, including proteasomal degradation. They can also act as sorting signals for vesicular trafficking in the secretory and endocytic pathway<sup>33</sup>. Given the importance of ubiquitylation for cellular proteins, it is likely that viral proteins might undergo similar modifications. The HSV1 protein pUL27 is known to be ubiquitylated on its cytoplasmic tail, and this modification has been linked to the protein's trafficking to multivesicular bodies<sup>11</sup>. Some herpesviral proteins can modify protein ubiquitylation. The HSV1 protein pRL2 can act as an E3-ubiquitin ligase<sup>34</sup> that promotes infection<sup>35</sup>, and the protein pUL36 contains an ubiquitin-specific protease domain<sup>36</sup>. The fact that the HSV1 proteome contains ubiquitin-modifying proteins highlights the importance of tightly controlled ubiquitylation and de-ubiquitylation events during the viral life cycle.

However, the extent of ubiquitylation on HSV1 proteins is not well known. To better understand the role of ubiquitination of herpesviral proteins, it would be necessary to identify which proteins are modified. A detailed knowledge of ubiquitylated residues would facilitate functional studies using viruses in which those residues have been mutated.

Here, we analyzed the 67 previously detected HSV1 proteins for ubiquitylated residues. Although no affinity enrichment method was used, we detected 10 ubiquitylated residues on nine viral proteins (Table III-1, Supplementary Table III-S5 for peptide details and spectra & Supplementary Table III-S6 for statistics of replicate experiments). To our

knowledge, only one of these sites has been previously published. Some of the modified sites were detected only in samples treated with inhibitors of DNA replication (Figure 3.2 A), indicating that ubiquitylation is dynamic and influenced by the environmental cues that define the viral proteome.

**Table III-1.** Ubiquitylation sites in HSV1 proteins.

HSV1 protein	Ubiquitylated residues			Residue published
	untreated	Acyclovir	PAA	
pUL1	K137, K213	K213	-	
pUL3	K120	-	-	
pUL4	K88	K88	-	
pUL15	K19	-	-	
pUL22	-	K716	K716	
pUL27	K72	K866	-	K63 in strain F <sup>11</sup>
pUL36	-	-	K461	
pUL47	-	K176	K176	
pUL55	-	-	K181	

To better understand which pathways of the viral life cycle might be affected and/or regulated by ubiquitylation, we grouped the modified viral proteins according to function and subcellular localisation. Interestingly, all ubiquitylated proteins could either localize to the nucleus and in some cases fulfil a known function inside the nucleus, or they can associate with cellular membranes and participate in membrane fusion events (Figure 3.2 B).

We detected ubiquitylation of proteins pUL22 and pUL27 that can facilitate membrane fusion, and of protein pUL1 that binds to pUL22 (Figure 3.2 C). The ubiquitylation of the cytoplasmic tail of pUL27 has been described previously, and might direct the trafficking of this protein to multivesicular bodies<sup>11</sup>. Taking into consideration that ubiquitylation of host proteins is well known to control vesicular trafficking<sup>33</sup>, these data suggest that herpesviral membrane protein trafficking might be regulated in a similar manner. Alternatively, protein ubiquitylation might function as a signal for proteasomal degradation. In both cases, the modification would allow a regulation of membrane fusion events, either by directing subcellular localisation, or by controlling protein amounts. Interestingly, we also detected ubiquitin residues on domains of both pUL22 and pUL27 that are predicted to be luminal. This could indicate that their topology differs from the prediction, or that these proteins can flip their topology as has previously been shown for



some transmembrane proteins in *E. coli*<sup>37, 38</sup>. Alternatively, protein ubiquitylation might occur after partial degradation and relocation of peptides into the cytosol, likely marking peptides for further proteasomal degradation.

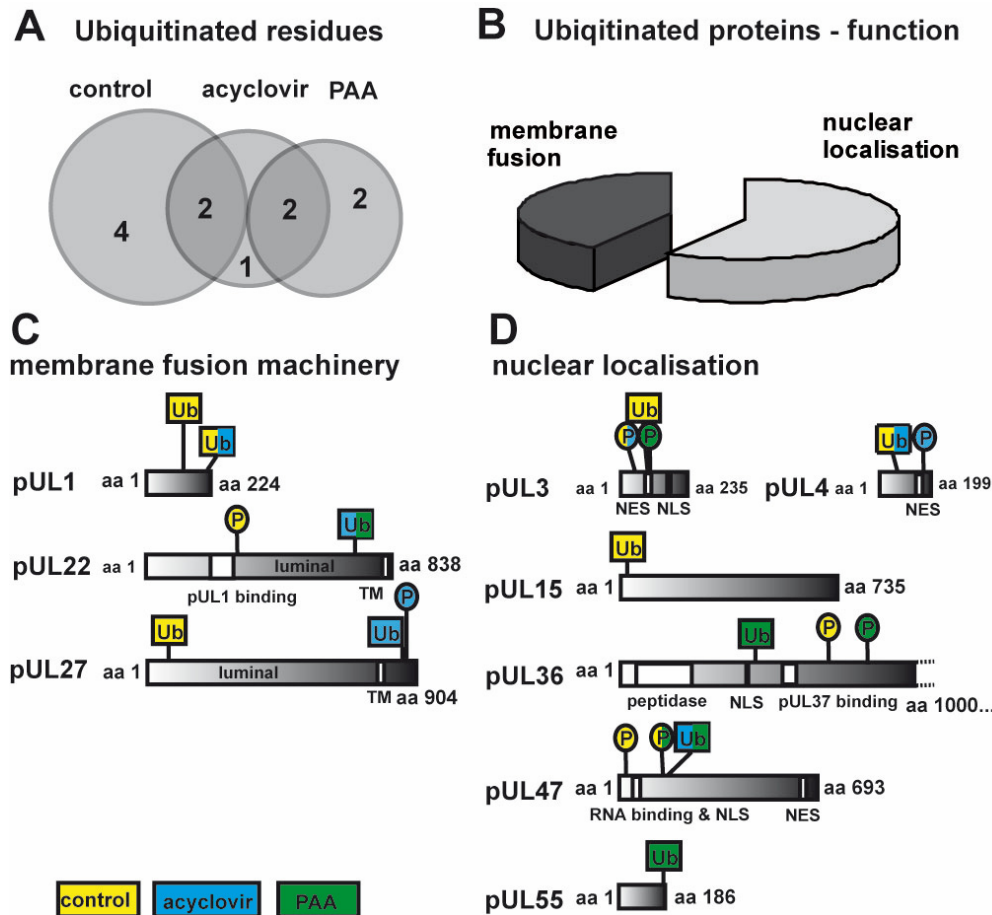


**Figure 3.2. Ubiquitylation of HSV1 proteins.**

We detected 11 ubiquitylation sites in nine HSV1 proteins. A: Ubiquitylation patterns were altered by acyclovir and PAA. B: Ubiquitylated proteins were grouped according to protein function and subcellular localisation. They fell into two different groups: proteins involved in membrane fusion, or proteins localizing to the nucleus. C & D: Schematic drawings of HSV1 proteins containing ubiquitylation sites. The colors denote the condition in which ubiquitylation was detected (yellow: control, blue: acyclovir, green: PAA). C: Ubiquitins found on fusion machinery pUL22, pUL27, and pUL1. D: Ubiquitins found on proteins with partial or predominant nuclear localisation. Ub: ubiquitin, P: phosphorylation, NLS: nuclear localisation signal, NES: nuclear exit signal, TM: transmembrane domain.

Furthermore, we detected ubiquitin residues on proteins that can localize to the nucleus during infection (Figure 3.2 D), indicating that ubiquitylation might regulate nuclear import or export, or intranuclear protein functions. The ubiquitylated proteins pUL3, pUL4,

pUL15, pUL36 and pUL47 contain nuclear localisation signals and / or nuclear export signals<sup>4, 39-41</sup>. In the case of pUL3, the ubiquitin residue is located directly within the nuclear export signal. As mentioned above, ubiquitylation might also serve to control the amounts of these proteins. A tightly controlled degradation of viral proteins is likely essential to facilitate the different stages of the viral life cycle.

Taken together, our data suggest a role for ubiquitylation in trafficking events during herpesviral infection. Our identification of ubiquitylated residues will facilitate further studies on the function of this modification on individual viral proteins.

#### **3.5.4. Phosphorylation of HSV1 regulatory proteins**

Phosphorylation of HSV1 proteins has been widely studied, and is known to regulate various aspects of the viral life cycle. The viral proteome contains two serine-threonine kinases, pUS3 and pUL13<sup>4, 42, 43</sup>, which are known to phosphorylate many cellular and viral proteins. One prominent highly phosphorylated protein is pRL2. Phosphorylation of the viral E3 ubiquitin ligase pRL2 on T67 allows binding to a cellular E3 ligase, thereby indirectly promoting viral transcription and replication<sup>44</sup>. A study using site-directed mutagenesis of putative phosphorylated residues indicated that phosphorylation in other regions of the protein also influenced productive infection<sup>45</sup>.

Although no phosphopeptide enrichment method was used in the present study, we identified 95 phosphorylated residues on 37 HSV1 proteins (Table III-2, Supplementary Table III-S7 for peptide details and spectra & Supplementary Table III-S8 for statistics of replicate experiments). Of these 37 proteins, at least a third have been previously shown to be phosphorylated by biochemical methods<sup>4, 46-48</sup>. However, to our knowledge only five of the 95 potential phosphorylated residues have been identified previously. Some published phosphorylation sites were not identified, either due the limited sensitivity of our approach, or because these proteins were not phosphorylated under our experimental conditions. Interestingly, a few phosphorylation sites were only detected in the presence of PAA and acyclovir, others only in the absence of these drugs (Figure 3.3 A).

**Table III-2.** Phosphorylation sites identified in HSV1 proteins. Confidence >75.

HSV1 protein	Phosphorylated residues			Residues published
	untreated	Acyclovir	PAA	
pRL2	S508, S514	S508	S508	
pRS1	S11, T21, S23, S80, S106, S157, T235, S491, S536, T772, S909, T1271, S534	S80, S106, T153, S157, T235, S491, S536, T772, T1271, S534	S80, T100, S106, T235, S491, S534, S536, T772, T1271	T1271 <sup>19</sup>
pUL3	S60	S60	S125	
pUL4	-	S187	-	
pUL6	-	S459	-	
pUL10	S391, S417	-	-	
pUL11	S66	S66		
pUL12	S604, S618	S604, T614, T621	S604	S604, T614 <sup>19</sup>
pUL13	S18, S91, S109, S119	-	S119, S293	
pUL17	-	-	T272	
pUL22	S326	-	-	
pUL23	-	-	Y239	
pUL24	T195	T120	-	
pUL25	-	T383	-	
pUL27	-	T868	-	
pUL28	-	S283	-	
pUL30	S1113			
pUL34	S42, S198	S198	S198	S198 <sup>53</sup>
pUL35	T111	-	-	
pUL36	T702	-	S832, T1618	
pUL37	S550, S977, S1054	T342	-	
pUL38	T110	-	-	
pUL39	T308	S100, T308	T308, T999	
pUL42	S358, S468	T95, S100	-	
pUL46	S478, S554, S557, S617, S679, S681	S478, S554, S557, S679, S681	S681	
pUL47	S20, S173	-	S173	
pUL49	S35, S71, S89, T114, S145, S277	S35, S89, S145	S35	
pUL50	S187	S187, T199	S187	
pUL51	S184, T190	T190	T190	
pUL54	S114, T132	S114, S116	-	S114 <sup>54</sup>
pUL56	S101	-	-	
pUS1	S22, T27, S135, T162, S167, T258	S167	S167	
pUS3	S139, S396	S396	S139	
pUS7	T341	-	-	
pUS8	S31, T451	-	-	
pUS9	S53	-	-	
pUS12	S81	-	-	

In grouping phosphorylated proteins according to subcellular localisation and function, we found that they mostly localize to the nucleus, where some of them are known to perform intranuclear functions (Figure 3.3 B). We further divided these proteins in groups as follows: (i) proteins that are localized to the nucleus but whose function is unknown, (ii) those that are involved in DNA replication and packaging, (iii) proteins involved in the regulation of gene expression, and (iv) those involved in nuclear egress.

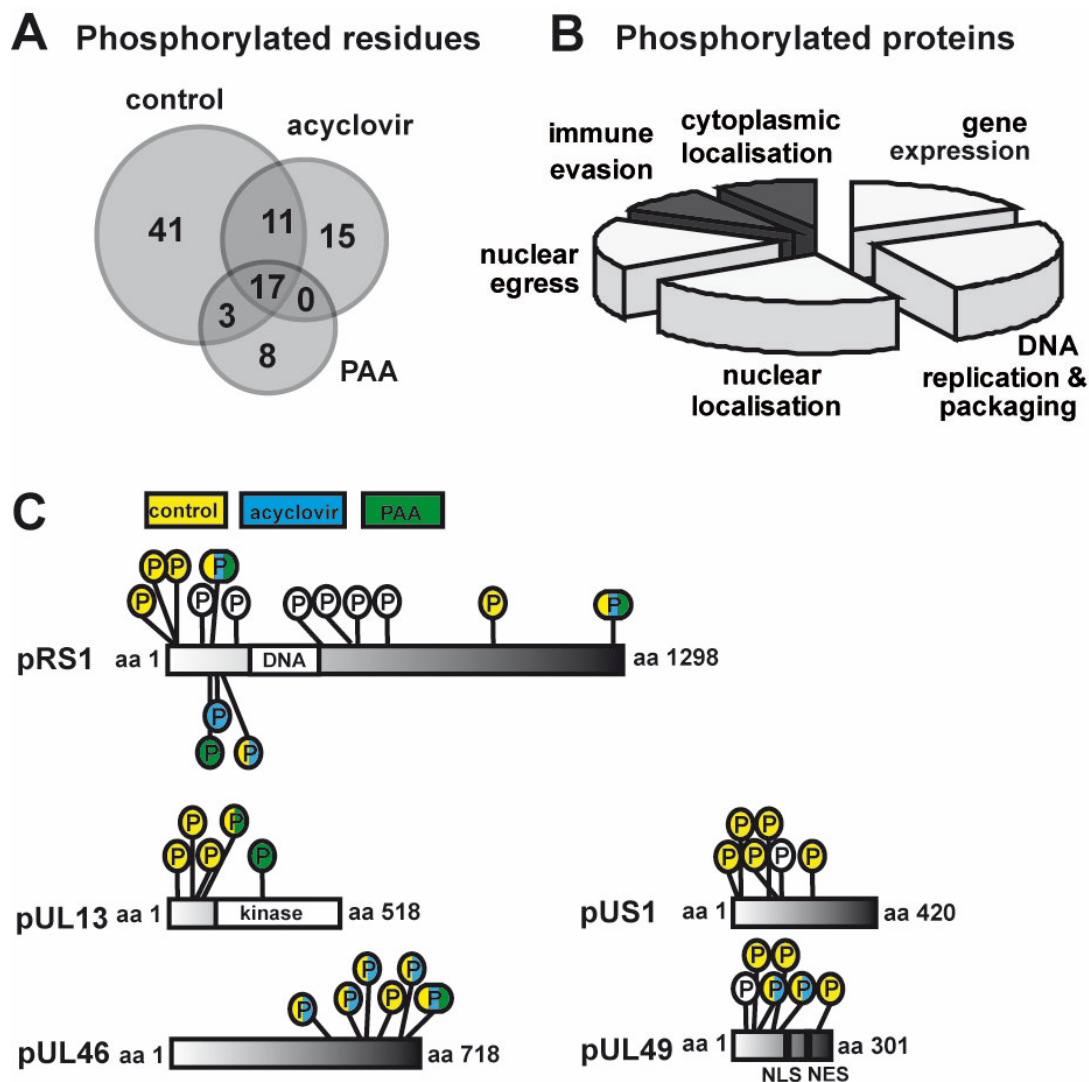


**Figure 3.3. Phosphorylation of HSV1 proteins.**

We detected 95 phosphorylation sites in 37 HSV1 proteins. A: Phosphorylation patterns were altered by acyclovir and PAA. B: Phosphorylated proteins were grouped according to protein function and subcellular localisation. They predominantly fulfilled functions in the nucleus (light segments), or were involved in immune evasion, or fulfilled a function in the cytosol (dark segments). C: Schematic drawings of HSV1 proteins containing more than four phosphorylation sites, detected with and without inhibitors (yellow: control, blue: acyclovir, green: PAA).

Next, we compared the abundance of phosphorylation sites on individual proteins. We detected five or more phosphorylation sites on pRS1, pUL46, pUL49, pUS1 and pUL13 (Figure 3.3 C), all of which are known to affect HSV1 gene expression, either directly by binding to promotor regions (pRS1) or indirectly by binding or modifying other regulatory proteins (pUL46, pUL49, pUL13, pUS1)<sup>43, 49 - 50</sup>.

These findings highlight the dynamics of phosphorylation and de-phosphorylation events, and point towards a possible role of this modification for the regulation of viral protein expression. Our identification of novel phosphosites should facilitate further studies on the role of phosphorylation of individual viral proteins, and the function of different phosphorylation patterns on proteins harbouring many phosphorylation sites.

### **3.5.5. Phosphorylated protein motifs display great variability**

Our data showed the down regulation of both HSV1 kinases pUL13 and pUS3 by the two DNA replication inhibitors (Figure 3.1 A). Interestingly, while acyclovir treatment reduced the amounts of pUL13 and pUS3 only moderately, PAA treatment almost completely abolished their expression. Consequently, changes in HSV1 protein phosphorylation patterns in the presence of acyclovir or PAA might be due to lower expression levels of the viral protein kinases pUS3 and pUL13, or might reflect a more complex regulation of cellular kinases. To shed additional light on this observation, we extracted and compared highly abundant phosphorylation sequence motifs with and without inhibitors (Figure 3.4 A) using motif-x<sup>29</sup>. For all three conditions, sequences containing the two residues 'SP' were found to be enriched. A higher number of common motifs were found for acyclovir and PAA compared to those detected in untreated cells. The 'SP' residues are reported as a putative minimal HSV2 pUL13 recognition motif (Figure 3.4 A)<sup>51</sup>. Since this motif is very short, it is difficult to infer whether protein phosphorylation was catalyzed by pUL13 or other kinases. Untreated samples contained 39 peptides that were phosphorylated on a SP motif. Upon acyclovir and PAA treatment, this number decreased to only 21 and 14 sites, respectively. Thus, the decrease in phosphorylated residues correlated with a reduced abundance of the viral kinase pUL13.

Five of the phosphorylation sites harbour a motif similar to that of the viral kinase pUS3<sup>52</sup> (Figure 3.4 B). Two sites were found on pUL46, one on pUS8, one on pUL54 and one on the kinase pUL13. Interestingly, this motif was detected less often after PAA or acyclovir

treatment, correlating with the lower expression level of pUS3 under these conditions. Overall, changes in phosphorylation of HSV1 substrates probably require a complex interplay of several cellular and viral kinases that might be regulated differentially when viral protein expression is altered following inhibitor treatment.

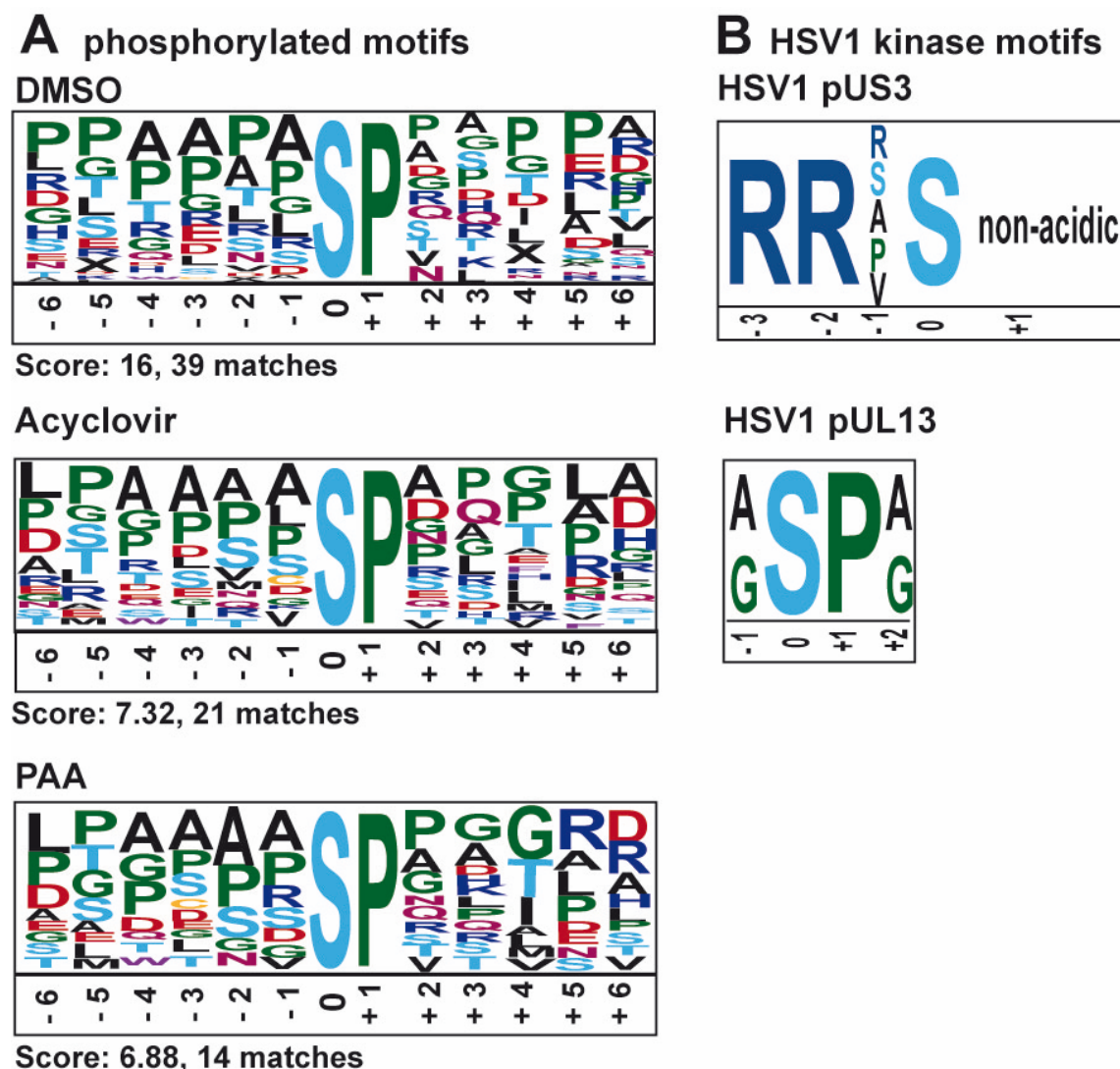


**Figure 3.4. Phosphorylation motifs.**

A: Phosphorylated motifs of HSV1 proteins detected in this study were clustered according to highly abundant amino acid sequences in contrast to the HSV1 proteome as a statistical background using motif-x. Heuristic scores from motif-x were calculated as the sum of the negative log of the binomial probabilities to generate the motifs. The size of the letter used to denote the amino acid located C-terminally (+) or N-terminally (-) of the phosphorylated S residue reflects how often this amino acid is found in phosphorylated motifs. B: Minimal amino acid sequences that function as phosphorylation motifs for the viral kinases pUS3 and pUL13 as published in <sup>51, 52</sup>.

### 3.6. Conclusions

Our study represents a comprehensive analysis of the intracellular HSV1 proteome with and without DNA replication inhibitor treatment. While many viral proteins responded to DNA replication inhibition as expected for their respective kinetic class, some immediate early and early proteins displayed an unexpected sensitivity to this inhibition. Conversely, some late proteins remained surprisingly unaffected, suggesting that the current model of HSV1 protein expression regulation might not be entirely suited to explain the more subtle differences of viral protein expression. HSV1 proteome analyses at different times of infection should help to clarify this issue.

We identified 10 ubiquitylation sites and 95 phosphorylation sites, most of which were previously unknown. Functional clustering indicated roles for modified proteins in viral protein transport regulation as well as regulation of viral protein expression. Knowledge of these modified residues opens the possibility for targeted mutagenesis of specific residues, and subsequent characterization of the functions of phosphorylation and ubiquitylation in the herpesviral life cycle. Future studies analysing certain fractions of infected cells at different times of infection should provide a better understanding on how HSV1 proteins are translocated through organelles to fulfill their functions, how this orchestrates the assembly of new viral particles, and to what extent these trafficking events are regulated by ubiquitylation and phosphorylation.

Taken together, our dataset provides new insights into HSV1 protein expression regulation, and identified novel protein modification sites. We hope that it will serve as a valuable resource for future functional studies on HSV1 biology.

### **3.7. Acknowledgement**

This work was supported by a Canadian Institutes of Health Research grant to MD and PT. MD and PT hold Canada Research Chairs in Cellular Microbiology and Proteomics and Bioanalytical Spectrometry, respectively. IRIC is supported in part by the Canadian Center of Excellence in Commercialization and Research, the Canada Foundation for Innovation and the Fonds de Recherche du Québec en Santé. CB was supported with a scholarship by the Natural Science and Engineering Research Council of Canada Vanier CGS, and KR received a fellowship from the German Research Foundation (RA 1608/4-1). We would like to thank Roger Lippé (Université de Montréal) for providing viruses and for critical reading of this manuscript. We are indebted to John Bergeron (McGill University, Montreal) for sharing antibodies. Furthermore we would like to thank Eric Bonneil (Institute for Research in Immunology and Cancer, Université de Montréal) for technical assistance with mass spectrometry analysis, and Olivier Caron-Lizotte (Institute for Research in Immunology and Cancer, Université de Montréal) for assistance with bioinformatics.

The authors declare no conflict of interest.



### 3.8. Abstract figure

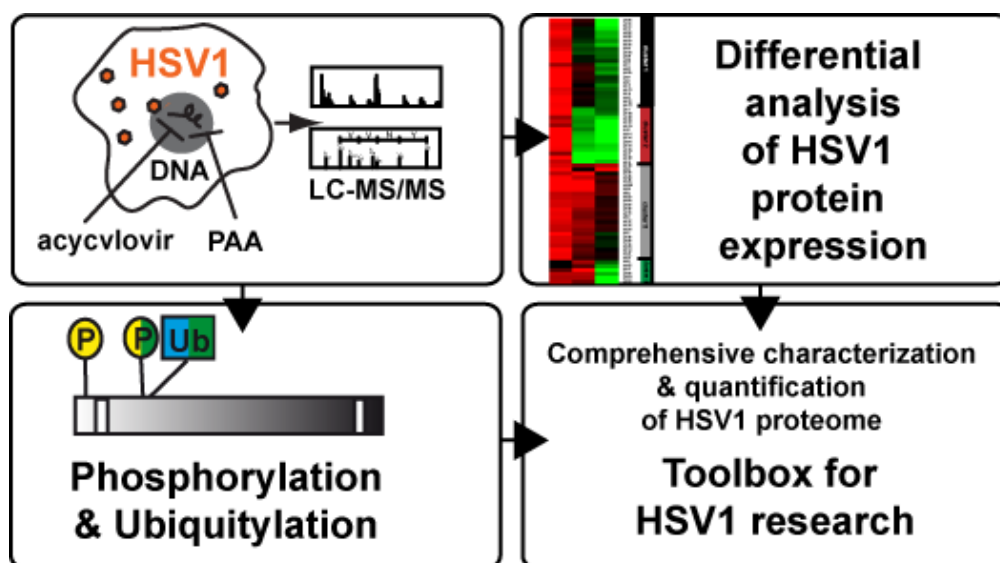


**Figure 3.5. Abstract figure.**  
Visual summary of the present study.

### 3.9. Supporting Information

#### 3.9.1. Supporting figures

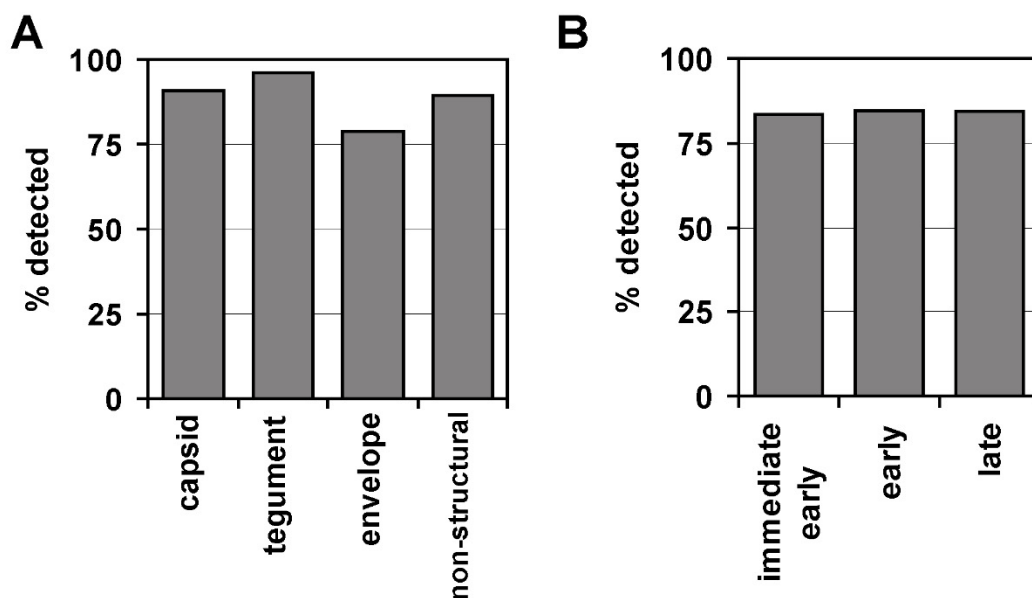


**Figure 3.S1. Coverage of HSV1 structural proteins and proteins of different kinetic classes.**

HSV1 proteins detected with two or more peptides and a score of 25 or higher. Of the 82 established HSV1 proteins, 67 were detected. Note that of the 15 undetected proteins, 7 are not detectable with this method since they are not contained in the database and/or are cleavage products of other proteins. The identified HSV1 proteins were grouped according to virus particle structure (A) or expression kinetics as published in reference<sup>4</sup> (B). Data summarizes three independent experiments analyzed in three technical replicates.

### 3.9.2. Supporting tables

**Table III-S1:** Summary of all HSV1 proteins that were identified in this study (under all experimental conditions) (CD-ROM).

**Table III-S2:** Summary of detailed peptide identifications in HSV1 infected cells treated with DMSO, acyclovir or PAA (CD-ROM).

**Table III-S3:** Statistics on peptides identified after DMSO, acyclovir and PAA treatment in replicate experiments (CD-ROM).

**Table III-S4:** Organisation of HSV1 proteins in clusters according to sensitivity to acyclovir and PAA (CD-ROM).

**Table III-S5:** Description of ubiquitylated peptides including links to spectra (CD-ROM).

**Table III-S6:** Statistics on ubiquitylated residues detected in replicate experiments (CD-ROM).

**Table III-S7:** Description of phosphorylated peptides including links to spectra (CD-ROM).

**Table III-S8:** Statistics on phosphorylated residues detected in replicate experiments (CD-ROM).

### 3.10. References

1. Klapper, P. E., and Cleator, G. M. (1997) Herpes simplex virus. *Intervirology* 40, 62-71
2. Müller, T., Hahn, E. C., Tottewitz, F., Kramer, M., Klupp, B. G., Mettenleiter, T. C., and Freuling, C. (2011) Pseudorabies virus in wild swine: a global perspective. *Arch Virol* 156, 1691 - 1705
3. Grünewald, K., Desai, P., Winkler, D. C., Heymann, J. B., Belnap, D. M., Baumeister, W., and Steven, A. C. (2003) Three-Dimensional Structure of Herpes Simplex Virus from Cryo-Electron Tomography. *Science* 302, 1396-1398
4. Roizman, B., and Campadelli-Fiume, G. (2007) Alphaherpes viral genes and their functions.
5. Penin, F., Dubuisson, J., Rey, F. A., Moradpour, D., and Pawlotsky, J.-M. (2004) Structural biology of hepatitis C virus. *Hepatology* 39, 5-19
6. Ganser-Pornillos, B. K., Yeager, M., and Pornillos, O. (2012) Assembly and Architecture of HIV. Viral Molecular Machines. In: Rossmann, M. G., and Rao, V. B., eds., pp. 441-465, Springer US
7. Roizman, B., Gu, H., and Mandel, G. (2005) The first 30 minutes in the life of a virus: unREST in the nucleus. *Cell Cycle* 4, 1019-1021
8. Roizman, B., Knipe, D. M., and Whitley, R. J. (2007) Herpes simplex virus. In: Fields, B. N., and Howley, P. M., eds. *Fundamental Virology*, 5th Ed., pp. 2502-2601, Lippincott Williams & Wilkins, Philadelphia
9. Boutell, C., Everett, R., Hilliard, J., Schaffer, P., Orr, A., and Davido, D. (2008) Herpes simplex virus type 1 ICP0 phosphorylation mutants impair the E3 ubiquitin ligase activity of ICP0 in a cell type-dependent manner. *J Virol* 82, 10647-10656
10. Imai, T., Arai, J., Minowa, A., Kakimoto, A., Koyanagi, N., Kato, A., and Kawaguchi, Y. (2011) Role of the herpes simplex virus 1 Us3 kinase phosphorylation site and endocytosis motifs in the intracellular transport and neurovirulence of envelope glycoprotein B. *J Virol* 85, 5003-5015
11. Calistri, A., Sette, P., Cancelotti, E., Forghieri, C., Comin, A., Göttlinger, H., Campadelli-Fiume, G., Palu, G., and Parolin, C. (2007) Intracellular trafficking and maturation of herpes simplex virus gB and virus egress require functional biogenesis of multivesicular bodies. *J Virol* 81, 11468 - 11478
12. Loret, S., Guay, G., and Lippe, R. (2008) Comprehensive characterization of extracellular herpes simplex virus type 1 virions. *J Virol* 82, 8605-8618
13. Santamaria, E., Sanchez-Quiles, V., Fernandez-Irigoyen, J. n., and Corrales, F. J. (2012) Contribution of MS-based proteomics to the understanding of Herpes Simplex Virus type 1 interaction with host cells. *Frontiers in Microbiology* 3

14. Padula, M. E., Sydnor, M. L., and Wilson, D. W. (2009) Isolation and Preliminary Characterization of Herpes Simplex Virus 1 Primary Enveloped Virions from the Perinuclear Space. *Journal of Virology* 83, 4757-4765
15. Michael, K., Böttcher, S., Klupp, B. G., Karger, A., and Mettenleiter, T. C. (2006) Pseudorabies virus particles lacking tegument proteins pUL11 or pUL16 incorporate less full-length pUL36 than wild-type virus, but specifically accumulate a pUL36 N-terminal fragment. *Journal of General Virology* 87, 3503-3507
16. Lippé, R. (2012) Deciphering Novel Host-Herpesvirus Interactions by Virion Proteomics. *Frontiers in Microbiology* 3, 181-190
17. Miettinen, J. J., Matikainen, S., and Nyman, T. A. (2012) Global Secretome Characterization of Herpes Simplex Virus 1-Infected Human Primary Macrophages. *J Virol* 86, 12770 - 12778
18. Vastag, L., Koyuncu, E., Grady, S. L., Shenk, T. E., and Rabinowitz, J. D. (2011) Divergent Effects of Human Cytomegalovirus and Herpes Simplex Virus-1 on Cellular Metabolism. *PLoS Pathog* 7, e1002124
19. Antrobus, R., Grant, K., Gangadharan, B., Chittenden, D., Everett, R. D., Zitzmann, N., and Boutell, C. (2009) Proteomic analysis of cells in the early stages of herpes simplex virus type-1 infection reveals widespread changes in the host cell proteome. *Proteomics* 9, 3913-3927
20. Skiba, M., Glowinski, F., Koczan, D., Mettenleiter, T. C., and Karger, A. (2010) Gene expression profiling of Pseudorabies virus (PrV) infected bovine cells by combination of transcript analysis and quantitative proteomic techniques. *Veterinary Microbiology* 143, 14-20
21. Kovacsics-Bankowski, M., and Rock, K. L. (1995) A phagosome-to-cytosol pathway for exogenous antigens presented on MHC class I molecules. *Science* 267, 243-246
22. Döhner, K., Radtke, K., Schmidt, S., and Sodeik, B. (2006) Eclipse Phase of Herpes Simplex Virus Type 1 Infection: Efficient Dynein-Mediated Capsid Transport without the Small Capsid Protein VP26. *J Virol* 80, 8211-8224
23. Blondeau, F., Ritter, B., Allaire, P. D., Wasiak, S., Girard, M., Hussain, N. K., Angers, A., Legendre-Guillemain, V., Roy, L., Boismenus, D., Kearney, R. E., Bell, A. W., Bergeron, J. J., and McPherson, P. S. (2004) Tandem MS analysis of brain clathrin-coated vesicles reveals their critical involvement in synaptic vesicle recycling. *Proc Natl Acad Sci U S A* 101, 3833 - 3838
24. Gilchrist, A., Au, C. E., Bell, A. W., GFernandez-Rodriguez, J., Lesimple, S., Nagaya, H., Roy, L., Gosline, S. J., Hallett, M., Paiement, J., Kearney, R. E., Nilsson, T., and Bergeron, J. J. (2006) Quantitative proteomics analysis of the secretory pathway. *Cell* 127, 1265 - 1281

25. Goyette, G., Boulais, J., Carruthers, N. J., Landry, C. R., Jutras, I., Duclos, S., Dermine, J. F., Michnick, S. W., Laboissière, S., Lajoie, G., Barreiro, L., Thibault, P., and Desjardins, M. (2012) Proteomic characterization of phagosomal membrane microdomains during phagolysosome biogenesis and evolution. *Mol Cell Proteomics* Aug. 20 [Epub ahead of print]
26. Rigbolt, K. T., Vanselow, J. T., and Blagoev, B. (2011) GProX, a User-Friendly Platform for Bioinformatics Analysis and Visualization of Quantitative Proteomics Data. *Mol Cell Proteomics* 10, O110.007450
27. Courcelles, M., Lemieux, S., Voisin, L., Meloche, S., and Thibault, P. (2011) Proteoconnections: A bioinformatics platform to facilitate proteome and phosphoproteome analysis. *Proteomics* 11, 2654 - 2671
28. Olsen, J. V., Blagoev, B., Gnad, F., Macek, B., Kumar, C., Mortensen, P., and Mann, M. (2006) Global, in vivo, and site-specific phosphorylation dynamics in signaling networks. *Cell* 127, 635 - 648
29. Schwartz, D., and Gygi, S. P. (2005) An iterative statistical approach to the identification of protein phosphorylation motifs from large-scale data sets. *Nature Biotechnology* 23, 1391-1398
30. De Clercq, E., and Field, H. J. (2006) Antiviral prodrugs – the development of successful prodrug strategies for antiviral chemotherapy. *British Journal of Pharmacology* 147, 1-11
31. Knopf, C. W. (1987) The Herpes Simplex Virus Type 1 DNA Polymerase Gene: Site of Phosphonoacetic Acid Resistance Mutation in Strain Angelotti is Highly Conserved. *Journal of General Virology* 68, 1429-1433
32. Stingley, S. W., Garcia Ramirez, J. J., Aguilar, S. A., Simmen, K., Sandri-Goldin, R. M., Ghazal, P., and K., W. E. (2000) Global analysis of Herpes Simplex Virus Type 1 Transcription using an Oligonucleotide-Based DNA Microarray. *J Virol* 74, 9916 - 9927
33. MacGurn, J. A., Hsu, P. C., and Emr, S. D. (2012) Ubiquitin and Membrane Protein Turnover: From Cradle to Grave. *Annu Rev Biochem* 81, 231 - 259
34. Vanni, E., Gatherer, D., Tong, L., Everett, R. D., and Boutell, C. (2012) Functional characterization of residues required for the herpes simplex virus 1 E3 ubiquitin ligase ICP0 to interact with the cellular E2 ubiquitin-conjugating enzyme UBE2D1 (UbcH5a). *J Virol* 86, 6323-6333
35. Boutell, C., Cuchet-Lourenco, D., Vanni, E., Orr, A., Glass, M., McFarlane, S., and Everett, R. D. (2011) A viral ubiquitin ligase has substrate preferential SUMO targeted ubiquitin ligase activity that counteracts intrinsic antiviral defence. *PLoS Pathog* 7, e1002245
36. Bolstad, M., Abaitua, F., Crump, C. M., and O'Hare, P. (2011) Autocatalytic activity of the ubiquitin-specific protease domain of herpes simplex virus 1 VP1-2. *J Virol* 85, 8738-8751

37. Rapp, M., Granseth, E., Seppälä, S., and von Heljne, G. (2006) Identification and evolution of dual-topology membrane proteins. *Nature Structural & Molecular Biology* 13, 112-116
38. Bowie, J. U. (2006) Flip-flopping membrane proteins. *Nature Structural & Molecular Biology* 13, 94-96
39. Zheng, C., Lin, F., Wang, S., and Xing, J. (2011) A novel virus encoded nucleocytoplasmic shuttling protein: the UL3 protein of herpes simplex virus type 1. *J Virol Methods* 177, 206 - 210
40. Pan, W. W., Long, J., Xing, J. J., and Zheng, C. F. (2011) Molecular determinants responsible for the subcellular localization of HSV-1 UL4 protein. *Virology* 26, 347 - 356
41. Yu, D., and Weller, S. K. (1998) Genetic Analysis of the UL15 Gene Locus for the Putative Terminase of Herpes Simplex Virus Type 1. *Virology* 243, 32 - 44
42. Mori, I. (2012) Herpes simplex virus US3 protein kinase regulates host responses and determines neurovirulence. *Microbiol Immunol* 56, 351-355
43. Asai, R., Ohno, T., Kato, A., and Kawaguchi, Y. (2007) Identification of proteins directly phosphorylated by UL13 protein kinase from herpes simplex virus 1. *Microbes Infect* 9, 1434-1438
44. Chaurushiya, M. S., Lilley, C. E., Aslanian, A., Meisenhelder, J., Scott, D. C., Landry, S., Ticau, S., Boutell, C., Yates, J. R., Schulman, B. A., Hunter, T., and Weitzman, M. D. (2012) Viral E3 Ubiquitin Ligase-Mediated Degradation of a Cellular E3: Viral Mimicry of a Cellular Phosphorylation Mark Targets the RNF8 FHA Domain. *Mol Cell* 46, 79 - 90
45. Mostafa, H. H., Thompson, T. W., Kushnir, A. S., Haenchen, S. D., Bayless, A. M., Hilliard, J. G., Link, M. A., Pitcher, L. A., Loveday, E., Schaffer, P. A., and Davido, D. J. (2011) Herpes simplex virus 1 ICP0 phosphorylation site mutants are attenuated for viral replication and impaired for explant-induced reactivation. *J Virol* 85, 12631-12637
46. Imai, T., Sagou, K., Arii, J., and Kawaguchi, Y. (2010) Effects of phosphorylation of herpes simplex virus 1 envelope glycoprotein B by Us3 kinase in vivo and in vitro. *J Virol* 84, 153-162
47. Stevely, W. S., Katan, M., Stirling, V., Smith, G. D., and Leader, D. P. (1985) Protein kinase activities associated with the virions of pseudorabies and herpes simplex virus. *J Gen Virol* 66, 661-673
48. Rojas, S., Corbin-Lickfett, K. A., Escudero-Paunetto, L., and Sandri-Goldin, R. M. (2010) ICP27 phosphorylation site mutants are defective in herpes simplex virus 1 replication and gene expression. *J Virol* 84, 2200 - 2211
49. Wagner, L. M., Lester, J. T., Sivrich, F. L., and DeLuca, N. A. (2012) The N terminus and C terminus of herpes simplex virus 1 ICP4 cooperate to activate viral gene expression. *J Virol* 86, 6862-6874

50. Bastian, T. W., and Rice, S. A. (2009) Identification of sequences in herpes simplex virus type 1 ICP22 that influence RNA polymerase II modification and viral late gene expression. *J Virol* 83, 128-139
51. Cano-Monreal, G. L., Tavis, J. E., and Morrison, L. A. (2008) Substrate specificity of the herpes simplex virus type 2 UL13 protein kinase. *Virology* 374, 1-10
52. Purves, F. C., Longnecker, R. M., Leader, D. P., and Roizman, B. (1987) Herpes simplex virus 1 protein kinase is encoded by open reading frame US3 which is not essential for virus growth in cell culture. *J Virol* 61, 2896-2901
53. Kato, A., Yamamoto, M., Ohno, T., Kodaira, H., Nishiyama, Y., and Kawaguchi, Y. (2005) Identification of proteins phosphorylated directly by the Us3 protein kinase encoded by herpes simplex virus 1. *J Virol* 79, 9325-9331
54. Zhi, Y., and Sandri-Goldin, R. M. (1999) Analysis of the phosphorylation sites of herpes simplex virus 1 regulatory protein ICP27. *J Virol* 73, 3246 - 3257



## **Chapter 4 : Nuclear envelope-derived autophagy contributes to MHC I antigen presentation of a viral protein that resides in the nuclear envelope**

Christina Bell<sup>1,2\*</sup>, Kerstin Radtke<sup>3\*</sup>, Luc English<sup>3</sup>, Diana Matheoud<sup>3</sup>,  
Magali Chemali<sup>3</sup>, Roger Lippé<sup>3</sup>, Pierre Thibault<sup>1,2,4</sup> & Michel  
Desjardins<sup>3,4</sup>

Manuscript in preparation for submission to *Immunity*

Institute for Research in Immunology and Cancer<sup>1</sup>, Department of Chemistry<sup>2</sup>,  
Department of Pathology and Cell Biology<sup>3</sup>, Université de Montréal, P.O. Box 6128,  
Station. Centre-ville, Montréal, Québec, Canada H3C 3J7

\*equal contribution

<sup>4</sup>Corresponding authors

**Key words:** herpes, HSV, NEDA, antigen, MHC, atg5, LC3a, nuclear envelope, T cell, autophagy

**Running title:** NEDA contributes to antigen presentation on MHC I

#### **4.1. Author contributions**

Christina Bell designed, executed and analyzed experiment, wrote the first complete draft and generated the figures. Kerstin Radtke designed, executed and analyzed experiment, wrote the first complete draft and generated the figures. Luc English contributed to project conception and experiments. Diana Matheoud and Magali Chemali contributed to molecular biology experiments. Roger Lippe provided HSV1 stocks, antibodies and expertise with the viral infection system. Pierre Thibault and Michel Desjardins designed the study, analyzed data, discussed results, wrote the manuscript and contributed as senior authors.

## 4.2. Summary

Herpes simplex virus 1 infection induces the formation of autophagosomes via a particular form of autophagy, referred to as nuclear envelope-derived autophagy (NEDA). The extent to which NEDA differs from macroautophagy and participates in the pathogenesis of HSV infection is still largely unknown. In the present study we showed that NEDA is an Atg5-independent pathway that participates in the capture of nuclear envelope-resident viral proteins and their processing and presentation on MHC class I molecules. Detailed proteomics characterization of autophagosomes revealed that NEDA leads to the specific targeting of nuclear envelope-resident proteins including gB to autophagosomes in an Atg5-independent manner. In contrast during macroautophagy mostly cytosolic proteins were transferred to the vacuolar compartment. These findings highlighted that various autophagic pathways can be induced to promote the capture of selective sets of viral proteins, thus actively shaping the nature of the immune response during infection.

### 4.3. Introduction

The ability to capture, process and present proteins and antigens, either endogenous or exogenous, is essential to initiate a sustained immune response against infectious diseases and to eliminate aberrant cells that appear during carcinogenesis<sup>1, 2</sup>. The last decade highlighted important contributions of various membrane trafficking pathways to the processing and presentation of endogenous or exogenous proteins on MHC class I or class II molecules (for a review see <sup>3</sup>). Cross-priming allows peptides from exogenous proteins to be presented on MHC class I molecules, enabling the production of reactive CD8+ T cells against a variety of intracellular pathogens<sup>4, 5</sup>. On the other hand, autophagy was shown to actively promote the capture and processing of endogenous proteins, including viral proteins, for presentation on MHC class II molecules<sup>6-8</sup>. These pathways take advantage of antigen processing machineries from the proteasome in the cytoplasm, and hydrolases within endocytic organelles to produce a wider diversity of peptides. Autophagy furthermore contributes to antimicrobial immunity both in direct ways as demonstrated by the xenophagic degradation of intracellular pathogens, and in indirect ways e.g. by modulating the activation of effector cells in adaptive immunity through the modulation of TLR signaling or antigen presentation<sup>9</sup>.

Complex trafficking events, related to autophagy, have also been shown to be actively engaged during herpes simplex virus 1 (HSV1) infection<sup>10-13</sup>. Infection with Herpes viruses causes diseases that afflict a large number of people worldwide. Debilitating and sometimes severe symptoms can occur through the entire life of infected individuals<sup>14</sup>. This reflects the fact that the immune system is unable to eliminate and mount an efficient immune response against the virus, which can remain latent for years. A hallmark of the limitation of the immune response during HSV1 infection in mice is the strong CD8+ T cell immunodominant response against a single epitope (SSIEFARL) from the viral glycoprotein B (gB)<sup>15, 16</sup>. Although the molecular mechanisms associated with immunodominance are extremely complex, it has been proposed that antigen processing and presentation are key steps of this process<sup>17</sup>. We have shown recently that autophagy participates in the processing and presentation of viral peptides during HSV1 infection.<sup>13</sup> Remarkably, while this virus is able to inhibit macroautophagy<sup>11</sup>, it can induce a particular form of autophagy characterized by the formation of autophagosomes made of a 4-layers membrane, originating from the coiling of the inner and outer membrane of the nuclear envelope<sup>13</sup>. This process, referred to as nuclear envelope-derived autophagy (NEDA),

occurs around 6 hours after infection. NEDA can take place in different types of mammalian cells, including macrophages and neurons, and requires the synthesis of late viral proteins<sup>12</sup>. The role of NEDA in the pathogenesis of viral infection, the host immune response, and its distinctive mechanism compared to macroautophagy are still poorly understood. Furthermore, the extent to which NEDA is involved in the processing of viral proteins and presentation of antigenic peptides remains to be established.

## 4.4. Results

### 4.4.1. Contribution of NEDA to viral antigen presentation

Previous reports underscored the role of autophagy in adaptive immunity by increasing MHC class II presentation of cytoplasmic antigens, including self or viral antigens, or by affecting MHC class I presentation by competing with the proteasome for substrates or influencing the peptidome pools through the control of levels of components of microRNA (miRNA) machinery<sup>9</sup>. The significance of autophagy in mounting an appropriate immune response against viral antigens, mostly through MHC class II presentation was also highlighted in recent studies<sup>6, 7</sup>. Interestingly, autophagosomes originating from the nuclear envelope (NEDA), were found to be an important source of viral peptides for proteasomal degradation and presentation through the MHC class I pathway<sup>13</sup>. Accordingly, we sought to examine how NEDA and macroautophagy regulate antigen processing and presentation following HSV1 infection, and how they might influence the nature of the immune response in infected macrophages. Classical autophagy (referred from this point on as macroautophagy) is an Atg5-dependent process that can be efficiently inhibited by treating cells with Phosphoinositide-3 kinase (PI3K) inhibitors like 3-methyl adenine (3-MA) and wortmannin and, more directly, by decreasing the expression of Atg5<sup>18</sup>. Interestingly, these two drugs did not alter the recruitment of the protein LC3b to the nuclear membrane, a hallmark of NEDA, during HSV1 infection (Fig. 4.1A). In contrast, the localization of LC3b to classical autophagosomes observed in the cytoplasm of uninfected cells after a mild heat shock is markedly decreased by these inhibitors. Furthermore, down-regulation of the expression of Atg5 by shRNA (Fig.4.S1) had no effect on the recruitment of a variant form of LC3, LC3a, a marker for NEDA, to the nuclear envelope (Fig. 4.1B), suggesting that NEDA is an Atg5-independent process. This was further confirmed using electron microscopy where the formation of 4-layers membrane autophagosomes on the nuclear envelope of HSV1-infected mouse embryonic fibroblasts (MEFs) was still observed in Atg5 <sup>-/-</sup> cells (Fig. 4.1C). Also, no significant changes in the distribution of LC3a on the nuclear rim was observed using immunofluorescence microscopy (Fig. 4.1D). These results clearly indicate that NEDA is an Atg5-independent process regulated by molecular mechanisms distinct from those of macroautophagy.

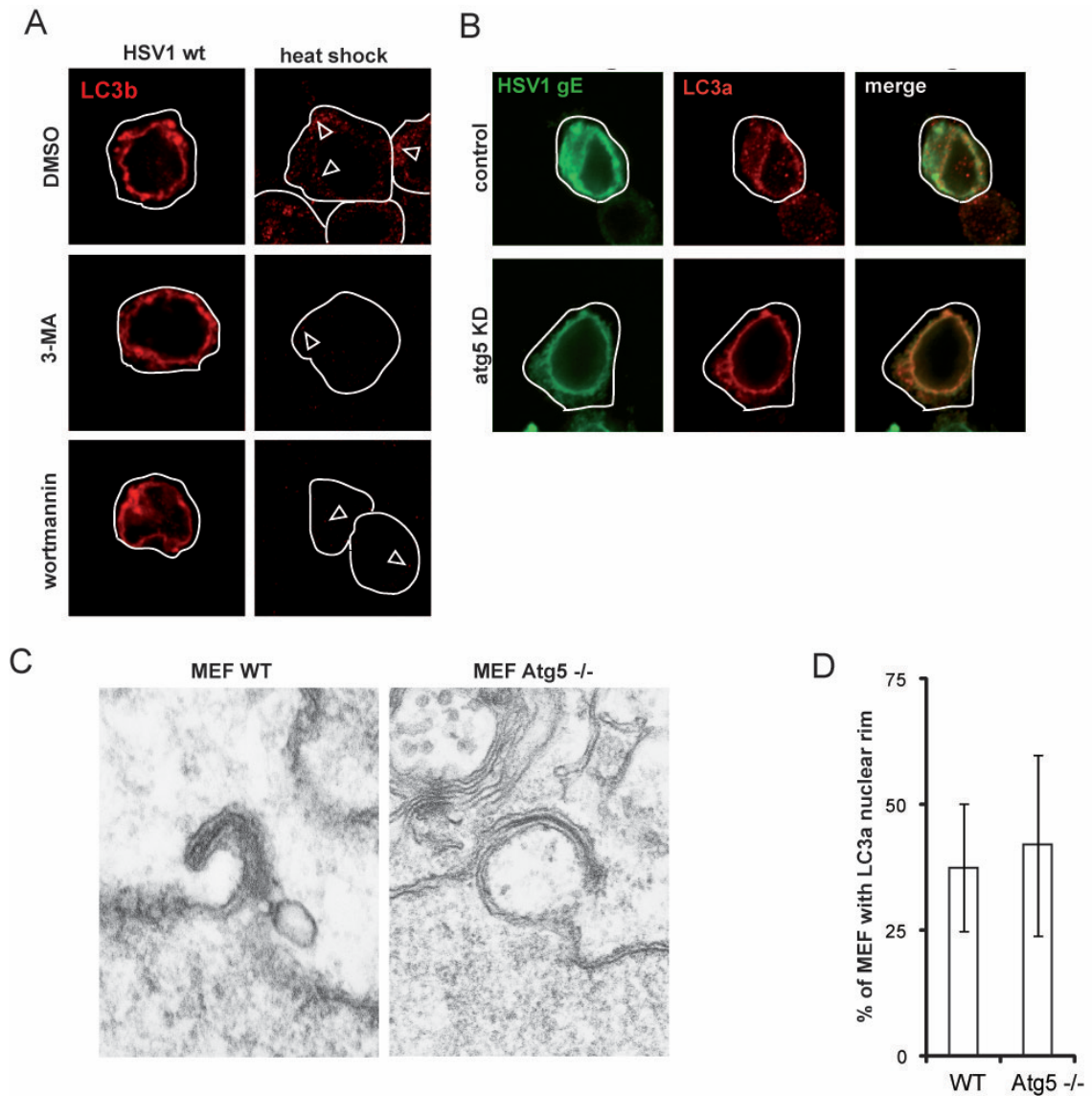


**Figure 4.1. NEDA is regulated differently than macroautophagy and is Atg5-independent.**

A. Macrophages were treated with the PI3K inhibitors 3-methyl adenine (3-MA) or wortmannin, or with DMSO as a control. Additionally, they were either infected with HSV1 WT, or left uninfected and treated with a heatshock. Immunofluorescence analysis with a LC3b antibody showed that LC3b accumulation around the nucleus and thus NEDA took place in infected cells despite the inhibitors. Heatshock treatment confirmed the efficient inhibition of macroautophagosome formation with 3-MA and wortmannin, since the number of LC3b positive punctae (arrowheads) was markedly reduced by both drugs. B. Immunofluorescence analysis of macrophages stably expressing shRNA against Atg5 or scrambled shRNA showed that HSV1 WT infection induced LC3b accumulation around the nucleus and thus NEDA even when Atg5 was down regulated. C. Four-membrane hooks characteristic for NEDA formed at the nuclear envelopes of HSV1 WT infected MEF cells with and without Atg5, as observed by electron microscopy. D. Quantification of three representative immunofluorescence experiments with about 200 cells showed that LC3a accumulated in the nuclear envelopes of HSV1 WT infected MEF cells similarly with and without Atg5. Error bars: SD

To determine whether NEDA plays a role in the capture of viral antigens and their processing for presentation on MHC class I molecules, we infected BMA macrophages with the wild type (WT) HSV1 that induces NEDA, or the HSV1 mutant  $\Delta PP1\alpha$  that does not trigger NEDA<sup>12</sup>, and quantified gB presentation as described previously<sup>13</sup>. The  $\Delta PP1\alpha$  mutant contains point mutations in the  $\Delta PP1\alpha$  binding domain of ICP34.5, which interferes with PP1 $\alpha$  binding. ICP34.5 via its PP1 $\alpha$  binding domain binds both PP1 $\alpha$  and eIF2 $\alpha$ , thus facilitating eIF2 $\alpha$  dephosphorylation and active translation, necessary for NEDA. Hence NEDA is not triggered anymore in the  $\Delta PP1\alpha$  mutant, while macroautophagy can still occur<sup>12</sup>. To determine if lytic vacuoles like autophagolysosomes are the primary sites of cytosolic antigen processing, we treated cells with the lysosomal acidification inhibitor Bafilomycin A1 (Baf). These experiments revealed that gB presentation was strongly reduced by Baf treatment in HSV1 WT, and to a much lesser extent in HSV1  $\Delta PP1\alpha$  infected cells (Fig. 4.2A), suggesting that vacuolar processing contributes to HSV1 antigen presentation when NEDA occurs. It is noteworthy that changes in CD8+ T cell activation following Baf treatment of either WT or  $\Delta PP1\alpha$  infected macrophages were not due to variable levels of MHC I molecules at the cell surface (Fig. 4.2B), or different expression levels of gB (Fig. 4.2C).



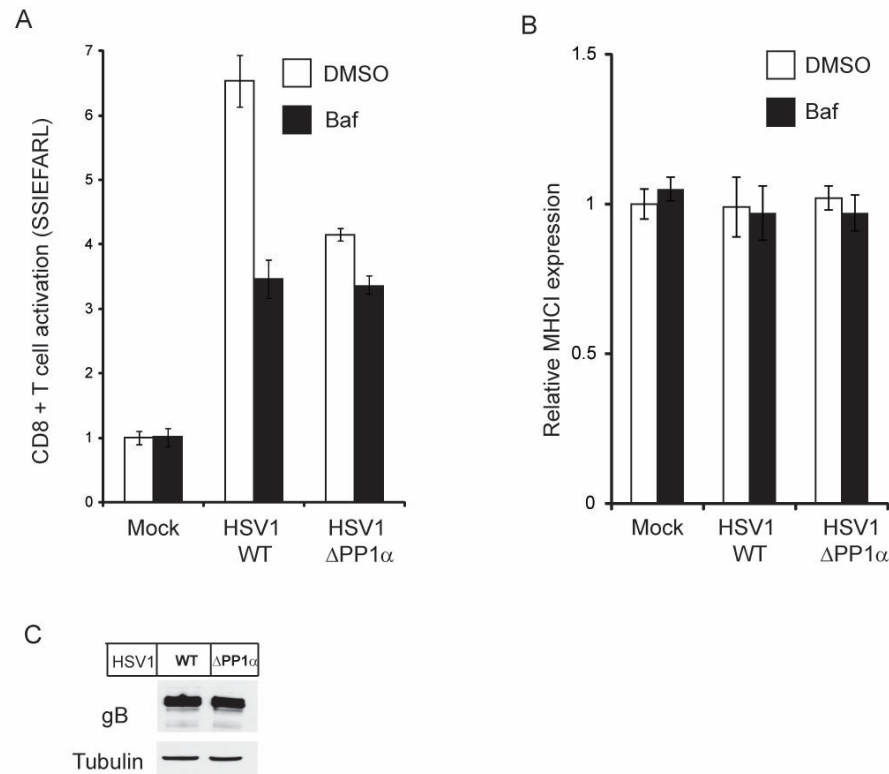


**Figure 4.2. NEDA contributes to the presentation of gB to MHC class I molecules.** A. Macrophages were infected with HSV1 WT that induces NEDA, or with HSV1  $\Delta$ PP1 $\alpha$  that does not. MHC I presentation of the viral protein gB was determined 9h pi by assessing the activation of 2E2 T cell hybridoma. Bafilomycin A1 (Baf) was added at 4 h pi to inhibit the vacuolar contribution to antigen presentation. Error bars: SD. B. Infection with HSV1 WT or  $\Delta$ PP1 $\alpha$  and treatment with Bafilomycin A1 does not affect MHC I expression levels. C. Infection levels are comparable in macrophages infected with HSV1 WT and  $\Delta$ PP1 $\alpha$  as assessed by western blot for gB. Tubulin was used as a loading control.

One of the remarkable features that distinguish NEDA from macroautophagy is the fact that the membrane required for autophagosome formation is recruited from the nuclear envelope, where several viral proteins, including gB, are highly enriched. To determine if gB present on the nuclear envelope can be captured for antigen presentation during NEDA, we expressed constructs where gB was linked to the ovalbumin peptide SIINFEKL (OVA) (Fig. 4.3A) and targeted either to the nuclear membrane or the lumen of the endoplasmic reticulum (ER) as a control (Fig. 4.3B). The addition of the SIINFEKL epitope allowed us to measure the level of antigen presentation using an OVA-specific CD8+ T cell hybridoma, rather than gB coming from the expression of the marker and the native viral protein during infection. In that context, HSV 1 infection is simply used to trigger NEDA (WT virus), or macroautophagy ( $\Delta$ PP1 $\alpha$  virus). Control experiments

indicated that NEDA was induced in cells expressing the gB/OVA constructs and infected with WT HSV 1 but not in cells infected with the  $\Delta PP1\alpha$  virus (data not shown). When BMA cells stably expressing these constructs were infected with WT HSV1, we observed that gB/OVA present on the nuclear envelope was effectively processed in a vacuolar compartment (Baf-sensitive) and presented to the OVA-specific CD8+ T cell hybridoma (Fig. 4.3C). In contrast, infection with the  $\Delta PP1\alpha$  virus led to a significant reduction presentation of gB/OVA by a mechanism largely unaffected by the Baf treatment. On the other hand, no change in CD8+T cell activation was observed when gB/OVA was expressed in the ER lumen of macrophage cells infected with the two distinct viruses and the ER luminal reporter antigen was presented mostly Bafilomycin A1 independently, suggesting that the ER itself can be recruited for the formation of autophagosomes during both NEDA (WT virus) and macroautophagy ( $\Delta PP1\alpha$ ) (Fig. 4.3C). Control experiments indicated that the level of expression of the gB/OVA constructs was not affected by the viral infection since similar levels were observed in mock cells (Fig. 4.3D). To confirm that NEDA participates in the presentation of viral antigens, we also monitored changes in CD8+ T cell activation of macrophages infected with WT or  $\Delta PP1\alpha$  HSV 1 virus following pharmacological inhibition of the Atg5-dependent autophagic pathway or shRNA silencing of Atg5. Control experiments performed on WT HSV1-infected macrophages treated with Acyclovir, a drug that inactivates DNA polymerases and incorporates itself into viral DNA chain, confirmed the inhibition of the vacuolar pathway in gB/OVA presentation (Fig. 4.3E). In contrast, WT HSV1-infected macrophages with knock down Atg5 or grown in the presence of 3 methyl adenine (3-MA), which blocks the formation of autophagosome via the inhibition of phosphatidylinositol 3-kinases, showed no significant changes in antigen presentation (Fig. 4.3E). It is noteworthy that Baf treatment of macrophages infected with WT HSV 1 showed a significant reduction of gB/OVA presentation confirming the Atg5-independent pathway and the role of NEDA in antigen processing. These results were in stark contrast with those from macrophages infected with  $\Delta PP1\alpha$  virus where Baf treatment no longer affected the presentation of the full-length gB/OVA in either WT or Atg5 knock-down cells, thus validating that macroautophagy is an Atg5-dependent pathway.

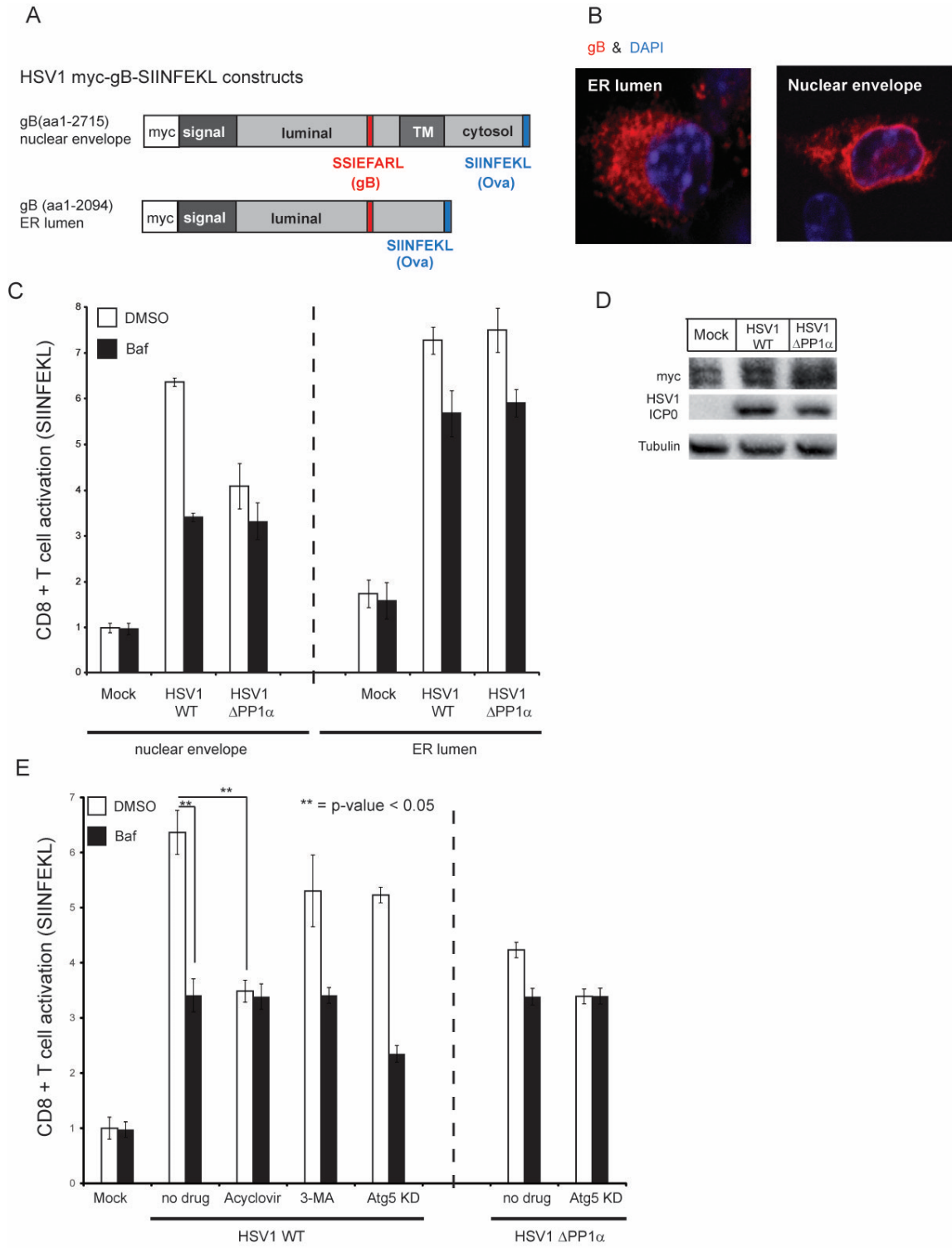


**Figure 4.3. NEDA contributes to MHC class I antigen presentation of a nuclear envelope-resident viral antigen.**

A. Construction of macrophage cell lines that stably express a reporter antigen in the nuclear envelope or the ER lumen. RAW macrophages were stably transfected to express H2kb, and a vector coding either for HSV1 gB full length-SIINFEKL or a truncated version that lacks the

transmembrane domain (TM). B. Immunofluorescence analysis with a gB antibody confirmed the localization of these constructs to be either mainly in the nuclear envelope and vesicular structures that might represent Golgi (nuclear envelope), or diffusely spread out throughout the ER and most notably absent from the nuclear envelope (ER lumen). C. Macrophage cell lines stably expressing a reporter antigen (SIINFEKL) either at the nuclear envelope or in the ER lumen were infected with HSV1 WT or HSV1  $\Delta$ PP1 $\alpha$  for 9h. Bafilomycin A1 (Baf) was added at 3h pi. The Bafilomycin A1-sensitive vacuolar antigen presentation of the nuclear envelope resident, but not the ER lumen resident reporter antigen was reduced strongly with HSV1  $\Delta$ PP1 $\alpha$  that does not induce NEDA. Error bars: SD. D: HSV1 WT and  $\Delta$ PP1 $\alpha$  do not alter expression of the full length gB-OVA-myc construct. E. The autophagic contribution to antigen presentation on MHC I is partially insensitive to macroautophagy inhibition. Antigen presentation with macrophages expressing the nuclear envelope resident reporter antigen containing SIINFEKL and either scrambled shRNA or shRNA against Atg5 were infected with HSV1 WT or mock infected for 9h, and treated with acyclovir or 3-MA at 2h pi. Bafilomycin A1 was added at 4h pi. Inhibition of NEDA with acyclovir strongly reduced the Bafilomycin A1-sensitive vacuolar contribution to antigen presentation. In contrast, inhibition of macroautophagy by 3-MA treatment or Atg5 knock down reduced the vacuolar contribution much less, indicating that NEDA could contribute to antigen presentation in the absence of macroautophagy. Bafilomycin A1 treatment no longer affected the presentation of the full-length gB/OVA construct in Atg5 knock-down cells infected with the  $\Delta$ PP1 $\alpha$  virus. Error bars: SD. (**Figure 4.3. continued**)

#### **4.4.2. Quantitative proteomics analyses of viral proteins in autophagolysosomes**

Thus far, our results highlight the fact that NEDA differs from macroautophagy, as an Atg5-independent process, and participates actively in the capture of viral antigens expressed in the nuclear envelope for antigen presentation during HSV1 infection. These features suggest that NEDA might provide an immunological advantage to the host during HSV1 infection by modulating the immune response via alternate antigen processing and presentation pathways. To determine how NEDA could influence the immune response and pathogenesis infection, we analyzed enriched autophagolysosomes (APL) formed in HSV1-infected macrophages, using mass spectrometry (MS)-based quantitative proteomics. Procedures to isolate autophagosomes based on their intrinsic density have been used in the past to characterize the composition of these organelles<sup>19-21</sup>. However, the fact that a large repertoire of host proteins can be captured by autophagy and be present in autophagosomes renders the identification of contaminants very difficult (see discussion). Thus, to characterize the composition of APLs and identify their viral content, we developed a novel organelle isolation method that takes advantage of a well-established flotation procedure shown to generate purified organelles with minimal contaminants<sup>22</sup> (Fig.4.4A). Previous reports indicated that autophagosomes formed during autophagy fuse with late endosome/lysosome-like organelles to generate APL<sup>23</sup>.

In that context, we filled the late endosome/lysosome compartment by internalizing small latex beads (100 nm) prior to HSV1 infection and autophagosome formation. Upon HSV1 infection, autophagosomes that fused with latex bead-containing compartments could be isolated by a simple flotation centrifugation. Latex bead-containing compartments (LB-C) isolated from uninfected cells were used as control to distinguish proteins associated with autophagosomes from those present on LBC. In addition to the 100 nm latex beads, we also used 800 nm beads for comparison. Electron microscopy experiments clearly indicated that 4-layered membrane autophagosomes containing viral capsids interact and fuse with LBC (Fig. 4.4B). Western blot analyses confirmed that the flotation method enabled the isolation of nuclear envelope-derived autophagosomes with the enrichment of the viral protein gB, the nuclear pore protein p62, and the autophagosome marker LC3b upon HSV1 infection of macrophage cells (Fig. 4.4C). The comparison of protein recovery yield from latex beads of different sizes indicated that beads of 800 nm generally provided higher recovery as indicated in Fig. 4.4C for the staining patterns of the different protein markers. These results demonstrated that this new cell fractionation approach is well suited to the rapid isolation of highly purified autophagosomes/APL for further characterization.

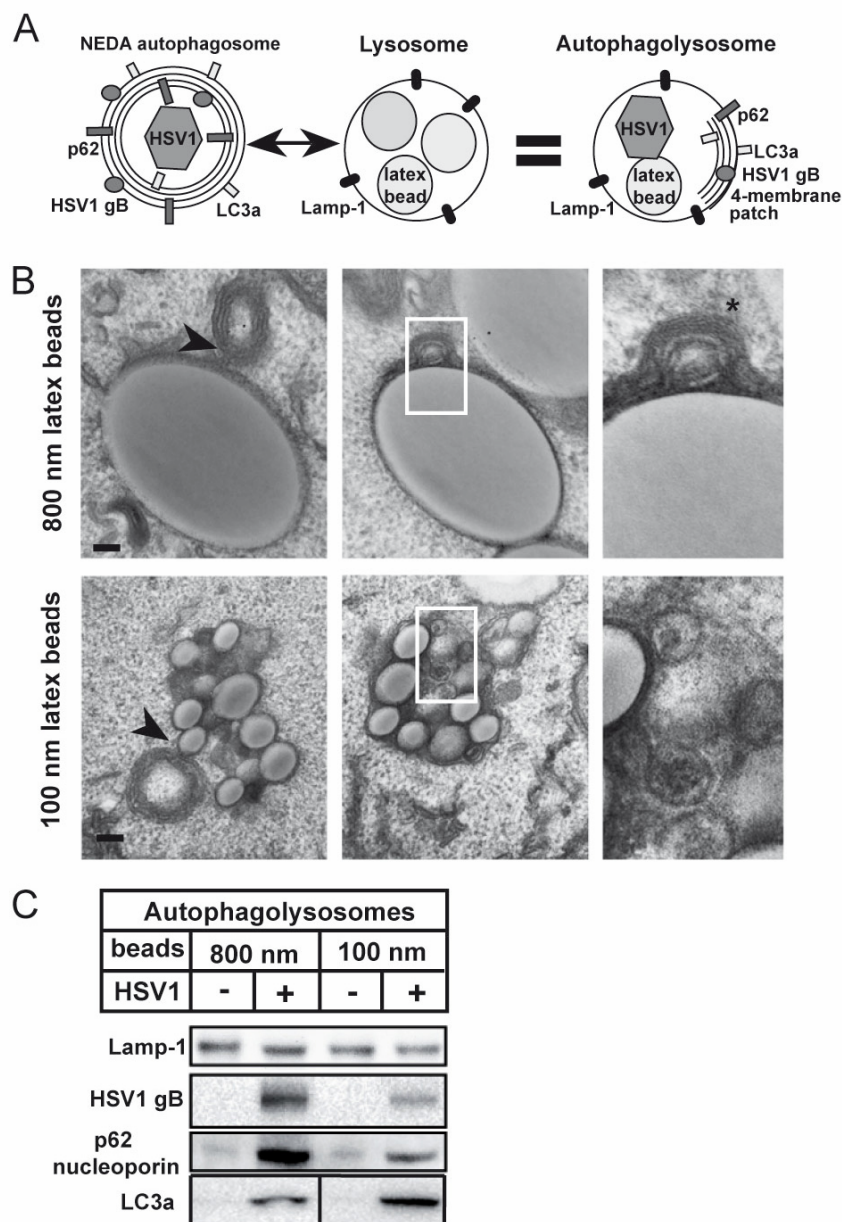


**Figure 4.4. A novel autophagolysosome isolation method.**

A. The isolation method is based on the loading of the lysosomal compartment with latex beads. To isolate APL, we filled lysosomes/phagolysosomes with latex beads and induced NEDA through HSV1 WT infection to promote the fusion of autophagosomes with latex bead-containing lysosomal compartments. B. Macrophages were preloaded with either 100 nm or 800 nm latex beads to fill the lysosomal compartments, and infected cells with HSV-1 to induce the formation of the typical 4-membrane layered autophagosomes associated with NEDA. 4-membrane layered structures were either closely associated with the 100 and 800 nm latexbead-compartment (LB-C) or fused with them. Electron microscopy also showed the presence of viral capsids within the lumen of LB-C, indicating that these compartments fused with autophagosomes to become APL. C. Western blotting showed that the nuclear membrane protein p62 nucleoporin was present in APL after infection, but absent from LB-C isolated from non-infected cells, confirming that the autophagosomes that fused with LB-C in infected cells were derived from the nuclear envelope. Since a higher enrichment of p62 was observed in APL formed with the 800 nm beads, these were used to perform subsequent experiments.

To determine whether NEDA selectively captures subsets of viral proteins, and study how this process could shape the nature of the immune response during HSV1 infection, we analyzed APL isolated from macrophages infected either with the WT or  $\Delta PP1\alpha$  mutant virus. We also analyzed total cell lysates (TCL) generated under the same conditions as controls for enrichment levels (Fig. 4.5A). Mass spectrometry analyses of APL protein extracts from macrophages infected with WT HSV1 enabled the identification of 54 viral proteins while a total of 60 viral proteins were identified for  $\Delta PP1\alpha$  HSV1 (Table IV-1 and Supplemental Table IV-S1). Analyses of TCL protein extracts from WT and  $\Delta PP1\alpha$  infected macrophages led to the identification of 63 and 58 viral proteins, respectively (Table IV-1 and Supplemental Table IV-S1). Altogether these proteomics analyses identified a total of 68 HSV1 representing a 83% coverage of the HSV1 proteome (82 proteins).

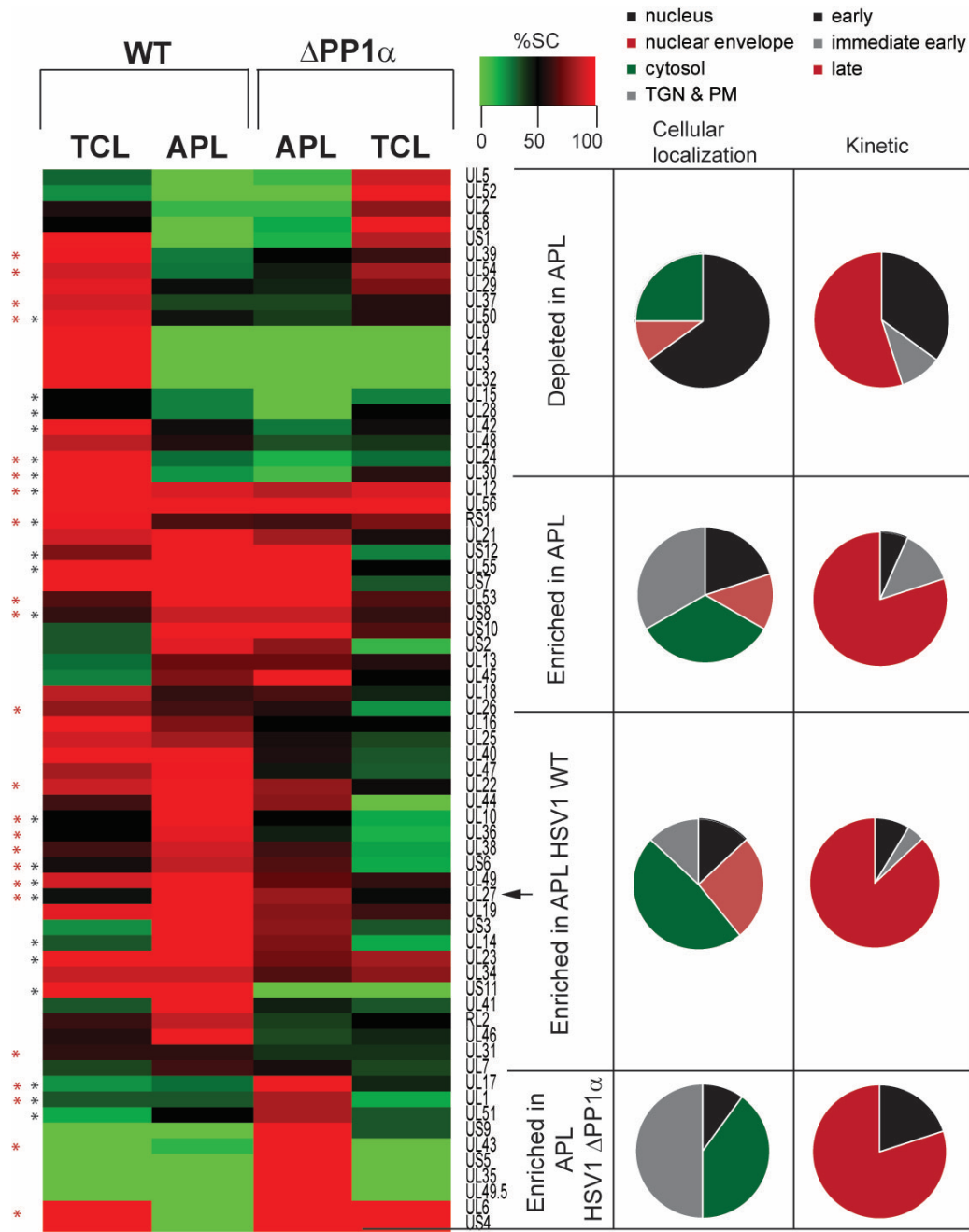
**Table IV-1.** Statistics of quantitative proteomics analysis of APL and TCL from HSV1 WT and HSV1  $\Delta PP1\alpha$  infected macrophages (Protein identifications (>1 peptides/protein); HSV1 proteome = 82 proteins).

	HSV1 WT		HSV1 $\Delta PP1\alpha$	
	TCL	APL	TCL	APL
<b>Distinct peptides</b>	1207	972	978	1065
<b>HSV1 proteins</b>	63	54	58	60
<b>% HSV1 proteome</b>	77	66	71	73

Quantitative analysis of protein abundance based on peptide spectral count revealed 4 clusters of viral proteins (Fig. 4.5A). The first cluster consisted of 20 HSV1 proteins corresponding to peptides highly abundant in the TCL but under-represented in the APL. We were able to assign a subcellular localization to most HSV1 proteins expressed in cells during infection based on earlier reports<sup>24, 25</sup>. Interestingly, 65% of the proteins within this cluster are expressed in the nucleus, suggesting that intra-nuclear proteins are not efficiently captured during NEDA, and are prevented from being processed within vacuolar compartments for antigen presentation during infection. The second cluster

consisted of 15 viral proteins highly abundant and/or enriched in APL isolated from cells infected with the WT or mutant viruses. The majority of these proteins are captured from the cytoplasm and cellular membranes (TGN/plasma membrane). The third cluster consisted of 23 proteins enriched in APL isolated from WT HSV1-infected cells. The capture of these proteins is probably linked to NEDA. In that context, it is interesting to note that a significant part (26%) of these proteins is associated with the nuclear envelope membrane. Finally, the fourth cluster consisted of 10 proteins that are specifically enriched in APL formed during infection with the  $\Delta PP1\alpha$  virus where NEDA does not occur. Indeed, none of these proteins are predominantly localized to the nuclear membrane nor captured during NEDA. For the most part, these viral proteins are coming from other membrane compartments within the cell such as the Trans-Golgi network (TGN)/plasma membrane, suggesting that the autophagic process responsible for the capture of these proteins is not NEDA, but possibly macroautophagy. Further differences are observed in the type of viral proteins captured and transferred to APL during infection. Indeed, a significantly higher proportion of late viral proteins is captured by the autophagic processes occurring during HSV1 infection. How different subsets of viral proteins would be specifically targeted to the APL is still unknown. Selective autophagy is thought to involve the labelling of cargo with ubiquitin and an adaptor protein that binds both ubiquitin and LC3<sup>26</sup>. Interestingly, we identified a number of ubiquitylated viral protein in our datasets suggesting a possible role for ubiquitin in the transfer of viral antigens to APL (Table IV-S2). Notably, we identified 28 ubiquitylation sites on 22 proteins in APL extracts from macrophages infected with WT HSV1, while 34 ubiquitylation sites on 24 proteins were detected upon  $\Delta PP1\alpha$  infection. However, mapping ubiquitylated proteins to specific clusters of proteins that are transferred to the APL (or not transferred) did not reveal any significant trend (Fig. 4.5) suggesting that ubiquitylation does not necessarily regulate the selective transfer of viral antigens to the APL during HSV1 infection.





Ubiquitylation in WT (\*) and  $\Delta PP1\alpha$ (\*)

**Figure 4.5. Quantitative proteomics analysis of APL extracts.**

BMA macrophages were infected with HSV1 WT and  $\Delta PP1\alpha$  at MOI 5. Autophagolysosomes (APL) and total cell lysate (TCL) were isolated 8h pi. Mass spectrometry analysis of HSV1 proteins in TCL and APL revealed four distinct clusters. Viral proteins were assigned according to their predominant subcellular localization. Viral nuclear envelope-resident proteins were detected most frequently in APL of HSV1 WT infected cells. TGN: Trans-Golgi-network; PM: Plasma membrane. Mostly later viral proteins were transferred to the APL. Several proteins were found to be ubiquitylated (\*) by mass spectrometry.

Several interesting observations can be highlighted from these data. We mentioned above that HSV1 infection is characterized by the induction of a CD8<sup>+</sup> T cell response preferentially directed against the SSIEFARL peptide of gB. Interestingly, gB (UL27) is present within the third cluster of proteins, preferentially enriched in APL from WT-infected cells where NEDA occurs (arrow in Fig. 4.5). When spectral peptide count was used to determine the relative abundance of the viral peptides present in APL and TCL from cells infected with WT or  $\Delta$ PP1 $\alpha$  virus, we observed that peptides from gB were more abundant in APL of WT-infected cells, while gB was only the third most abundant protein identified in the TCL. In contrast, gB peptides are more abundant in both APL and TCL extracts of  $\Delta$ PP1 $\alpha$  infected cells (Fig. 4.6A). However, gB is significantly enriched in the APL of macrophages infected with WT compared to  $\Delta$ PP1 $\alpha$  HSV1 virus (Fig. 4.6A). Western Blot analysis confirmed the preferential transfer of gB to the APL, and the appearance of small bands of lower molecular weight, suggesting its degradation and processing within APL (Fig. 4.6B). Interestingly, it has been known since more than a decade that the cytotoxic T cell response to HSV-1 infection in mice is almost entirely directed against a single gB immunodominant epitope (SSIEFARL)<sup>15</sup>. These observations suggest that NEDA might contribute to the immunodominance by promoting the transfer of gB to degradative compartments, such as APL, for antigen processing.

Western blot analyses further indicated that Atg5KD does not affect the enrichment of gB in APL during WT infection (Fig. 4.6B), suggesting that the capture of this protein occurs independently of Atg5. Comparison of viral proteome data from the APL of WT and  $\Delta$ PP1 $\alpha$  infected cells showed that a higher sequence coverage of gB was observed in macrophages infected with WT (56%) compared to  $\Delta$ PP1 $\alpha$  HSV1 (48%) (Fig. 4.6C). We also noted that different gB sequences were identified in these extracts, possibly reflecting the different composition of lytic enzymes within APL of infected macrophages. This is also highlighted by the presence of different ubiquitylated residues on gB with different viruses. An extracted ion chromatogram (XIC) for a representative peptide of gB shows its preferential localization in APL isolated from WT HSV1-infected cells (Fig. 4.6D).

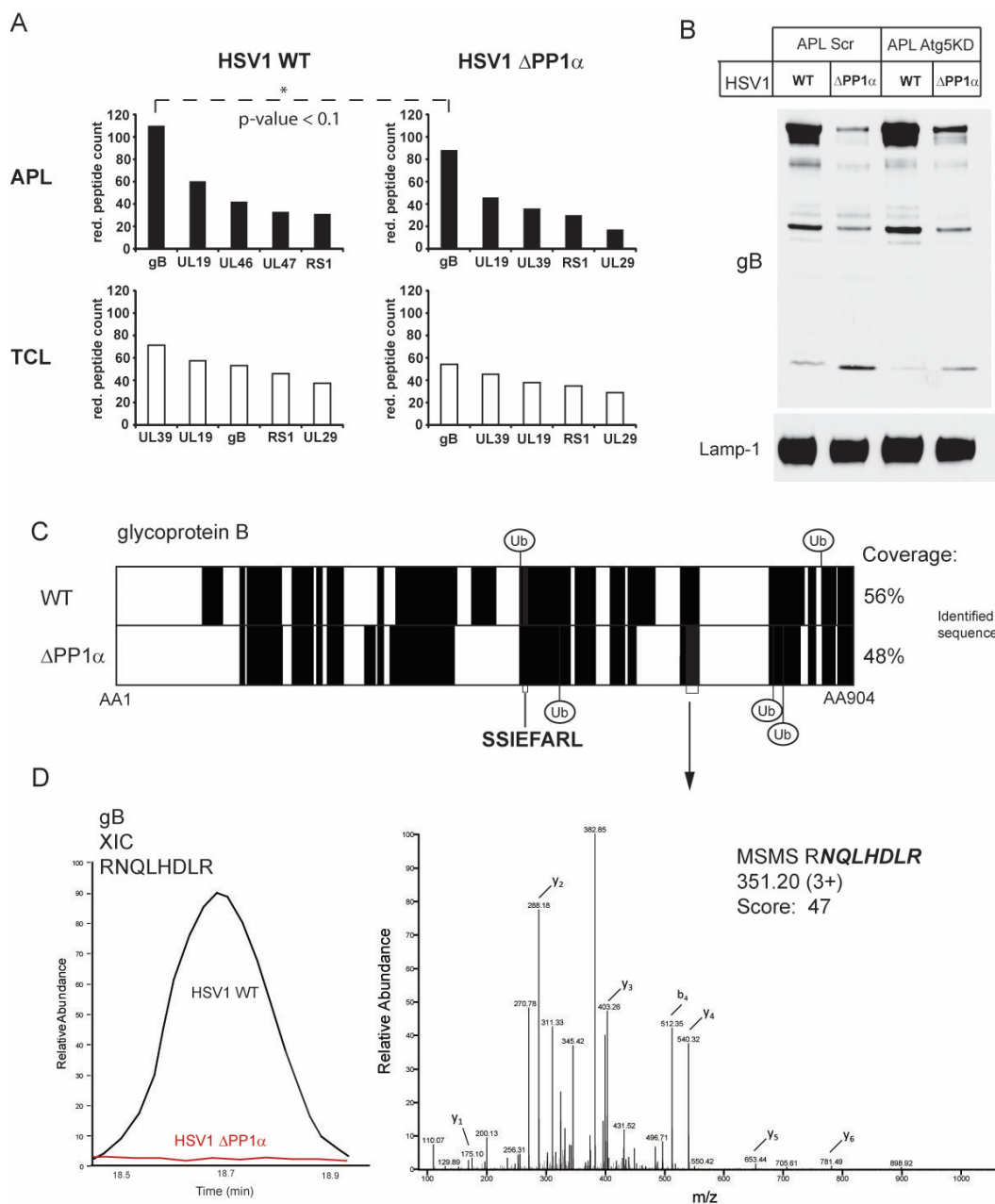


**Figure 4.6. NEDA leads to the enrichment of gB on the APL.**

A. Redundant peptide count of the five most abundant proteins in each sample. gB is significantly enriched in APL infected with HSV1 WT compared to  $\Delta PP1\alpha$  infection ( $p$ -value > 0.1). B. Western Blot analysis of APL extracts from BMA Scr and Atg5KD macrophages confirmed the preferential transfer of gB to the APL during HSV1 WT infection. This transfer is Atg5 independent. C: Comparison of gB sequence coverage in the APL from HSV1 WT and  $\Delta PP1\alpha$  infected macrophages, ub: ubiquitylation site detected by mass spectrometry. D. Extracted ion chromatogram (XIC) of a representative peptide of gB (RNQLHDLR) shows the stronger abundance in the APL of HSV1 WT infected macrophages.

Our proteomics analyses provide the first evidence that NEDA is functionally distinct from macroautophagy by the composition of viral proteins found in the corresponding APL compartments which on the other hand could impact the nature of the antigens presented on MHC molecules during infection. We also noted that viral proteins more abundant in APL of HSV1  $\Delta$ PP1 $\alpha$ -infected macrophages corresponded mostly to cytosolic proteins, suggesting that classical macroautophagy could also be involved (Fig. 4.5 and 4.7A). The increase in abundance of UL17 in the APL of HSV1  $\Delta$ PP1 $\alpha$  infected cells was also confirmed by comparing the extracted ion chromatograms of the corresponding peptides. A representative profile of a peptide from UL17 is shown in Figure 4.7B along with its MS/MS spectrum.

The specific transfer of different viral proteins according to the type of autophagic pathway prompted us to further investigate the role of Atg5 in the transfer of specific antigens. The subset of the protein enriched in the APL during HSV1  $\Delta$ PP1 $\alpha$  infection was probed by Western blotting. Accordingly we mainly detected UL1, UL17, UL51 and US4 in the APL extracts of macrophages infected with HSV1  $\Delta$ PP1 $\alpha$  (Figure 4.7C). In Atg5 KD macrophages, these proteins were no longer detected in the corresponding extracts suggesting that the specific transfer of viral proteins to the APL during HSV1  $\Delta$ PP1 $\alpha$  infection is Atg5-dependent. In contrast proteins enriched on the APL of HSV1 WT-infected macrophages revealed that proteins such as gB (Fig. 4.6B) and gH (Fig. 4.7D) are preferentially transferred to the APL during viral infection. Importantly, these analyses also revealed that the transfer of these viral proteins is Atg5 independent as gB and gH and can still be detected on the APL even in Atg5 KD cells (Fig. 4.7D).

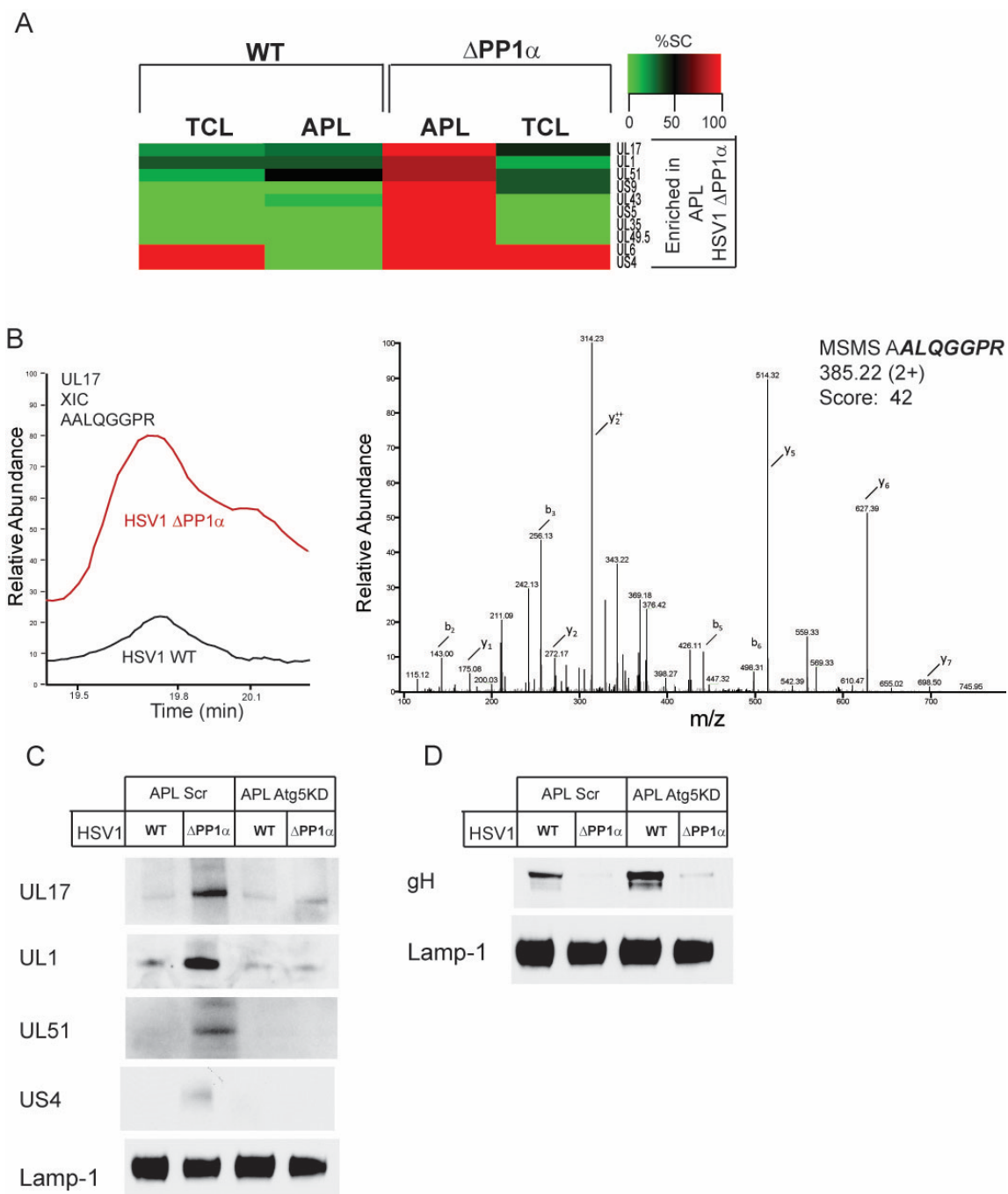


**Figure 4.7. Atg5-dependent transfer of a specific subset of proteins to the APL during  $\Delta PP1\alpha$  infection.**

A. Cluster of proteins that are selectively transferred to the APL during HSV1  $\Delta PP1\alpha$  infection. Atg5-dependent and independent antigen transfer to the APL. B. Mass Spectrometry analysis confirms the increase in abundance of UL17 in the APL of HSV1  $\Delta PP1\alpha$  infected macrophages as shown by the XIC of a representative peptide of UL17 (AALQGGPR). C. Western Blot analysis for proteins selectively transferred to the APL during HSV1  $\Delta PP1\alpha$  infection UL17, UL1, UL51 and US4 in APL extracts reveals that the transfer of viral antigens to the APL during  $\Delta PP1\alpha$  infection is Atg5-dependent. D. Western Blot analysis for gH, enriched in the APL upon HSV1 WT infection, reveals that the transfer of viral antigens to the APL through NEDA is Atg5-independent.

## 4.5. Discussion

It was only recently that autophagy was shown to play a role in the presentation of viral proteins on both MHC class I and class II molecules. The group of Münz initially showed that EBNA1, a viral protein expressed during Epstein-Barr virus (EBV) infection in EBV-positive lymphoma cells<sup>6</sup> was presented on MHC class II molecules. This important finding indicated that autophagy was a cellular process that could actively shape the CD4+ T cell immune response during infection. On the other hand, we were able to show that autophagy also contributes to the capture of endogenous viral proteins for processing in vacuolar compartments and presentation on MHC class I molecules during HSV1 infection<sup>13</sup>. This is of potential immunological interest as vacuolar processing of viral proteins by autophagy could lead to the generation of peptides not usually produced by proteasomal processing in the cytoplasm within the classical MHC class I presentation pathway. For example, it was shown that aminopeptidases present in the cytoplasm contributed to preferential amino acid cleavage, enhancing the presentation of certain peptides to cytotoxic T cells during HIV infection<sup>27</sup>. In the case of HSV1 infection, we have shown that a particular type of autophagic response was observed, characterized by the formation of 4-layers membrane autophagosomes generated from the coiling of the nuclear envelope. However, the contribution of this process, referred to as NEDA, to antigen presentation was not demonstrated. Also, it was not yet well understood how NEDA differs from macroautophagy.

Our results clearly indicate that unlike macroautophagy, NEDA is an Atg5-independent process that contributes directly to the capture of viral antigens, their processing, and their presentation on MHC class I molecules (Fig.4.1 and Fig.4.2). While macroautophagy is inhibited by PI3K inhibitors such as 3-MA or by Atg5KD, NEDA is not affected (Fig. 4.1). Macroautophagy inhibition only partially reduce MHC class I antigen presentation, while inhibition of NEDA with acyclovir almost completely abolishes any vacuolar contribution to antigen presentation (Fig. 4.3E). This clearly shows that NEDA strongly contributes to MHC1 antigen presentation during HSV1 infection and also highlights functional differences between NEDA and macroautophagy. This could suggest that gB is processed differently in autophagosomes derived from NEDA and macroautophagy, hence resulting in the creation of more antigenic peptides during NEDA and thus more efficient antigen presentation on MHC class I molecules.

During macroautophagy bulk cytoplasm is engulfed and degraded in the APL<sup>23</sup>. NEDA is a more selective process and autophagosomes are functionally different as they originate from the nuclear envelope. To investigate the selectivity of viral antigen captured for antigen presentation during NEDA, we localized gB to the nuclear envelope (Fig. 4.3A and 4.3B) and monitored its presentation to CD8<sup>+</sup> T cells using our novel antigen presentation system<sup>28</sup>. Our data indicated that NEDA specifically contributes to the presentation of a specific subset of viral antigens localized to the nuclear envelope, while it did not significantly contribute to the presentation of ER resident antigens to MHC class I molecules (Fig. 4.3C).

To further understand how NEDA contributes to MHC class I antigen processing and presentation it is crucial to characterize the composition of autophagosomes formed during this process. To our knowledge no previous investigations reported the proteome of APL and only four previous studies described the use of mass spectrometry to identify autophagosomal proteins<sup>19-21, 29</sup>. While these approaches were mostly based on density gradient isolation<sup>19-21</sup>, they identified only a limited number of autophagosome proteins, as most proteins were associated to metabolic processes<sup>19</sup> or had unknown functions. The conclusions from these studies were limited by the fact that autophagosomes were isolated by density gradient centrifugation<sup>30</sup>, an approach where contaminants can co-migrate and can consequently hamper the identification of *bona fide* autophagosomal proteins. Furthermore, the overlap between all four autophagosomal proteomes is alarmingly low<sup>21</sup>, raising questions about co-purified contaminants or unselective capture during cytosolic bulk degradation.

To characterize the proteome of the APL formed by NEDA, an efficient cell fractionation approach was developed to isolate these compartments. It is known that an APL is formed by the fusion of an autophagosome with a lysosome (or a phagolysosome)<sup>31</sup>. Thus, we reasoned that by filling the lysosomal compartment with latex beads prior to the stimulation of autophagy, it should be possible to isolate APL by a well-established flotation method (Fig. 4.4). The advantage of the flotation method is that it yields highly purified fractions devoid of cellular contaminants<sup>22</sup>. Here we show that this isolation technique yields pure APL extracts (Fig. 4.4) and the isolation method can be directly integrated into our well-established LC-MS/MS workflow.

This new method for APL isolation is applicable to the investigation of several different types of autophagy and can be employed to investigate how different stimuli shape the

APL proteome. The availability of this technique for proteomics analyses of APL would be of immediate impact to the field of autophagy as it provides the ability to perform sub-cellular fractionation and conduct large-scale study on APL under different experimental paradigms. The analysis of different types of selective autophagy pathways using our technique could provide important insights into cargo recognition, cargo receptors or even more on the origin of the phagophore membrane used to form the autophagosome.

The selectivity of NEDA in preferentially capturing nuclear envelope derived proteins was confirmed by detailed proteomics analyses of the APL (Fig. 4.5). In contrast to macroautophagy, NEDA was found to be an Atg5-independent autophagy process. Interestingly, gB was found to be one of the most abundant viral proteins enriched on the nuclear envelope during infection with WT HSV1. This observation could partly explain the immunodominance of gB, where the cytotoxic T cell response to HSV-1 infection in mice is almost entirely directed against a single gB immunodominant epitope corresponding to the peptide SSIEFARL<sup>15</sup>. In fact, more than 50% of the CD8<sup>+</sup> T cells present in infected mice are directed against this single epitope. The other reactive viral epitopes in mice are unknown<sup>16</sup>. A study examining the CD4<sup>+</sup> T cell repertoire in HSV-1 infected human patients also detected gB as the most abundantly presented protein, followed by gD, and ICP4<sup>32</sup>. While the cellular processes responsible for gB immunodominance are poorly understood, our results suggest that NEDA could contribute to immunodominance by promoting the transfer of high amounts of gB to degradative compartments, such as APL, for antigen processing. Immunodominance leads to an inefficient immune response, and NEDA could be beneficial for the HSV1 infection by limiting the immune response to a single epitope of the viral protein gB. NEDA inhibition by e.g. Acyclovir treatment could possibly represent a novel therapeutic avenue to reduce the damaging effects of immunodominance. Obviously, further studies will be required to validate this hypothesis.

Comprehensive proteomics analyses revealed another striking finding where different viral proteins were transferred to the APL according to the type of autophagy. A subset of mostly cytosolic or trans-golgi network resident proteins was preferentially transferred to the APL during infection with the  $\Delta PP1\alpha$  virus (Fig. 4.5). Importantly, this transfer was Atg5-dependent, while most proteins transferred to the APL during HSV1 WT infection were trafficked in an Atg5-independent manner. The fact that many cytosolic proteins were transferred to the APL during  $\Delta PP1\alpha$  infection in an Atg5-dependent way, suggest



that macroautophagy contributes to this transfer. Our results clearly show that different types of autophagy can be induced to promote the capture of subsets of viral proteins for antigen processing and presentation. Our study represent the first contribution highlighting that the nature of the immune response can be shaped by modulating the autophagic process during infection. By stimulating distinct autophagic pathways, one could promote the recruitment of different organelles to the APL and hence capture specific sets of viral proteins for processing and antigen presentation. Taken together, our study highlights that harnessing the contribution of autophagy in antigen presentation has the potential to minimize the deleterious effects of immunodominance in viral infection, and to activate an immune response against disease epitopes less often detected.

## 4.6. Experimental Procedures

### 4.6.1. Cells, viruses, and antibodies

The BMA3.1A7 macrophage cell line was derived from C56/BL6 mice<sup>33</sup>. BMA3.1A7, RAW, MEF WT (kindly provided by Gilbert Arthur, University of Manitoba, Canada) and MEF atg5<sup>-/-</sup> (kindly provided by N. Mizushima (Medical and Dental University, Tokyo) were cultured in Dulbecco's modified Eagle's medium (DMEM) containing 10% (vol/vol) fetal calf serum (FCS) and 2 mM glutamine. The gB HSV-specific CD8<sup>+</sup> T cell hybridoma HSV-2.3.2E2 (kindly provided by G. Arthur, University of Manitoba, Canada, ) and the OVA-specific CD8<sup>+</sup> B3Z T cell hybridoma (kindly provided by W. Heath, University of Melbourne) were cultivated in RPMI with 5% FBS. The HSV1 strains 17+ WT (kindly provided by Beate Sodeik, Medizinische Hochschule Hannover, Germany) and HSV1 17+  $\Delta$ PP1 $\alpha$ <sup>12</sup> were propagated in BHK-21 cells (ATCC CCL-10), and titers were determined on Vero cells (ATCC CCL-81) as previously described<sup>34</sup>.

The following primary antibodies against cellular proteins were used: rabbit polyclonal to cleaved LC3b (AP1806a; Abgent), rabbit polyclonal antibody to cleaved LC3a (AP1805a; Abgent), mouse monoclonal anti-tubulin antibody (GTU-88; Sigma), mouse monoclonal anti-nuclear pore complex/p62 antibody (610497, BD Transduction Laboratories), mouse monoclonal anti-GAPDH (MAB374, Millipore), a mouse monoclonal anti-atg5 antibody (NB110-74818, Novus Biologicals) for immuno blot, a rabbit polyclonal anti-atg5 antibody (PAB0712, Abnova) for immunofluorescence, and a rat polyclonal anti-lamp1 antibody that was contributed by J. Thomas August to the Developmental Studies Hybridoma Bank, University of Iowa. The rabbit polyclonal anti-myc antibody (ab9010; abcam) was used to detected myc-tagged proteins. Viral proteins were detected with mouse monoclonal antibodies against HSV1/2 gB (10-H44, Fitzgerald for immunofluorescence; clone 10B7, ab6506 Abcam for immuno blots), a mouse monoclonal antibody against HSV1 gE (H600, VirusSys), a mouse monoclonal against ICP0 (clone5H7, ab6515 , Abcam), a mouse monoclonal antibody against gH (BBH1, Abcam), a mouse-monoclonal antibody against gG (H1379, ab53471, Abcam) and mouse-monoclonal antibodies againsts UL17, UL1 and UL51 (kindly provided by Roger Lippé , Université de Montréal).

#### **4.6.2. Generation of pIRES-gB1-2715 Nuclear Envelope and pIRES-gB1-2094 ER lumen vectors**

The HSV1 gB sequence was amplified from purified HSV1 F DNA as described previously<sup>28</sup>. The full length gene (coding for aa 1-2715) was transferred into pIRES-EGFG without a localisation signal, and the C-terminally truncated gene that did not code for a transmembrane region (aa1-2094) was cloned into pIRES-EGFP-KDEL that contains the ER retention signal KDEL, both kindly provided by Claude Perreault (Université de Montréal).

#### **4.6.3. Generation of stable RAW gB-nuclear envelope & RAW gB-ER lumen cell lines**

RAW cells containing the MHC I isoform kb were described previously<sup>28</sup>. In order to generate the RAW gB-nuclear envelope and RAW gB-ER lumen cell lines, the RAW kb cells were transfected with the two pIRES-gB vectors described above. Stable clones were selected with 0.5 mg/ml G418 starting 24h after transfection. After 8 days individual cells expressing high levels of eGFP were selected and isolated using a BD FACS Vantage sorter. These cells were cultivated to derive at monoclonal stable cell lines.

#### **4.6.4. Infection and drug treatment**

Cells were inoculated at a multiplicity of infection (MOI) of 5-10 on a rocking platform at 37°C for 30 min. The inoculum was removed and replaced with cell culture medium, and infected cells were incubated until 8 h postinfection (hpi) for APL isolations, immunofluorescence analysis and electron microscopy. For antigen presentation experiments, cells were incubated until 9 hpi. The PI3K inhibitors wortmannin (681675, Calbiochem) and 3-MA (011M4006, Sigma) were added at 2 hpi at final concentrations of 50  $\mu$ M or 10 mM, respectively. Bafilomycin A1 (MT-800, KAMIYA Biomedical Company) was added at 3 h pi at a final concentration of 1  $\mu$ M. For heatshock treatment, cells were incubated at 42°C for 20 min.

#### 4.6.5. Antigen presentation assays

Infected macrophages were fixed for 10 min sharp with 1% (WT/vol) paraformaldehyde at room temperature, followed by three washes with DMEM containing 10% FBS and 1mM glycine (Sigma). The 2E2 or B3Z T cell hybridoma were added at a ratio of two T cells per macrophage to detect SSIEFARL (HSV1 gB) or SIINFEKL (ovalbumin) presentation, respectively. The T cells were incubated for 12 to 14h at 37C, and then collected and lysed by treatment with 0.125 M Tris base, 0.01 M cyclohexane diaminotetraacetic acid, 50% (vol/vol) glycerol, 0.025% (vol/vol) Triton X-100 and 0.003 M dithiothreitol, pH 7.8 for 10 min on a shaker. The beta-galactosidase substrate (0.15 mM chlorophenol red b-D-galactopyranoside (10884308001, Roche) in 1 mM MgSO<sub>4</sub> x 7 H<sub>2</sub>O, 10 mM KCl, 0.39M NaH<sub>2</sub>PO<sub>4</sub> \_ H<sub>2</sub>O, 0.6 M Na<sub>2</sub>HPO<sub>4</sub> x 7 H<sub>2</sub>O, pH 7.8) was added for 2–4 h at 37C. Cleavage of chlorophenol red-b-D-galactopyranoside was measured in a spectrophotometer at 595 nm. The SSIEFARL or SIINFEKL peptides were added together with the T cell hybridoma to control MHC I surface levels.

#### 4.6.6. Autophagolysosome isolation

BMA3.1A7 macrophages were infected with HSV1 WT or  $\Delta$ PP1 $\alpha$  virus at a MOI of 10 for 30 min. After a 15 min washing step with (DMEM) containing 10% (vol/vol) fetal calf serum (FCS) and 2 mM glutamine, macrophages were pulsed for 30min with latexbeads (0.8  $\mu$ m, 1:100) followed by a chase until 10h post infection. Autophagolysosomes (APL) were isolated according to flotation on a sucrose gradient adapted from Desjardins et al.<sup>35</sup>. Total cell lysates were also obtained for controls of enrichment levels. All cell fractions were prepared in biological triplicates.

#### 4.6.7. Mass spectrometry analysis of APL

Twenty micrograms of total cell lysate or isolated APL were separated on a 4–12% precast NuPAGE gel (NP0321, Invitrogen). After Coomassie staining, lanes were separated into 12 pieces using an in-house cutting device. The gel pieces were reduced with Dithiothreitol (DTT; D9163, Sigma Aldrich), alkylated by Chloroacetamide (C0267, Sigma-Aldrich) and digested with trypsin (ratio 1:25; V5111, Promega). After triple peptide extraction using 90% acetonitrile, extracts were combined, dried and

resuspended in 5% acetonitrile, 0.2% formic acid (FX0440-7, EMD). Peptides were separated on a 150  $\mu\text{m}$  i.d., 15 cm reversed phase nano-LC column (Jupiter C18, 3  $\mu\text{m}$ , 300 Å; 04A-4263 Phenomenex) with 0.2% formic acid used for loading. Peptides were eluted with a gradient of 5–40% acetonitrile within 70 min on an Eksigent 2D-nanoLC (Dublin) operating at a flow-rate of 600 nL/min. The nano-LC was then coupled to an LTQ-Orbitrap Elite mass spectrometer (Thermo-Electron), and samples were injected in an interleaved manner. The apparatus was operated in a data-dependent acquisition mode with a 1 s survey scan at 120,000 resolution, followed by 12 product ion scans (MS/MS) of the most abundant precursors above a threshold of 10,000 counts in the LTQ-part of the instrument. CID was performed in the LTQ at 35% collision energy and an Activation Q of 0.25.

The centroided MS/MS data were merged into single peak-list files (Distiller, v2.4.2.0) and analyzed with the Mascot search engine v2.3.01 (Matrix Science) against the forward and reversed HSV1 Uniprot release 2011 database. Mascot was searched with a parent ion tolerance of 10 ppm and a fragment ion mass tolerance of 0.5 Da. Carbamidomethylation of cysteine; oxidation of methionine; deamidation; phosphorylation of serine, threonine, and tyrosine residues were specified as variable modifications. The false discovery rate (FDR), was calculated as the percentage of positive hits in the decoy database versus the target database, and a FDR of 1% was considered for both proteins and peptides. Relative protein abundance was determined using a redundant peptide counting approach (spectral counts)<sup>36</sup>. The value of redundant peptide counts from 3 identification cycles (on 3 independent biological replicates) was used to generate heatmaps. Unsupervised clustering was performed using the Graphical Proteomics Data Explorer (GProX) software platform in default settings<sup>37</sup>.

#### **4.6.8. Immunofluorescence**

For immunofluorescence analysis, cells were fixed and permeabilized with Cytofix/Cytoperm according to manufacturer's instructions (51-2091KZ, BD Biosciences). Proteins of interest were labeled with the primary antibodies listed above and the corresponding secondary antibodies coupled to Alexa 488 or Alexa 568 (Invitrogen – Molecular Probes). Cells were then embedded with ProLong Gold antifade (Invitrogen) and analyzed with a confocal microscope (LSM510, Leica Microsystems).

Images were adapted with Adobe Photoshop CS3. Linear contrast adjustments were performed equally for all images within one experiment.

#### **4.6.9. SDS-PAGE & immunoblots**

Proteins in isolated APL and cell lysates were separated by SDS PAGE on 12% gels (Mini-PROTEAN TGX, 456-1043, Bio-Rad) and transferred onto nitrocellulose membrane (Pall Corporation). Proteins of interest were detected with the primary antibodies listed above, followed by appropriate secondary antibodies coupled to horseradish peroxidase (Jackson Immuno Research) for enhanced chemiluminescence detection (Western Lightning Plus, NEL105001EA, PerkinElmer). If required, membranes were stripped by incubation with 2% SDS, 100 mM beta-mercaptoethanol, and 50 mM Tris (pH 6.8) at 56°C for 15 min and re-probed with other antibodies. Images were analyzed and linearly contrast enhanced with Adobe Photoshop CS3.

#### **4.6.10. Electron microscopy**

For morphological analysis, infected cells were fixed in 2.5% (vol/vol) glutaraldehyde (Canemco), embedded in Epon (Mecalab), and thin sectioned as described previously<sup>38</sup>. Images were analyzed and contrast enhanced with Adobe Photoshop CS3.

## **4.7. Acknowledgements**

This work was supported by a Canadian Institutes of Health Research grant to MD and PT. MD and PT hold Canada Research Chairs in Cellular Microbiology and Proteomics and Bioanalytical Spectrometry, respectively. IRIC is supported in part by the Canadian Center of Excellence in Commercialization and Research, the Canada Foundation for Innovation and the Fonds de Recherche du Québec en Santé. CB was supported with a scholarship by the Natural Science and Engineering Research Council of Canada Vanier CGS, and KR received a fellowship from the German Research Foundation (RA 1608/4-1). We would like to thank Johanne Duron (Université de Montréal) for her help with the viral infection system, Eric Bonneil (Université de Montréal) for technical assistance with mass spectrometry analysis, Olivier Caron-Lizotte and Mathieu Courcelles (Université de Montréal) for assistance with bioinformatics.

## 4.8. Supplemental data

### 4.8.1. Supplementary figures

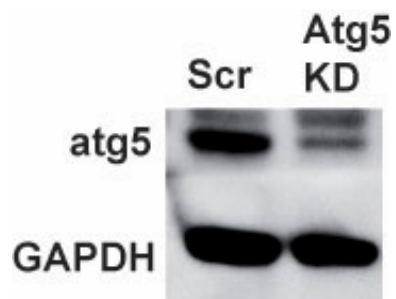


**Figure 4.S1. Atg5 knockdown efficiency.**

The efficiency of Atg5 knockdown after shRNA treatment of RAW264.7 cells with scrambled shRNA (scr) or anti Atg5 shRNA was validated in immuno blot with an anti Atg5 antibody and an anti GAPDH antibody as a loading control.



#### 4.8.2. Supplemental tables

**Table IV-S1:** HSV1 protein identifications (under all experimental conditions) (CD-ROM).

**Table IV-S2:** List of ubiquitylated peptides including links to spectra (CD-ROM).

## 4.9. References

1. Janeway, C. A., Travers, P., Walport, M., and Shlomchik, M. J. (2001) The recognition and effector mechanisms of adaptive immunity.
2. Dermime, S., Armstrong, A., Hawkins, R. E., and Stern, P. L. (2002) Cancer vaccines and immunotherapy. *British medical bulletin* 62, 149-162
3. Neefjes, J., Jongsma, M. L. M., Paul, P., and Bakke, O. (2011) Towards a systems understanding of MHC class I and MHC class II antigen presentation. *Nat Rev Immunol* 11, 823-836
4. Houde, M., Bertholet, S., Gagnon, E., Brunet, S., Goyette, G., Laplante, A., Princiotta, M. F., Thibault, P., Sacks, D., and Desjardins, M. (2003) Phagosomes are competent organelles for antigen cross-presentation. *Nature* 425, 402-406
5. Ackerman, A. L., Kyritsis, C., Tampé, R., and Cresswell, P. (2003) Early phagosomes in dendritic cells form a cellular compartment sufficient for cross presentation of exogenous antigens. *Proceedings of the National Academy of Sciences* 100, 12889-12894
6. Paludan, C., Schmid, D., Landthaler, M., Vockerodt, M., Kube, D., Tuschl, T., and Münz, C. (2005) Endogenous MHC Class II Processing of a Viral Nuclear Antigen After Autophagy. *Science* 307, 593-596
7. Nimmerjahn, F., Milosevic, S., Behrends, U., Jaffee, E. M., Pardoll, D. M., Bornkamm, G. W., and Mautner, J. (2003) Major histocompatibility complex class II-restricted presentation of a cytosolic antigen by autophagy. *European Journal of Immunology* 33, 1250-1259
8. Schmid, D., Pypaert, M., and Münz, C. (2007) Antigen-Loading Compartments for Major Histocompatibility Complex Class II Molecules Continuously Receive Input from Autophagosomes. *Immunity* 26, 79-92
9. Deretic, V., Saitoh, T., and Akira, S. (2013) Autophagy in infection, inflammation and immunity. *Nature Reviews Immunology* 13, 722-737
10. Tallóczy, Z., Jiang, W., Virgin, H. W., Leib, D. A., Scheuner, D., Kaufman, R. J., Eskelinen, E.-L., and Levine, B. (2002) Regulation of starvation- and virus-induced autophagy by the eIF2 $\alpha$  kinase signaling pathway. *Proceedings of the National Academy of Sciences* 99, 190-195
11. Orvedahl, A., Alexander, D., Tallóczy, Z., Sun, Q., Wei, Y., Zhang, W., Burns, D., Leib, D. A., and Levine, B. (2007) HSV-1 ICP34.5 Confers Neurovirulence by Targeting the Beclin 1 Autophagy Protein. *Cell Host & Microbe* 1, 23-35
12. Radtke, K., English, L., Rondeau, C., Leib, D., Lippé, R., and Desjardins, M. (2013) Inhibition of the Host Translation Shutoff Response by Herpes Simplex Virus 1 Triggers Nuclear Envelope-Derived Autophagy. *Journal of Virology* 87, 3990-3997

13. English, L., Chemali, M., Duron, J., Rondeau, C., Laplante, A., Gingras, D., Alexander, D., Leib, D., Norbury, C., Lippe, R., and Desjardins, M. (2009) Autophagy enhances the presentation of endogenous viral antigens on MHC class I molecules during HSV-1 infection. *Nat Immunol* 10, 480-487
14. Whitley, R. J., and Roizman, B. (2001) Herpes simplex virus infections. *The Lancet* 357, 1513-1518
15. Wallace, M. E., Keating, R., Heath, W. R., and Carbone, F. R. (1999) The Cytotoxic T-Cell Response to Herpes Simplex Virus Type 1 Infection of C57BL/6 Mice Is Almost Entirely Directed against a Single Immunodominant Determinant. *Journal of Virology* 73, 7619-7626
16. Sheridan, P. A., and Beck, M. A. (2009) The dendritic and T cell responses to herpes simplex virus-1 are modulated by dietary vitamin E. *Free Radical Biology and Medicine* 46, 1581-1588
17. Akram, A., and Inman, R. D. (2012) Immunodominance: A pivotal principle in host response to viral infections. *Clinical Immunology* 143, 99-115
18. Levine, B., and Kroemer, G. (2008) Autophagy in the Pathogenesis of Disease. *Cell* 132, 27-42
19. Øverbye, A., Brinchmann, M. F., and Seglen, P. O. (2007) Proteomic Analysis of Membrane-Associated Proteins from Rat Liver Autophagosomes. *Autophagy* 3, 300-322
20. Dengjel, J., Høyer-Hansen, M., Nielsen, M. O., Eisenberg, T., Harder, L. M., Schandorff, S., Farkas, T., Kirkegaard, T., Becker, A. C., Schroeder, S., Vanselow, K., Lundberg, E., Nielsen, M. M., Kristensen, A. R., Akimov, V., Bunkenborg, J., Madeo, F., Jäättelä, M., and Andersen, J. S. (2012) Identification of Autophagosome-associated Proteins and Regulators by Quantitative Proteomic Analysis and Genetic Screens. *Molecular & Cellular Proteomics* 11
21. Mancias, J. D., Wang, X., Gygi, S. P., Harper, J. W., and Kimmelman, A. C. (2014) Quantitative proteomics identifies NCOA4 as the cargo receptor mediating ferritinophagy. *Nature* 509, 105-109
22. Stuart, L. M., Boulais, J., Charriere, G. M., Hennessy, E. J., Brunet, S., Jutras, I., Goyette, G., Rondeau, C., Letarte, S., Huang, H., Ye, P., Morales, F., Kocks, C., Bader, J. S., Desjardins, M., and Ezekowitz, R. A. B. (2007) A systems biology analysis of the Drosophila phagosome. *Nature* 445, 95-101
23. Yang, Z., and Klionsky, D. J. (2010) Mammalian autophagy: core molecular machinery and signaling regulation. *Current Opinion in Cell Biology* 22, 124-131
24. Xing, J., Wang, S., Li, Y., Guo, H., Zhao, L., Pan, W., Lin, F., Zhu, H., Wang, L., and Li, M. (2011) Characterization of the subcellular localization of herpes simplex virus type 1 proteins in living cells. *Medical microbiology and immunology* 200, 61-68

25. Salsman, J., Zimmerman, N., Chen, T., Domagala, M., and Frappier, L. (2008) Genome-wide screen of three herpesviruses for protein subcellular localization and alteration of PML nuclear bodies. *PLoS pathogens* 4, e1000100
26. Kraft, C., Peter, M., and Hofmann, K. (2010) Selective autophagy: ubiquitin-mediated recognition and beyond. *Nature cell biology* 12, 836-841
27. Zhang, S. C., Martin, E., Shimada, M., Godfrey, S. B., Fricke, J., Locastro, S., Lai, N. Y., Liebesny, P., Carlson, J. M., Brumme, C. J., Ogbechie, O. A., Chen, H., Walker, B. D., Brumme, Z. L., Kavanagh, D. G., and Le Gall, S. (2012) Aminopeptidase Substrate Preference Affects HIV Epitope Presentation and Predicts Immune Escape Patterns in HIV-Infected Individuals. *The Journal of Immunology* 188, 5924-5934
28. Bell, C., English, L., Boulais, J., Chemali, M., Caron-Lizotte, O., Desjardins, M., and Thibault, P. (2013) Quantitative Proteomics Reveals the Induction of Mitophagy in Tumor Necrosis Factor- $\alpha$ -activated (TNF $\alpha$ ) Macrophages. *Molecular & Cellular Proteomics* 12, 2394-2407
29. Gao, W., Kang, J. H., Liao, Y., Ding, W.-X., Gambotto, A. A., Watkins, S. C., Liu, Y.-J., Stolz, D. B., and Yin, X.-M. (2010) Biochemical Isolation and Characterization of the Tubulovesicular LC3-positive Autophagosomal Compartment. *Journal of Biological Chemistry* 285, 1371-1383
30. Strømhaug, P. E., Berg, T. O., Fengsrud, M., and Seglen, P. O. (1998) Purification and characterization of autophagosomes from rat hepatocytes. *Biochem. J.* 335, 217-224
31. Sanjuan, M. A., Dillon, C. P., Tait, S. W. G., Moshiah, S., Dorsey, F., Connell, S., Komatsu, M., Tanaka, K., Cleveland, J. L., Withoff, S., and Green, D. R. (2007) Toll-like receptor signalling in macrophages links the autophagy pathway to phagocytosis. *Nature* 450, 1253-1257
32. Jing, L., Schiffer, J. T., Chong, T. M., Bruckner, J. J., Davies, D. H., Felgner, P. L., Haas, J., Wald, A., Verjans, G. M. G. M., and Koelle, D. M. (2013) CD4 T-Cell Memory Responses to Viral Infections of Humans Show Pronounced Immunodominance Independent of Duration or Viral Persistence. *Journal of Virology* 87, 2617-2627
33. Kovacsovics-Bankowski, M., and Rock, K. (1995) A phagosome-to-cytosol pathway for exogenous antigens presented on MHC class I molecules. *Science* 267, 243-246
34. Sodeik, B., Ebersold, M. W., and Helenius, A. (1997) Microtubule-mediated Transport of Incoming Herpes Simplex Virus 1 Capsids to the Nucleus. *The Journal of Cell Biology* 136, 1007-1021
35. Desjardins, M., Celis, J. E., van Meer, G., Dieplinger, H., Jahraus, A., Griffiths, G., and Huber, L. A. (1994) Molecular characterization of phagosomes. *Journal of Biological Chemistry* 269, 32194-32200
36. Bell, C., Desjardins, M., Thibault, P., and Radtke, K. (2013) Proteomics Analysis of Herpes Simplex Virus Type 1-Infected Cells Reveals Dynamic Changes of Viral

Protein Expression, Ubiquitylation, and Phosphorylation. *Journal of Proteome Research* 12, 1820-1829

37. Rigbolt, K. T. G., Vanselow, J. T., and Blagoev, B. (2011) GProX, a User-Friendly Platform for Bioinformatics Analysis and Visualization of Quantitative Proteomics Data. *Molecular & Cellular Proteomics* 10

38. Griffiths, G., Quinn, P., and Warren, G. (1983) Dissection of the Golgi complex. I. Monensin inhibits the transport of viral membrane proteins from medial to trans Golgi cisternae in baby hamster kidney cells infected with Semliki Forest virus. *The Journal of Cell Biology* 96, 835-850



## **Chapter 5 : Conclusion**

## 5.1. Conclusion and Discussion

Understanding the molecular mechanisms governing cell functions is essential to prevent diseases and develop therapeutic approaches. In that context, proteomics is a key enabling technology that continues to have a major impact on the understanding of how cells work, as proteins and their interacting complexes are the major actors performing and regulating cell functions. Proteomics has already led to several major discoveries and has provided direct insights into the understanding of the immune system<sup>1, 2</sup>.

Autophagy is a highly conserved lysosomal degradation pathway that plays an essential role in cellular homeostasis. Although autophagy was first proposed to be a source of nutrients during stress, new data suggests that this process has implications in cancer, immune response, neurodegeneration, development and aging<sup>3</sup>. Recently, autophagy was shown to be involved in the presentation of endogenous proteins on MHC class II molecules<sup>4</sup>. Our lab has furthermore shown that autophagy contributes to the presentation of viral proteins on MHC class I molecules<sup>5</sup>. Protein degradation in vacuolar compartments is of particular interest for disease progressions like cancer and viral infections, as this process complements classical proteasome cleavage, providing a way to expose additional immunogenic epitopes. Autophagy is now recognized as a vacuolar pathway involved in antigen presentation and has also been linked in various other ways to processes in innate and adaptive immunity rendering autophagy an emerging immunological paradigm. Bulk degradation of proteins by autophagy causes major cellular remodeling and modulates the proteomics composition of a cell<sup>6</sup>. MS-based proteomics is hence an ideal approach to follow protein dynamics in autophagy pathways. However, proteomics analyses of protein dynamics during autophagy are still scarce and only very few studies have utilized proteomics techniques to investigate different aspects of autophagy.

Consequently the main focus of this thesis was to develop an approach to define the molecular mechanisms governing the involvement of autophagy in innate and adaptive immunity using novel quantitative proteomics methods together with functional assays. This objective was successfully completed and documented in the preceding chapters of this thesis. An integrated proteomics research program was established to unravel the molecular machines associated with autophagy and to decipher the fine details of the molecular mechanisms governing the functions of the autophagosome in antigen



presentation using a systems biology approach. To study how autophagosome and antigen presentation are modulated in macrophages, we first conducted several comprehensive proteomics studies under different conditions known to stimulate autophagy. In this context, we employed cytokine activation as well as viral infections since both stimuli are known to modulate autophagy in various complex ways.

### **5.1.1. An unexpected role for TNF- $\alpha$ in the induction of mitophagy**

While cytokines such as IFN- $\gamma$ , TNF- $\alpha$  and IL-1 $\beta$  have been reported to induce autophagy, IL-4, IL-13 and IL-10 may antagonize this degradation process<sup>7</sup>. Cytokines are also crucial components of the immune system and play a central role in mounting an efficient immune response against pathogens. Classically, macrophages are activated by a priming stimulus by the proinflammatory cytokine IFN- $\gamma$  followed by a microbial trigger. Following this activation macrophages release a variety of proinflammatory cytokines such as IL-1, IL-6 and TNF- $\alpha$ <sup>8</sup>. Interestingly, TNF- $\alpha$  is not only produced by macrophages, but can also act back on macrophages and synergize with IFN- $\gamma$  to modulate the activity of macrophages through the induction of signaling cascades and changes in gene expression. Several pathways induced by TNF- $\alpha$  have been described in the literature including apoptosis<sup>9</sup> or autophagy<sup>10-12</sup>, which may be cell type dependent. Relatively few studies have investigated the molecular mechanisms and signaling associated with the activation of macrophages by TNF- $\alpha$ . To date no comprehensive analysis has been performed.

Our work, outlined in chapter 2 of this thesis, describes the first comprehensive analysis of TNF- $\alpha$  activation of macrophages by label-free quantitative proteomics and provided important insights on how TNF- $\alpha$  actively shapes the activity of macrophages. Quantitative proteomics analysis highlighted the consistent down regulation of mitochondrial proteins in response to TNF- $\alpha$  activation as well as the differential regulation of several proteins involved in protein degradation, vesicular trafficking, and immune response. Importantly, integration of our proteomics dataset with several bioinformatics tools as well as novel functional assays revealed an unsuspected role of TNF- $\alpha$  activation in macrophages leading to the selective degradation of mitochondrial proteins by mitophagy. Functional flow cytometry assays established the reduction of the

healthy mitochondria population upon TNF- $\alpha$  stimulation and confirmed that mitochondria are selectively degraded upon TNF- $\alpha$  stimulation by Atg5-dependent mitophagy. Fluorescence microscopy analysis revealed that mitochondria are indeed sequestered in autophagosome structures and confirmed the enhanced mitophagic activity in TNF- $\alpha$  activated macrophages. Complementary morphological analyses by electron microscopy showed the engulfment of mitochondria in double membrane structures during TNF- $\alpha$  stimulation.

Our quantitative proteomics dataset also highlighted the upregulation of cPLA<sub>2</sub>, an enzyme known to modulate the induction of ROS, a well-established feature of the macrophage's microbicidal activity to kill pathogenic invaders such as bacteria. Increased levels of ROS lead to the damage of mitochondria characterized by the depolarization of the mitochondrial membrane potential. Damaged mitochondria are eliminated as part of the mitochondrial quality control mechanism by mitophagic degradation<sup>13</sup>. This suggests that TNF- $\alpha$  induced mitophagy involves the induction of ROS. Using a novel antigen presentation system we showed that the induction of mitophagy by TNF- $\alpha$  enabled the processing and presentation of mitochondrial antigens on MHC class I molecules in an Atg5 dependent manner, expanding the role of autophagy in the processing of intracellular antigens and their presentation by MHC class I molecules. Taken together, these findings highlight a novel, unsuspected role for TNF- $\alpha$  in mitophagy and in the processing and presentation of mitochondrial antigens by MHC class I molecules.

### **5.1.2. Potential roles of TNF- $\alpha$ induced mitophagy**

Mitochondria execute several pivotal metabolic functions in the cell, including oxidative phosphorylation, and represent the main source of cellular energy. However mitochondria can also cause harm to the cell<sup>14</sup>. If damaged by, for example, oxidation of mitochondrial lipids or proteins, mitochondria release high levels of Ca<sup>2+</sup> and cytochrome c, hence inducing apoptosis<sup>15</sup>. Mitophagy has evolved as a mitochondrial quality control mechanisms to prevent cellular damage by aiding in the removal of damaged or superfluous mitochondria and by preserving a population of healthy mitochondria<sup>13</sup>. The finding that TNF- $\alpha$  stimulation induces mitophagy might seem unsuspected at first, although it might be anticipated considering the association of ROS, mitochondrial damage and mitophagy. It can be hypothesized that TNF  $\alpha$  induced ROS production can

damage mitochondria, which in turn could lead to the release of cytochrome c and the induction of apoptosis. Indeed, TNF- $\alpha$  is known to induce apoptosis in several cell types<sup>9</sup>. In macrophages, mitophagy may have evolved as a compensation mechanism to counteract the effects of mitochondrial damage caused by the microbicidal activity of macrophages via the selective degradation of impaired mitochondria. This ensures the survival of classically activated macrophages and hence the elucidation of an efficient immune response.

Another functional hallmark of mitophagy is the selectivity for cargo selection. Mitophagy uses specific signals to recognize and remove damaged mitochondria. Loss of mitochondrial membrane potential leads to Pink1 accumulation on the outer membrane of dysfunctional mitochondria. This leads to the recruitment of Parkin, which tags mitochondrial proteins by ubiquitylation for subsequent degradation by mitophagy<sup>13</sup>. The regulation of Pink1 and Parkin upon TNF- $\alpha$  stimulation was not determined in our study. This is likely due to the time frame chosen for sample collection or due to the sample preparation used, which enriched for membrane proteins and might hence result in the loss of only weakly associated membrane proteins. Interestingly, we detected a number of ubiquitylated mitochondrial proteins which could mediate their recruitment to autophagosomes via binding to cargo receptors and LC3. Recently, it was found that Parkin also plays a role in the ubiquitin mediated xenophagic degradation of *M. tuberculosis*<sup>16</sup>. Parkin ubiquitylates phagosomes containing *M. tuberculosis* and targets the vesicles for lysosomal destruction. This finding is very exciting and provides an unexpected functional link between mitophagy and infectious diseases. In that context, it should be noted that TNF- $\alpha$ , as a proinflammatory cytokine, also executes a key function in the elimination of internalized bacteria. Furthermore, TNF- $\alpha$  also plays an important role in the protective immune response to *M. tuberculosis*. It is tempting to speculate that mitophagy in macrophages might have evolved from the xenophagic degradation pathway used to eradicate pathogenic invaders. These pathways seem distinct, however the evolutionary origin of mitochondria from a bacterial endosymbiont, suggests that perhaps autophagic mechanisms are shared between these pathways. Autophagy of mitochondria and bacteria share a lot of commonalities including specific recognition signals such as ubiquitylation, specific cargo receptors as well as a similar shaped autophagosome structures. It is reasonable to propose that the induction of mitophagy presented a survival advantage in TNF- $\alpha$  activated macrophages, which macrophages

might have been selected for during evolution and thus established mitophagy as a survival mechanism. Alternatively, recent research revealed that dysfunctional mitochondria may serve as a danger signal, resulting in the activation of several innate immune receptors such as the NLRP3-inflammasome<sup>17</sup>. Considering that several studies also indicated a modulation of host mitochondria dynamics<sup>18</sup> during intracellular infection with several pathogens such as *L. monocytogenes*, it can be hypothesized that damaged mitochondria may serve as a signal for intracellular infection and activation of xenophagy, as speculated by Manzanillo et al.<sup>16</sup>. In that context, TNF- $\alpha$  induced mitophagy likely improves the pathogen killing abilities of macrophages, while simultaneously ensuring macrophage survival.

Another scenario can be proposed, where TNF- $\alpha$  induced mitophagy might have developed as a proviral function. During viral infection, the virus relies on the host's protein synthesis machinery to express all proteins needed for assembly of the virions and thus for its viral spread. If cells undergo apoptosis in the presence of high levels of TNF- $\alpha$ , the viral proliferative capacity is reduced. Keeping the cell alive by the induction of mitophagy and the removal of dysfunctional, harmful mitochondria allows the virus to continue to proliferate and propagate much more efficiently. Strikingly, our results showed that TNF- $\alpha$  not only induced mitophagy, but this process also contributed to MHC class I antigen presentation. The fact that TNF- $\alpha$  not only degraded mitochondrial proteins to prevent further damage to the cell, but also utilizes the mitochondrial antigens to promote a CD8<sup>+</sup> T cell response, suggests an even more defined role of this process in the development of a specific immune response.

### **5.1.3. TNF- $\alpha$ induced mitophagy contributes to antigen presentation: 'Shaping an efficient immune response'**

Several studies have reported the contribution of autophagy to antigen presentation<sup>4, 5, 19</sup>. Until now, studies only reported the contribution of bulk macroautophagy to both MHC class I and II processing and presentation. Our study represents the first report showing that selective autophagy, more specifically mitophagy, can also contribute to antigen presentation on MHC class I molecules. The notion that autophagic pathways can be modulated to promote the capture of specific sets of endogenous antigens for presentation on MHC molecules has fundamental implications for the immune response.

Previous studies have shown that antigens predominantly presented on MHC class I and II molecules derive from cytosolic or vacuolar origins (lysosome, endosome)<sup>20, 21</sup>. Mitochondrial proteins are usually not presented or presented in very low abundance. Interestingly, a recent study on the MHC class II immunopeptidome showed that autophagy promotes MHC class II presentation of peptides from intracellular source proteins. While proteins from the lysosome, nucleus or cytoskeleton were preferentially presented in cells undergoing autophagy, mitochondria proteins represented only 0.2% of all peptides presented<sup>22</sup>. These findings suggest that antigens localized in mitochondria can evade their detection by the immune system. This is important as there are several viruses known to localize parts of their proteome to mitochondria, hence evading immune detection. Examples include human immunodeficiency virus (HIV) protein Vpr, Hepatitis B virus (HBV) protein X, Hepatitis C virus (HCV) protein NS2 and Epstein barr virus (EBV) protein BHRF1, to mention a few<sup>23</sup>. HSV1 protein UL12.5 also localizes to mitochondria<sup>24</sup>. Interestingly, many viral proteins targeted to mitochondria control apoptosis<sup>23</sup>. This is in agreement with the complex interplay between apoptosis, autophagy and TNF- $\alpha$  activation, outlined above. The cell's ability to increase the presentation of mitochondrial antigen by the stimulation of mitophagy with TNF- $\alpha$  could improve the immune detection of some viruses and thus limit viral spread. Inducing the selective degradation of mitochondrial proteins by TNF- $\alpha$  opens up important possibilities to shape the immunopeptidome presented to T cells. This could open up novel avenues to develop therapeutic approaches and vaccines against infectious diseases such as viral infection.

#### **5.1.4. HSV1 infection and autophagy**

After having investigated cytokines as potent stimulators or modulators of autophagy, we set out to investigate the complex interactions between viral infections and autophagy.

HSV1 infection induces a novel form of autophagy, termed nuclear envelope derived autophagy (NEDA). NEDA results in the formation of autophagosomes that originate from the nuclear envelope. The role of NEDA in the pathogenesis of viral infection, whether it benefits the host or the virus, is poorly understood. NEDA is regulated differently than macroautophagy and is induced in response to ICP34.5 binding to PP1 $\alpha$ <sup>25</sup>, hence depending on the production of late viral proteins. How this autophagic process differs

mechanistically from classical macroautophagy still needs to be elucidated. Macroautophagy was recently reported to contribute to efficient processing and presentation of a viral antigen in murine macrophages during HSV1 infection<sup>5</sup>. However, the extent to which NEDA is involved in the processing and presentation of viral proteins and peptides remains to be established. To further understand how NEDA and its involvement in antigen presentation is regulated, we first characterized our experimental system.

#### **5.1.5. A comprehensive characterization of viral protein expression in macrophages**

The definition of the viral proteome in infected cells is crucial for our understanding on how HSV1 executes its functions. In addition to protein expression levels, ubiquitylation and phosphorylation play an important role for HSV1 protein function, subcellular localization, or stability. No complete data exists of the expression of the whole viral proteome as well as of posttranslational modifications on HSV1 proteins. To address this, we performed a comprehensive quantitative analysis of the HSV1 proteome of infected cells by mass-spectrometry-based proteomics as described in chapter 3.

LC-MS/MS analysis identified a total of 67 structural and non-structural viral proteins (82% of the proteome). Different kinetic classes of viral protein expression were investigated using two different inhibitors of DNA replication. Our data suggest that the classification into immediate early, early and late proteins might not totally reflect expression profiles in infected cells and protein expression might be controlled in a more complex manner in HSV1 infected cells. Our analysis also identified 90 novel phosphorylation sites and ten novel ubiquitylation sites on different viral proteins. Interestingly, all ubiquitylated proteins could either localize to the nucleus or participate in membrane fusion events suggesting that ubiquitylation might affect viral protein trafficking and localization. Taken together, our dataset provides new insights into HSV1 protein expression regulation and generated comprehensive phosphorylation and ubiquitylation sites maps, which served as a resource for my third project outlined in chapter 4.

### **5.1.6. NEDA is Atg5-independent and contributes to MHC class I antigen presentation**

During HSV1 infection, viral proteins are degraded by the proteasome to generate peptides that are loaded on MHC class I molecules and presented at the cell surface to stimulate a CD8+ T cell response. Interest in NEDA stems from its potential ability to complement classical proteasome cleavage by the generation of non-traditional, immunogenic epitopes, distinct from those generated during classical autophagy. Our results outlined in chapter 4 clearly show that NEDA is an Atg5-independent pathway, different from macroautophagy, that contributes to the presentation of an epitope of gB to CD8+ T cells. During macroautophagy bulk cytoplasm is engulfed and degraded in the autophagolysosome<sup>26</sup>. NEDA is a more selective process and autophagosomes derive from the nuclear envelope. Indeed, our data, obtained using our novel antigen presentation assay, indicate that NEDA selectively captures antigens and specifically contributes to the presentation of a particular subset of viral antigens localized to the nuclear envelope. Clearly, NEDA exhibits functional differences to macroautophagy. To gain further insights into NEDA contribution to MHC class I antigen processing and presentation, we characterized the composition of autophagosomes formed during this process.

### **5.1.7. A novel autophagosome isolation method**

To date, very little work has been done to decipher the proteome of autophagosomes and only few previous studies described the use of mass spectrometry to identify autophagosomal proteins<sup>27-30</sup>. To characterize the proteome of the autophagosome formed by NEDA, an efficient cell fractionation approach had to be developed to isolate these compartments. We developed a new isolation method based on the loading of the lysosomal compartment with latex beads, a unique tool to obtain very pure cell extracts, upon autophagy induction. We monitored the transfer of HSV1 antigens into autophagolysosomes (APL) using MS based proteomics. This isolation technique yields pure APL extracts and the isolation method can be directly integrated into our well-established LC-MS/MS workflow. This new APL isolation method is amenable for the investigation of several different types of autophagy and can be used to investigate how different stimuli shape the autophagosome proteome. This new technique is expected to

have a great impact on the autophagy field since meaningful large-scale datasets for the different autophagy types can now be generated. This new method can potentially revolutionize the field of autophagy research. The analysis of different types of selective autophagy pathways using our technique could provide important insights into cargo recognition, cargo receptors or on the origin of the phagophore membrane used to form the autophagosome in a previously inaccessible and comprehensive manner. Based on hypothesis driven research, new concepts can be established from the large-scale proteomics datasets, which can be ultimately tested using our immunological follow-up screens.

#### **5.1.8. Selectivity of NEDA: beneficial for host or virus?**

Detailed proteomics analyses of the APL confirmed the selectivity of NEDA to favorably capture nuclear envelope derived proteins. Interestingly, gB, found to be enriched on the nuclear envelope during infection was also the most abundant protein in the APL during HSV1 WT infection, while it was significantly less abundant in NEDA-deficient systems. It has been established, that the cytotoxic T cell response to HSV-1 infection in mice is almost entirely directed against a single gB immunodominant epitope corresponding to the peptide SSIEFARL<sup>31</sup>. The cellular processes responsible for gB immunodominance are poorly understood. Our results support the hypothesis that NEDA contributes to immunodominance by promoting the transfer of high amounts of gB to degradative compartments, such as APL, for antigen processing. Immunodominance leads to an inefficient immune response. This would thus suggest that NEDA is an autophagic pathway that is beneficial for the virus by limiting the immune response to a single epitope of the viral protein gB. NEDA induction might represent a novel viral evasion mechanism and NEDA inhibition might hence represent a novel therapeutic avenue to reduce the damaging effects of immunodominance. However, further investigations are required to support this proposal. In contrast, previous studies argued that enhancing antigen presentation is an important means by which autophagy combats intracellular microbes and counteracts the effect of viral immune evasion<sup>32</sup>. The premise is that the host immune system retaliates by degrading proteins for presentation to MHC class I molecules that would generally not access the classical antigen presentation pathway. This research was conducted on macroautophagy, while our work focused specifically on NEDA.



Comprehensive proteomics analysis revealed another meaningful finding. Different viral protein subsets were transferred to the APL whether NEDA occurred or not. A subset of mostly cytosolic proteins was preferentially transferred to the APL during infection in a NEDA deficient system in an Atg5 dependent manner, while the transfer of most proteins transferred to the APL during HSV1 WT infection was Atg5 independent. Since many cytosolic proteins were transferred to the APL in NEDA deficient systems in an Atg5-dependent manner, it is reasonable to propose that macroautophagy contributes to this transfer.

#### **5.1.9. Autophagy can shape the immune response by selectively targeting different protein subsets: a novel concept**

The integration of all results obtained during my PhD revealed an important new concept in immunology: different selective autophagy pathways can be induced to promote the capture of different subsets of proteins for antigen processing and presentation. While TNF- $\alpha$  induces the presentation of antigens localized in mitochondria, NEDA specifically targets proteins localized at the nuclear envelope. In contrast, macroautophagy samples cytosolic proteins and targets them to the autophagosome. The notion that autophagic pathways can be modulated to promote the capture of specific sets of endogenous antigens that are usually undetected for presentation on MHC molecules opens up novel avenues for therapeutic interventions. Indeed we are the first to demonstrate that the nature of the immune response can be actively shaped by modulating the autophagic process during infection. By stimulating distinct autophagic pathways, the recruitment of different organelles to autophagosomes and hence the capture of specific sets of viral proteins for processing and antigen presentation could be promoted. Modulating the autophagic response could be used to shape the repertoire of viral peptides presented by MHC I molecules during HSV-1 infection.

The mechanism responsible for the selective transfer of various subsets of viral proteins by different autophagic conditions remains to be elucidated. NEDA and macroautophagy are two functionally distinct processes, which may account for their specificity or non-specificity in the sampling of antigens. While NEDA autophagosomes originate from the nuclear envelope, the origin of the phagophore membrane during macroautophagy is still under debate. The different origin of the membrane could contribute to the capture of

different antigen subsets. NEDA enriches for proteins localized at the nuclear envelope such as gB, since autophagosomes are derived from nuclear membranes. The different origins of autophagosomes formed during NEDA and macroautophagy can also influence the properties of these compartments. Different enzymes, proteases or lysosomal content might be recruited that can result in differential processing of the proteins in the vesicle. The improved presentation of antigens upon NEDA induction suggests that NEDA autophagosomes contain proteases and peptidases that cleave viral proteins to derive antigens that are preferentially presented on MHC class I molecules.

Other factors may be responsible for the selectivity of NEDA as opposed to macroautophagy, which mostly recruits cytosolic proteins. Indeed, macroautophagy is Atg5-dependent, while NEDA is not. Recently, another Atg5-independent pathway has been characterized, where autophagosomes originate from the trans-golgi network<sup>33</sup>. Ubiquitylation of viral proteins might also play a role in the capture of specific subsets of viral proteins to the autophagosome. Different cargo receptors could be present in the autophagosomes that target different ubiquitylated motifs. It should be noted that we did not find modulation based on ubiquitylation patterns in our experiments. This could be attributed, in part, to the small number of ubiquitylation sites identified in this work. A large-scale analysis of ubiquitylation sites in the APL using affinity-enrichment would provide much needed information on this matter. Finally, NEDA is characterized by the presence of LC3a on the autophagosomal membrane, whereas during macroautophagy LC3b, a homologue of LC3a is enriched on the autophagosome. During selective autophagy the LIR motif<sup>34</sup> is crucial for the selective targeting of cargo to the autophagosomal membrane. LC3a may act to recruit specific cargo containing a LC3a interacting motif, not yet identified to date.

In conclusion, the application of quantitative proteomics methods allowed for the identification of alterations occurring in autophagosomes during disease and inflammatory conditions, including viral infections. Our established systems biology approach that combined mass spectrometry-based quantitative proteomics with novel antigen presentation assays revealed new immunological insights providing a greater understanding on autophagosome functions in antigen processing and presentation and their modulation. My PhD thesis research highlights the importance of autophagy in antigen presentation and its potential to shape an appropriate immune response against disease epitopes that are less often detected.

## 5.2. Future perspectives

The finding that autophagic pathways can be modulated to promote the capture of specific sets of endogenous antigens for presentation on MHC molecules has implications well beyond the scope of this thesis. Indeed, the possibility to shape the composition of the peptides presented to T cells opens novel avenues to develop therapeutic approaches and vaccines against infectious diseases and cancer. In the context of the strong immunodominance often associated with these diseases, the ability to modify the immunopeptidome of antigen presenting cells has the potential to activate a T cell response against a broader set of microbial and cancer epitopes.

### 5.2.1. Iterative proteomics: Autophagy and antigen presentation - 'network of influence'

The mechanisms by which NEDA or mitophagy mediate their contribution to antigen presentation remain to be elucidated. In order to be able to modulate and shape the immune response through the induction of different autophagy pathways, it is crucial to truly understand how these pathways are regulated and how they modulate and contribute to antigen presentation. The definition of the composition of the autophagosome isolated from different autophagic conditions will provide important insights into the distinct functional properties of these vesicles. In chapter 4 of this thesis, we performed a detailed characterization of the viral proteome transferred to the APL during NEDA and macroautophagy. In addition to the viral proteome data, this dataset contains important insights into the host proteome targeted to the autophagosome. Indeed, preliminary analysis of our dataset show the modulation of protein interaction networks associated to lysosomal degradation as well as ion transport. This suggests, that different autophagic pathways might influence the degradative capabilities of the autophagosome and thus modulate the processing of antigens. Further analyses with regard to the autophagosome composition are currently ongoing.

Importantly, the interaction of proteins into networks and molecular machines is at the base of most biological functions. To understand the molecular mechanisms regulating the functional properties of autophagosomes, and the role played by these organelles in antigen presentation, we developed a novel approach as a continuation of my PhD

research, where the links between proteins are identified by proteomics analyses and functional assays. This approach highlights a novel type of network that we call "networks of influence". The method to decipher these networks, called Iterative Proteomics, is based on proteomics analyses aimed to determine how a single autophagosome protein "influences" the overall proteome of this organelle. Hence, autophagosomes can be isolated from cells using the method described in this thesis, where a single protein is knockdown, and analyzed by quantitative mass spectrometry. The modulated proteins are further studied by generating corresponding knockdown cell lines where their functional properties are tested. The resolution of the networks expands as additional cycles of proteomic analyses/shRNA knock down/APL functional assays are performed. Iterative Proteomics is a novel approach to study how groups of proteins interact and "influence" each other. The networks identified by this approach are not necessarily representative of direct protein-protein interaction, but rather based on the fact that these proteins influence a given functional pathway by modulating the presence of each other. Preliminary results already show the strength of this method. Several proteins identified by mass spectrometry-based proteomics to be differentially regulated such as *Irgm1* or *Cxcl10* directly modulated antigen presentation, while other proteins such as *Tmem176b* modulated antigen presentation via the regulation of NEDA induction. This further highlights the potential of quantitative proteomics to investigate complex immunological paradigms in a comprehensive manner, which should become more common in future research.

### **5.2.2. Quantitative proteomics approaches to investigate selectivity in autophagy pathways**

Understanding how selectivity is achieved in different autophagy processes is central to our capability to modulate these pathways. Concepts regarding selective autophagy are just starting to emerge. In recent years, it became clear that ubiquitylation not only plays a role in the UPS system, but is also essential for the selective targeting of cargo to autophagosomes<sup>35</sup>. Ubiquitylated proteins can be recognized by cargo receptors such as p62 which recruit them for autophagic degradation. In addition the LIR motif also plays an important role to recruit cargo for autophagosomal degradation<sup>34</sup>.

In order to get a more comprehensive view on the role of ubiquitylation in autophagy selectivity, it would be of key importance to obtain a large-scale repertoire of ubiquitylation sites in autophagosomes isolated under different autophagic conditions such as NEDA or mitophagy. Large-scale proteomics analysis of the ubiquitinome is now achievable<sup>36, 37</sup>. Antibody-based affinity approaches for the specific di-Gly fragment characteristic of ubiquitylation allows for the routine identification of up to 10 000 ubiquitylation sites in mammalian cells<sup>37</sup>. The major shortcoming of the methods developed to date is the need for high protein quantities. Autophagosome isolation results in limited protein quantities (though it can be up-scaled), thus making the large scale analysis of ubiquitylation very challenging. Improvements in method development such as higher affinity antibodies in combination with higher sensitivity mass spectrometry instruments, such as the Orbitrap Fusion<sup>38</sup>, should make the comprehensive analysis of the autophagosome ubiquitinome possible in the near future. Comparative analysis of these sites should provide important insights on how this cargo selectivity is exerted and if it is indeed ubiquitin-dependent. The ubiquitinome together with the autophagosome proteome could also likely serve as a valuable resource for advanced bioinformatics analysis to define the LIR motif in more detail. Even more, this should aid in the identification of additional motifs. There are several homologs of LC3 in mammals, however the role of most of these homologs has not yet been established. Interestingly, LC3a is a specific marker for NEDA. Ubiquitylated and non-modified proteins present in the autophagosome in HSV1 WT infected cells could be computationally analyzed to define a LC3a interacting motif. This could provide a basis to predict which protein subsets will be preferentially transferred to the autophagosome under different conditions.

### **5.2.3. Modulation of the Immuno-peptidome by selective autophagy**

Promoting the transfer of different sets of viral proteins to APL, where they are actively processed, will influence the nature of the viral peptides presented on MHC class I molecules and shape the repertoire of CD8+ cytotoxic T cells. Thus, it would be interesting to investigate how various autophagic pathways affect the composition of the MHC class I peptides presented at the surface of HSV-1-infected cells. Our lab developed a mass-spectrometry platform to identify immunopeptides loaded on MHC class I molecules, which can be used to monitor the immuno-peptidome in a high-

throughput manner<sup>39-41</sup>. Integration of immunopectidomics and autophagosome proteomics under different autophagy conditions can reveal, if the immunopectidome reflects the autophagosomal composition or if it is rather shaped by the classical pathway of antigen processing. Furthermore, these results could be nicely complemented by the identification of the peptidome in autophagosomes. To this end, autophagosomes could be isolated and peptides extracted using molecular weight cutoffs. This would allow to determine peptide cleavage sites and the corresponding proteases and peptidase responsible for the cleavage, an important information usually lost in proteomics workflows following trypsin digestion. Peptides present in the autophagosome could then be correlated to the immunopectidome to get a complete view on autophagy's contribution to antigen processing and presentation.

Remarkably, the ability to follow changes to the APL proteome during the activation of various autophagic pathways, and their effect on the nature of the viral immunopectidome, will provide an opportunity to test whether the viral peptides produced by APL under various conditions are relevant to the immune response engaged in infected mice. The identity of the viral peptides recognized by T cells is unknown. Identifying these peptides is important to develop vaccination protocols, and/or methods to boost the immune response during infection by promoting the processing and presentation of viral epitopes proven to be reactive. The characterization of the viral immunopectidome would provide the unique opportunity to test whether the identified peptides correspond to the ones recognized by reactive CD8<sup>+</sup> T cells in infected animals.

Taken together, the research performed during this PhD thesis as well as future research continues to deepen our understanding on how autophagy and its contribution to antigen presentation is actively modulated.

### 5.3. References

1. Trost, M., English, L., Lemieux, S., Courcelles, M., Desjardins, M., and Thibault, P. (2009) The phagosomal proteome in interferon- $\gamma$ -activated macrophages. *Immunity* 30, 143-154
2. Houde, M., Bertholet, S., Gagnon, E., Brunet, S., Goyette, G., Laplante, A., Princiotta, M. F., Thibault, P., Sacks, D., and Desjardins, M. (2003) Phagosomes are competent organelles for antigen cross-presentation. *Nature* 425, 402-406
3. Choi, A. M., Ryter, S. W., and Levine, B. (2013) Autophagy in human health and disease. *New England Journal of Medicine* 368, 651-662
4. Paludan, C., Schmid, D., Landthaler, M., Vockerodt, M., Kube, D., Tuschl, T., and Münz, C. (2005) Endogenous MHC Class II Processing of a Viral Nuclear Antigen After Autophagy. *Science* 307, 593-596
5. English, L., Chemali, M., Duron, J., Rondeau, C., Laplante, A., Gingras, D., Alexander, D., Leib, D., Norbury, C., Lippe, R., and Desjardins, M. (2009) Autophagy enhances the presentation of endogenous viral antigens on MHC class I molecules during HSV-1 infection. *Nat Immunol* 10, 480-487
6. Kristensen, A. R., Schandorff, S., Hoyer-Hansen, M., Nielsen, M. O., Jaattela, M., Dengjel, J., and Andersen, J. S. (2008) Ordered organelle degradation during starvation-induced autophagy. *Molecular & Cellular Proteomics*
7. Harris, J. (2011) Autophagy and cytokines. *Cytokine* 56, 140-144
8. Mosser, D. M., and Edwards, J. P. (2008) Exploring the full spectrum of macrophage activation. *Nature Reviews Immunology* 8, 958-969
9. Sidoti-de Fraisse, C., Rincheval, V., Risler, Y., Mignotte, B., and Vayssiere, J.-L. (1998) TNF- $\alpha$  activates at least two apoptotic signaling cascades. *Oncogene* 17, 1639-1651
10. Jia, G., Cheng, G., Gangahar, D. M., and Agrawal, D. K. (2006) Insulin-like growth factor-1 and TNF-[ $\alpha$ ] regulate autophagy through c-jun N-terminal kinase and Akt pathways in human atherosclerotic vascular smooth cells. *Immunol Cell Biol* 84, 448-454
11. Baregamian, N., Song, J., Bailey, C. E., Papaconstantinou, J., Evers, B. M., and Chung, D. H. (2009) Tumor Necrosis Factor- $\alpha$ ; and Apoptosis Signal-Regulating Kinase 1 Control Reactive Oxygen Species Release, Mitochondrial Autophagy and C-Jun N-Terminal Kinase/P38 Phosphorylation During Necrotizing Enterocolitis. *Oxidative Medicine and Cellular Longevity* 2, 297-306
12. Keller, C. W., Fokken, C., Turville, S. G., Lünemann, A., Schmidt, J., Münz, C., and Lünemann, J. D. (2011) TNF- $\alpha$  Induces Macroautophagy and Regulates MHC Class II Expression in Human Skeletal Muscle Cells. *Journal of Biological Chemistry* 286, 3970-3980

13. Ashrafi, G., and Schwarz, T. (2012) The pathways of mitophagy for quality control and clearance of mitochondria. *Cell Death & Differentiation* 20, 31-42
14. Saraste, M. (1999) Oxidative Phosphorylation at the fin de siècle. *Science* 283, 1488-1493
15. Parsons, M. J., and Green, D. R. (2010) Mitochondria in cell death. *Essays Biochem* 47, 99-114
16. Manzanillo, P. S., Ayres, J. S., Watson, R. O., Collins, A. C., Souza, G., Rae, C. S., Schneider, D. S., Nakamura, K., Shiloh, M. U., and Cox, J. S. (2013) The ubiquitin ligase parkin mediates resistance to intracellular pathogens. *Nature* 501, 512-516
17. Zhou, R., Yazdi, A. S., Menu, P., and Tschopp, J. (2011) A role for mitochondria in NLRP3 inflammasome activation. *Nature* 469, 221-225
18. Stavru, F., Bouillaud, F., Sartori, A., Ricquier, D., and Cossart, P. (2011) *Listeria monocytogenes* transiently alters mitochondrial dynamics during infection. *Proceedings of the National Academy of Sciences* 108, 3612-3617
19. Tey, S.-K., and Khanna, R. (2012) Autophagy mediates transporter associated with antigen processing-independent presentation of viral epitopes through MHC class I pathway. *Blood* 120, 994-1004
20. Chicz, R. M., Urban, R. G., Gorga, J. C., Vignali, D., Lane, W. S., and Strominger, J. L. (1993) Specificity and promiscuity among naturally processed peptides bound to HLA-DR alleles. *The Journal of experimental medicine* 178, 27-47
21. Lechler, R., Aichinger, G., and Lightstone, L. (1996) The endogenous pathway of MHC class II antigen presentation. *Immunological reviews* 151, 51-79
22. Dengjel, J., Schoor, O., Fischer, R., Reich, M., Kraus, M., Müller, M., Kreymborg, K., Altenberend, F., Brandenburg, J., Kalbacher, H., Brock, R., Driessen, C., Rammensee, H.-G., and Stevanovic, S. (2005) Autophagy promotes MHC class II presentation of peptides from intracellular source proteins. *Proceedings of the National Academy of Sciences* 102, 7922-7927
23. Boya, P., Pauleau, A.-L., Poncet, D., Gonzalez-Polo, R.-A., Zamzami, N., and Kroemer, G. (2004) Viral proteins targeting mitochondria: controlling cell death. *Biochimica et Biophysica Acta (BBA) - Bioenergetics* 1659, 178-189
24. Corcoran, J. A., Saffran, H. A., Duguay, B. A., and Smiley, J. R. (2009) Herpes Simplex Virus UL12.5 Targets Mitochondria through a Mitochondrial Localization Sequence Proximal to the N Terminus. *Journal of Virology* 83, 2601-2610
25. Radtke, K., English, L., Rondeau, C., Leib, D., Lippe, R., and Desjardins, M. (2013) Inhibition of the Host Translation Shut-off Response by Herpes Simplex Virus 1 triggers Nuclear Envelope-derived Autophagy. *J Virol* 87, 3990-3997
26. Yang, Z., and Klionsky, D. J. (2009) An overview of the molecular mechanism of autophagy. *Curr Top Microbiol Immunol* 335, 1-32



27. Mancias, J. D., Wang, X., Gygi, S. P., Harper, J. W., and Kimmelman, A. C. (2014) Quantitative proteomics identifies NCOA4 as the cargo receptor mediating ferritinophagy. *Nature* 509, 105-109
28. Gao, W., Kang, J. H., Liao, Y., Ding, W.-X., Gambotto, A. A., Watkins, S. C., Liu, Y.-J., Stolz, D. B., and Yin, X.-M. (2010) Biochemical Isolation and Characterization of the Tubulovesicular LC3-positive Autophagosomal Compartment. *Journal of Biological Chemistry* 285, 1371-1383
29. Dengjel, J., Høyer-Hansen, M., Nielsen, M. O., Eisenberg, T., Harder, L. M., Schandorff, S., Farkas, T., Kirkegaard, T., Becker, A. C., Schroeder, S., Vanselow, K., Lundberg, E., Nielsen, M. M., Kristensen, A. R., Akimov, V., Bunkenborg, J., Madeo, F., Jäättelä, M., and Andersen, J. S. (2012) Identification of Autophagosome-associated Proteins and Regulators by Quantitative Proteomic Analysis and Genetic Screens. *Molecular & Cellular Proteomics* 11
30. Øverbye, A., Brinchmann, M. F., and Seglen, P. O. (2007) Proteomic Analysis of Membrane-Associated Proteins from Rat Liver Autophagosomes. *Autophagy* 3, 300-322
31. Wallace, M. E., Keating, R., Heath, W. R., and Carbone, F. R. (1999) The Cytotoxic T-Cell Response to Herpes Simplex Virus Type 1 Infection of C57BL/6 Mice Is Almost Entirely Directed against a Single Immunodominant Determinant. *Journal of Virology* 73, 7619-7626
32. Tey, S.-K., and Khanna, R. (2012) Host immune system strikes back. *Autophagy* 8, 1-3
33. Nishida, Y., Arakawa, S., Fujitani, K., Yamaguchi, H., Mizuta, T., Kanaseki, T., Komatsu, M., Otsu, K., Tsujimoto, Y., and Shimizu, S. (2009) Discovery of Atg5/Atg7-independent alternative macroautophagy. *Nature* 461, 654-658
34. Birgisdottir, Å. B., Lamark, T., and Johansen, T. (2013) The LIR motif—crucial for selective autophagy. *Journal of cell science* 126, 3237-3247
35. Kraft, C., Peter, M., and Hofmann, K. (2010) Selective autophagy: ubiquitin-mediated recognition and beyond. *Nature cell biology* 12, 836-841
36. Kim, W., Bennett, E. J., Huttlin, E. L., Guo, A., Li, J., Possemato, A., Sowa, M. E., Rad, R., Rush, J., and Comb, M. J. (2011) Systematic and quantitative assessment of the ubiquitin-modified proteome. *Molecular cell* 44, 325-340
37. Udeshi, N. D., Svinkina, T., Mertins, P., Kuhn, E., Mani, D. R., Qiao, J. W., and Carr, S. A. (2013) Refined Preparation and Use of Anti-diglycine Remnant (K-ε-GG) Antibody Enables Routine Quantification of 10,000s of Ubiquitination Sites in Single Proteomics Experiments. *Molecular & Cellular Proteomics* 12, 825-831
38. Senko, M. W., Remes, P. M., Canterbury, J. D., Mathur, R., Song, Q., Eliuk, S. M., Mullen, C., Earley, L., Hardman, M., Blethrow, J. D., Bui, H., Specht, A., Lange, O., Denisov, E., Makarov, A., Horning, S., and Zabrouskov, V. (2013) Novel Parallelized Quadrupole/Linear Ion Trap/Orbitrap Tribrid Mass Spectrometer Improving Proteome Coverage and Peptide Identification Rates. *Analytical Chemistry* 85, 11710-11714

39. Caron, E., Vincent, K., Fortier, M. H., Laverdure, J. P., Bramoullé, A., Hardy, M. P., Voisin, G., Roux, P. P., Lemieux, S., and Thibault, P. (2011) The MHC I immunopeptidome conveys to the cell surface an integrative view of cellular regulation. *Molecular systems biology* 7
40. de Verteuil, D., Muratore-Schroeder, T. L., Granados, D. P., Fortier, M.-H., Hardy, M.-P., Bramoullé, A., Caron, É., Vincent, K., Mader, S., and Lemieux, S. (2010) Deletion of immunoproteasome subunits imprints on the transcriptome and has a broad impact on peptides presented by major histocompatibility complex I molecules. *Molecular & Cellular Proteomics* 9, 2034-2047
41. Fortier, M.-H., Caron, É., Hardy, M.-P., Voisin, G., Lemieux, S., Perreault, C., and Thibault, P. (2008) The MHC class I peptide repertoire is molded by the transcriptome. *The Journal of experimental medicine* 205, 595-610

## **Appendix : Scientific Contributions**

## Publications

Christina Bell, Guanghou Shui, Markus Wenk, Michel Desjardins, Pierre Thibault. Combined proteomics and lipidomics analyses enable the characterization of phagosome maturation in activated macrophages. *In preparation for submission*

Mélanie Dieudé\*, Christina Bell\*, Shijie Qi, Nicolas Pallet, Julie Turgeon, Chanel Béland, Déborah Beillevaire, Matthieu Rousseau, Diane Gingras, Christiane Rondeau, Claude Perreault, Yves Durocher, Michel Desjardins, Eric Boilard, Pierre Thibault and Marie-Josée Hébert. Nanovesicles released by apoptotic endothelial cells induce anti-LG3 production and accelerate vascular rejection. *In preparation for submission*.

\* = equal contribution

Christina Bell\*, Kerstin Radtke\*, Luc English, Diana Matheoud, Magali Chemali, Roger Lippe, Pierre Thibault, Michel Desjardins. Nuclear envelope-derived autophagy contributes to MHC I antigen presentation of a nuclear envelope resident viral protein. *In preparation for submission*.

\* = equal contribution

Christina Bell, Luc English, Jonathan Boulais, Magali Chemali, Olivier Caron-Lizotte, Michel Desjardins, Pierre Thibault. Quantitative proteomics reveals the induction of mitophagy in TNF- $\alpha$  activated macrophages. *Mol Cell Proteomics*, 2013 September, 12 (9): 2394-407 – *September 2013 Cover*

Nicolas Pallet, Isabelle Sirois, Christina Bell, Laila-Aicha Hanafi, Katia Hamelin, Melanie Dieude, Christiane Rondeau, Pierre Thibault, Michel Desjardins, Marie-Josée Hébert. A comprehensive characterization of membrane vesicles released by autophagic human endothelial cells. *Proteomics*, 2013 Apr, 13 (7): 1108-20

Christina Bell, Michel Desjardins, Pierre Thibault, Kerstin Radtke. Proteomics analyses of Herpes Simplex Virus Type-1 infected cells Reveals Dynamic Changes of Viral Protein Expression, Ubiquitylation and Phosphorylation. *J Proteome Res*, 2013 April, 12(4): 1820-9

Francois-Xavier Campbell-Valois, Matthias Trost, Magali Chemali, Brian D.Dill, Annie Laplante, Sophie Duclos, Shayan Sadeghi, Christiane Rondeau, Isabel Morrow, Christina Bell, Kiyokata Hatsuzawa, Pierre Thibault, Michel Desjardins. Quantitative proteomics reveals that only a subset of the endoplasmatic reticulum contributes to the phagosome. *Mol Cell Proteomics*, 2012 Jul; 11(7): M111.016378

Christina Bell, Geoffrey T. Smith, Michael J. Sweredoski, Sonja Hess. Characterization of the *Mycobacterium tuberculosis* Proteome by Liquid Chromatography Mass Spectrometry-based Proteomics Techniques.: A Comprehensive Resource for Tuberculosis Research. *J Proteome Res* 2012 Jan 1; 11(1):119-30

## Book Chapters

Christina Bell, Michel Desjardins, Pierre Thibault, Kerstin Radtke. Autophagy's contribution to innate and adaptive immunity: an overview. "Autophagy, Infection and the Immune Response". Wiley, accepted, expected publication 2014

## Conference Contributions (selected highlights)

Christina Bell, Guanghou Shui, Markus Wenk, Michel Desjardins, Pierre Thibault. Combined proteomics and lipidomics analyses enable the characterization of phagosome maturation in activated macrophages. *6<sup>th</sup> Annual CNPN Symposium*, Montréal, QC, Canada, April 14-16, 2014. Poster Presentation

Christina Bell, Guanghou Shui, Markus Wenk, Michel Desjardins, Pierre Thibault. Combined proteomics and lipidomics analyses enable the characterization of phagosome maturation in activated macrophages. *61<sup>st</sup> ASMS Conference on Mass Spectrometry*, Minneapolis, MN, USA, June 9-13, 2013. Poster Presentation

Christina Bell, Luc English, Jonathan Boulais, Magali Chemali, Olivier Caron-Lizotte, Michel Desjardins, Pierre Thibault. Quantitative proteomics reveals the specific autophagic elimination of mitochondria in TNF- $\alpha$  activated macrophages. *Keystone Symposia on Autophagy, Inflammation and Immunity*, Montréal, QC, Canada, February 17-22, 2013. Oral Presentation

Christina Bell, Luc English, Roger Lippe, Michel Desjardins, Pierre Thibault. The phagosome proteome of HSV-1 infected macrophages reveals novel insights on the role of membrane trafficking in MHC-class-I presentation. *60<sup>th</sup> ASMS Conference on Mass Spectrometry*, Vancouver, BC, Canada, May 20-24, 2012. Oral Presentation

Christina Bell, Luc English, Matthias Trost, Magali Chemali, Michel Desjardins, Pierre Thibault. Quantitative subcellular proteomics analyses of TNF- $\alpha$  activated mouse macrophages highlight the selective degradation of mitochondria proteins by mitophagy. *59<sup>th</sup> ASMS Conference on Mass Spectrometry*, Denver, CO, USA, June 5-9, 2011. Poster Presentation

Christina Bell, Matthias Trost, Luc English, Michel Desjardins, Pierre Thibault. Quantitative proteomics analysis of TNF- $\alpha$  activated macrophages reveals the selective degradation of mitochondria proteins. *The 23<sup>rd</sup> Annual Mass Spectrometry Workshop, Canadian Society for Mass Spectrometry*, Lake Louise, December 2-4, 2010. Oral Presentation

Christina Bell, Matthias Trost, Michel Desjardins, Pierre Thibault. Performance of different fractionation methods for quantitative proteomics analyses of membrane proteins from control and TNF- $\alpha$  activated mouse macrophages. *58<sup>th</sup> ASMS Conference on Mass Spectrometry*, Salt Lake City, UT, USA, May 23-27, 2010. Poster Presentation

Christina Bell, Michael J. Sweredoski, Sonja Hess. Characterization of *Mycobacterium tuberculosis* membrane and surface-exposed proteins by liquid chromatography mass spectrometry-based proteomics techniques. *NIBS Seminar*, National Institute of Biological Sciences, Beijing, China, August 10, 2009. Invited Speaker

Christina Bell, Michael J. Sweredoski, Sonja Hess. Characterization of *Mycobacterium tuberculosis* membrane and surface-exposed proteins by liquid chromatography mass spectrometry-based proteomics techniques. *57<sup>th</sup> ASMS Conference on Mass Spectrometry*, Philadelphia, PA, USA, May 31-June 4, 2009. Oral Presentation